Organic Micropollutants in Small River Systems

–

Occurrence, Fate and Effects

Dissertation

Der Mathematisch-Naturwissenschaftlichen Fakultät

der Eberhard Karls Universität Tübingen

zur Erlangung des Grades eines

Doktors der Naturwissenschaften

(Dr. rer. nat.)

vorgelegt von

M.Sc. Maximilian Eckhard Müller

aus Radolfzell am Bodensee

Tübingen

2020

„Das Leben ist kein Jammertal,
am wenigsten im Ammertal“

Gedruckt mit Genehmigung der Mathematisch-Naturwissenschaftlichen Fakultät der Eberhard Karls Universität Tübingen

Tag der mündlichen Qualifikation:	19.11.2020
Stellvertretender Dekan:	Prof. Dr. József Fortágh
1. Berichterstatter:	Prof. Dr. Christian Zwiener
2. Berichterstatterin:	Prof. Dr. Beate I. Escher
3. Berichterstatter:	Prof. Dr. Andreas Schäffer

Abstract

The number of anthropogenic organic chemicals is continuously increasing and with it their substantial use in, for instance, industrial and domestic applications, agriculture and medical use. Many of these compounds are intentionally synthesized to be persistent (e.g., flame retardants, coatings) or bioactive (e.g., pesticides, pharmaceuticals), with some exhibiting the unintended characteristic of being bioaccumulative (e.g., polycyclic aromatic hydrocarbons, per- and polyfluoroalkyl substances). Thus, they pose an imminent risk to the environment with potentially far-reaching implications. Organic micropollutants are released into the aquatic environment through various input sources such as surface runoff, wastewater treatment plant effluents, combined sewer overflows, industrial sites or are, in the case of pesticides, intentionally dispersed into the environment. Inputs can be point or diffuse sources that are often not easy to identify and characterize. Rivers act as a conduit for micropollutant transport, integrating diffuse and point sources within their entire catchment and hosting important transformation processes. Therefore, the present work aimed to gain a detailed understanding of the occurrence and (toxic) effects of organic micropollutants in rivers that is required to predict their fate in the environment.

In this doctoral thesis, I investigated the chemical and toxicological profile of the Ammer River, in Southwest Germany, under varying hydrological conditions. The Ammer River is representative of small rivers in karstic systems and in densely populated temperate climate regions. I characterized input sources and the fate of organic micropollutants at the scale of the Ammer catchment via a combination of chemical analysis (liquid chromatography–mass spectrometry) and environmentally relevant *in-vitro* bioassays, during a series of field sampling campaigns. Organic indicator chemicals were selected based on their application, environmental relevance, occurrence in previous studies and degradability in order to indicate different input sources and in-stream processes. The bioanalytical test battery was further improved and complemented by the development of a novel *in-vitro* bioassay (Oxygen Consumption Rate assay) that can account for two different modes of action of mitochondrial toxicity in environmental samples.

Under dry weather conditions and using chemical analysis and *in-vitro* bioassays, I identified a wastewater treatment plant as the major input source of organic micropollutants governing the chemical and toxicological profile of the Ammer River. Organic micropollutants were uncovered to be discharged from different input sources, with the wastewater treatment plant as the dominant input source of pharmaceuticals, industrial and household chemicals and biocides. In an 8 km long section of the Ammer, downstream of the wastewater treatment plant, compound concentrations and biological effects decreased and dilution and loss processes were uncovered. The tributaries in that river section contributed little to the overall load of compounds and mixture effects in the Ammer due to their relatively low discharge, but showed a different chemical and toxicological profile.

During a storm event, the chemical and toxicological profile of the Ammer significantly changed. The numbers, concentrations and fluxes of organic micropollutants and associated effects were generally higher and suspended particulate matter turned out to be an important transport vector for effects and for hydrophobic target compounds. Organic micropollutants discharged from agricultural and urban areas, combined sewer overflow and the wastewater treatment plant. Thus, changing hydrological conditions may trigger the occurrence and the increase of organic micropollutant concentrations, mass fluxes, associated effects and the importance of particle-facilitated transport in rivers, which can pose a risk to the aquatic environment and are, at present, not considered in risk assessment and management options. Although both approaches, chemical analysis and *in-vitro* bioassays, are complementary as they cover different compounds and compound classes, they showed a similar pollution profile of the Ammer.

In this thesis I showed that the chemical and toxicological profile of a river is highly variable in time and space, specifically driven by varying hydrological conditions that act to partition input sources of organic micropollutants, and thus their individual mass-flux contribution. It is therefore important for the investigation of the fate of organic micropollutants in rivers, of factors driving in-stream processes (e.g., degradation, sorption) and for future regulatory monitoring efforts to consider and properly capture these spatiotemporal variations.

Zusammenfassung

Die Anzahl anthropogener organischer Chemikalien nimmt kontinuierlich zu und damit auch ihre reichhaltigen Anwendungen in, beispielsweise, industriellen und häuslichen Anwendungen, der Landwirtschaft und medizinischen Gebrauch. Viele dieser Verbindungen sind persistent (e.g., Flammschutzmittel, Beschichtungen), bioaktiv (e.g., Pestizide, Arzneimittel) oder bioakkumulierend (e.g., polyzyklische aromatische Kohlenwasserstoffe, per- und polyfluorierte Alkylverbindungen) und stellen somit ein Risiko für die Umwelt mit potentiell weitreichenden Folgen dar. Diese organischen Mikroschadstoffe können über verschieden Quellen in die Umwelt eingetragen werden, wie beispielsweise dem Abfluss von landwirtschaftlichen, urbanen und industriellen Oberflächen, Kläranlagen, Überlauf von Regenrückhaltebecken oder werden gar absichtlich in der Umwelt verbreitet, wie im Falle von Pestiziden. Diese Quellen können einen punktuellen oder eher diffusen Eintrag aufweisen und sind oftmals nicht einfach auszumachen und zu charakterisieren. Flüsse integrieren punktuelle und diffuse Eintragsquellen in ihrem gesamten Einzugsgebiet und beherbergen darüber hinaus wichtige Transport- und Transformationsprozesse. Ziel der vorliegenden Arbeit war es daher, ein detailliertes Verständnis des Auftretens und der (toxischen) Auswirkungen organischer Mikroverunreinigungen in Flüssen zu erlangen, das zur Vorhersage ihres Schicksals in der Umwelt erforderlich ist.

In dieser Doktorarbeit untersuchte ich das chemische und toxikologische Profil der Ammer in Süd-Deutschland, unter verschiedenen hydrologischen Bedingungen. Die Ammer ist charakteristisch für kleine Flüsse in Karstsystemen dicht besiedelter Länder der gemäßigten Klimazone. In Feldstudien habe ich mit einer Kombination aus chemischer Analytik (Flüssigchromatographie mit Massenspektrometrie-Kopplung) und umweltrelevanten *in-vitro* Biotests, Eintragsquellen und das Schicksal organischer Mikroschadstoffe auf Einzugsgebietsebene identifiziert und charakterisiert. Um verschiedene Eintragsquellen und Prozesse im Fluss kenntlich zu machen wurden organischer Indikatorverbindungen, basierend auf Anwendung, Umweltrelevanz, Auftreten in ähnlichen Studien und Abbaubarkeit, ausgewählt. Die angewandte, bioanalytische Test-Batterie wurde ferner durch die Entwicklung eines *in-vitro* Biotests, welcher zwei verschiedene Wirkmechanismen der Mitochondrientoxizität in Umweltproben zu messen vermag, ergänzt.

Unter Trockenwetter-Bedingungen identifizierte ich mittels chemischer Analytik und *in-vitro* Biotests eine Kläranlage als die Haupteintragsquelle organsicher Mikroschadstoffe, welche das chemische und toxikologische Profil der Ammer dominierte. Unterschiedliche Eintragsquellen organischer Mikroschadstoffe wurden aufgedeckt, dominiert von der Kläranlage als Haupteintragsquelle von Arzneimitteln, Bioziden und Chemikalien aus industriellen und häuslichen Anwendungen. In einem 8 km langem Teilstück der Ammer, unterhalb der Kläranlage, sanken die Konzentrationen der detektierten Verbindungen und die biologischen Effekte und es wurden Verdünnungs- und Verlustprozesse enthüllt. Aufgrund ihres geringen

Abflusses erbrachten die Zuflüsse nur einen geringen Beitrag zum Gesamtfluss der detektierten Verbindungen und der Mischungseffekte. Darüber hinaus zeigten sie ein unterschiedliches chemisches und toxikologisches Profil.

Während eines Regenereignisses zeigte die Ammer ein gänzlich anderes chemisches und toxikologisches Profil. Die Anzahl, Konzentrationen und Massenflüsse organischer Mikroschadstoffe und damit einhergehender Effekte waren wesentlich höher als unter Trockenwetter-Bedingungen. Suspendierte Partikel stellten sich während eines Regenereignisses als wichtige Transportvektoren, von Effekten und von hydrophoben Zielsubstanzen heraus. Der Eintrag organischer Mikroschadstoffe konnte dabei auf Regenrückhaltebeckenüberlauf, landwirtschaftliche und urbane Gebieten und die Kläranlage zurückgeführt werden. Demzufolge können Änderungen der hydrologischen Bedingungen das Auftreten und eine Erhöhung der Schadstoffkonzentrationen, -massenflüsse und damit einhergehender Effekte und eine steigende Bedeutung des Partikel-vermittelten Transports hervorrufen, welche ein Risiko für die aquatische Umwelt darstellen können und in der gegenwärtigen Risikobewertung und -bewältigung nicht berücksichtigt werden. Obwohl beide Ansätze, chemische Analytik und Biotests, unterschiedliche Verbindungen und Verbindungsklassen abdecken zeigten sie ein ähnliches Belastungsprofil der Ammer.

In dieser Arbeit habe ich gezeigt, dass das chemische und toxikologische Profil eines Flusses zeitlich und räumlich sehr unterschiedlich ist, insbesondere aufgrund unterschiedlicher hydrologischer Bedingungen, die die Eingangsquellen organischer Mikroschadstoffe und damit ihren individuellen Massenflussbeitrag gewichten. Es ist daher wichtig für die Untersuchung des Schicksals organischer Mikroschadstoffe in Flüssen, von Faktoren, die In-Stream-Prozesse antreiben (z. B. Abbau, Sorption), und für zukünftige regulatorische Überwachungsbemühungen, diese räumlich-zeitlichen Variationen zu berücksichtigen und richtig zu erfassen.

Danksagung

Mein erster und ganz besonderer Dank gilt meinem Doktorvater Prof. Dr. Christian Zwiener, der mir die Promotion in diesem spannenden Thema ermöglichte. Ebenfalls möchte ich mich ganz besonders bei meiner Doktormutter Prof. Dr. Beate Escher bedanken. Ich hatte wirklich ganz besonderes Glück diese Arbeit unter der Betreuung zweier Wissenschaftler anzufertigen, welche erfahrene und etablierte Experten ihres jeweiligen Faches sind. Vielen Dank für die stetige Unterstützung, das Einbringen fachlicher Expertise, das mir entgegengebrachte Vertrauen und die stets erquickenden Gespräche. Ein ganz besonderer Dank gilt ebenfalls meinem ehemaligen Mentor und Lehrer Prof. Dr. Andreas Schäffer für sein Interesse an dieser Arbeit und seine Funktion als Berichterstatter meiner Dissertation.

Ebenfalls möchte ich mich für das eingebrachte Fachwissen meiner Projektpartner Dr. Martina Werneburg, Dr. Marc Schwientek, M.Sc. Clarissa Glaser und besonders Prof. Dr. Christiane Zarfl, für ihr Interesse an dieser Arbeit und ihre Funktion als Prüferin meiner Disputation, bedanken.

Ein besonderer Dank gilt auch der Deutschen Forschungsgemeinschaft DFG und allen Mitgliedern des Sonderforschungsbereichs CAMPOS (SFB 1253), die diese Arbeit überhaupt erst möglich machten.

Einen herzlichen Dank möchte ich auch meinen Freunden, Kolleginnen und Kollegen der Arbeitsgruppe Umweltanalytik an der Universität Tübingen richten. Besonders danken möchte ich dabei M.Sc. Boris Bugsel, Stephanie Nowak und Dr. Markus Schmitt für ihre Hilfe im Labor, an den Massenspektrometern und die hilfreichen fachlichen und erbaulichen Gespräche. Auch M.Sc. Maria König, Dr. Rita Schlichting und Jenny John vom UFZ-Leipzig möchte ich für ihre Unterstützung im Labor danken.

Darüber hinaus möchte ich Dr. Adrian Mellage, Dr. Thomas Wendel, M.Sc. Klaus Röhler, M.Sc. Simon Martin, M.Sc. Stefan Klingler, Sara Cafisso und M.Sc. Johanna Schlögl, für das sehr angenehme Arbeitsklima und die ein oder andere Portion Spätzle oder Runde Bier, meinen Dank aussprechen.

Nicht zuletzt möchte ich mich von ganzem Herzen bei Dr. Anne-Katrin Müller für die fachlichen Gespräche als auch die persönliche Unterstützung bedanken.

Meinen Eltern, meinem Bruder und meinen Großeltern, die mich dorthin gebracht haben wo ich heute bin, widme ich einen ganz besonderen Dank.

Petri Heil!

Contents

1. Introduction

1.1. Organic micropollutants in the aquatic environment

One of the major problems humanity is facing at present and in the future is the availability of clean and safe drinking water (Connor 2015). In August 2020 more than 22000 unique substances were registered under the European legislation REACH (Registration, Evaluation, Authorisation and Restriction of Chemicals) by the European Chemicals Agency for use on the European market (ECHA 2020) and more than 160 million compounds were registered in the Chemical Abstract Service (CAS 2020). A substantial portion of anthropogenic compounds is constantly, intentionally or unintentionally, emitted into the environment. In industrialized countries most anthropogenic compounds for industrial and household applications, such as protection and cleaning agents, pharmaceuticals and personal care products, make their way into municipal sewerage systems. To the detriment of our environment, many of the aforementioned compounds are designed to be persistent in order to meet their requirements. That means, for instance, flame retardants and protection agents are required to have a long life-expectancy (Li et al. 2012; Roosens et al. 2010). Also pharmaceuticals can be poorly degradable as they need to reach their target site before being metabolized (Glassmeyer et al. 2008). Such anthropogenic compounds, that are poorly degradable in wastewater treatment, may thus enter rivers via wastewater treatment effluents (point source). Veterinary drugs can enter the environment by dispersion as manure (diffuse source), (Sarmah et al. 2006). In addition, direct runoff from urban and industrial areas or wastewater bypassing municipal sewerage systems constitute important diffuse and point pollutant sources worldwide, owing to missing infrastructure or combined sewer overflow (CSO), (Shao et al. 2006; Singh et al. 2004). Other anthropogenic compounds such as pesticides are directly dispersed into the environment.

Once in rivers, these organic micropollutants partition from water to the environmental compartments air, water, biota and suspended materials (**Figure 1**). Their behavior and distribution is determined by their (1) compound-specific physicochemical properties (polarity, water solubility, lipid solubility, adsorption capacity, vapor pressure, degradability and molecular structure), (2) the system properties of the receiving environment (pH, temperature, flow rates, redox potential, salinity, suspended materials, solar radiation) and their (3) input characteristics and quantities (Schwarzenbach et al. 2016). Hence, the different partitioning behavior of

these compounds leads to different transport pathways in environmental compartments. Organic micropollutants that tend to adsorb onto mineral surfaces or to organic carbon of soil particles, in, for instance, agricultural areas, can be introduced into rivers by erosion (Giménez et al. 2012; Liu 2019). Or if adsorbed to sediment particles in rivers, they may be released and become bioavailable during sediment disturbance events, such as storm events and floods (Eggleton and Thomas 2004). Furthermore, micropollutants associated to sewage sludge can enter rivers in cases of CSO (Eganhouse and Sherblom 2001). Therefore, suspended particulate matter (SPM) can act as an important vector of micropollutant transport in rivers (Aminot et al. 2018; Boulard et al. 2019; da Silva et al. 2011).

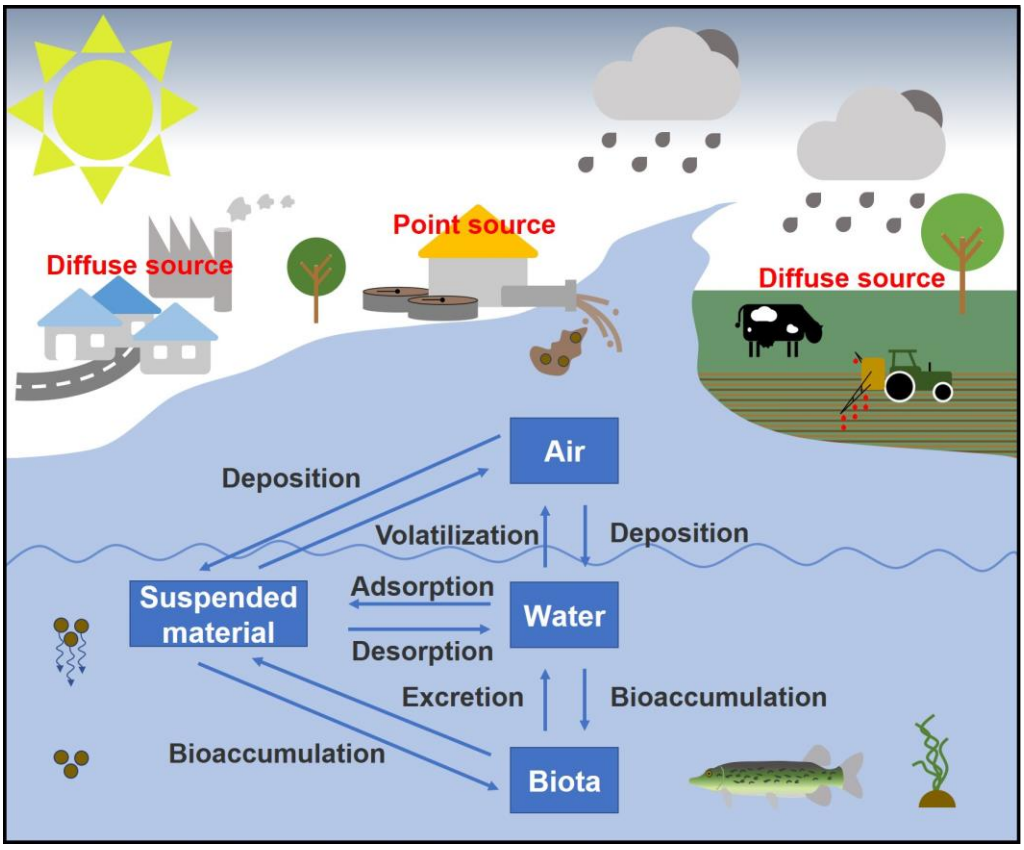

Figure 1: Conceptual graph of different input sources, their characteristics and the distribution of organic micropollutants between the compartments air, water, biota and suspended materials in rivers.

As a consequence, organic micropollutants are regularly detected in surface waters all around the globe (Bradley et al. 2020; Casado et al. 2019; Heeb et al. 2012; Loos et al. 2009) and (may) pose a risk to the aquatic environment (Fent 2013). Their input sources into rivers, be it point sources like treated or untreated wastewaters or diffuse sources such as runoff and leachate from agricultural and urban areas, are often challenging to track (Schwarzenbach et al. 2010). Their vast number and great variety of physicochemical properties is the major challenge in assessing their occurrence and fate in the environment (Schwarzenbach et al. 2016). Thus, to obtain a comprehensive picture of the pollution profile in surface waters, sophisticated screening approaches and methods are required that cover a broad range of organic micropollutants.

1.2. Environmental analysis of organic micropollutants

1.2.1. Chemical analysis

Liquid chromatography coupled to mass spectrometry (LC-MS) is a commonly used analytical approach to qualify and quantify pollutants in environmental samples. A simplified and conceptual illustration of LC-MS is given in **Figure 2**. Sample analytes in a mobile phase (eluent) are chromatographically separated based on their interaction to a stationary phase (column). Before entering the mass spectrometer, they pass the ion source in which they become transferred in the gaseous phase in an ionized form. Drawn into the mass spectrometer by electrostatic attraction, ions are further separated based on their mass to charge ratio before being detected. In high resolution mass spectrometry (HRMS) different ions with same nominal masses can be distinguished allowing the identification of their atomic compositions.

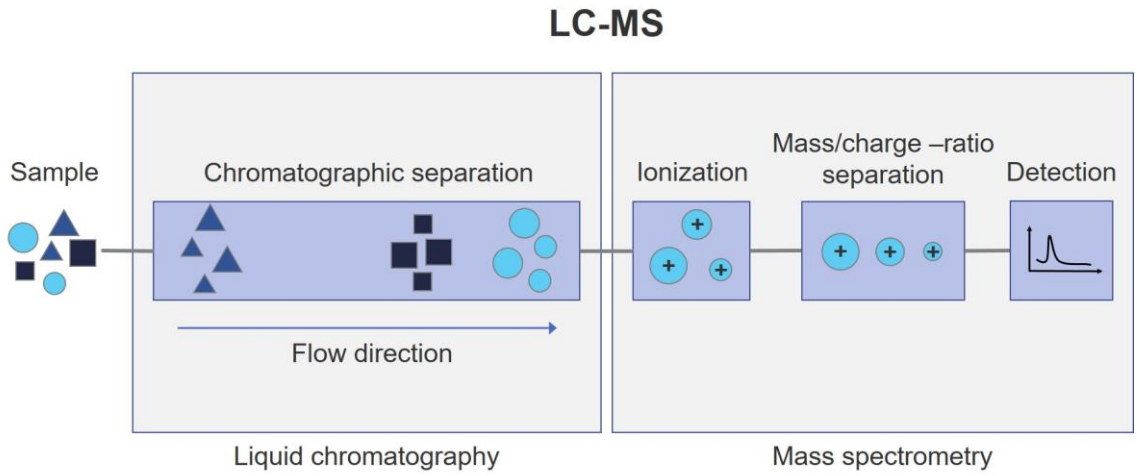

Figure 2: Conceptual illustration of liquid chromatography coupled to mass spectrometry (LC-MS). First, analytes in a sample are chromatographically separated. In a second step, analytes are transferred in the gaseous phase in an ionized form, separated by their mass to charge ratio and subsequently detected.

A powerful approach to quantify analytes in a sample and in the lower ng L^{-1} range is the target screening, using for instance an LC coupled to a triple quadrupole (QQQ) mass spectrometer by electrospray ionization (ESI), which requires a piori analyte selection and, ideally, analytical standards for identity confirmation. A high resolution time-of-flight (TOF) mass spectrometer can overcome this limitation with high mass accuracy (<3 ppm) and high resolving power (>20000 at m/z ≈ 300) in full scan mode.

With information on the exact mass of the suspect (suspect screening) or without any information prior to the measurement (non-target screening) analytes can be further verified by the aid of analytical standard solutions, chromatographic retention time, fragmentation and isotope patterns (Krauss et al. 2010; Moschet et al. 2013b; Zedda and Zwiener 2012). These mass spectrometric applications are among the draught horses of environmental analysis (Casado et al. 2019; Ccanccapa-Cartagena et al. 2019; Lege et al. 2019; Ruff et al. 2015; Tisler and Zwiener 2018).

1.2.2. Bioanalytical tools

Although LC-MS yields valuable information on analyte identity, quantity and to some extend physicochemical properties, the data acquisition does not provide information on the toxicity of mixtures of chemicals in a sample. For the latter, effect-based screening tools come into play, generating an integrated signal of all compounds affecting the same endpoint. This is very useful if pollution in a particular environmental compartment is suspected but the triggers are unknown or may not be analyzed, as it can give a hint on whether further action is needed or not. The principle of so-called bioassay relies on the exposure of a biological organism against a compound or a compound mixture that generates a measurable lethal response, also referred to as endpoints. Endpoints can be, for instance, algal growth inhibition, immobilization of daphnids (usually *Daphnia magna*) (OECD 2004) or impaired zebrafish embryo development (Legler et al. 2000).

High throughput *in-vitro* bioassays are a cost-efficient alternative to animal testing, they cover toxic transformation products and mixture effects, such as concentration addition, synergism or antagonism by combined exposure of organic micropollutants in environmental samples (Altenburger et al. 2018; Pomati et al. 2006). Hence, providing insights into the mixture toxicity of a sample, and allowing to estimate the potential associated risk of exposure to compound mixtures by using model-based extrapolation to whole organisms or communities (Brinkmann et al. 2014; Rostami-Hodjegan and Tucker 2007). Thus, *in-vitro* bioassays have become an attractive alternative to complement chemical analysis in risk assessment (Brack et al. 2018). *In-vitro* bioassays mostly use reporter gene cell lines indicative of a specific mode of action (MoA). These MoAs can be adaptive stress response (Welch 1993), binding to hormone receptor or receptors involved in metabolic pathways, such as the

peroxisome proliferator-activated receptor (Neale et al. 2017a). Activation of the associated nuclear receptors or transcription factors initiate the expression of a reporter protein, for instance, a fluorescent protein or the enzyme luciferase, yielding a measurable signal (upper half of **Figure 3**). This measurable signal enables the derivation of a concentration-response curve and finally an effect concentration (EC). ECs can be transferred into effect units (EU, reciprocal of the effect concentration), for an easier understanding as high EUs relate to high effects. Aside from the analytes acting according to a specific MoA, every compound in a sample contributes in a specific or unspecific way to cell viability (e.g., physico-chemical disruption of membranes or proteins, induction of mitochondrial disruption, apoptosis, oxidative stress or heat shock response) and therewith to cytotoxicity (lower half of **Figure 3**). Such cytotoxic interference can mask the specific effects, lead to false positive results and needs to be measured in parallel (Escher et al. 2020; Fay et al. 2018; Judson et al. 2016). The cytotoxic concentration (IC) can provide information on the overall chemical load of a sample. Effect concentrations derived from *in-vitro* bioassays with environmentally relevant MoAs can be converted into bioanalytical equivalent concentrations (BEQ_{bio}), describing the concentration of a well understood single compound exerting the same effect as measured in the sample.

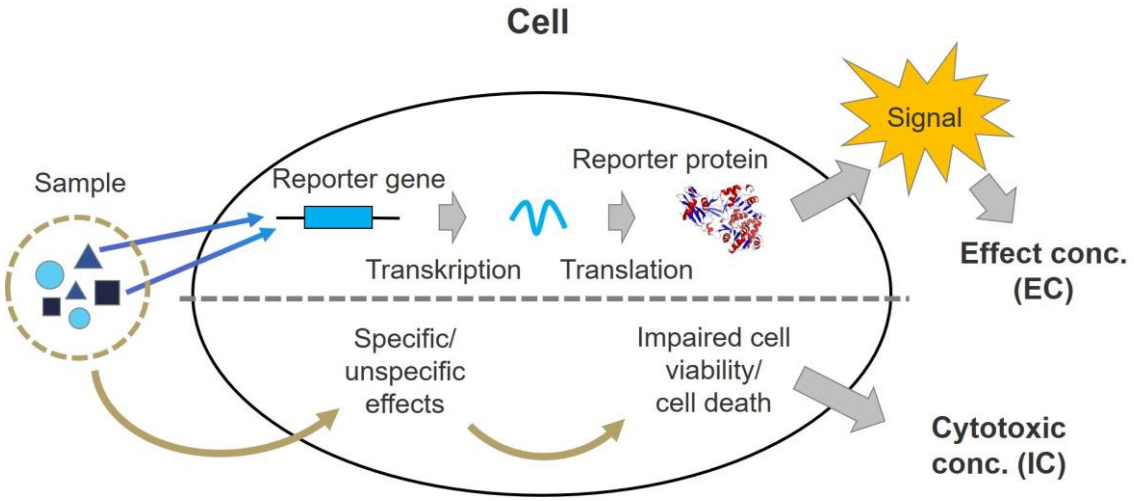

Figure 3: Conceptual illustration of a reporter gene bioassay. Reporter protein expression is initiated by receptor binding or induction of transcription factors by sample analytes acting according to the mode of action of the assay (illustrated in the upper half of the cell). The synthesized reporter protein mediates a measurable signal allowing derivation of effect concentrations (EC). All compounds in a sample specifically or unspecifically affect cell viability (illustrated in the lower half of the cell) that is measurable, for instance, as cell growth inhibition allowing derivation of cytotoxic concentrations (IC).

Not all important modes of action can be quantified by reporter gene assays, among them is the interference with energy metabolism in mitochondria. Mitochondrial toxicity is a commonly exerted MoA of pesticides, such as substituted phenols which act as uncouplers of oxidative phosphorylation (Terada 1990) like bromoxynil or the fungicide family of strobilurines target the inhibition of the fungal electron transport chain (Bartlett et al. 2002). Since oxidative phosphorylation in mitochondria is the main energy supplier in almost all eukaryotic organisms (Dykens et al. 1999; McBride et al. 2006), its disturbance can ultimately result in cell death and consequently high environmental relevance can be attributed. Pesticides are intentionally distributed in the environment in order to provoke adverse effects. Thus, one aim of this work was to develop a new *in-vitro* bioassay that can quantitatively detect pesticide classes that induce disruption of oxidative phosphorylation and other mitochondrial toxic compounds in environmental samples.

For mitochondrial toxicants oxidative phosphorylation offers essentially three main target sites: ATP-synthase, the inner mitochondrial membrane and the electron transport chain (**Figure 4**). *In-vitro* test systems such as the mitochondrial membrane potential assay (MPP) (Sakamuru et al. 2016) can reflect oxidative phosphorylation activity, however, they fail to yield more precise information on the disturbed target sites.

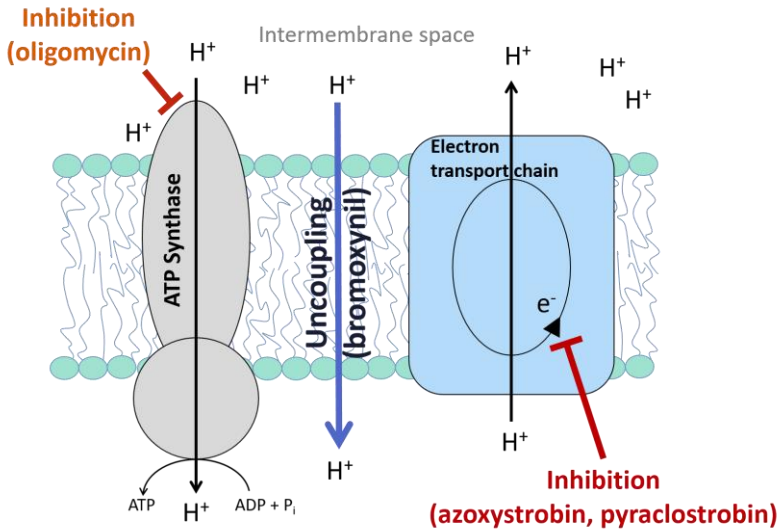

Figure 4: Conceptual graph of the main components, ATP-synthase, inner mitochondrial membrane and the electron transport chain, in oxidative phosphorylation. ATP-synthase may be inhibited by oligomycin, the membrane uncoupled by the herbicide bromoxynil and the electron transport chain inhibited by the fungicides azoxystrobin and pyraclostrobin. Figure adapted from Müller et al. (2019).

Monitoring the cellular oxygen consumption rate (OCR), however, allows further characterization of the toxicant's MoA as the OCR can increase, decrease or remain constant (Attene-Ramos et al. 2013).Therefore, I hypothesized that by measuring the oxygen consumption rate *in-vitro*, using the Agilent Seahorse XF^{e}96 Extracellular Flux Analyzer, different modes of action of micropollutants and micropollutant mixtures may be identified and quantified. This assay was developed and integrated in an existing test battery of reporter gene assays for water quality assessment.

1.2.3. Combining chemical analysis with *in-vitro* bioassays

As with every other analytical screening technique, both chemical analysis and *in-vitro* bioassays are limited to a certain analytical window, determined by sample preparation, chromatography or ionization technique and the bioavailability of the analytes. Their analytical windows may overlap and both approaches have to be considered as complementary, providing a more complete picture of the pollution profile of a sample.

A way to link chemical analysis with *in-vitro* bioassays is to model the expected cumulative effect based on the concentrations and effects of the individual compounds detected in a sample (König et al. 2017; Neale et al. 2015). The more the effect measured in a sample can be explained by the effect caused by the detected analytes the greater the overlap of the detection windows of chemical analysis and *in-vitro* bioassay. However, this presupposes the absence of mixture effects (Jonker et al. 2016), but as extensive experiments with more than 200 realistic environmental mixtures have shown, the assumption of additivity is justified (Neale et al. 2020). This type of modelling is also referred to as "Iceberg Modelling". Helpful tools to estimate poor quality of surface water are environmental quality standards (EQS) set by the Water framework Directive. These EQSs are concentration thresholds of individual compounds, that distinguish between acceptable and unacceptable surface water quality. Escher et al. (2018) proposed an algorithm that translates EQS into their corresponding effect-based trigger value (EBT). These EBTs represent effect threshold levels to differentiate between good and poor surface water quality. In this thesis, *in-vitro* bioassays were applied, primarily as bioanalytical tools to identify input sources and transport vectors of organic micropollutants and to trace changes of water quality.

The complementary combination of chemical analysis and *in-vitro* bioassays has previously been used for example to assess surface water quality of large streams (Neale et al. 2015), wastewaters and their impact on river water quality (Farré and Barceló 2003; König et al. 2017; Neale et al. 2017b), to track pesticides in agricultural areas (Lundqvist et al. 2019b) and waste- and drinking water treatment (Jia et al. 2015; Lundqvist et al. 2019a; Neale et al. 2012; Nivala et al. 2018).

1.3. Indicator chemicals and -effects

A very effective and commonly utilized approach in environmental analysis is to trace organic indicator chemicals, not only to characterize input sources of organic micropollutants (Tran et al. 2019), but also water treatment efficiency (Jin and Peldszus 2012), attenuation processes (Guillet et al. 2019; Jaeger et al. 2019; Jobelius et al. 2010) and potable reuse (Salgot et al. 2006). Depending on the study purpose these indicator chemicals must meet certain criteria, e.g., partitioning properties, degradability, emission characteristics and local regulatory frameworks (Jekel et al. 2015). The indicator chemicals used within the present work were used to represent either input sources or in-stream processes.

In order to reflect inputs from wastewater treatment plants into rivers (point source), an indicator chemical should stem from applications that finally lead it into the municipal sewerage systems. It should be poorly degradable during wastewater treatment and be continuously emitted by the WWTP effluent into the receiving river (Clara et al. 2004). These requirements are often met by pharmaceuticals (e.g., carbamazepine, hydrochlorothiazide, sulfamethoxazole).

Emissions from agricultural areas (diffuse source) may be reflected by pesticides used for widely cultivated crops (e.g., bentazone, azoxystrobin). However, the application of pesticides in agriculture varies seasonally and regionally (Vryzas et al. 2009). This together with the additional use of many pesticides as biocides in urban areas, may limit their representativeness and hamper input source identification.

Micropollutant input into rivers by urban run-off may be reflected by, for instance, biocides used in building materials and facades to prevent root penetration and algal growth (e.g., mecoprop, terbutryn) or flame retardants and plasticizers from rubber and plastic materials (e.g., tris(1-chloro-2-propyl) phosphate, triphenylphosphate), (Bucheli et al. 1998; Burant et al. 2018; Burkhardt et al. 2011).

To reflect in-stream processes (e.g., photolysis, biodegradation) an organic indicator chemicals should exhibit a defined reactivity towards the considered process (Jekel et al. 2015).

Along with organic indicator chemicals, *in-vitro* bioassays allow to assess input sources of organic micropollutants, e.g., hormonal effects in treated wastewater or manure (Lorenzen et al. 2004; Peterson et al. 2000).

1.4. Study site

The Ammer River in Southwest Germany was chosen as the study site for this work. The Ammer receives organic micropollutants from various input sources, spanning both point and diffuse contributions, such as WWTPs, agricultural, forestry and urban areas. In addition, it is representative for small rivers in karstic systems and in densely populated areas of temperate climate. Covering an area of approximately 238 km² the Ammer catchment is embedded in the upper Neckar River Basin, between the Swabian Alb in the Southeast and the Black Forest in the West. Under base flow conditions the river is mainly fed by gypsum and limestone aquifers and treated wastewater from one WWTP (WWTP1) upstream of Altingen with 80,000 person equivalents and a second smaller one (WWTP2) between Hailfingen and Tailfingen with 9,000 person equivalents, see **Figure 5**. The catchment upstream of the gauge in Pfäffingen, is dominated by agricultural (71%), urban (17%) and forestry (12%) land use (Grathwohl et al. 2013). The average annual flow is 0.44 $m^3 s^{-1}$ at the gauge in Pfäffingen (orange house in **Figure 5**). In this work a Lagrangian sampling was performed by following the same water parcel as it flows downstream (Antweiler et al. 2014).

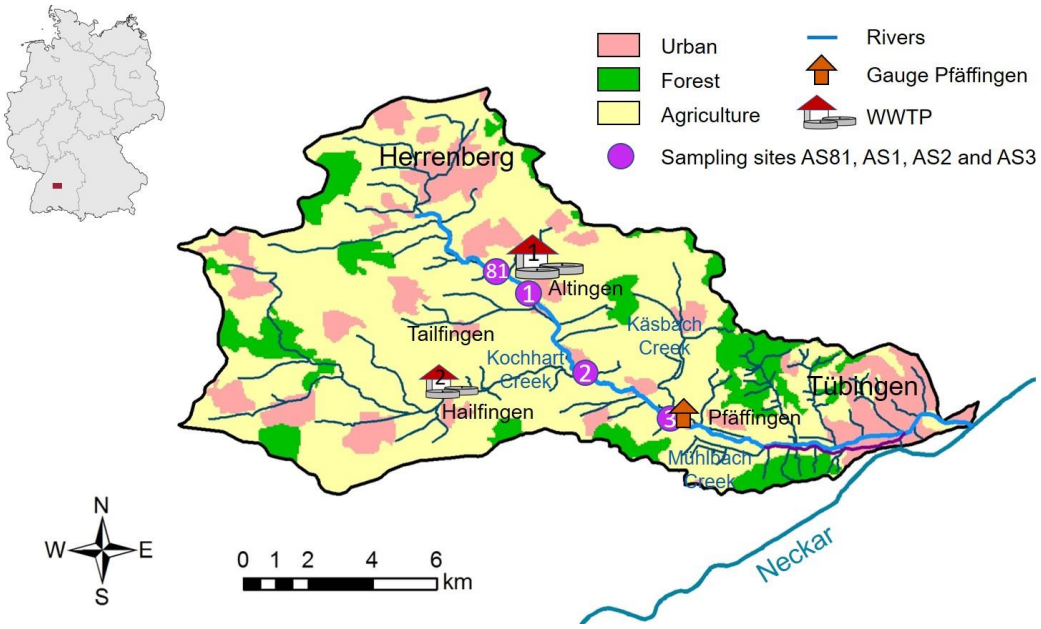

Figure 5: Ammer River catchment, in Southwestern Germany, its land use, the gauge in Pfäffingen and the two wastewater treatment plants, WWTP1 and WWTP2. The Ammer main stem from source to mouth is highlighted in light blue and bifurcates into the Ammer Canal (purple line) in Tübingen. Purple dots indicate sites where automated sampling was performed. Figure adapted from Müller et al. (2018).

1.5. Applied analytical methods

To assess the chemical profile of the Ammer River, target and suspect screening was applied on a set of compounds from different compound classes, such as herbicides, fungicides, insecticides, pharmaceuticals and industrial and household chemicals (Table S4 of *Publication 4*). These compounds were selected based on their application, occurrence in previous studies (Loos et al. 2009; Moschet et al. 2014) and environmental relevance. They may serve as indicator chemicals for different input sources and represent different degrees of degradability under environmental conditions. This set of compounds was continuously increased throughout the three field studies performed in this work (**Figure 6**). Compounds detected by suspect screening during the first field study were later included in the target screening.

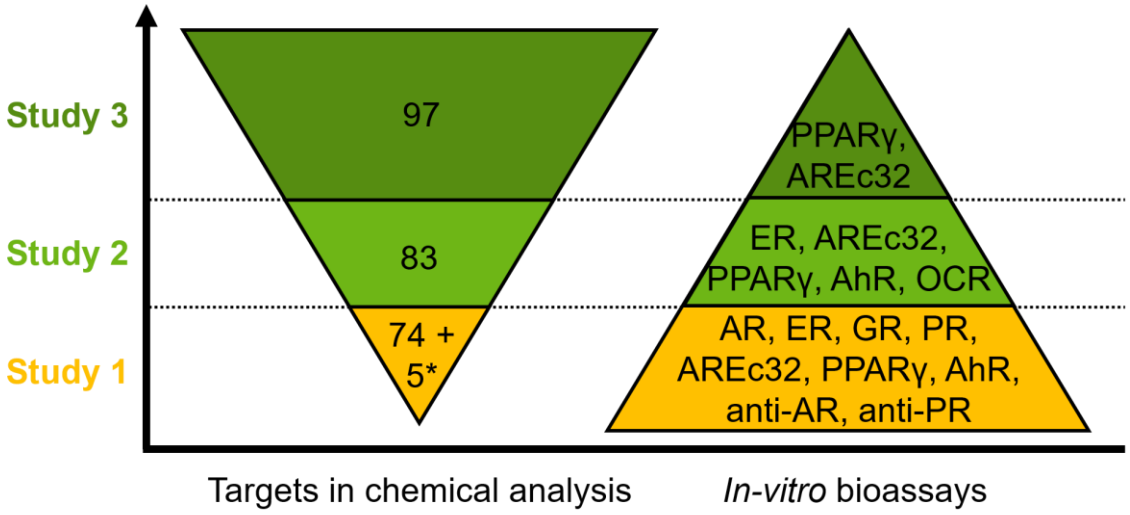

Figure 6: Conceptual graph of the number of screened targets (left pyramid, *suspects) in chemical analysis and of the number of applied *in-vitro* bioassays (right pyramid), during the three field studies.

To get an inventory of active mixtures present in the Ammer River a test battery of seven *in-vitro* bioassays with environmentally relevant MoAs, through different toxicity pathways, was applied. The MoAs screened for covered aryl hydrocarbon receptor induction (AhR-CALUX) and peroxisome proliferator activated receptor activity (PPARγ-Bla), both involved in cell metabolism (Brennan et al. 2015; Neale et al. 2017a). Cellular stress response was examined by oxidative stress response (AREc32), (Escher et al. 2012; Escher et al. 2013; Welch 1993). Binding to hormone

receptors was represented by examining estrogenicity (ER-Bla), glucocorticogenic activity (GR-Bla), androgenicity (AR-Bla) and progestagenic activity (PR-Bla), (Huang et al. 2011; Invitrogen 2007; 2010; König et al. 2017). To identify possible antagonists present in the samples that suppress the effect of an agonist, the assays for androgenicity and progestagenic activity were additionally performed in antagonistic mode (Anti AR-Bla and Anti PR-Bla). Over the three field studies performed in this work, this test battery was reduced to assays that were most relevant for the research question addressed and the test battery was further complemented by the Oxygen Consumption Rate assay (OCR) developed within this work.

1.6. Scientific context and relevance

Understanding of fate and behavior of organic micropollutants on the catchment scale is especially relevant in small rivers which are more prone to chemical pollution as a result of relatively smaller dilution ratios (Lorenz et al. 2017). Rivers integrate organic micropollutants within their entire catchments and host important transformation and transport processes. While prominent transformation processes and the fate of organic micropollutants have been comprehensively studied under controlled laboratory conditions, bench-scale findings are poorly transferable to natural systems. Results from laboratory studies do not adequately account for the environmental (dynamic) boundary conditions characteristic of surface water systems. Turbidity, average water depth, chemical composition of the river water and sediment, sorption and sedimentation, radiation, canopy shading, temperature and water exchange between hyporheic zone and stream channel, among others, may all in parallel determine the fate and effects of micropollutants in rivers. A deeper understanding of the distribution and behavior of organic micropollutants on the catchment scale is the underlying motivation for developing models capable of predicting future trends in water quality. Therefore, analytical methods and approaches are required that can appropriately identify and characterize input sources of organic micropollutants and trace changes of the water quality in rivers.

It is further important to improve and develop new effect-based screening tools to capture compound classes that may not be covered by chemical analysis alone and that allow to link chemical contamination with ecological effects in future works. So far effect-based screening tools are not implemented in a regulatory context and

governmental monitoring efforts but there are several recommendations concerning the revision of the Water Framework Directive in the European Union (Altenburger et al. 2019; Brack et al. 2019a; Brack et al. 2019b; Brack et al. 2016; Brack et al. 2017; Brack et al. 2018; EU 2013/39; van Gils et al. 2019).

1.7. Objectives and scope of the thesis

The objectives of the present work were to (1) improve and develop environmental screening techniques and (2) to investigate input sources, occurrence and fate of organic micropollutants in a small river catchment under different hydrological conditions. To this end, the following questions were addressed:

- Can the combination of the two complementary screening approaches chemical analysis and *in-vitro* bioassays be used to identify input sources of organic micropollutants and changes of the water quality in a river, on a catchment scale?
- Can mitochondrial toxicity serve as an additional and more specific endpoint for the screening of commonly used pesticide classes?
- What is the influence of diffuse input sources such as agricultural land use compared to point sources such as treated wastewater on the micropollutant and effect profile of a small river under dry (baseflow) weather conditions?
- What are the dynamics of micropollutant concentrations and mass fluxes and associated effects during a storm event?
- To what extend is suspended particulate matter involved in transport of micropollutants and micropollutant mixtures during a storm event?

The objectives of the present work were tackled during three field studies at the Ammer River:

Study 1: Grab samples from the main stem and tributaries of the Ammer River and one sample of the Goldersbach River, as reference, were collected and characterized by chemical analysis and a battery of seven environmentally relevant *in-vitro* bioassays. Selected target compounds and the average cytotoxicity were used to reflect in-stream processes (*Publication 1*).

Study 2: Lagrangian sampling of the Ammer and time-resolved sampling at three sampling sites (AS1, AS2 and AS3, see **Figure 5**) was performed in a 7.7 km long river section, downstream of WWTP1, plus grab samples of all tributaries in that river stretch. All samples were analyzed by chemical analysis and four *in-vitro* bioassays. (*Publication 3*). Moreover, four six-hour composite samples were collected upstream and downstream of the first reach (AS1 and AS2, see **Figure 5**) using large volume-solid phase extraction devices (LV-SPE). These samples were used to examine a new multi-endpoint mitochondrial toxicity assay developed within this thesis (*Publication 2*).

Study 3: Time resolved sampling of river water samples was performed at two sampling sites (AS81 and AS2, see **Figure 5**) during a storm event. Suspended particulate matter was separated from the water phase by filtration. Both phases were extracted and measured by chemical analysis and two *in-vitro* bioassays. This study served to elucidate the role of particulate matter for the fate and transport of organic micropollutants (*Publication 4*).

2. Summary of the three field studies

2.1. Analysis of organic micropollutants and associated effects on the catchment scale

As a first inventory of input sources and loss and dilution processes of organic micropollutants along the entire length of the Ammer River, the combination of chemical analysis and bioanalytical tools (*in-vitro* bioassays) was applied in a field study on July 2017 (**Study 1**, *Publication 1*). Samples were collected at nine sampling sites of the Ammer River, from source to mouth, at three sites from two Ammer tributaries and at one site of the Kleiner Goldersbach, in the Goldersbach catchment (**Figure 7**).

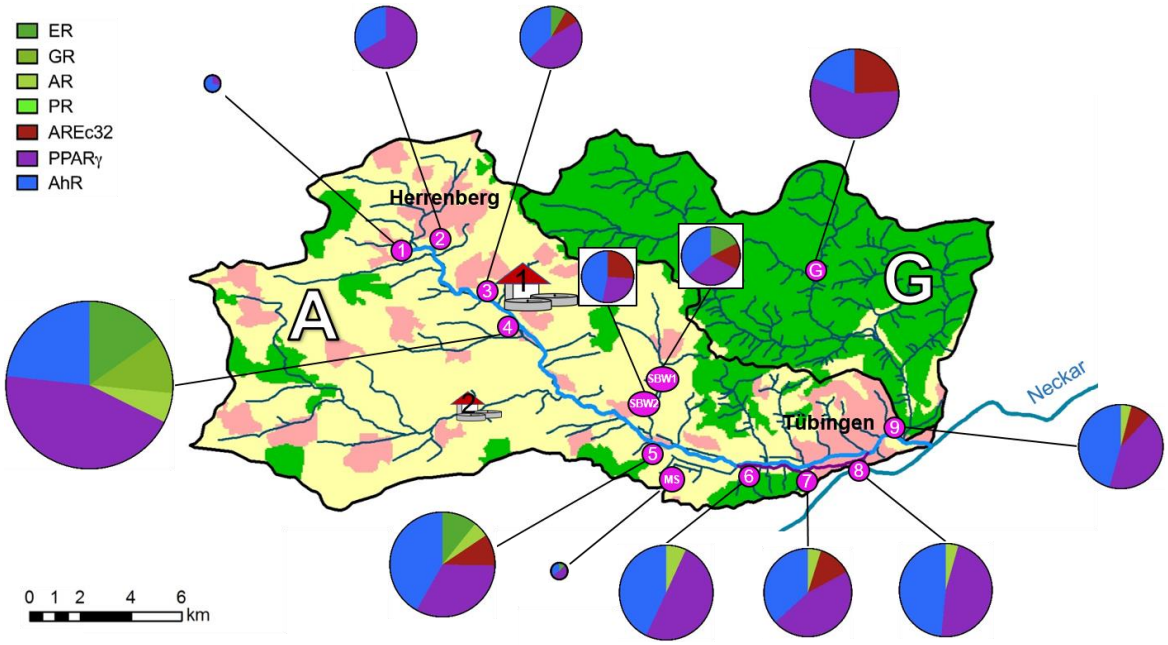

Figure 7: Sampling sites (purple dots) in the Ammer (A) and Goldersbach (G) catchment. Pie charts show the average cytotoxicity (chart size) and the toxicological patterns (chart colors) revealed by the *in-vitro* bioassays. Red and white houses represent the wastewater treatment plants located in the Ammer catchment. Figure adapted from Müller et al. (2018).

The sample extracts were screened for 79 suspect and target compounds from different compound classes (i.e., herbicides, fungicides, insecticides, pharmaceuticals and industrial and household chemicals, see Table S1 &2 of *Publication 1*). The sample extracts were also measured in the *in-vitro* bioassays battery described in chapter 1.5.

21 out of 79 suspect and target analytes were detected in the samples taken from the Ammer River and its tributaries Schönbrunnen and Mühlbach. The detected analytes were assigned to the concentration classes depicted in **Figure 8** and included 14 pharmaceuticals, 4 herbicides (bentazone, isoproturon, diuron and fluconazone) the insecticide thiamethoxam, the herbicide metabolite atrazine-desethyl and the pharmaceutical metabolite metoprolol acid.

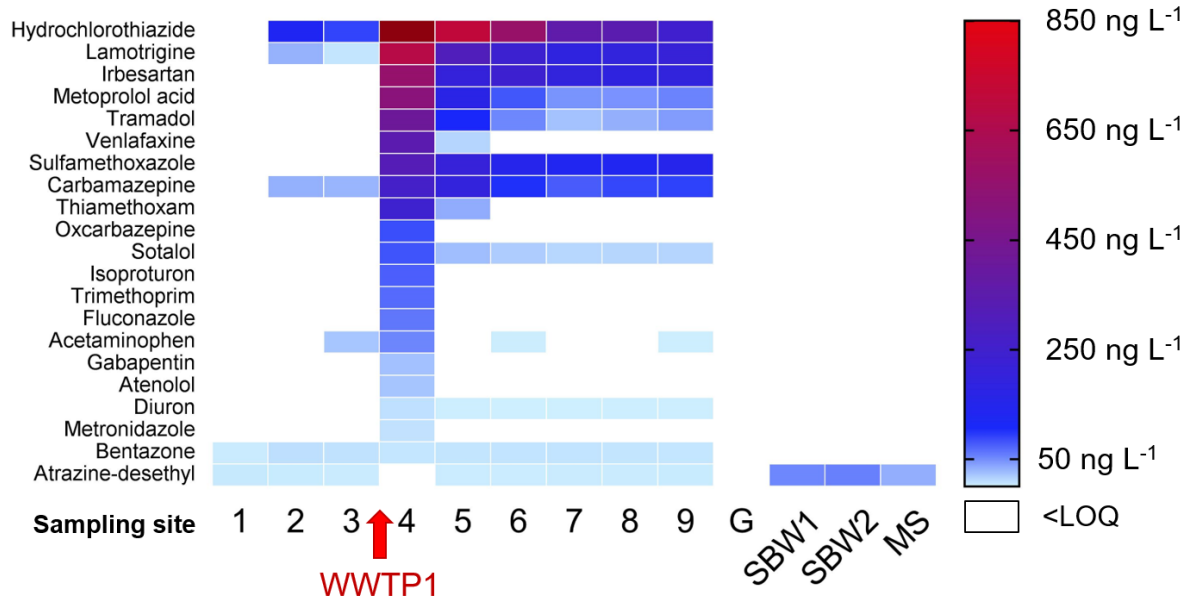

Figure 8: Detected suspect and target compounds in the extracts of the samples collected along the Ammer main stem (1 to 9), from the tributaries Schönbrunnen (SB) and Mühlbach (MS) and from the Kleiner Goldersbach (G) creek in the Goldersbach catchment. Concentration of hydrochlorothiazide at site 4 was 1.9 µg L^{-1}, colored in dark red as it was exceeding the concentration scale. LOQ = limit of quantification. Figure adapted from Müller et al. (2018).

For all compounds, except for bentazone and atrazine-desethyl, highest concentrations were measured at site 4 downstream of the effluent of WWTP1. For these compounds the WWTP1 effluent can be considered as the main input source, which is not surprising as had a contribution of 81% to the Ammer by the time of sampling. Upstream of WWTP1 bentazone and atrazine-desethyl and the pharmaceuticals acetaminophen, carbamazepine, hydrochlorothiazide and lamotrigine were detected in the Ammer and are indicative for further input sources. The four mentioned pharmaceuticals suggest the impact of wastewater, for instance, from leaking sewers or contaminated groundwater from the city of Herrenberg. The herbicide and the herbicide metabolite atrazine-desethyl were the only compounds that were also detected in the Ammer source and point towards contamination from

agricultural land use. In the samples taken from the Schönbrunnen, that is surrounded by agricultural areas, only atrazine-desethyl was detected suggesting the former use of the herbicide atrazine in this area. Between sampling site 6 and 9 some compounds indicated a rather conservative behavior, i.e. the pharmaceuticals carbamazepine and sulfamethoxazole as supported by previous literature (Clara et al. 2004; Martindale 1993; Zhou and Moore 1994). Therefore, both compounds were selected as indicator chemicals to reflect dilution. In comparison to carbamazepine and sulfamethoxazole, the pharmaceuticals sotalol and tramadol showed a faster concentration decreased between site 4 and 9. Since sotalol is moderately degradable by indirect photolysis, hydrolysis and biodegradation (Letzel 2008; Piram et al. 2008) and tramadol is moderately photolabile (Bergheim et al. 2012), both compounds indicate potential in-stream processes occurring between site 4 and 9.

For a better understanding of the toxicological profile of the Ammer River, measured effects and cytotoxicity were visualized by pie charts included into the map of the catchment (**Figure 7**). Each pie chart shows the effect profile (displayed by the EUs) and the average cytotoxicity (pie chart size) measured in the assays. Highest effects and cytotoxicity in all assays for agonistic endpoints, except for progestagenic activity (PR-Bla), were measured in the sample taken at site 4 (Table 3 of *Publication 1*), downstream of WWTP1 which dominated the toxicity pattern of the samples taken further downstream at sites 5 to 9. The toxicological profile of the Ammer changed after passing WWTP1 and showed additional hormonal effects measured in AR-Bla, ER-Bal and GR-Bla. This reveals the input of hormones by the effluent of WWTP1. The presence of hormones upstream of WWTP1 at site 3 was suggested by estrogenicity measured in ER-Bla, pointing towards additional input sources. This could be for example the potential impact by wastewater, as already suggested by the detected compounds, or animal manures used in agriculture that had been described as sources of hormones in literature (Lorenzen et al. 2004). Between site 4 and 5 the cytotoxicity and specific effects in all agonistic assays declined. In that stretch the course of the average cytotoxicity aligned between the concentration courses of the indicator chemicals carbamazepine and sotalol and can thus be mainly ascribed to dilution. From site 6 to 9 the concentrations of the indicator chemicals carbamazepine, sulfamethoxazole, tramadol and sotalol and the average cytotoxicity only slightly decreased and the effect pattern marginally changed. Thus, no substantial inputs of

additional water, organic micropollutants or degradation can be assumed in this river stretch.

The information provided by the chemical analysis and the *in-vitro* bioassays are complementary. For example, herbicides detected by the chemical analysis may not be specifically covered by the applied bioassays. On the other hand, no hormones detectable by the assays AR, ER, GR and PR and no hydrophobic compounds, such as polycyclic aromatic hydrocarbon, detectable in the AhR assay were included in the target and suspect list. For example, the sample from the Kleiner Goldersbach showed effects in AhR-Bla, AREc32 and PPARγ-Bla and cytotoxicity that was similar to the Ammer River, although none of the compounds screened for was detected. It becomes clear that it is important to combine different screening approaches to cover the broadest possible spectrum of different compounds and compound classes.

In the course of developing and improving analytical screening techniques for environmental pollutants, with focus on pesticides, a new *in-vitro* bioassay for mitochondrial toxicity, using the Seahorse XF^e96 Extracellular Flux Analyzer, was developed within this work (*Publication 2*). The method is based on measuring the oxygen consumption rate (OCR) in cells over time, whilst consecutively applying reference compounds for ATP-synthase inhibition (oligomycin), uncoupling of the mitochondrial membrane (2,4-dinitrophenol) and inhibition of the electron transport chain (mix of rotenone and antimycin A). In parallel measurements, one of the reference compounds was replaced by the sample or a negative control (buffer). The OCR decrease or increase, respectively, induced by the sample and normalized to the basal respiration in comparison to the reference compound and the negative control allows quantification and subsequent derivation of an effect concentration (EC). Hence, this approach allows one to use three individual experimental designs that target the MoAs ATP-synthase inhibition, uncoupling of the mitochondrial membrane and inhibition of the electron transport chain. All three experimental designs were validated with single chemicals of known mechanism and achieved Z-factors (Zhang et al. 1999) above 0.6 indicating precise and reproducible data acquisition.

One aspect of the following field study in 2018 (**Study 2)** was to collect water extracts to investigate the occurrence of mitochondrial toxic chemicals in the environment. Four six-hour composite samples at the two sampling sites AS1 and AS2 (**Figure 5**), located approximately 3 km apart, were generated using LV-SPE devices (*Publication 2*). The upstream sampling site AS1 was located around 500 m downstream of WWTP1 and

the sampling at AS2 (located in Reusten) was delayed for 133 minutes to account for the travel time of each water parcel (mean flow velocity = 0.39 m s^{-1}). In *Publication 2,* AS1 is denoted as SS1 and AS2 is denoted as SS2. The water LV-SPE extracts of AS1 and AS2 were then tested in the OCR assay in the experimental designs for uncoupling and electron transport chain inhibition (**Figure 9 A & B**).

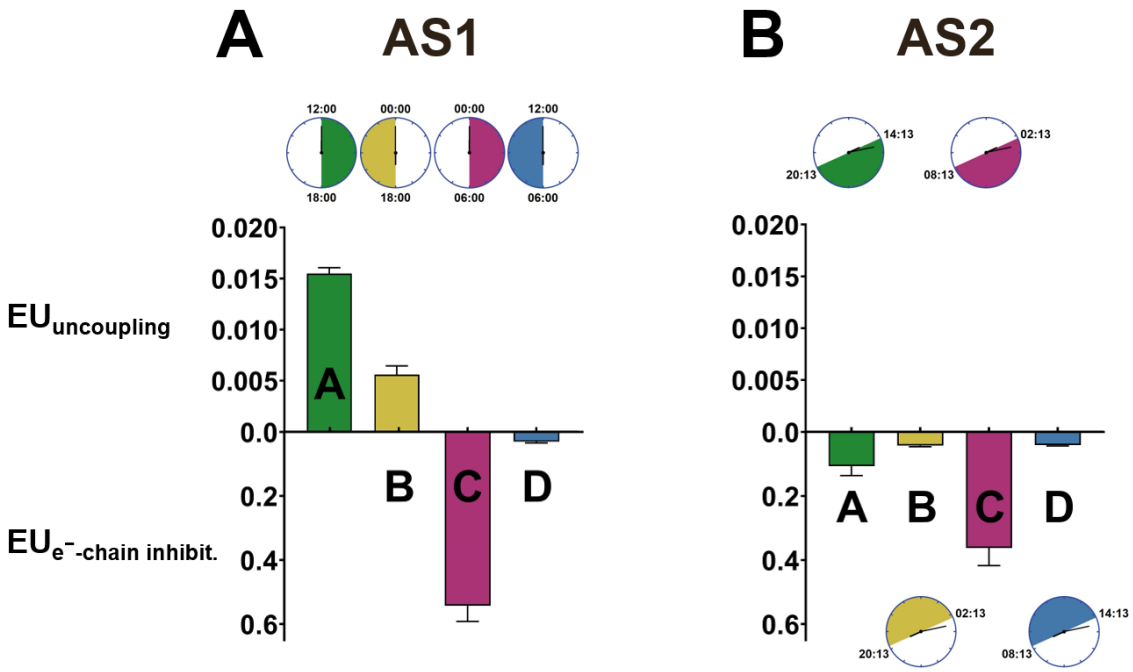

Figure 9: LV-SPE extracts of the four six hours composite samples A, B, C and D taken at AS1 (A) and AS2 (B) and measured in the experimental designs for uncoupling (upper half of each graph) and electron transport chain inhibition (lower half of each graph). The measured effects are expressed as effect units (EU, reciprocal of the derived effect concentration causing 10% effect EC_{10}), since high EUs relate to high effects.

In the first two composite samples from AS1 uncoupling activity was detected, whereas in all other composite samples electron transport chain inhibition was observed. Interestingly, at AS1 a transition from uncoupling activity to electron transport chain inhibition occurred within 24 hours. Another transition was observed from uncoupling activity at AS1 to electron transport chain inhibition at AS2 within the first 12 hours. It indicates degradation of uncouplers or additional input of electron transport chain inhibitors between both sampling sites. Importantly, the EC_{10} values of the samples AS1-C (1.84 ± 0.17 REF), AS2-A (9.34 ± 1.77 REF) and AS2-C (2.76 ± 0.42 REF) for electron transport chain inhibition were below an enrichment factor of 10 emphasizing

the environmental relevance of chemicals that disrupt mitochondrial functions and can thus damage a cell to death (Meyer et al. 2013).

Performed in the experimental designs for uncoupling and electron transport chain inhibition, binary mixture experiments with chemicals of known mechanism confirmed the environmental samples´ dominant MoAs. With the developed OCR assay uncoupling of the mitochondrial membrane and electron transport chain inhibition against a background of numerous nonspecifically acting compounds in environmental samples were quantified and changes of the water quality over time and space were revealed in the Ammer River.

In *Publication 2* it was highlighted that the developed OCR assay reaches its limits when it comes to mixtures of components with different MoAs or compounds with multiple target sites in the oxidative phosphorylation. Uncoupling was experimentally shown to be masked by electron transport chain inhibition. ATP-synthase inhibition would be masked by uncouplers, since an inhibited ATP-synthase would be bypassed by the uncoupler resulting in a decreasing electro chemical gradient and with it an upregulated oxygen consumption (Hatefi 1985). Electron transport chain inhibitors would mask ATP-synthase inhibition too, as in both cases the OCR decreases.

2.2. Characterization of emission sources

The highest spatial differences of micropollutant concentrations, effects and average cytotoxicity were observed between WWTP1 and the Pfäffingen gauge in **Study 1**. To characterize input sources of organic micropollutants and to assess the influence of tributaries on the chemical and toxicological profile of the Ammer, the following field study (**Study 2**) focused exclusively on that defined stretch (*Publication 3*). **Study 2** was performed in June 2018 after a longer dry weather period and under base flow conditions (743 L s^{-1} at the gauge in Pfäffingen). Between several meters upstream of the WWTP1 effluent and the gauge Pfäffingen, Lagrangian sampling was performed by collecting grab samples of the Ammer main stem upstream of each tributary inlet (**Figure 10**).

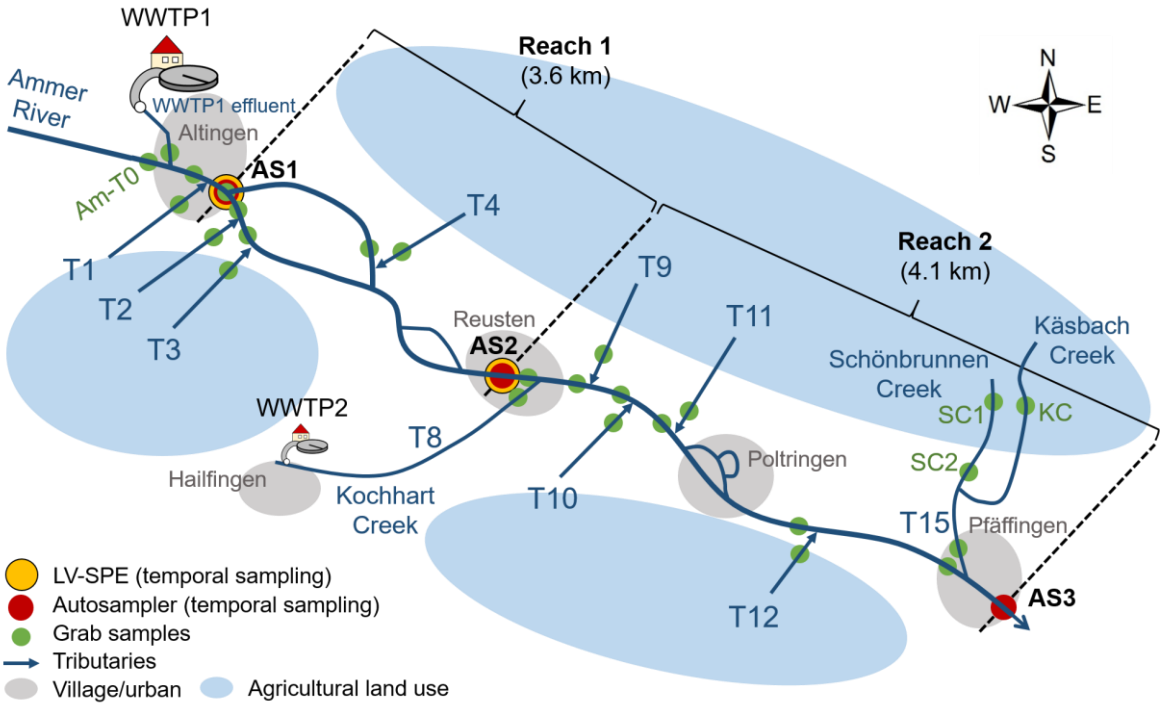

Figure 10: Conceptual illustration of the studied river section of the Ammer. Sampling sites are highlighted by green (grab samples), red (autosamplers) and yellow (LV-SPE) dots. Tributaries, except for the Kochhart Creek, Schönbrunnen Creek and Käsbach Creek, are highlighted by blue arrows. Grab samples from the tributaries are named after the tributary. Grab samples from the Ammer main stem are named according to the next downstream tributary. Figure adapted from Müller et al. (2020a).

Using autosamplers, hourly composite samples were collected at three sampling sites (AS1, AS2 and AS3), dividing the study site into two river reaches (reach 1: 3.6km,

reach 2: 4.1 km). Grab samples of each tributary were collected as well. The extracts of the water samples were analyzed by target screening for an extended number of 83 compounds, including the same compounds considered in the previous chapter (chapter 2.1.). The water extracts were moreover measured in four *in-vitro* bioassays covering the MoAs aryl hydrocarbon receptor induction (AhR-CALUX), peroxisome proliferator activated receptor activity (PPARγ-Bla), oxidative stress response (AREc32) and estrogenicity (ER-Bla).

In the Ammer River and its tributaries 28 of the target compounds (9 pesticides, 13 pharmaceuticals and 6 industrial and household chemicals [IHCs]) were detected and assigned to the concentration classes in **Figure 11 A**. A hierarchical cluster analysis revealed different compound profiles of the samples from the main stem downstream of WWTP1 and the samples from the tributaries. Upstream of WWTP1, at Am-T0, only the pharmaceutical carbamazepine the IHC 4&5-methylbenzotriazole and the herbicide bentazone were detected, similar to **Study 1**. In the WWTP1 effluent, which contributed to 51% to the Ammer discharge at AS1, 13 pharmaceuticals, 5 IHCs and 4 pesticides were detected (Table S5 of *Publication 3*). The concentrations of azoxystrobin, tris(2-butoxyethyl)phosphate (TBEP) and triphenylphosphate (TPP), detected in the WWTP1 effluent, had decreased below the limit of quantification by >70% in the Ammer main stem at the next downstream sampling site (Am-T1). Since biodegradation is not a reasonable removal process due to the travel time of about 5 minutes, sorption to organic carbon of sediment or SPM and sedimentation may be considerable attenuation processes given the relatively high octanol-water partitioning constants (5.1 for azoxystrobin, 4.3 for TBEP and 4.1 for TPP, predicted from ACD/Labs (2020)). 10 pharmaceuticals, 3 pesticides and 3 IHCs were transported throughout the studied river section as they still occurred at the most downstream sampling site Am-T15. In the tributary T8 (Kochhart Creek), which receives the effluent of WWTP2, 11 pharmaceuticals, 5 pesticides and 5 IHCs were detected, whereas the compound composition and concentrations were different to the WWTP1 effluent. The tributaries T9 and T10 appeared to be impacted by the WWTP2 effluent as well. Benzotriazole, carbamazepine, irbesartan and lamotrigine were found in T9 and 4&5-methylbenzotriazole, metoprolol and lamotrigine were found in T10, all of which are typical wastewater pollutants. A possible explanation could be that water from T8 percolated into the karstic groundwater and introduced T9 and T10 further downstream, as described in a previous study (Harreß 1973).

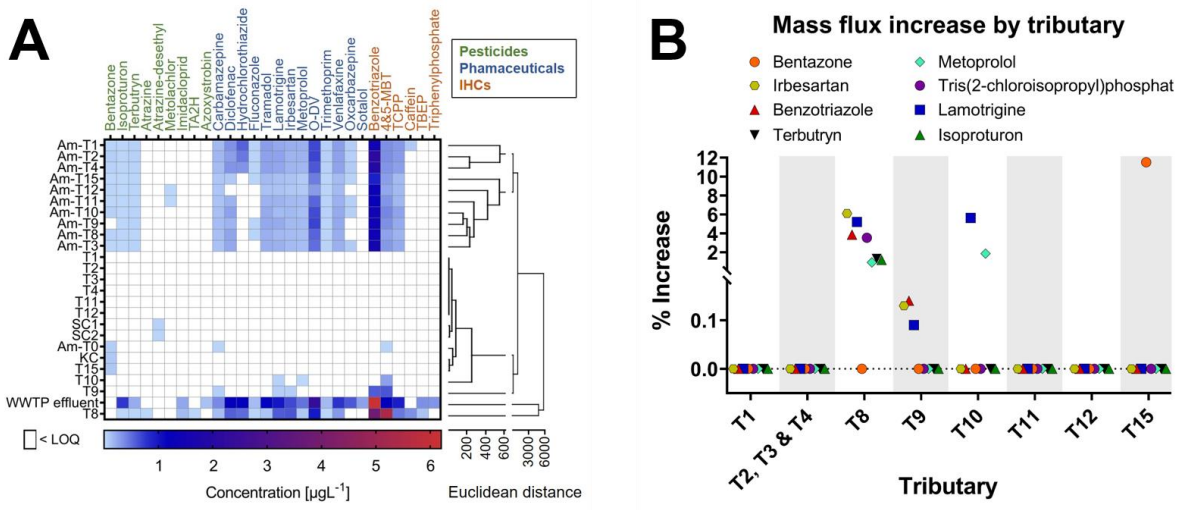

Figure 11: (A) Concentrations of target analytes detected in the grab samples. Similarities of the samples´ compound profiles, expressed as the Euclidean distance, are visualized in a hierarchical cluster analysis with the unweighted pair-group method using arithmetic averages. (B) Mass flux increases (ΔJ_i, increase in percentage) of selected compounds in the Ammer main stem caused by the respective tributary. Am-T = Ammer tributary; KC = Käsbach Creek; SC = Schönbrunnen Creek; 4&5-MTB = 4&5-methylbenzotriazole; O-DV = O-desmethylvenlafaxine; TA2H = terbuthylazine-2-hydroxy; TBEP = tris(2-butoxyethyl)phosphate; TCPP = tris(1-chloro-2-propyl)phosphate; LOQ = limit of quantification. Figure adapted from Müller et al. (2020a).

In the samples of T15 and its tributaries Schönbrunnen Creek and Käsbach Creek the herbicide bentazone and the degradation product atrazine-desethyl were detected, suggesting contamination from agricultural land use. None of the target compounds were detected in the tributaries T1, T2, T3, T4, T11 and T12. To assess the influence of the tributaries on the abundance of compounds in the main stem, the mass flux increase of selected compounds caused by the tributaries was calculated and depicted in **Figure 11 B**. These compounds represent different compound classes and applications and thus point (e.g., lamotrigine via wastewater) and diffuse (e.g., bentazone used in agriculture) input sources. The influence of the tributaries on the mass fluxes in the Ammer was generally insignificant (≤10%). Highest mass flux increase (10.4%) was caused by T15, which is surrounded by agricultural land use, for the herbicide bentazone. As bentazone was not detected in the WWTP1 effluent and the wastewater impacted T8, wastewater was no significant input pathway of this herbicide. A likely input pathway into the Ammer is the use of bentazone in agriculture.

The samples of the Ammer and its tributaries showed effects in the *in-vitro* bioassays for aryl hydrocarbon receptor induction (AhR-CALUX), peroxisome proliferator activated receptor activity (PPARγ-Bla), oxidative stress response (AREc32) and estrogenicity (ER-Bla), see **Figure 12 A**. The samples of the Ammer downstream of WWTP1 and the effects of the samples from the tributaries showed a different effect profile in a hierarchical cluster analysis, similar to the compound profiles. In the Ammer upstream of WWTP1 effects were measured in all applied assays, though relatively low (Table S6 of *Publication 3*). The WWTP1 effluent showed the highest effects in the assays for aryl hydrocarbon receptor induction (AhR-CALUX), peroxisome proliferator activated receptor activity (PPARγ-Bla) and estrogenicity (ER-Bla) and appeared to dominate the effect profile in the Ammer further downstream, regarding these endpoints. The tributaries had an insignificant influence (<10%) on the effect fluxes in the Ammer (**Figure 12 B**). Highest effect flux increase was caused by T2, T3 and T4 together in the ER-Bla. Input from T8 and T10 increased the effect fluxes in the Ammer, measured in AhR-Bla, ER-Bla and PPARγ-Bla, by approximately 1 to 5%. Thus, the tributaries had little influence on the compound and effect profile of the Ammer, due to their low discharge.

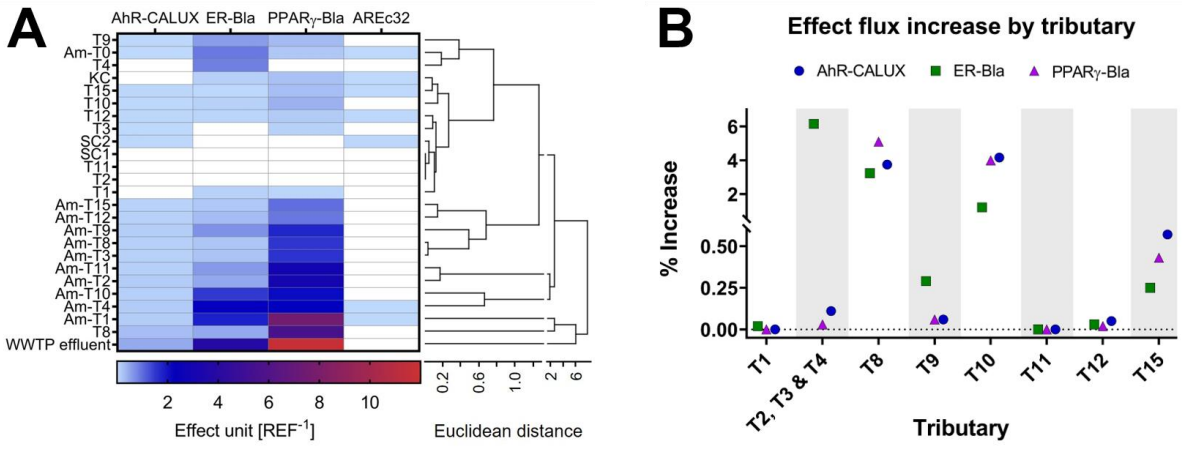

Figure 12: (A) Effects measured in the assays AhR-CALUX, ER-Bla, PPARγ-Bla and AREc32, expressed as effect units. Similarities of the samples´ effect profiles, expressed as the Euclidean distance, are visualized in a hierarchical cluster analysis with the unweighted pair-group method using arithmetic averages. (B) Effect flux increases (ΔJ_i, increase in percentage) of effects in AhR-CALUX, ER-Bla and PPARγ-Bla in the Ammer main stem caused by the respective tributary. Am-T = Ammer tributary; KC = Käsbach Creek; SC = Schönbrunnen Creek. Figure adapted from Müller et al. (2020a).

The Lagrangian sampling over 24 hours at AS1, AS2 and AS3 uncovered a decreasing temporal variability of the overall chemical burden and the average cytotoxicity with increasing distance from the most dominant input source WWTP1 (**Figure 13 A & B**), mainly driven by dilution. The variations in the chemical profiles at AS1, AS2 and AS3 were driven by compounds that showed no significant concentration decrease along the river flow path (e.g., benzotriazole, 4- & 5-methylbenzotriazole and TCPP) and compounds that dissipated from the water phase more readily (e.g., diclofenac and hydrochlorothiazide). In reach 1 and reach 2 (**Figure 13 B**) the average cytotoxicity attenuated for 12.3 and 17.8% which was mainly attributed to dilution (reach 1: 10.3%, reach 2: 22.7%).

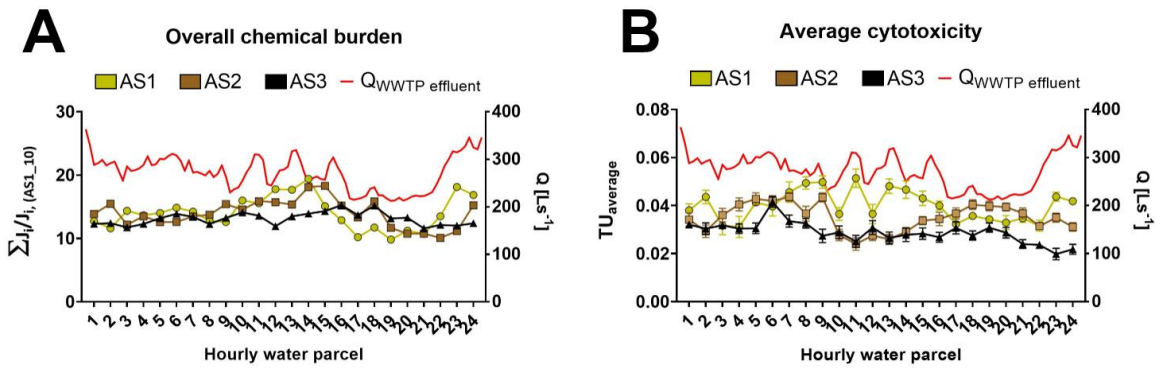

Figure 13: (A) Overall chemical burden, expressed as the sum of normalized mass fluxes of detected compounds, in the Ammer at AS1, AS2 and AS3 over 24 hours. (B) Average cytotoxicity $TU_{average}$ measured in the assays AhR-CALUX, ER-Bla, PPARγ-Bla and AREc32 at AS1, AS2 and AS3 over 24 hours. The discharge of the WWTP1 effluent is displayed on the right vertical axis. Figure reprinted from Müller et al. (2020a).

The compound and effect profile of the Ammer and its tributaries were very similar in that river section, although only at maximum 0.12% of the measured effects (in AhR-Bla, ER-Bla, PPARγ-Bla and AREc32) could be explained by the detected target compounds based on iceberg modelling (see **Supplemental Information**, chapter 6.1). A comparison to effect-based trigger values revealed threshold exceedance in the Ammer main stem at AS1, AS2 and AS3 in all assays, except for AREc32 (Table S10 & S11 of *Publication 3*). The samples of many tributaries and the Ammer upstream of WWTP1 were compliant with EBTs. Although, no target compounds were detected, T1, T2 and KC exceeded the EBT in ER and T12 the EBT in AREc32, again underlining the complementarity of both chemical analysis and bioassays.

To further explore the changes of the water quality in reach 1 (between AS1 and AS2) observed in the OCR assay (**Figure 9**), extracts of the intermediate tributaries T1, T2, T3 and T4 were measured for electron transport chain inhibition at one concentration level (40 REF, n=2, **Figure 14**). Although the WWTP1 effluent and T3 pointed towards electron transport chain inhibition, in two independent experiments, the measured effect levels were below the limit of detection of 9.6 % effect.

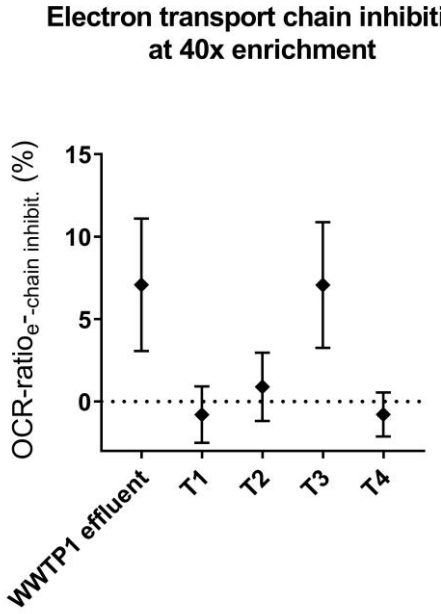

Figure 14: Extracts of the WWTP1 effluent and the tributaries T1, T2, T3 and T4 between AS1 and AS2 measured for electron transport chain inhibition at REF 40.

The target compounds diclofenac, lamotrigine and carbamazepine were detected in the Ammer River at the time of sampling (**Figure 11 A**). The latter compounds have been shown to impair mitochondrial oxidative phosphorylation by other researchers (Berger et al. 2010; Syed et al. 2016). Therefore, they were measured as single compounds for electron transport chain inhibition (**Figure 15 A-D**). Benzotriazole was also tested on account of the relatively high concentrations (6 µg L^{-1}) measured in the water samples. Electron transport chain inhibition was shown for diclofenac, lamotrigine and benzotriazole. None of the tested compounds showed changes in cell viability during the OCR experiment. However, their effect concentrations (EC_{10}) were far above (~100000x) the concentrations measured in the Ammer River, so that at maximum only 0.06% (in AS1-D) of the electron transport chain inhibition measured in the Ammer could be explained by diclofenac, lamotrigine and benzotriazole (see **Supplemental Information**, chapter 6.1).

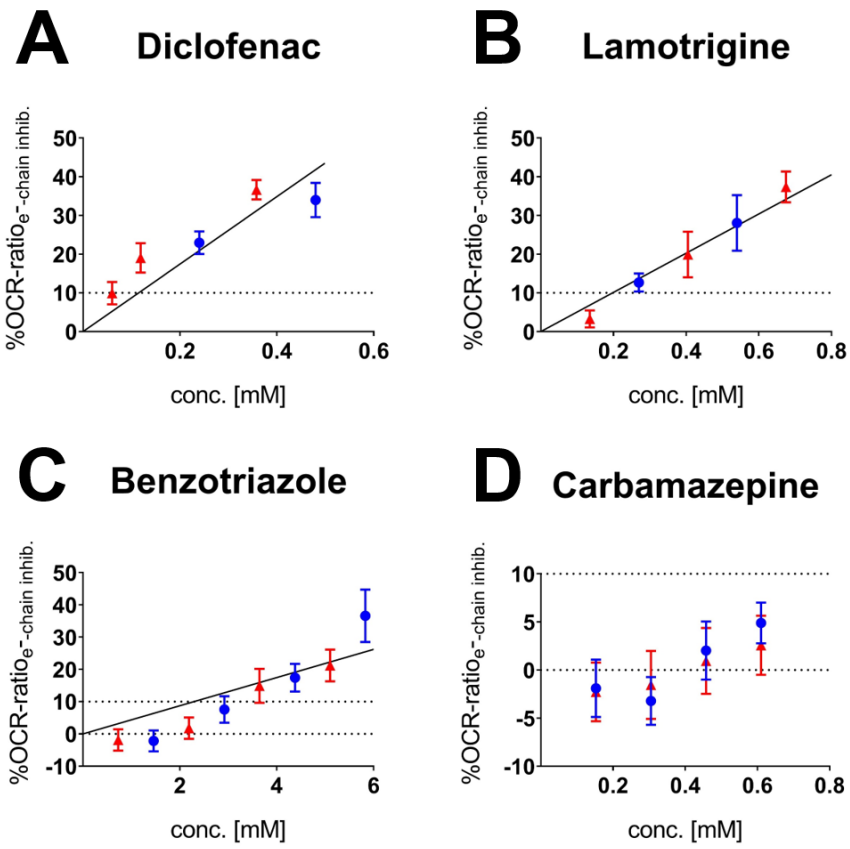

Figure 15: Single compounds diclofenac, lamotrigine, benzotriazole and carbamazepine measured for electron transport chain inhibition.

2.3. Storm event-driven occurrence and transport of organic micropollutants and associated effects

In order to assess the impact of changes in hydrological conditions on the occurrence of organic micropollutants and associated effects in a river and the role of SPM in micropollutant transport, river water was sampled during a storm event (**Study 3**), *Publication 4*. A thunder cell came from southwest and passed the upper Ammer catchment during the night of 27th to 28th of July 2019, from 18:30 to 22:45 (all times are given as Central European Summer Time, UTC+2h), with precipitation up to 80 mm h^{-1} and a maximum discharge of 8603 L s^{-1} at the gauge the investigated storm event almost reached the HQ2 classification (11650 L s^{-1}) of a biennial flood (LUBW 2020), see **Figure 16**. At the two sampling sites AS81, under the A81 highway bridge upstream of the WWTP1, and at AS3 at the gauge station in Pfäffingen (**Figure 16**) autosamplers collected one liter of river water every 30 minutes during a six-hour period. The sampling at AS3 was delayed for 53 minutes. In *Publication 4* AS81 is denoted as AS1 and AS3 is denoted as AS2. SPM was separated from the river water by filtration and both phases were then individually extracted.

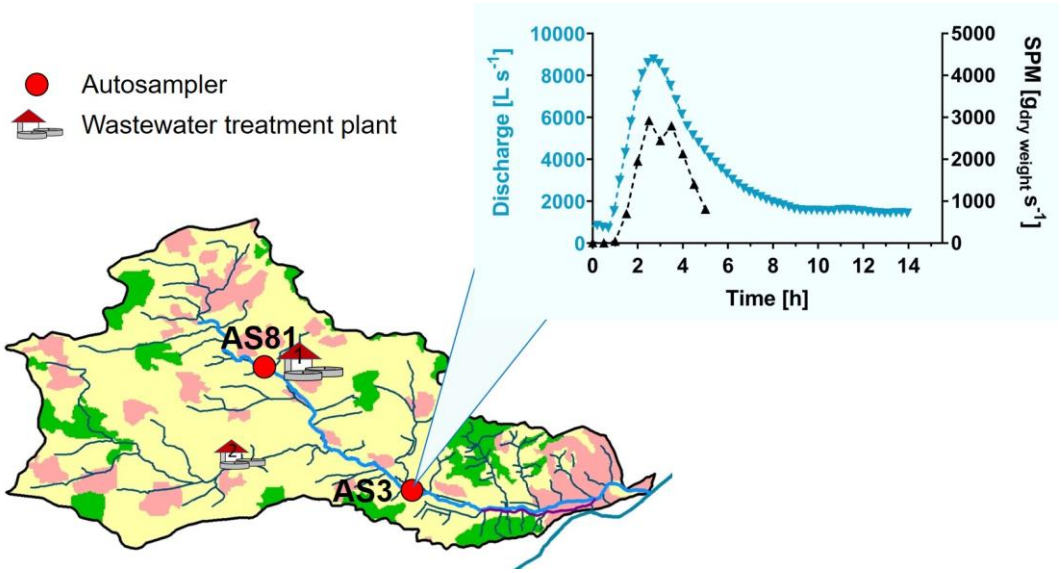

Figure 16: Locations of the sampling sites AS81 and AS3 in the Ammer catchment. Discharge Q and suspended particulate matter (SPM) flux in the Ammer River at AS3, during the storm event of **Study 3**. Figure adapted from Müller et al. (2018).

SPM and water extracts were analyzed by target screening for 97 compounds, including the compounds considered in **Study 1** and **2**, and two *in-vitro* bioassays indicative for oxidative stress response (AREc32), and for aryl hydrocarbon receptor induction (AhR-CALUX).

At AS81 27 target compounds (11 pesticides, 9 pharmaceuticals and 7 IHCs) and at AS3 33 target compounds (10 pesticides, 17 pharmaceuticals and 6 IHCs) were detected in the water extracts (Table S11 of *Publication 4*), with 25 compounds detected at both sites. PFHxA (perfluorohexanoic acid) and propiconazole disappeared between both sites and 8 additional compounds were found at AS2. In **Study 1** and **Study 2**, during dry weather conditions, 9 and 15 of these compounds were below the limit of quantification. Thus, a higher number of compounds was detected during the storm event than under dry weather conditions, in **Study 1** and **Study 2**.

Potential input sources upstream of AS81 and between AS3 were characterized based on the usages, applications and mass flux dynamics of the detected compounds. The compounds´ mass flux dynamics can be subdivided into three groups (**Figure 17,** Table S13 of *Publication 4*). Compounds of Group 1 showed higher or equally high average mass fluxes at AS81 compared to AS3. Group 2 compounds showed a ten times higher average mass flux at AS3 than at AS81. Compounds of Group 3 were detected at AS81 and showed average mass fluxes at AS3 that had increased by a factor less than 10.

For Group 1 compounds it can be assumed that they were mainly introduced from different input sources of the upper Ammer catchment, upstream of AS81. The anthropogenic markers for untreated wastewater caffeine and paracetamol (Buerge et al. 2003; Kasprzyk-Hordern et al. 2009) suggest input from combined sewer overflow (CSO, **Figure 17 A & B**). The biocides carbendazim and diuron are used to preserve outdoor materials and façades and indicate input from urban areas.

Group 2 comprises pharmaceuticals and IHCs (**Figure 17 C & D**) that typically find their way into the environment through treated wastewater. For the dynamics of these compounds a major impact by WWTP1 can be assumed. The mass fluxes of selected Group 2 compounds at AS3 increased during the storm event and followed the discharge.

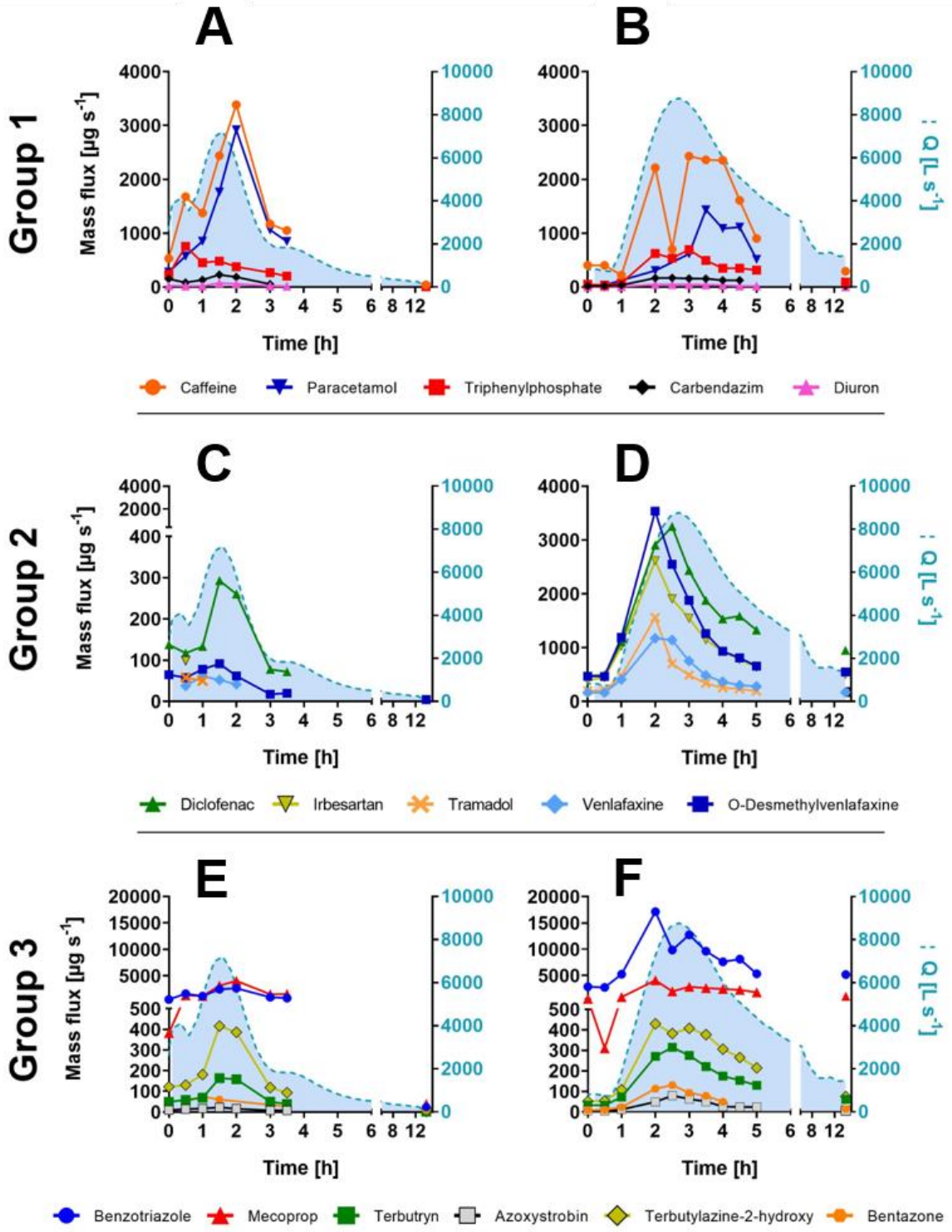

Figure 17: Mass fluxes (µg s^{-1}) of selected compounds in water during the storm event that fell into three groups: Group 1) those that showed a higher or equally high average mass flux at AS81 (A) compared to AS3 (B); Group 2) showed a 10x higher average mass flux at AS3 (D) than at AS81 (C); Group 3) detected at AS81 (E) with moderately increased average mass fluxes (below a factor of 10) at AS3 (F). Mass fluxes are depicted on the left vertical axis, while discharge is depicted as light blue area and on the right vertical axis. MCPA: (4-chloro-2-methylphenoxy)acetic acid. Figure reprinted from Müller et al. (2020b).

For Group 3 compounds input upstream of AS81, as they were detected at AS81, and input between AS81 and AS3, as their mass fluxes had increased between both sites, can be assumed. The pesticides azoxystrobin, bentazone and mecoprop, which are commonly used in agriculture, and the pesticide transformation product terbutylazine-2-hydroxy suggest input from agricultural areas. Mecoprop is moreover incorporated in roof sealings and felts to prevent root penetration and terbutryn in façade paintings. Both compounds may become washed off by rainfall and thus enter rivers (Bucheli et al. 1998; Burkhardt et al. 2011).

Compared to the base flow and dry weather condition during **Study 2**, generally higher concentrations and mass fluxes of organic micropollutants were observed during the storm event conditions of **Study 3**. For example, concentrations were by factors of 4 for benzotriazole, 7 for TCPP, 3 for 4&5-methylbenzotriazole, 3 for carbamazepine, 2 for isoproturon and 3 for bentazone higher under storm event conditions. The mass fluxes, however, had increased by factors of 26 for benzotriazole, 77 for TCPP, 26 for 4&5-methylbenzotriazole, 17 for carbamazepine, 15 for isoproturon and 18 for bentazone. The absolute total mass of all compounds, that were detected in both **Study 2** and **Study 3**, passing AS3 over 12 h was accounted for 122 g during **Study 2** and 1028 g in **Study 3**. Although this estimation is based on only 18 compounds, a pollutant load difference of one order of magnitude between dry and wet weather conditions can be assumed.

In the SPM extracts a total number of 16 compounds (10 pesticides, 2 pharmaceuticals and 4 IHCs) were detected. These included pesticides used in agriculture (e.g., azoxystrobin, bixafen, diflufenican, prochloraz) or to preserve outdoor materials (e.g., isoproturon, terbutryn) and indicate inputs from agricultural and urban areas. The widely used plasticizer and flame retardant triphenylphosphate was detected at AS81 (upstream of WWTP1) and may stemmed from urban runoff and/or CSO, as already suggested by the organic indicator chemicals detected in the water extracts. However, it remains unclear whether these micropollutants sorbed onto SPM in the Ammer River or were transported into the Ammer in a particle-facilitated manner.

The micropollutants azoxystrobin, isoproturon and the organophosphates triphenylphosphate, tris(1-chloro-2-propyl) phosphate and (tris(2-butoxyethyl) phosphate were detected in both water and on SPM. These compounds are neutral at pH 7.4, have octanol-water partition coefficients logK_{ow} above 4, except for isoproturon with 2.8 (Table S10 of *Publication 4*), and predominantly partition to the organic carbon

of SPM (Kim et al. 2017; Kodešová et al. 2011; Worrall et al. 1996). At both sampling sites, the observed concentration ratio between water and SPM (R_i) agreed well with the concentration ration between water and organic carbon at equilibrium (K_d), see **Figure 18**. Albeit the environmental conditions and parameters (e.g., ion-, dissolved organic carbon- and SPM concentrations) may change rapidly in a river during a storm event the results indicate that compound concentrations on SPM and in water could be equilibrated. For triphenylphosphate, tris(1-chloro-2-propyl) phosphate, (tris(2-butoxyethyl) phosphate and isoproturon, even at relatively low SPM concentrations, more than 15% of the total mass flux was attributed to SPM.

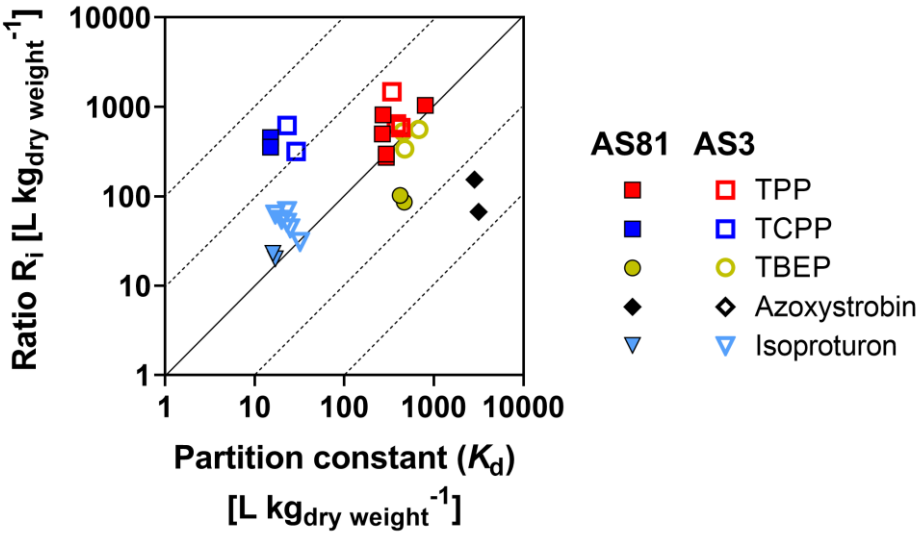

Figure 18: Observed concentration ratio (R_i in L kg^{-1}) versus the partition constant (K_d) between water and organic carbon of SPM during the storm event, for the compounds azoxystrobin, isoproturon, TPP (triphenylphosphate), TBEP (tris(2-butoxyethyl) phosphate) and TCPP (tris(1-chloro-2-propyl) phosphate), at AS81 (filled symbols) and AS3 (empty symbols). Figure adapted from Müller et al. (2020b).

The effect equivalents in the water extracts measured in AREc32 and AhR-CALUX were higher than under dry weather and base flow conditions (Table S17 & S18 of *Publication 4*). During the storm event the effects in water, measured in AREc32, varied at maximum by a factor of 1.9 at AS81 and by a factor of 2.8 at AS3 (**Figure 19 A & B**). The tentative effect-based trigger value for AREc32 is 140 $\mu g_{dichlorvos}$ L^{-1} and was exceeded in all water samples during the actual storm event. In the SPM extracts from AS81 and AS3 the measured effects remained constant and increased only after the event (**Figure 19 A & B**). The effect equivalents in the water and the SPM extracts

measured in AhR-CALUX followed the water and SPM discharge at AS81 and, with a slight delay, at AS3 (**Figure 19 C & D**). The tentative effect-based trigger value for AhR-CALUX is 4.3 $ng_{benzo[a]pyrene}$ L^{-1} and was exceeded in all water samples. Thus, the comparison to EBTs pointed towards poor overall water quality with respect to the mixture effect endpoints of oxidative stress response and aryl hydrocarbon receptor induction. The distribution ratio (R_{BEQ}) of effects in water and associated to SPM varied between 10^3 and 10^4 in AREc32 and between 10^3 and 10^5 in AhR-CALUX, at both sampling sites (Figure S3 of *Publication 4*). This indicates that micropollutants causing the effects in the respective assay were mainly associated to SPM.

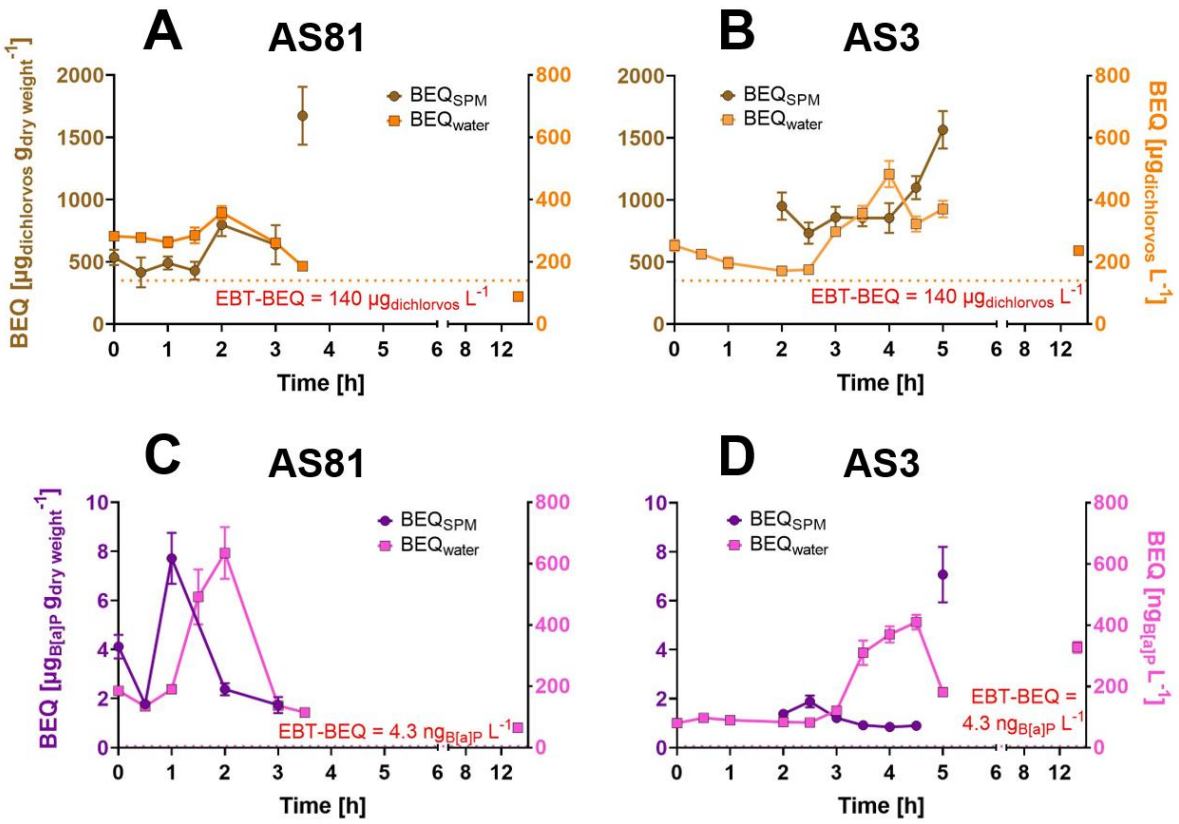

Figure 19: Effects in water and on SPM at AS81 and AS3, measured in AREc32 (A & B, dichlorvos-EQ) and AhR-CALUX (C & D, B[a]P-EQ), over time. Effect-based trigger values for AREc32 and AhR-CALUX, updated by Neale et al. (2020), are visualized by dotted lines. Figure adapted from Müller et al. (2020b).

The bioanalytical effect fluxes (BEF) in water and on SPM, measured in AREc32 and in AhR-CALUX, increased during the storm event at AS81 and AS3(**Figure 20 A-D**). In both assays and at both sites the BEF_{SPM} followed the SPM flux and the BEF_{water} followed the discharge with a slight delay. Although the mass of SPM was ~1000 times

lower than the mass of water, the BEF_{SPM} was as high or even higher than BEF_{water} because the measured BEQs of SPM were much higher than the BEQs of water. Hence, highlighting the significant contribution of SPM to water quality following a storm event.

In summary, during the investigated storm event micropollutant numbers, concentrations, mass fluxes, effects and effect fluxes increased and were generally higher than under dry weather conditions and SPM was shown to play an important role in effect transport.

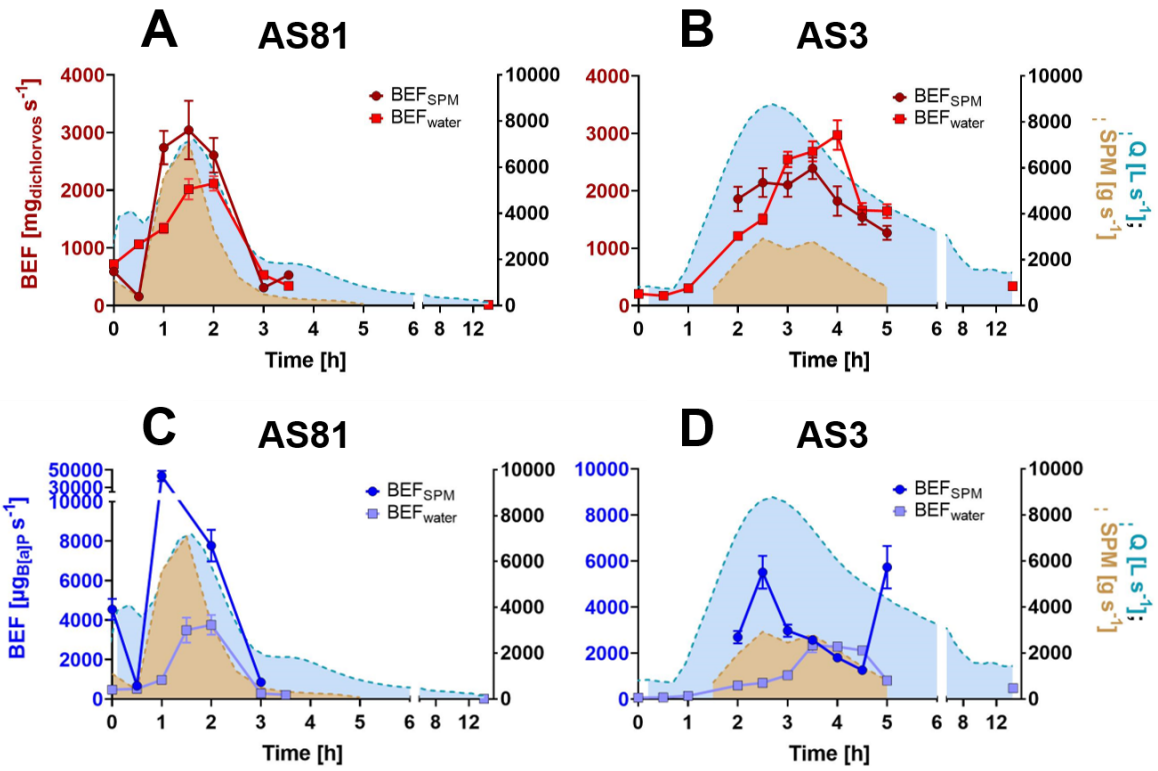

Figure 20: Time courses if the bioanalytical effect fluxes at AS81 and AS3, in water (BEF_{water}) and associated to SPM (BEF_{SPM}), measured in AREc32 (A & B) and AhR-CALUX (C & D) and displayed on the left vertical axes. Discharges of water (blue area) and SPM (brown area) are displayed on the right vertical axes. Figure adapted from Müller et al. (2020b).

3. General discussion

In this chapter, the research questions raised in **chapter 1.5** are revisited and the relevance of the results and implications for environmental research and monitoring are critically discussed and evaluated.

3.1. Environmental trace analysis

3.1.1. The "Analytical Window"

In this thesis, I showed that the combination of chemical analysis and a battery of environmentally relevant *in-vitro* bioassays, including a newly-developed bioassay that quantifies mitochondrial toxicity, can reflect changes in water quality and identify and characterize input sources of organic micropollutants in a small river on the catchment scale.

Previous studies on the occurrence of organic micropollutants in rivers on the catchment scale primarily used chemical analysis alone (Berenzen et al. 2005; Boulard et al. 2019; Moschet et al. 2013a; Ruff et al. 2015) but often screened for much higher numbers of target compounds in environmental samples (Chiaia-Hernandez et al. 2012; Gago-Ferrero et al. 2019; Moschet et al. 2014; Munz et al. 2017; Tousova et al. 2017). Screening for more compounds is costly, but allows for a more comprehensive assessment of the chemical profile. In this work, the number of screened target compounds had chronologically increased to a final number of 97. However, besides target screening the application of suspect screening helped to achieve a more complete picture of the chemical profile in **Study 1** (Hollender et al. 2017; Moschet et al. 2013b).

In this work chemical analysis and *in-vitro* bioassays revealed a very similar pollution profile, although they covered different compounds and compound classes (see **Supplemental Information,** chapter 6.1). An explanation could be that the detected target compounds and the effect causing compounds had the same input sources or the same driving forces. A hierarchical cluster analysis revealed the similarities of detected compound classes (pesticides, pharmaceuticals, IHCs) and measured effects during **Study 2**, under base flow conditions (**Figure 21**). Pesticides and pharmaceuticals were most similar, likely because for most pesticides and pharmaceuticals the WWTP1 effluent was the major input source. Greatest similarities between a compound class and effects were found for IHCs and aryl hydrocarbon

receptor induction (AhR-CALUX). Although their analytical windows hardly overlapped (at maximum 0.12%), the detected IHCs and the compounds active in AhR-CALUX showed a similar profile in the Ammer and they maybe had similar input sources or driving forces. Little similarity was observed for compound classes and estrogenicity (ER-Bla). There is also little similarity of compound classes and oxidative stress (AREc32), however, which is also attributed due to the fact that most samples showed no effects because of cytotoxic interference.

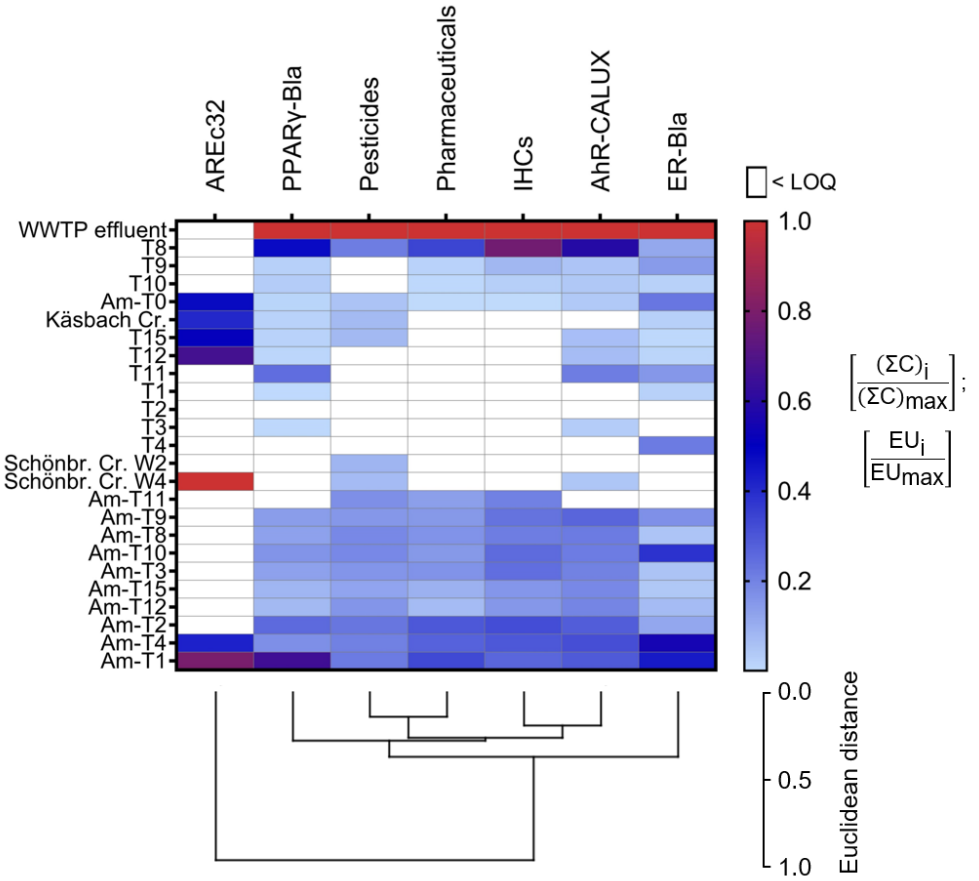

Figure 21: Similarities between the compound classes pesticides, pharmaceuticals and industrial and houshold chemicals (IHCs) and aryl hydrocarbon receptor induction (AhR-CALUX), estrogenicity (ER-Bla), oxidative stress response (AREc32) and peroxisome proliferator activated receptor activity (PPARγ-Bla) represented in a hierarchical cluster analysis with the unweighted pair-group method using arithmetic averages. Differences between compound classes and bioassays are expressed by the Euclidean distance. Results were generated in Study 2.

It is difficult to explain which chemicals are responsible for the effects observed in the bioassays if the analytical windows of chemical analysis and bioassays hardly overlap. In other studies, up to 80, 71% of the activity in ER and AhR and even up to

100% of the activity in AR-Bla, anti AR-Bla, anti GR-Bla and photosystem II inhibition could be explained by detected compounds, under the assumption of concentration addition, and in many cases the majority of the explained fraction was attributed to only a few compounds (Könemann et al. 2018; König et al. 2017; Neale et al. 2015; Neale et al. 2017b). But this requires extensive single compound testing and it is not sufficient to test only the most promising compounds according to their chemical structure. As an example, the pesticides propiconazole and terbuthylazine were unexpectedly uncovered to be active in AhR (Neale et al. 2017b) and Lundqvist et al. (2019b) found co-occurrence of pesticides and AhR activation in river samples from agricultural areas.

To identify input sources of organic micropollutants and changes of the water quality in a river, it is not absolutely necessary to be capable of explaining which compounds are responsible for the occurring effects. It is more important to capture a broad spectrum of compounds and compound classes. Therefore, a diverse list of target or suspect compounds and *in-vitro* bioassays covering diverse endpoints are advantageous. For this purpose, adaptive stress response pathways (e.g., oxidative stress response) are beneficial as they are crucial to cell viability and may become activated by a broad range of various stressors (Simmons et al. 2009), other than the rather selective receptor mediated endpoints.

In the water samples collected during **Study 1** no or only little glucocorticoid activity (GR-Bla), androgenicity (AR-Bla), anti androgenicity (Anti AR-Bla), progestagenic activity (PR-Bla) and anti progestagenic activity (Anti PR-Bla) was measured, all of which capture hormonal effects. A similar effect signature was reflected by a European-wide demonstration program for effect-based monitoring of surface waters, in which Tousova et al. (2017) took water samples in four European river basins at 18 sampling sites. In this study, glucocorticoid activity in 22%, androgenicity in 11%, anti androgenicity in 0% of the neutral sorbent (Chromabond HR-X) extracts of all samples. Whereas, estrogenicity was measured in 78% of the samples. Estrogenic compounds were measured in surface waters worldwide (Adeel et al. 2017), are incompletely removed during wastewater treatment (Völker et al. 2019) and estrogenicity is among the most frequently observed hormonal effects (Tousova et al. 2017). Of the hormonal effects measured in the Ammer, estrogenicity was highest. Thus, it was deemed suitable to represent hormonal effects in the subsequent studies, while the assays GR-Bla, AR-Bla, Anti AR-Bla, PR-Bla and Anti PR-Bla were not further considered.

Cytotoxicity was defined by cell growth inhibition and was measured as a side parameter, concurrent to the effect in every bioassay, to avoid false positive results due to cytotoxic interferences. Although the dosing for measuring cytotoxicity was not purposively conducted, in **Study 1** and **Study 2** the average cytotoxicity (expressed in toxic units TU) downstream of WWTP1, which governed the toxicological and chemical profile of the Ammer, declined along the river flow and mirrored dilution. Other studies showed that cytotoxicity can be used as an endpoint to evaluate the pollution profile of surface water (Sousa et al. 2017; Yuan et al. 2005) and settling particulate matter during a flood event (Hollert et al. 2000) and bioremediation efficiency (Sun et al. 2017). Results herein, showed that cytotoxicity can be used as a surrogate for the overall chemical burden along a river.

3.1.2. Indicator chemicals and -effects

In the present work organic indicator chemicals were shown to be very useful tools to identify and characterize input sources of organic micropollutants. However, their use in different applications, for example as pesticides in agriculture and as biocides in urban areas, together with regional and seasonal variations can make it difficult to trace back their origin and thus may limit their representativeness. This also goes along with a limited applicability on other study sites. For the selection of appropriate indicator chemicals, I therefore recommend to first acquire a comprehensive chemical inventory, of the studied environmental compartment, covering different compounds and compound classes. From this inventory compounds that most satisfy the requirements outlined in chapter 1.3. are selected.

Aside from organic indicator chemicals *in-vitro* bioassays can indicate input sources of organic micropollutants as well. In **Study 1** the WWTP1 was shown to be the major input source of the hormonal effects androgenicity (AR-Bla) and glucocorticogenic activity (GR-Bla) in the Ammer catchment. Thus, these hormonal endpoints may serve as indicators for input of wastewater into rivers in future studies. WWTP1 was also the major input source of estrogenicity (ER-Bla), however, estrogenicity was shown in previous studies to be introduced from agricultural areas as well (Lorenzen et al. 2004; Peterson et al. 2000; Scott et al. 2018).

3.1.3. Oxygen Consumption Rate (OCR) assay

Disturbance of the oxidative phosphorylation may be caused by a broad spectrum of micropollutants pertaining to different compound classes, and may not be restricted to a single specific compound. Hence, the developed OCR assay can be used to assess mitochondrial toxicity in environmental samples and trace changes of the water quality along a river, while the measured effects cannot be dedicated to a specific class of micropollutants.

The Seahorse XF^{e}96 Extracellular Flux Analyzer used in the OCR assay was applied by other researchers to measure environmental samples (Probert et al. 2018) and micropollutants (Attene-Ramos et al. 2013). However, previous applications have not been able to quantitatively distinguish between different MoAs, nor account for the absolute effect of a sample relative to a reference compound. Compared to other methodologies, following the OCR does not require isolation of mitochondria and addition of labels, reporters or dyes. Nevertheless, mitochondria as major energy suppliers in eukaryotic cells, their crucial involvement in cell metabolism (McBride et al. 2006) and their disturbance may ultimately lead to cell death make it to an endpoint of high environmental relevance and should thus be focus of further environmental research.

3.2. Impacts of changes in hydrological conditions

Under dry weather conditions the chemical and toxicological profile of the Ammer River was governed by the WWTP1 in Altingen. In **Study 1** and **2** WWTP1 contributed to 81 and 51% of the Ammer discharge and the proposed effect-based trigger values for estrogenicity and activation of PPARγ were not compliant with samples taken downstream of WWTP1 while being compliant with effects in samples taken upstream. In a number of wastewater impacted rivers Kolpin et al. (2004) and Loraine and Pettigrove (2006) found generally higher numbers and concentrations of organic wastewater contaminants, such as pharmaceuticals and personal care products, under low flow conditions, and thus a higher portion of treated wastewater, compared to normal and high flow conditions. In **Study 2** tributaries from agricultural and urban areas were found to have only minor influence on the mass and effect fluxes in the Ammer. In the same river section and during a storm event (**Study 3**) numbers, concentrations and fluxes of micropollutants and associated effects in the water phase had increased many times over. This agrees with Ccanccapa et al. (2016), Vryzas et al. (2009), Szöcs et al. (2017) and (Neale et al. 2020). Szöcs et al. (2017) and Neale et al. (2020) recorded a high spatial and temporal variability of the chemical and effect profile in water of small German rivers, mostly influenced by agriculture and/or wastewater, following rainfall. Neale et al. (2020) found a generally higher micropollutant burden under rain event conditions, by comparing *in-vitro* effect data to studies of other small rivers under dry weather conditions. In the present work it was observed that the increase of the mass fluxes of detected compounds in water was more pronounced than the increase of concentrations. In similar studies concentrations were highest right at the beginning of a storm event and then decreased as dilution kicked in (Benotti and Brownawell 2007; Madoux-Humery et al. 2013; Phillips et al. 2012). The findings of this work were based on comparing the chemical and effect profile of the Ammer River between dry weather conditions and a storm event, which was relatively intense but lasted only several hours until the discharge had returned back to almost base flow conditions. In agricultural tributaries of the Ammer River, Zarfl et al. (2020) showed an increasing mass flux of the herbicide metamitron during a storm event, lasting for several days, while the majority of the detected herbicides showed highest mass fluxes at the beginning of the rain event. If lasting longer, for

instance several days or weeks, a storm event may elevate compounds that are not rapidly mobilized.

Since the many factors influencing transport, erosion, remobilization and deposition of particulate matter can vary between events, even if hydrograph shapes are similar (Eder et al. 2014; Giménez et al. 2012; Soler et al. 2008), the significance of SPM in micropollutants transport may vary as well. In the past, most studies focused on hydrophobic organic compounds in sediments and SPM, such as polycyclic aromatic hydrocarbons and halogenated aromatic hydrocarbons (McCready et al. 2006; Van Metre and Mahler 2005). However, biodegradability, bioavailability and mobility affecting sorption also accounts for hydrophilic organic compounds (Schwarzenbach et al. 2006). The compounds detected in the SPM extracts of **Study 3** comprised hydrophobic and hydrophilic compounds. Thus, SPM poses a transport vector also for hydrophilic compounds. This finding is in agreement with Boulard et al. (2019), da Silva et al. (2011) and Martínez-Hernández et al. (2014). In **Study 1** and **2** the river water was visually very clear and micropollutant transport via SPM was thus neglected. Considering micropollutant transport via SPM during dry weather conditions would have required larger sample volumes to obtain sufficient SPM for analysis. In a previous study, Boulard et al. (2019) found that numbers and concentrations of pharmaceuticals bound to SPM increased with an increasing wastewater portion. It would therefore be interesting to assess the role of SPM in micropollutant transport under dry weather conditions and over longer monitoring time scales.

The present work showed that changes of hydrological conditions during storm events have considerable impact on the compound and effect profile of rivers. Compared to dry weather conditions, during storm events organic micropollutants may become mobilized from agricultural and urban runoff (Burant et al. 2018; Tran et al. 2019; Zgheib et al. 2011a), introduced by combined sewer overflow (Gasperi et al. 2008) and due to reduced residence time in WWTPs (**Figure 22**). In the past, storm events had caused severe ecological and human health problems such as the *Cryptosporidium hominis* pest in Sweden 2010/2011 (Ridderstedt et al. 2018; Smittskyddsinstitutet 2011). The identification of toxicity drivers, in rivers during storm events, by priority substances alone, outlined by the European Water Framework Directive (EU 2013/39), is insufficient, environmental parameters (e.g., pH, temperature, flow rates, redox potential, salinity, turbidity, suspended materials) and the chemical composition may change in a relatively short time, hampering the

determination of travel times of water packages. Although the micropollutant burden was generally higher during storm event conditions, dry weather conditions after longer dry periods may pose a risk to the aquatic environment as well due to the relatively high portion of treated wastewater. It is therefore important to elucidate chemical pollution in rivers and in-steam processes during different and changing hydrological condition.

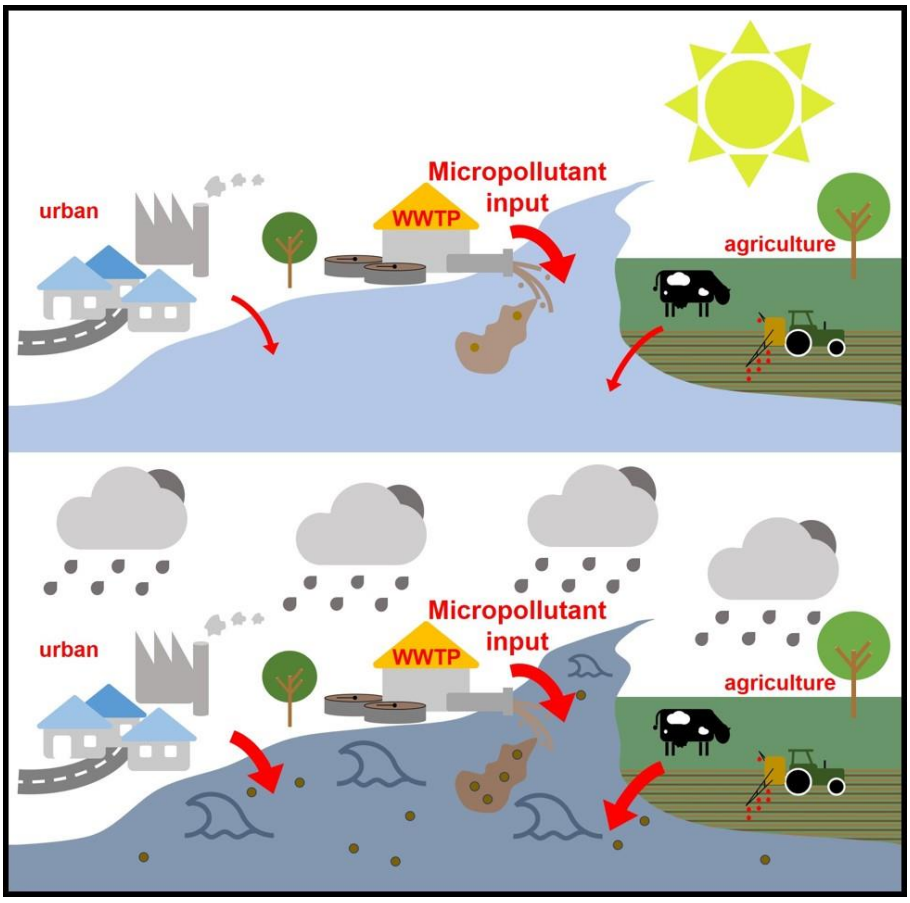

Figure 22: Conceptual illustration of the influence of micropollutant inputs from urban (left arrows) and agricultural (right arrows) areas and of treated wastewater (central arrow) under dry weather (upper half) and storm event (lower half) conditions, visualized by the arrow thickness.

3.3. Transferability of results

Catchment scale monitoring of organic micropollutant fate and transport is a challenging task. A comprehensive assessment of the environmental fate of organic micropollutants in rivers requires that a range of hydrogeological parameters, such as travel times, advection and dispersion of the river water, groundwater inflow and hyporheic exchange are considered (Glaser et al. 2019; Lawrence et al. 2013; Manamsa et al. 2016; Schmadel et al. 2016). In some cases, sampling strategies can improve the comparability of studies in different river segments and catchments. Meteorological conditions together with the regional application and consumption behavior of pesticides, pharmaceuticals and IHCs determine input sources and characteristics (Boulard et al. 2019; Burant et al. 2018; McKee et al. 2017; Wittmer et al. 2010) and should be considered as well.

In anthropogenically influenced catchments, field studies on the fate of micropollutants can generate transferrable information (from site to site) on the downstream propagation of compounds and effects in both the water column and SPM in rivers. Most importantly, the influence of dynamic hydrology provides valuable information on the chemical and toxicological response of systems to environmental changes, on the scale of single precipitation events (see *Publication 4*).

When it comes to the individual consideration of particulate matter and water, the separation cutoff, that is, the operational definition between particulate and dissolved phases can limit the comparability of different studies. For instance, various studies investigating the contamination of SPM used filtration with different pore sizes (Baborowski et al. 2004; Kim and Sansalone 2008; Zgheib et al. 2011b), applied centrifugation (Heemken et al. 2000) or used traps for assessing the settleable particle fraction (Boulard et al. 2019; Hollert et al. 2000). In some cases, no clear information on the cutoff between water and particulate matter is provided (Álvarez-Ruiz et al. 2015). It is noteworthy that contaminants associated to particulate matter below the “particulate”-cutoff would be ascribed to the aqueous phase. Therefore, it would be beneficial for the transferability of results to use a standardized separation procedure with a small cutoff, such as the DIN (38409-2) with a cutoff at 1.5 µm, in future investigations.

4. Conclusion & Outlook

In this thesis I showed that the chemical and toxicological profile of a river is driven by varying hydrological conditions, that control input sources of organic micropollutants, and thus their individual mass-flux contribution, and is highly variable in time and space. It is therefore important to consider and properly capture these spatiotemporal variations to investigate the fate of organic micropollutants in rivers, to examine factors driving in-stream processes (e.g., sorption, degradation) and for future regulatory monitoring efforts.

During the investigated storm event, additional micropollutant transport via SPM played an important role. As micropollutant mixtures associated to SPM can potentially exhibit toxicity it is important to further examine what compounds and effects are associated to SPM and how they are linked to particle properties and particle origin. To what extend can SPM act as a sink or source and what are the sorption kinetics and the bioavailability of organic micropollutants and effects associated to SPM? The latter is an important question that should be central to future research that builds on the work outlined herein.

Although during the investigated storm event the total micropollutant load over 12 h in the Ammer River water was around a magnitude higher compared to base flow conditions, further research is needed to assess the annual proportion of the storm event driven micropollutant loads. Also, after longer dry weather periods and in densely populated areas, treated wastewater can represent a major volume fraction of the discharge in smaller rivers potentially leading to adverse effects on the aquatic environment and drinking water quality. It is therefore important to elucidate the impact of different hydrological conditions on the chemical and toxicological profile of a river and to assess their influence on the aquatic environment on the long term.

Chemical analysis combined with effect data from a river catchment may provide the basis to develop models that can predict in-stream processes and hazardous situations without extensive sampling and analytical effort. In light of sustaining a “good chemical status” according to the European water framework directive (EU 2013/39) chemical analysis could be complemented with selected bioassays in the future to obtain a first impression of the compound, effect inventory, dominant input sources (by the aid of organic indicator chemicals and indicator effects) and characteristics of a river catchment. Future monitoring efforts, should then focus on previously identified hot spots or hot moments for environmental risk assessment and management.

5. References

ACD/Labs. ChemSpider data base. 2020. Royal Society of Chemistry; [accessed 2020]. http://www.chemspider.com/.

Adeel M, Song X, Wang Y, Francis D, Yang Y. 2017. Environmental impact of estrogens on human, animal and plant life: a critical review. *Environ Int*. 99:107-119.

Altenburger R, Brack W, Burgess RM, Busch W, Escher BI, Focks A, Hewitt LM, Jacobsen BN, de Alda ML, Ait-Aissa S. 2019. Future water quality monitoring: improving the balance between exposure and toxicity assessments of real-world pollutant mixtures. *Environ Sci Eur*. 31(1):1-17.

Altenburger R, Scholze M, Busch W, Escher BI, Jakobs G, Krauss M, Krüger J, Neale PA, Ait-Aissa S, Almeida AC. 2018. Mixture effects in samples of multiple contaminants–An inter-laboratory study with manifold bioassays. *Environ Int*. 114:95-106.

Álvarez-Ruiz R, Andrés-Costa MJ, Andreu V, Picó Y. 2015. Simultaneous determination of traditional and emerging illicit drugs in sediments, sludges and particulate matter. *J Chromatogr A*. 1405:103-115.

Aminot Y, Fuster L, Pardon P, Le Menach K, Budzinski H. 2018. Suspended solids moderate the degradation and sorption of waste water-derived pharmaceuticals in estuarine waters. *Sci Total Environ*. 612:39-48.

Antweiler RC, Writer JH, Murphy SF. 2014. Evaluation of wastewater contaminant transport in surface waters using verified Lagrangian sampling. *Sci Total Environ*. 470:551-558.

Attene-Ramos MS, Huang R, Sakamuru S, Witt KL, Beeson GC, Shou L, Schnellmann RG, Beeson CC, Tice RR, Austin CP. 2013. Systematic study of mitochondrial toxicity of environmental chemicals using quantitative high throughput screening. *Chem Res Toxicol*. 26(9):1323-1332.

Baborowski M, von Tümpling Jr W, Friese K. 2004. Behaviour of suspended particulate matter (SPM) and selected trace metals during the 2002 summer flood in the River Elbe (Germany) at Magdeburg monitoring station. *Hydrol Earth Syst Sc*. 8(2):135-150.

Bartlett DW, Clough JM, Godwin JR, Hall AA, Hamer M, Parr-Dobrzanski B. 2002. The strobilurin fungicides. *Pest Manag Sci*. 58(7):649-662.

Benotti MJ, Brownawell BJ. 2007. Distributions of pharmaceuticals in an urban estuary during both dry-and wet-weather conditions. *Environ Sci Technol*. 41(16):5795-5802.

Berenzen N, Lentzen-Godding A, Probst M, Schulz H, Schulz R, Liess M. 2005. A comparison of predicted and measured levels of runoff-related pesticide concentrations in small lowland streams on a landscape level. *Chemosphere*. 58(5):683-691.

Berger I, Segal I, Shmueli D, Saada A. 2010. The effect of antiepileptic drugs on mitochondrial activity: a pilot study. *J Child Neurol*. 25(5):541-545.

Bergheim M, Gieré R, Kümmerer K. 2012. Biodegradability and ecotoxicitiy of tramadol, ranitidine, and their photoderivatives in the aquatic environment. *Environ Sci Pollut Res*. 19(1):72-85.

Boulard L, Dierkes G, Schlüsener MP, Wick A, Koschorreck J, Ternes TA. 2019. Spatial distribution and temporal trends of pharmaceuticals sorbed to suspended particulate matter of German rivers. *Water Res*.115366.

Brack W, Aissa SA, Backhaus T, Dulio V, Escher BI, Faust M, Hilscherova K, Hollender J, Hollert H, Müller C. 2019a. Effect-based methods are key. The European Collaborative Project SOLUTIONS recommends integrating effect-based methods for diagnosis and monitoring of water quality. *Environ Sci Eur*. 31(1):1-6.

Brack W, Ait-Aissa S, Backhaus T, Birk S, Barceló D, Burgess R, Cousins I, Dulio V, Escher BI, Focks A. 2019b. Strengthen the European collaborative environmental research to meet European policy goals for achieving a sustainable, non-toxic environment. *Environ Sci Eur*. 31(1):1-9.

Brack W, Ait-Aissa S, Burgess RM, Busch W, Creusot N, Di Paolo C, Escher BI, Hewitt LM, Hilscherova K, Hollender J. 2016. Effect-directed analysis supporting monitoring of aquatic environments—an in-depth overview. *Sci Total Environ*. 544:1073-1118.

Brack W, Dulio V, Ågerstrand M, Allan I, Altenburger R, Brinkmann M, Bunke D, Burgess RM, Cousins I, Escher BI, Hernández FJ, Hewitt LM, Hilscherová K, Hollender J, Hollert H, Kase R, Klauer B, Lindim C, Herráez DL, Miège C, Munthe J, O'Toole S, Posthuma L, Rüdel H, Schäfer RB, Sengl M, Smedes F, van de Meent D, van den Brink PJ, van Gils J, van Wezel AP, Vethaak AD, Vermeirssen E, von der Ohe PC, Vrana B. 2017. Towards the review of the European Union Water Framework Directive: Recommendations for more efficient assessment and management of chemical contamination in European surface water resources. *Sci Total Environ*. 576:720-737.

Brack W, Escher BI, Müller E, Schmitt-Jansen M, Schulze T, Slobodnik J, Hollert H. 2018. Towards a holistic and solution-oriented monitoring of chemical status of European water bodies: how to support the EU strategy for a non-toxic environment? *Environ Sci Eur*. 30(1):1-11.

Bradley PM, Journey CA, Button DT, Carlisle DM, Huffman BJ, Qi SL, Romanok KM, Van Metre PC. 2020. Multi-region assessment of pharmaceutical exposures and predicted effects in USA wadeable urban-gradient streams. *PLoS One*. 15(1):e0228214.

Brennan JC, He G, Tsutsumi T, Zhao J, Wirth E, Fulton MH, Denison MS. 2015. Development of species-specific Ah receptor-responsive third generation CALUX cell lines with enhanced responsiveness and improved detection limits. *Environ Sci Technol*. 49(19):11903-11912.

Brinkmann M, Eichbaum K, Buchinger S, Reifferscheid G, Bui T, Schäffer A, Hollert H, Preuss TG. 2014. Understanding receptor-mediated effects in rainbow trout: in vitro–in vivo extrapolation using physiologically based toxicokinetic models. *Environ Sci Technol*. 48(6):3303-3309.

Bucheli TD, Müller SR, Voegelin A, Schwarzenbach RP. 1998. Bituminous roof sealing membranes as major sources of the herbicide (R, S)-mecoprop in roof runoff waters: potential contamination of groundwater and surface waters. *Environ Sci Technol*. 32(22):3465-3471.

Buerge IJ, Poiger T, Müller MD, Buser H-R. 2003. Caffeine, an anthropogenic marker for wastewater contamination of surface waters. *Environ Sci Technol*. 37(4):691-700.

Burant A, Selbig W, Furlong ET, Higgins CP. 2018. Trace organic contaminants in urban runoff: Associations with urban land-use. *Environ Pollut*. 242:2068-2077.

Burkhardt M, Zuleeg S, Vonbank R, Schmid P, Hean S, Lamani X, Bester K, Boller M. 2011. Leaching of additives from construction materials to urban storm water runoff. *Water Sci Technol*. 63(9):1974-1982.

CAS. Chemical Abstracts Service. 2020. American Chemical Society; [accessed 2020]. https://www.cas.org/support/documentation/chemical-substances.

Casado J, Brigden K, Santillo D, Johnston P. 2019. Screening of pesticides and veterinary drugs in small streams in the European Union by liquid chromatography high resolution mass spectrometry. *Sci Total Environ*. 670:1204-1225.

Ccanccapa-Cartagena A, Pico Y, Ortiz X, Reiner EJ. 2019. Suspect, non-target and target screening of emerging pollutants using data independent acquisition: Assessment of a Mediterranean River basin. *Sci Total Environ*. 687:355-368.

Ccanccapa A, Masiá A, Andreu V, Picó Y. 2016. Spatio-temporal patterns of pesticide residues in the Turia and Júcar Rivers (Spain). *Sci Total Environ*. 540:200-210.

Chiaia-Hernandez AC, Krauss M, Hollender J. 2012. Screening of lake sediments for emerging contaminants by liquid chromatography atmospheric pressure photoionization and electrospray ionization coupled to high resolution mass spectrometry. *Environ Sci Technol*. 47(2):976-986.

Clara M, Strenn B, Kreuzinger N. 2004. Carbamazepine as a possible anthropogenic marker in the aquatic environment: investigations on the behaviour of Carbamazepine in wastewater treatment and during groundwater infiltration. *Water Res*. 38(4):947-954.

Connor R. 2015. The United Nations world water development report 2015: water for a sustainable world. UNESCO publishing. ISBN: 9231000713

da Silva BF, Jelic A, López-Serna R, Mozeto AA, Petrovic M, Barceló D. 2011. Occurrence and distribution of pharmaceuticals in surface water, suspended

solids and sediments of the Ebro river basin, Spain. *Chemosphere*. 85(8):1331-1339.

DIN. 38409-2. 1987. German standard methods for the examination of water, waste water and sludge; parameters characterizing effects and substances (group H); determination of filterable matter and the residue on ignition (H 2). Deutsche Industrienorm.

Dykens JA, Davis RE, Moos WH. 1999. Introduction to mitochondrial function and genomics. *Drug Dev Res*. 46(1):2-13.

ECHA. Registered substances in the European Union. 2020. European Chemicals Agency; [accessed 2020 22/8]. https://echa.europa.eu/information-on-chemicals/registered-substances.

Eder A, Exner-Kittridge M, Strauss P, Blöschl G. 2014. Re-suspension of bed sediment in a small stream–results from two flushing experiments. *Hydrol Earth Syst Sc*. 18(3):1043-1052.

Eganhouse R, Sherblom P. 2001. Anthropogenic organic contaminants in the effluent of a combined sewer overflow: impact on Boston Harbor. *Mar Environ Res*. 51(1):51-74.

Eggleton J, Thomas KV. 2004. A review of factors affecting the release and bioavailability of contaminants during sediment disturbance events. *Environ Int*. 30(7):973-980.

Escher BI, Aït-Aïssa S, Behnisch PA, Brack W, Brion F, Brouwer A, Buchinger S, Crawford SE, Du Pasquier D, Hamers T, Hettwer K, Hilscherová K, Hollert H, Kase R, Kienle C, Tindall AJ, Tuerk J, van der Oost R, Vermeirssen E, Neale PA. 2018. Effect-based trigger values for in vitro and in vivo bioassays performed on surface water extracts supporting the environmental quality standards (EQS) of the European Water Framework Directive. *Sci Total Environ*. 628-629:748-765.

Escher BI, Dutt M, Maylin E, Tang JYM, Toze S, Wolf CR, Lang M. 2012. Water quality assessment using the AREc32 reporter gene assay indicative of the oxidative stress response pathway. *J Environ Monit*. 14(11):2877-2885.

Escher BI, Henneberger L, König M, Schlichting R, Fischer FC. 2020. Cytotoxicity Burst? Differentiating Specific from Nonspecific Effects in Tox21 in Vitro Reporter Gene Assays. *Environ Health Perspect*. 128(7):077007.

Escher BI, van Daele C, Dutt M, Tang JYM, Altenburger R. 2013. Most Oxidative Stress Response In Water Samples Comes From Unknown Chemicals: The Need For Effect-Based Water Quality Trigger Values. *Environ Sci Technol*. 47(13):7002-7011.

EU. 2013/39. Directive 2013/39/EU of the European Parliament and of the Council of 12 August 2013 amending Directives 2000/60/EC and 2008/105/EC as regards priority substances in the field of water policy Text with EEA relevance.

Farré M, Barceló D. 2003. Toxicity testing of wastewater and sewage sludge by biosensors, bioassays and chemical analysis. *Trends Analyt Chem*. 22(5):299-310.

Fay KA, Villeneuve DL, Swintek J, Edwards SW, Nelms MD, Blackwell BR, Ankley GT. 2018. Differentiating pathway-specific from nonspecific effects in high-throughput toxicity data: a foundation for prioritizing adverse outcome pathway development. *Toxicol Sci*. 163(2):500-515.

Fent K. 2013. Ökotoxikologie: Umweltchemie-Toxikologie-Ökologie. Georg Thieme Verlag. ISBN: 3131693045

Gago-Ferrero P, Bletsou AA, Damalas DE, Aalizadeh R, Alygizakis NA, Singer HP, Hollender J, Thomaidis NS. 2019. Wide-scope target screening of> 2000 emerging contaminants in wastewater samples with UPLC-Q-ToF-HRMS/MS and smart evaluation of its performance through the validation of 195 selected representative analytes. *J Hazard Mater*.121712.

Gasperi J, Garnaud S, Rocher V, Moilleron R. 2008. Priority pollutants in wastewater and combined sewer overflow. *Sci Total Environ*. 407(1):263-272.

Giménez R, Casalí J, Grande I, Díez J, Campo MA, Álvarez-Mozos J, Goñi M. 2012. Factors controlling sediment export in a small agricultural watershed in Navarre (Spain). *Agric Water Manag*. 110:1-8.

Glaser C, Schwientek M, Zarfl C. 2019. Designing field-based investigations of organic micropollutant fate in rivers. *Environ Sci Pollut Res*.1-17.

Glassmeyer ST, Koplin DW, Furlong ET, Focazio M. 2008. Environmental presence and persistence of pharmaceuticals: an overview.

Grathwohl P, Rügner H, Wöhling T, Osenbrück K, Schwientek M, Gayler S, Wollschläger U, Selle B, Pause M, Delfs J-O. 2013. Catchments as reactors: a comprehensive approach for water fluxes and solute turnover. *Environ Earth Sci*. 69(2):317-333.

Guillet G, Knapp JL, Merel S, Cirpka OA, Grathwohl P, Zwiener C, Schwientek M. 2019. Fate of wastewater contaminants in rivers: Using conservative-tracer based transfer functions to assess reactive transport. *Sci Total Environ*. 656:1250-1260.

Harreß HM. 1973. Hydrogeologische Untersuchungen im Oberen Gäu [PhD thesis]. Eberhard Karls Universität Tübingen.

Hatefi Y. 1985. The mitochondrial electron transport and oxidative phosphorylation system. *Annu Rev Biochem*. 54(1):1015-1069.

Heeb F, Singer H, Pernet-Coudrier B, Qi W, Liu H, Longrée P, Müller B, Berg M. 2012. Organic micropollutants in rivers downstream of the megacity Beijing: sources and mass fluxes in a large-scale wastewater irrigation system. *Environ Sci Technol*. 46(16):8680-8688.

Heemken O, Stachel B, Theobald N, Wenclawiak B. 2000. Temporal variability of organic micropollutants in suspended particulate matter of the River Elbe at Hamburg and the River Mulde at Dessau, Germany. *Arch Environ Contam Toxicol*. 38(1):11-31.

Hollender J, Schymanski EL, Singer HP, Ferguson PL. 2017. Nontarget screening with high resolution mass spectrometry in the environment: ready to go? *Environ Sci Technol*. (51):11505-11512.

Hollert H, Duerr M, Erdinger L, Braunbeck T. 2000. Cytotoxicity of settling particulate matter and sediments of the Neckar River (Germany) during a winter flood. *Environ Toxicol Chem*. 19(3):528-534.

Huang R, Xia M, Cho M-H, Sakamuru S, Shinn P, Houck KA, Dix DJ, Judson RS, Witt KL, Kavlock RJ. 2011. Chemical genomics profiling of environmental chemical modulation of human nuclear receptors. *Environ Health Perspect*. 119(8):1142.

Invitrogen. Validation & Assay Performance Summary. 2007. GeneBLAzer® GR-UAS-bla HEK 293T Cells; [accessed 2018 06/13]. https://tools.thermofisher.com/content/sfs/manuals/GR_valpak_with_DAcells.pdf.

Invitrogen. Validation & Assay Performance Summary. 2010. GeneBLAzer® AR-UAS-bla GripTite™ Cells; [accessed 2018 05/26]. https://tools.thermofisher.com/content/sfs/manuals/geneblazer_ARGripTite_man.pdf.

Jaeger A, Posselt M, Betterle A, Schaper J, Mechelke J, Coll C, Lewandowski J. 2019. Spatial and temporal variability in attenuation of polar organic micropollutants in an urban lowland stream. *Environ Sci Technol*. 53(5):2383-2395.

Jekel M, Dott W, Bergmann A, Dünnbier U, Gnirß R, Haist-Gulde B, Hamscher G, Letzel M, Licha T, Lyko S, Miehe U, Sacher F, Scheurer M, Schmidt CK, Reemtsma T, Ruhl AS. 2015. Selection of organic process and source indicator substances for the anthropogenically influenced water cycle. *Chemosphere*. 125:155-167.

Jia A, Escher BI, Leusch FD, Tang JY, Prochazka E, Dong B, Snyder EM, Snyder SA. 2015. In vitro bioassays to evaluate complex chemical mixtures in recycled water. *Water Res*. 80:1-11.

Jin X, Peldszus S. 2012. Selection of representative emerging micropollutants for drinking water treatment studies: A systematic approach. *Sci Total Environ*. 414:653-663.

Jobelius C, Ruth B, Griebler C, Meckenstock RU, Hollender J, Reineke A, Frimmel FH, Zwiener C. 2010. Metabolites indicate hot spots of biodegradation and biogeochemical gradients in a high-resolution monitoring well. *Environ Sci Technol*. 45(2):474-481.

Jonker M, van Gestel CA, Kammenga JE, Laskowski R, Svendsen C. 2016. Mixture toxicity: linking approaches from ecological and human toxicology. CRC press. ISBN: 1439830096

Judson R, Houck K, Martin M, Richard AM, Knudsen TB, Shah I, Little S, Wambaugh J, Woodrow Setzer R, Kothya P. 2016. Editor's Highlight: analysis of the effects of cell stress and cytotoxicity on in vitro assay activity across a diverse chemical and assay space. *Toxicol Sci*. 152(2):323-339.

Kasprzyk-Hordern B, Dinsdale RM, Guwy AJ. 2009. Illicit drugs and pharmaceuticals in the environment–forensic applications of environmental data, part 2: pharmaceuticals as chemical markers of faecal water contamination. *Environ Pollut*. 157(6):1778-1786.

Kim J-Y, Sansalone JJ. 2008. Event-based size distributions of particulate matter transported during urban rainfall-runoff events. *Water Res*. 42(10-11):2756-2768.

Kim U-J, Oh JK, Kannan K. 2017. Occurrence, removal, and environmental emission of organophosphate flame retardants/plasticizers in a wastewater treatment plant in New York State. *Environ Sci Technol*. 51(14):7872-7880.

Kodešová R, Kočárek M, Kodeš V, Drábek O, Kozák J, Hejtmánková K. 2011. Pesticide adsorption in relation to soil properties and soil type distribution in regional scale. *J Hazard Mater*. 186(1):540-550.

Kolpin DW, Skopec M, Meyer MT, Furlong ET, Zaugg SD. 2004. Urban contribution of pharmaceuticals and other organic wastewater contaminants to streams during differing flow conditions. *Sci Total Environ*. 328(1-3):119-130.

Könemann S, Kase R, Simon E, Swart K, Buchinger S, Schlüsener M, Hollert H, Escher BI, Werner I, Ait-Aissa S. 2018. Effect-based and chemical analytical methods to monitor estrogens under the European Water Framework Directive. *Trends Analyt Chem*. 102:225-235.

König M, Escher BI, Neale PA, Krauss M, Hilscherová K, Novák J, Teodorović I, Schulze T, Seidensticker S, Hashmi MAK. 2017. Impact of untreated wastewater on a major European river evaluated with a combination of in vitro bioassays and chemical analysis. *Environ Pollut*. 220:1220-1230.

Krauss M, Singer H, Hollender J. 2010. LC–high resolution MS in environmental analysis: from target screening to the identification of unknowns. *Anal Bioanal Chem*. 397(3):943-951.

Lawrence JE, Skold ME, Hussain FA, Silverman DR, Resh VH, Sedlak DL, Luthy RG, McCray JE. 2013. Hyporheic zone in urban streams: a review and opportunities for enhancing water quality and improving aquatic habitat by active management. *Environ Eng Sci*. 30(8):480-501.

Lege S, Eisenhofer A, Heras JEY, Zwiener C. 2019. Identification of transformation products of denatonium–occurrence in wastewater treatment plants and surface waters. *Sci Total Environ*. 686:140-150.

Legler J, Broekhof JL, Brouwer A, Lanser PH, Murk AJ, van der Saag PT, Vethaak AD, Wester P, Zivkovic D, van der Burg B. 2000. A novel in vivo bioassay for (xeno-) estrogens using transgenic zebrafish. *Environ Sci Technol*. 34(20):4439-4444.

Letzel M. 2008. Verhalten prioritärer organischer Stoffe der Wasserrahmenrichtlinie in Kläranlagen und beim Eintrag in oberirdische Gewässer. *Bayerisches Landesamt für Umwelt (LfU), München*.

Li B, Danon-Schaffer MN, Li LY, Ikonomou MG, Grace JR. 2012. Occurrence of PFCs and PBDEs in landfill leachates from across Canada. *Water, Air, Soil Pollut*. 223(6):3365-3372.

Liu Y. 2019. Modelling the Fate of Sediments and Micropollutants in Rivers [PhD thesis]. Eberhard Karls Universität Tübingen.

Loos R, Gawlik BM, Locoro G, Rimaviciute E, Contini S, Bidoglio G. 2009. EU-wide survey of polar organic persistent pollutants in European river waters. *Environ Pollut*. 157(2):561-568.

Loraine GA, Pettigrove ME. 2006. Seasonal variations in concentrations of pharmaceuticals and personal care products in drinking water and reclaimed wastewater in southern California. *Environ Sci Technol*. 40(3):687-695.

Lorenz S, Rasmussen JJ, Süß A, Kalettka T, Golla B, Horney P, Stähler M, Hommel B, Schäfer RB. 2017. Specifics and challenges of assessing exposure and effects of pesticides in small water bodies. *Hydrobiologia*. 793(1):213-224.

Lorenzen A, Hendel JG, Conn KL, Bittman S, Kwabiah AB, Lazarovitz G, Masse D, McAllister TA, Topp E. 2004. Survey of hormone activities in municipal biosolids and animal manures. *Environ Toxicol*. 19(3):216-225.

LUBW. Daten- und Kartendienst der LUBW. 2020. Baden-Württemberg State Institute for the Environment, Survey and Nature Conservation; [accessed 2020 05/15]. https://udo.lubw.baden-wuerttemberg.de/projekte/api/processingChain?ssid=62abf969-105e-4ab2-8b20-b07c853b14d6&selector=abflussBW.Hochwasser.bwabfl%3Abwabfl_sel_hq_pegel.sel.

Lundqvist J, Mandava G, Lungu-Mitea S, Lai FY, Ahrens L. 2019a. In vitro bioanalytical evaluation of removal efficiency for bioactive chemicals in Swedish wastewater treatment plants. *Sci Rep*. 9(1):7166.

Lundqvist J, von Brömssen C, Rosenmai AK, Ohlsson Å, Le Godec T, Jonsson O, Kreuger J, Oskarsson A. 2019b. Assessment of pesticides in surface water samples from Swedish agricultural areas by integrated bioanalysis and chemical analysis. *Environ Sci Eur*. 31(1):53.

Madoux-Humery A-S, Dorner S, Sauvé S, Aboulfadl K, Galarneau M, Servais P, Prévost M. 2013. Temporal variability of combined sewer overflow contaminants: evaluation of wastewater micropollutants as tracers of fecal contamination. *Water Res*. 47(13):4370-4382.

Manamsa K, Lapworth D, Stuart M. 2016. Temporal variability of micro-organic contaminants in lowland chalk catchments: New insights into contaminant sources and hydrological processes. *Sci Total Environ*. 568:566-577.

Martindale W. 1993. The Extra Pharmacopoeia. London: Pharmaceutical Press. ISBN: 9780853693000

Martínez-Hernández V, Meffe R, Herrera S, Arranz E, de Bustamante I. 2014. Sorption/desorption of non-hydrophobic and ionisable pharmaceutical and personal care products from reclaimed water onto/from a natural sediment. *Sci Total Environ*. 472:273-281.

McBride HM, Neuspiel M, Wasiak S. 2006. Mitochondria: more than just a powerhouse. *Curr Biol*. 16(14):R551-R560.

McCready S, Birch GF, Long ER. 2006. Metallic and organic contaminants in sediments of Sydney Harbour, Australia and vicinity—a chemical dataset for evaluating sediment quality guidelines. *Environ Int*. 32(4):455-465.

McKee LJ, Bonnema A, David N, Davis JA, Franz A, Grace R, Greenfield BK, Gilbreath AN, Grosso C, Heim WA. 2017. Long-term variation in concentrations and mass loads in a semi-arid watershed influenced by historic mercury mining and urban pollutant sources. *Sci Total Environ*. 605:482-497.

Meyer JN, Leung MC, Rooney JP, Sendoel A, Hengartner MO, Kisby GE, Bess AS. 2013. Mitochondria as a target of environmental toxicants. *Toxicol Sci*. 134(1):1-17.

Moschet C, Götz C, Longrée P, Hollender J, Singer H. 2013a. Multi-level approach for the integrated assessment of polar organic micropollutants in an international lake catchment: the example of Lake Constance. *Environ Sci Technol*. 47(13):7028-7036.

Moschet C, Piazzoli A, Singer H, Hollender J. 2013b. Alleviating the reference standard dilemma using a systematic exact mass suspect screening approach with liquid chromatography-high resolution mass spectrometry. *Anal Chem*. 85(21):10312-10320.

Moschet C, Wittmer I, Simovic J, Junghans M, Piazzoli A, Singer H, Stamm C, Leu C, Hollender J. 2014. How a complete pesticide screening changes the assessment of surface water quality. *Environ Sci Technol*. 48(10):5423-5432.

Müller ME, Escher BI, Schwientek M, Werneburg M, Zarfl C, Zwiener C. 2018. Combining in vitro reporter gene bioassays with chemical analysis to assess changes in the water quality along the Ammer River, Southwestern Germany. *Environ Sci Eur*. 30(1):20.

Müller ME, Vikstrom S, König M, Schlichting R, Zarfl C, Zwiener C, Escher BI. 2019. Mitochondrial toxicity of selected micropollutants, their mixtures, and surface water samples measured by the oxygen consumption rate in cells. *Environ Toxicol Chem*. 38(5):1000-1011.

Müller ME, Werneburg M, Glaser C, Schwientek M, Zarfl C, Escher BI, Zwiener C. 2020a. Influence of emission sources and tributaries on the spatial and temporal patterns of micropollutant mixtures and associated effects in a small river. *Environ Toxicol Chem*. 39(7):1382-1391.

Müller ME, Zwiener C, Escher BI. 2020b. Storm event-driven occurrence and transport of dissolved and sorbed organic micropollutants and associated effects in the Ammer River, Southwestern Germany. *Environ Toxicol Chem*.

Munz NA, Burdon FJ, De Zwart D, Junghans M, Melo L, Reyes M, Schönenberger U, Singer HP, Spycher B, Hollender J. 2017. Pesticides drive risk of micropollutants in wastewater-impacted streams during low flow conditions. *Water Res*. 110:366-377.

Neale PA, Ait-Aissa S, Brack W, Creusot N, Denison MS, Deutschmann B, Hilscherová K, Hollert H, Krauss M, Novak J, Schulze T, Seiler T-B, Serra H, Shao Y, Escher BI. 2015. Linking in vitro effects and detected organic micropollutants in surface water using mixture-toxicity modeling. *Environ Sci Technol*. 49(24):14614-14624.

Neale PA, Altenburger R, Aït-Aïssa S, Brion F, Busch W, de Aragão Umbuzeiro G, Denison MS, Du Pasquier D, Hilscherová K, Hollert H, Morales DA, Novák J, Schlichting R, Seiler T-B, Serra H, Shao Y, Tindall AJ, Tollefsen KE, Williams TD, Escher BI. 2017a. Development of a bioanalytical test battery for water quality monitoring: fingerprinting identified micropollutants and their contribution to effects in surface water. *Water Res*. 123(Supplement C):734-750.

Neale PA, Antony A, Bartkow ME, Farre MJ, Heitz A, Kristiana I, Tang JY, Escher BI. 2012. Bioanalytical assessment of the formation of disinfection byproducts in a drinking water treatment plant. *Environ Sci Technol*. 46(18):10317-10325.

Neale PA, Braun G, Brack W, Carmona E, Gunold R, König M, Krauss M, Liebmann L, Liess M, Link M, Schäfer RB, Schlichting R, Schreiner VC, Schulze T, Vormeier P, Weisner O, Escher BI. 2020. Assessing the mixture effects in in-vitro bioassays of chemicals occurring in small agricultural streams during rain events. *Environ Sci Technol*. 54(13):8280-8290.

Neale PA, Munz NA, Aït-Aïssa S, Altenburger R, Brion F, Busch W, Escher BI, Hilscherová K, Kienle C, Novák J. 2017b. Integrating chemical analysis and bioanalysis to evaluate the contribution of wastewater effluent on the micropollutant burden in small streams. *Sci Total Environ*. 576:785-795.

Nivala J, Neale PA, Haasis T, Kahl S, König M, Müller RA, Reemtsma T, Schlichting R, Escher BI. 2018. Application of cell-based bioassays to evaluate treatment efficacy of conventional and intensified treatment wetlands. *Environ Sci-Wat Res*. 4(2):206-217.

OECD. 2004. Test No. 202: Daphnia sp. Acute Immobilisation Test.

Peterson E, Davis R, Orndorff H. 2000. 17 β-Estradiol as an indicator of animal waste contamination in mantled karst aquifers. *J Environ Qual*. 29(3):826-834.

Phillips P, Chalmers A, Gray J, Kolpin D, Foreman W, Wall G. 2012. Combined sewer overflows: an environmental source of hormones and wastewater micropollutants. *Environ Sci Technol*. 46(10):5336-5343.

Piram A, Salvador A, Verne C, Herbreteau B, Faure R. 2008. Photolysis of β-blockers in environmental waters. *Chemosphere*. 73(8):1265-1271.

Pomati F, Castiglioni S, Zuccato E, Fanelli R, Vigetti D, Rossetti C, Calamari D. 2006. Effects of a complex mixture of therapeutic drugs at environmental levels on human embryonic cells. *Environ Sci Technol*. 40(7):2442-2447.

Probert PM, Leitch AC, Dunn MP, Meyer SK, Palmer JM, Abdelghany TM, Lakey AF, Cooke MP, Talbot H, Wills C. 2018. Identification of a xenobiotic as a potential environmental trigger in primary biliary cholangitis. *J Hepatol*. 69(5):1123-1135.

Ridderstedt F, Widerström M, Lindh J, Lilja M. 2018. Sick leave due to diarrhea caused by contamination of drinking water supply with Cryptosporidium hominis in Sweden: a retrospective study. *J Water Health*. 16(5):704-710.

Roosens L, D'Hollander W, Bervoets L, Reynders H, Van Campenhout K, Cornelis C, Van Den Heuvel R, Koppen G, Covaci A. 2010. Brominated flame retardants and perfluorinated chemicals, two groups of persistent contaminants in Belgian human blood and milk. *Environ Pollut*. 158(8):2546-2552.

Rostami-Hodjegan A, Tucker GT. 2007. Simulation and prediction of in vivo drug metabolism in human populations from in vitro data. *Nat Rev Drug Discov*. 6(2):140-148.

Ruff M, Mueller MS, Loos M, Singer HP. 2015. Quantitative target and systematic non-target analysis of polar organic micro-pollutants along the river Rhine using high-resolution mass-spectrometry–identification of unknown sources and compounds. *Water Res*. 87:145-154.

Sakamuru S, Attene-Ramos MS, Xia M. 2016. Mitochondrial membrane potential assay. High-Throughput Screening Assays in Toxicology. Springer. p. 17-22.

Salgot M, Huertas E, Weber S, Dott W, Hollender J. 2006. Wastewater reuse and risk: definition of key objectives. *Desalination*. 187(1-3):29-40.

Sarmah AK, Meyer MT, Boxall AB. 2006. A global perspective on the use, sales, exposure pathways, occurrence, fate and effects of veterinary antibiotics (VAs) in the environment. *Chemosphere*. 65(5):725-759.

Schmadel NM, Ward AS, Kurz MJ, Fleckenstein JH, Zarnetske JP, Hannah DM, Blume T, Vieweg M, Blaen PJ, Schmidt C. 2016. Stream solute tracer timescales changing with discharge and reach length confound process interpretation. *Water Resour Res*. 52(4):3227-3245.

Schwarzenbach RP, Egli T, Hofstetter TB, Von Gunten U, Wehrli B. 2010. Global water pollution and human health. *Annu Rev Environ Resour*. 35:109-136.

Schwarzenbach RP, Escher BI, Fenner K, Hofstetter TB, Johnson CA, Von Gunten U, Wehrli B. 2006. The challenge of micropollutants in aquatic systems. *Science*. 313(5790):1072-1077.

Schwarzenbach RP, Gschwend PM, Imboden DM. 2016. Environmental organic chemistry. John Wiley & Sons. ISBN: 1118767233

Scott PD, Coleman HM, Khan S, Lim R, McDonald JA, Mondon J, Neale PA, Prochazka E, Tremblay LA, Warne MSJ. 2018. Histopathology, vitellogenin and chemical body burden in mosquitofish (Gambusia holbrooki) sampled from six river sites receiving a gradient of stressors. *Sci Total Environ*. 616:1638-1648.

Shao M, Tang X, Zhang Y, Li W. 2006. City clusters in China: air and surface water pollution. *Front Ecol Environ*. 4(7):353-361.

Simmons SO, Fan C-Y, Ramabhadran R. 2009. Cellular stress response pathway system as a sentinel ensemble in toxicological screening. *Toxicol Sci*. 111(2):202-225.

Singh KP, Mohan D, Sinha S, Dalwani R. 2004. Impact assessment of treated/untreated wastewater toxicants discharged by sewage treatment plants on health, agricultural, and environmental quality in the wastewater disposal area. *Chemosphere*. 55(2):227-255.

Smittskyddsinstitutet S. 2011. Cryptosporidium i Östersund-Smittskyddsinstitutets arbete med det dricksvattenburna utbrottet i Östersund 2010–2011 (How the Swedish Institute for Communicable Disease Control worked with the waterborne outbreak in Östersund 2010–2011). Smittskyddsinstitutet Sweden.

Soler M, Latron J, Gallart F. 2008. Relationships between suspended sediment concentrations and discharge in two small research basins in a mountainous Mediterranean area (Vallcebre, Eastern Pyrenees). *Geomorphology*. 98(1-2):143-152.

Sousa JMdCe, Peron AP, e Sousa LdS, de Moura Holanda M, Lima AdMV, de Oliveira VA, da Silva FCC, de Morais Lima LHG, Matos LA, de Moura Dantas SMM. 2017. Cytotoxicity and genotoxicity of Guaribas river water (Piauí, Brazil), influenced by anthropogenic action. *Environ Monit Assess*. 189(6):301.

Sun J, Zhang R, Qin L, Zhu H, Huang Y, Xue Y, An S, Xie X, Li A. 2017. Genotoxicity and cytotoxicity reduction of the polluted urban river after ecological restoration: a field-scale study of Jialu River in northern China. *Environ Sci Pollut Res*. 24(7):6715-6723.

Syed M, Skonberg C, Hansen SH. 2016. Mitochondrial toxicity of diclofenac and its metabolites via inhibition of oxidative phosphorylation (ATP synthesis) in rat liver mitochondria: Possible role in drug induced liver injury (DILI). *Toxicol In Vitro*. 31:93-102.

Szöcs E, Brinke M, Karaoglan B, Schäfer RB. 2017. Large scale risks from agricultural pesticides in small streams. *Environ Sci Technol*. 51(13):7378-7385.

Terada H. 1990. Uncouplers of oxidative phosphorylation. *Environ Health Perspect*. 87:213-218.

Tisler S, Zwiener C. 2018. Formation and occurrence of transformation products of metformin in wastewater and surface water. *Sci Total Environ*. 628:1121-1129.

Tousova Z, Oswald P, Slobodnik J, Blaha L, Muz M, Hu M, Brack W, Krauss M, Di Paolo C, Tarcai Z, Seiler T-B, Hollert H, Koprivica S, Ahel M, Schollée JE, Hollender J, Suter MJF, Hidasi AO, Schirmer K, Sonavane M, Ait-Aissa S, Creusot N, Brion F, Froment J, Almeida AC, Thomas K, Tollefsen KE, Tufi S, Ouyang X, Leonards P, Lamoree M, Torrens VO, Kolkman A, Schriks M, Spirhanzlova P, Tindall A, Schulze T. 2017. European demonstration program on the effect-based and chemical identification and monitoring of organic pollutants in European surface waters. *Sci Total Environ*. 601-602:1849-1868.

Tran NH, Reinhard M, Khan E, Chen H, Nguyen VT, Li Y, Goh SG, Nguyen QB, Saeidi N, Gin KY-H. 2019. Emerging contaminants in wastewater, stormwater runoff, and surface water: Application as chemical markers for diffuse sources. *Sci Total Environ*. 676:252-267.

van Gils J, Posthuma L, Cousins IT, Lindim C, de Zwart D, Bunke D, Kutsarova S, Müller C, Munthe J, Slobodnik J. 2019. The European Collaborative Project SOLUTIONS developed models to provide diagnostic and prognostic capacity and fill data gaps for chemicals of emerging concern. *Environ Sci Eur*. 31(1):72.

Van Metre PC, Mahler BJ. 2005. Trends in hydrophobic organic contaminants in urban and reference lake sediments across the United States, 1970− 2001. *Environ Sci Technol*. 39(15):5567-5574.

Völker J, Stapf M, Miehe U, Wagner M. 2019. Systematic review of toxicity removal by advanced wastewater treatment technologies via ozonation and activated carbon. *Environ Sci Technol*. 53(13):7215-7233.

Vryzas Z, Vassiliou G, Alexoudis C, Papadopoulou-Mourkidou E. 2009. Spatial and temporal distribution of pesticide residues in surface waters in northeastern Greece. *Water Res*. 43(1):1-10.

Welch WJ. 1993. How cells respond to stress. *Sci Am*. 268(5):56-64.

Wittmer I, Bader H-P, Scheidegger R, Singer H, Lück A, Hanke I, Carlsson C, Stamm C. 2010. Significance of urban and agricultural land use for biocide and pesticide dynamics in surface waters. *Water Res*. 44(9):2850-2862.

Worrall F, Parker A, Rae J, Johnson A. 1996. Equilibrium adsorption of isoproturon on soil and pure clays. *Eur J Soil Sci*. 47(2):265-272.

Yuan J, Wu X-J, Lu W-Q, Cheng X-L, Chen D, Li X-Y, Liu A-L, Wu J-J, Xie H, Stahl T. 2005. Chlorinated river and lake water extract caused oxidative damage, DNA migration and cytotoxicity in human cells. *Int J Hyg Environ Health*. 208(6):481-488.

Zarfl C, Adolphi C, Best N, Degenhardt R, Glauch L, König M, Schlichting R, Schwientek M, Werneburg M, Zwiener C, Escher BI. 2020. Dynamics of mixture effects and causative chemicals during rain events in rivers in agricultural and urban areas. Conference Poster, SETAC Europe Annual Meeting 2020. Dublin, Ireland.

Zedda M, Zwiener C. 2012. Is nontarget screening of emerging contaminants by LC-HRMS successful? A plea for compound libraries and computer tools. *Anal Bioanal Chem*. 403(9):2493-2502.

Zgheib S, Moilleron R, Chebbo G. 2011a. Influence of the land use pattern on the concentrations and fluxes of priority pollutants in urban stormwater. *Water Sci Technol*. 64(7):1450-1458.

Zgheib S, Moilleron R, Saad M, Chebbo G. 2011b. Partition of pollution between dissolved and particulate phases: what about emerging substances in urban stormwater catchments? *Water Res*. 45(2):913-925.

Zhang J-H, Chung TD, Oldenburg KR. 1999. A simple statistical parameter for use in evaluation and validation of high throughput screening assays. *J Biomol Screen*. 4(2):67-73.

Zhou W, Moore DE. 1994. Photochemical decomposition of sulfamethoxazole. *Int J Pharm*. 110(1):55-63.

6. Supplemental Information

6.1. Iceberg modeling (Study 2)

To evaluate the overlap of the detected target compounds and the applied *in-vitro* bioassays during **Study 2** iceberg modelling was applied. The cumulative effect BEQ_{chem} induced by the detected target compounds were predicted and calculated based on the concentration of a quantified target compound and its effect or cytotoxicity data, according to König et al. (2017). Therefore, the relative effect potencies (REP_i) were computed by Equation S1, based on the effect data of the detected chemicals (EC_{10} [i]) and the reference compound (EC_{10} [reference]).

$$REP_i = \frac{EC_{10}\ (reference)}{EC_{10}\ (i)} \qquad (S1)$$

Effect data for single chemicals was obtained from Escher et al. (2018), Escher et al. (2020) and Neale et al. (2020). Metaphorically speaking, the effect of a sample measured in a bioassay (BEQ_{bio}) stands for the entire body of an iceberg, whereas the effect that can be explained by the quantified target compounds (BEQ_{chem}) represents the uncovered tip of the iceberg visible above the surface. BEQ_{chem} was calculated using Equation S2.

$$BEQ_{chem} = \sum_{i=i}^{n} REP_i \times C_i \qquad (S2)$$

The more effect is explained by the detected target analytes the greater the overlap of the detection windows of chemical analysis and *in-vitro* bioassay. In the grab samples and the temporally resolved samples at AS1, AS2 and AS3 at maximum only three of 27 detected target analytes were found to be active in the applied *in-vitro* bioassays and the effects explained were in all samples and assays below 0.12%, see **Figure SI 1 and 2**. Since here only little of the measured effects could be explained, the analytical windows of the chemical analysis and the four *in-vitro* bioassays appear to hardly overlap. Hence, the application of chemical analysis and the *in-vitro* bioassays is a complementary combination.

The electron transport chain inhibition measured in the LV-SPE samples of **Study 2** was explained by at maximum 0.06%, by the detected target compounds diclofenac, lamotrigine and benzotriazole (**Figure S3**).

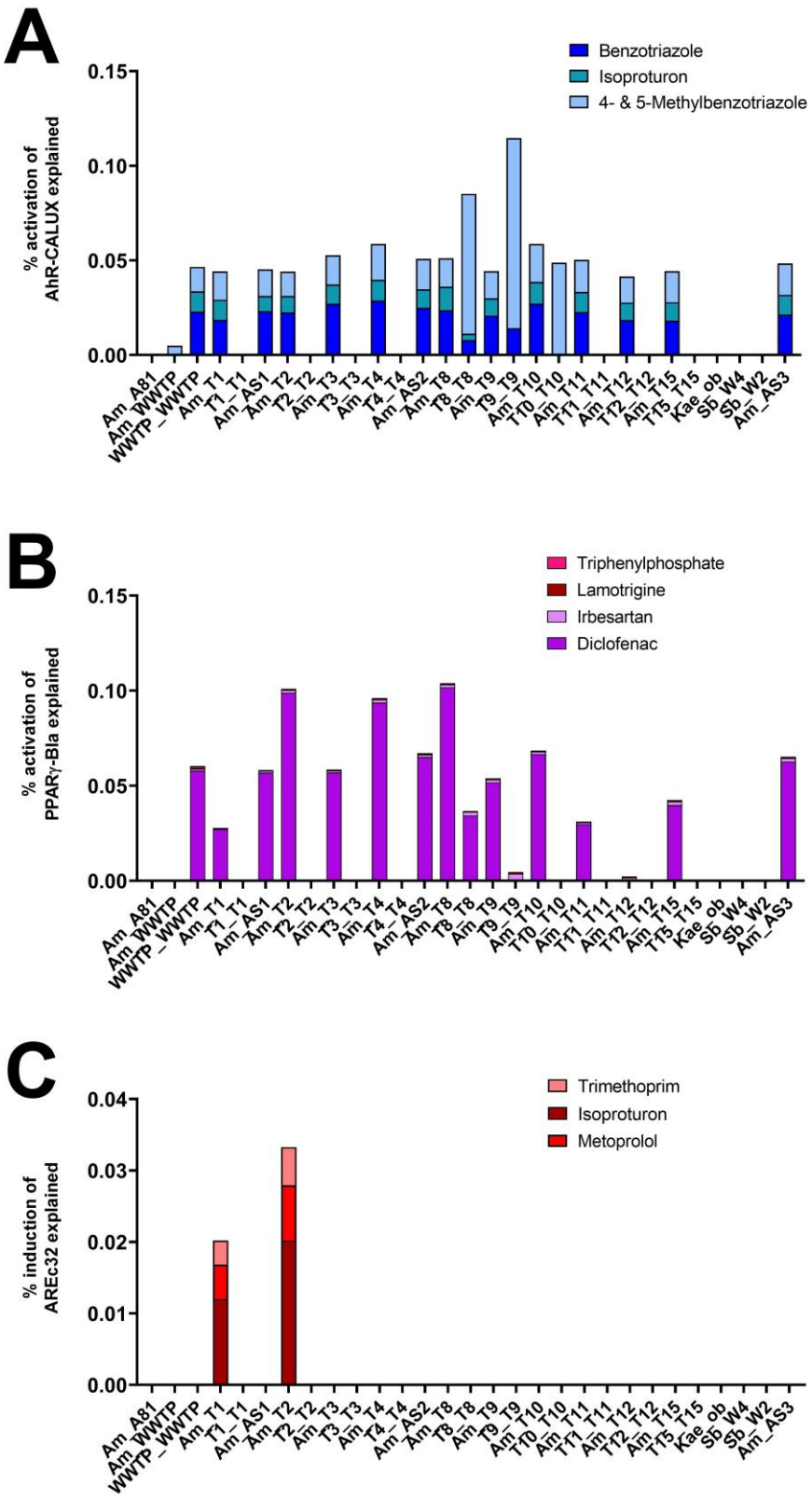

Figure SI 1: % Activation or induction of the grab samples measured in the in-vitro bioassays AhR-CALUX (A), PPARγ-Bla (B) and AREc32 (C) explained by the quantified target compounds.

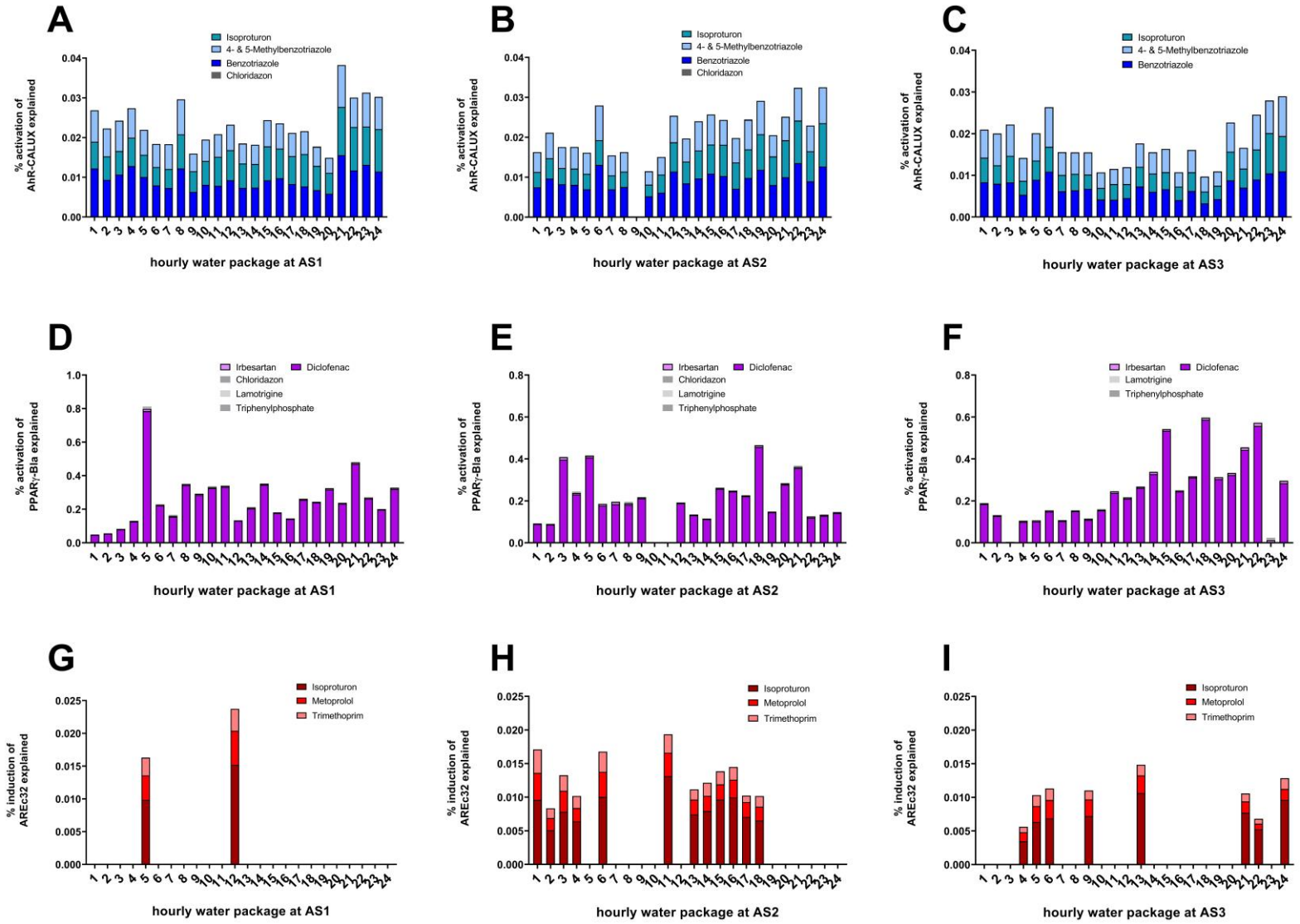

Figure SI 2: % Activation or induction of the temporally resolved taken samples at AS1 (A, D and G), AS2 (B, E and H) and AS3 (C, F and I) measured in the in-vitro bioassays AhR-CALUX (A to C), PPARγ-Bla (D to F) and AREc32 (G to I) explained by the quantified target compounds.

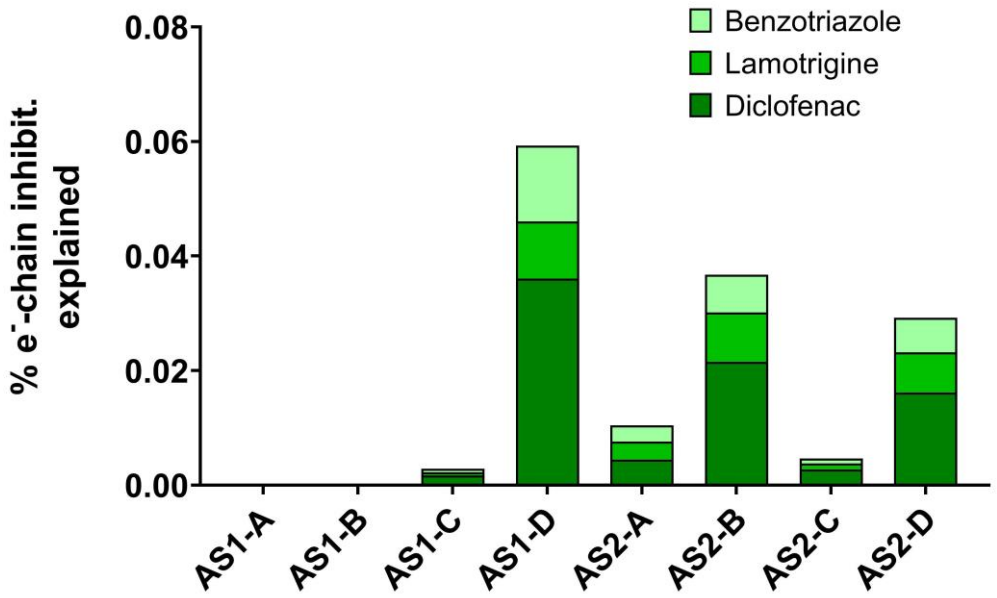

Figure SI 3: % Electron transport chain inhibition, measured in the LV-SPE samples of Study 2, explained by the detected target compounds benzotriazole, lamotrigine and diclofenac.

7. Thesis publications

Publication 1

Combining *in vitro* reporter gene bioassays with chemical analysis to assess changes in the water quality along the Ammer River, Southwestern Germany

Maximilian E. Müller [a], Beate I. Escher [a,b], Marc Schwientek [a], Martina Werneburg [a], Christiane Zarfl [a] and Christian Zwiener [a]

[a]Eberhard Karls University of Tübingen, Center for Applied Geoscience, 72074 Tübingen, Germany

[b]UFZ – Helmholtz Centre for Environmental Research, 04318 Leipzig, Germany

Published in *Environmental Sciences Europe*, DOI: 10.1186/s12302-018-0148-y

Müller *et al. Environ Sci Eur (2018) 30:20*
https://doi.org/10.1186/s12302-018-0148-y

Environmental Sciences Europe

RESEARCH

Open Access

Combining in vitro reporter gene bioassays with chemical analysis to assess changes in the water quality along the Ammer River, Southwestern Germany

Maximilian E. Müller[1], Beate I. Escher[1,2], Marc Schwientek[1], Martina Werneburg[1], Christiane Zarfl[1] and Christian Zwiener[1*]

Abstract

Background: Rivers receive water and associated organic micropollutants from their entire catchment, including from urban, agricultural and natural sources, and constitute an important environmental component for catalyzing pollutant turnover. Environmental removal processes were extensively investigated under laboratory conditions in the past but there is still a lack of information on how organic micropollutants attenuate on the catchment scale. The aim of this study was to describe the chemical and toxicological profile of a 4th order river and to characterize in-stream processes. We propose indicator chemicals and indicator in vitro bioassays as screening methods to evaluate micropollutant input and transport and transformation processes of the chemical burden in a river. Carbamazepine and sulfamethoxazole were selected as indicators for dilution processes and the moderately degradable chemicals tramadol and sotalol as indicators for potential in-stream attenuation processes. The battery of bioassays covers seven environmentally relevant modes of action, namely estrogenicity, glucocorticogenic activity, androgenicity progestagenic activity and oxidative stress response, as well as activation of the peroxisome proliferator-activated receptor and the aryl hydrocarbon receptor, using the GeneBLAzer test battery and the AhR-CALUX and AREc32 assays.

Results: Both approaches, targeted chemical analysis and in vitro bioassays, identified a wastewater treatment plant (WWTP) as a major input source of organic micropollutants that dominantly influenced the water quality of the river. Downstream of the WWTP the amount of detected chemicals and biological effects decreased along the river flow. The organic indicator chemicals of known degradability uncovered dilution and potential loss processes in certain river stretches. The average cytotoxic potency of the river water decreased in a similar fashion as compounds of medium degradability such as the pharmaceutical sotalol.

Conclusions: This study showed that the indicator chemical/indicator bioassay approach is suitable for identifying input sources of a mixture of organic micropollutants and to trace changes in the water quality along small rivers. This method forms the necessary basis for evaluating the natural attenuation processes of organic micropollutants on a catchment scale, especially when combined with enhanced sampling strategies in future studies.

Keywords: LC–MS analysis, In vitro bioassays, Bioanalytical equivalent concentration, Organic indicator chemicals, Catchment scale, Wastewater

*Correspondence: christian.zwiener@uni-tuebingen.de
[1] Center for Applied Geoscience, Eberhard Karls University of Tübingen, 72074 Tübingen, Germany
Full list of author information is available at the end of the article

Background

Rivers collect water, sediments and solute fluxes, and integrate the input of chemicals within their entire catchment. The chemical burden of an anthropogenically impacted river is mostly governed by pharmaceuticals, pesticides, chemicals of industrial use and their transformation products [1, 2]. Their input sources can be point sources such as wastewater effluents or diffuse sources such as runoff and leaching from agricultural and urban regions [3]. Surface waters are environmental compartments that host important transport and transformation processes of organic micropollutants. Sophisticated screening methods are needed to characterize the input sources of organic micropollutants and their natural attenuation on the catchment scale. Targeted chemical analysis is typically used in water quality monitoring programs [4] and provides important information about the concentration of selected compounds, but is often insufficient to reflect the large number of different chemicals present in a sample [5]. Moreover, the analytical window of detectable chemicals is limited due to their physicochemical properties. In vitro bioassays that are based on reporter gene cell lines that mediate a measurable signal (effect) when exposed to a chemical can be a complementary analytical tool as they detect micropollutants, transformation products and their mixtures, which may not be covered by the chemical analysis [6]. A combined chemical and toxicological approach has the potential for a comprehensive assessment of water quality [7] and it has been proposed to complement the chemical status assessment with effect-based methods, for instance in the Water Framework Directive [5, 8]. Besides the specific effect in a bioassay, cytotoxicity can give information about the total chemical load of a sample.

In previous studies, diverse batteries of in vitro bioassays were used to assess the chemical burden of wastewater, recycled water, surface water and drinking water (e.g., from Australia [9], the US [10], Europe (multinational) [11], the Netherlands [12], Slovenia [13], France [14]), the impact of untreated wastewater on surface waters [15] and the efficiency of nature-based [16], conventional [17] and advanced [18] wastewater treatment technologies.

Effect-based methods have also been applied together with chemical analysis to characterize the surface waters of larger river systems such as the Danube river [19], but little work has been done on the catchment scale in smaller order rivers and creeks.

The use of indicator chemicals that are indicative for certain input sources or biotic and abiotic transformation processes can be applied to interpret the results from chemical analysis. Organic indicator chemicals have been used previously for studying drinking water treatment [20], evaluating the impact of sewer leakages on groundwater [21], natural attenuation processes in contaminated groundwater [22], surveilling hospital effluents [23] and potable reuse [24]. A chemical that is used as an indicator must meet certain criteria that will depend on the study purpose [25], e.g., emission, degradability and partitioning properties [26].

The aim of this study was to investigate a 4th order stream using a combination of bioanalytical tools and chemical analytics and test their power in characterizing input sources and dilution and loss processes of organic chemicals in rivers. The Ammer River is a tributary of the Neckar River located in Southwestern Germany, close to Tübingen, that receives input from wastewater treatment plants (WWTP) and flows through urban and agricultural areas. The water quality of the Ammer River was monitored at nine sampling sites from the source to the mouth, where it flows into the Neckar River, using LC–HRMS targeting 79 known pollutants that may serve as indicator chemicals. We considered chemicals from different compound classes and input sources, like pharmaceuticals, insecticides, fungicides, herbicides and household chemicals. These compounds also represent different degrees of degradability under environmental conditions, like the rather persistent carbamazepine and sulfamethoxazole, the biodegradable sotalol and venlafaxine, or diclofenac which is also photodegraded. We also applied a test battery of seven in vitro bioassays covering seven environmentally relevant modes of action, namely estrogenicity [15], glucocorticogenic activity [27], androgenicity [15], progestagenic activity [15], oxidative stress response [28, 29], peroxisome proliferator-activated receptor activity [30] and aryl hydrocarbon receptor induction [31]. The assays for androgenicity and progestagenic activity were also performed in antagonistic mode to identify possible antagonists present in the samples that suppress the effect of an agonist.

Methods

Chemicals and reagents

Methanol, acetonitrile, water, formic acid and acetic acid were all LC/MS grade and purchased from Optima®, Thermo Fisher Scientific (Waltham, US-MA). Ethyl acetate was provided by Acros Organics, Thermo Fisher Scientific (Waltham, US-MA). 79 chemicals were monitored including pharmaceuticals, herbicides, fungicides, insecticides, antibiotics and other substances of anthropogenic origin (for details see Additional file 1: Tables S1 and S2).

Sampling sites

The Ammer River with a catchment size of approximately 238 km^2 is located in Southwestern Germany, and flows over a distance of approximately 22 km from Herrenberg to Tübingen, where it flows into the river Neckar. At

the time of sampling (July 18th, 2017), the Ammer River was mainly fed by karstic springs emerging from limestone and gypsum aquifers and treated wastewater. All sampling sites are listed in Table 1. With a discharge of 0.40 $m^3 s^{-1}$ at the gauge Pfäffingen (sampling site 5), the flow was below the average annual low flow (0.44 $m^3 s^{-1}$). The pump station Herrenberg uses water from a limestone spring for drinking water treatment. Five kilometers downstream of the spring the Ammer River receives effluent from the catchment's largest WWTP [80,000 PE (population equivalent)]. The contribution of treated wastewater at site 4 was estimated to be 81% based on electrical conductivity measurements (see Additional file 1: Section S1 and Table S3). The Ammer River receives input from a second WWTP (9000 PE) located between the villages Hailfingen and Tailfingen through the small Kochart Creek, which plays a minor role in water and chemical input due to its size.

Six sampling sites along the main stem and three sampling sites along the Ammer Canal were chosen to characterize and identify input sources that affect the water quality (Table 1, Fig. 1). The samples were taken within 8 h along the flow direction, starting at the Ammer source, in order to reduce the effects of transient flow. Furthermore, samples were taken from the "Kleiner Goldersbach (G)", a remote tributary within a nature reserve that was expected to be unaffected by domestic and industrial wastewaters, and the tributaries Schönbrunnen (SB) and Mühlbach (MS).

Table 1 Numbering and description of the sampling locations, in accordance with Fig. 1

Index	Sampling site location	Geographic coordinates
1	Ammer source	48°35′03.4″N 8°51′17.7″E
2	Pump station Herrenberg	48°35′02.7″N 8°51′48.5″E
3	Ammer upstream of WWTP	48°34′04.7″N 8°53′30.7″E
4	Ammer downstream of WWTP	48°33′48.8″N 8°54′00.6″E
5	Ammer downstream of Käsbach mouth	48°31′34.7″N 8°57′50.9″E
6	Ammer canal downstream of Mühlbach mouth	48°31′12.7″N 9°00′18.9″E
7	Ammer canal	48°31′10.0″N 9°01′24.1″E
8	Ammer canal at Nonnenhaus	48°31′17.9″N 9°03′20.2″E
9	Ammer upstream of Goldersbach mouth	48°31′37.7″N 9°04′28.8″E
G	Kleiner Goldersbach creek	48°34′33.5″N 9°02′06.0″E
SB W1	Schönbrunnen weir 1	48°32′37.1″N 8°57′54.3″E
SB W2	Schönbrunnen weir 2	48°32′21.4″N 8°57′41.9″E
MS	Mühlbach source	48°31′04.8″N 8°58′43.3″E

Sampling and sample preparation

Grab samples of water were collected at each sampling site, from the middle of the water body at half depth on July 18th 2017. Solid phase extraction (SPE) was used for analyte preconcentration. 500 mg Oasis HLB (waters) cartridges were preconditioned with 10 mL methanol and 10 mL ethyl acetate. Two liters of river water from each sampling site were passed through the extraction cartridges using a vacuum manifold (Phenomenex®). After extraction, the sorbents were aspirated to dryness by vacuum and stored at −20 °C until they were eluted with 10 mL methanol and 10 mL ethyl acetate. The eluates were combined and passed through a 0.2 µm polyethersulfone filter (PES, 0.2 µm, Agilent Captiva Premium Syringe filter) to remove any remaining solid particles. Subsequently, the extracts were reduced to dryness by a gentle stream of nitrogen at 40 °C (Barkey Vapotherm basis mobil II) and reconstituted in methanol to achieve an enrichment factor of 1000. The extracts were stored at −20°C until measurement. To check for background signals caused by the SPE procedure, a blank was provided by extracting 2 L of MilliQ (Thermo Fisher Scientific, GenPure Pro UV-TOC).

Chemical analysis

Target screening analysis of the sample extracts was performed by liquid chromatography (Agilent 1290 LC) coupled to high resolution mass spectrometry (Agilent 6550 iFunnel Q-TOF-MS). Analyte separation was achieved by an Agilent Poroshell 120 EC-C18 column (2.7 µm particle size, 4.6 × 150 mm) and a gradient program using water/acetonitrile both with 0.1% formic acid in the case of positive ESI or with 0.1% acetic acid in the case of negative ESI. External calibration solutions were prepared for identification and quantitation. Reference standard solutions were first measured in an All-Ion Fragmentation (AIF) mode, which allows acquisition of mass fragmentation data without precursor selection. Data analysis and evaluation were performed by Mass Hunter Qualitative Analysis B.07.00 and Mass Hunter Quantitative Analysis software B.06.00 (Agilent Technologies, CA, USA). The data acquired by AIF were evaluated by the Find by Formula (FBF) algorithm to identify target compounds based on accurate mass, retention time and accurate mass fragments to reduce the number of false positives. To assess matrix effects on quantification, standard addition of all analytes at about 30 µg L^{-1} was used exemplarily for samples from sites 2 (pump station Herrenberg), 4 (Ammer downstream WWTP) and 8 (Ammer canal Nonnenhaus). Signal suppression or enhancement of the target compounds in the Ammer main stem was calculated and considered for quantification based on the following scheme: matrix effect of sample 2 was considered for samples 1, 2 and 3, matrix effect of sample 4 was

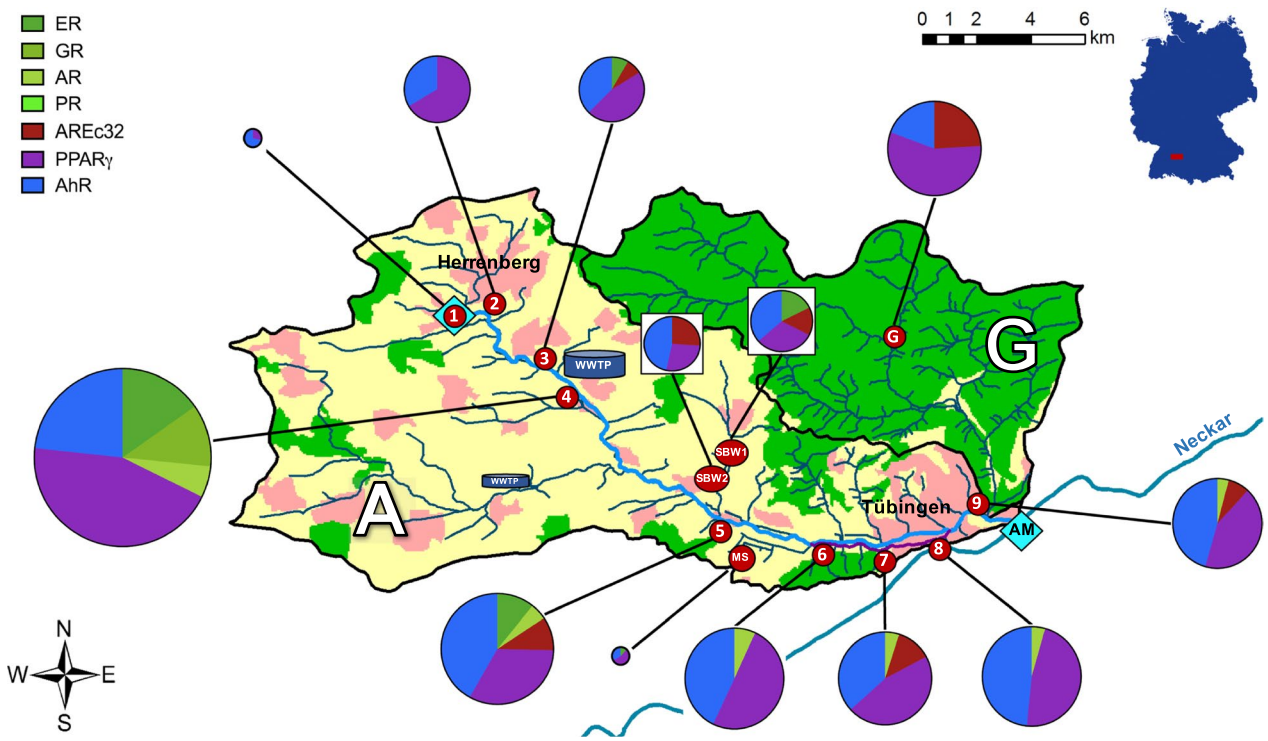

Fig. 1 Catchments of the river Ammer (A) and its tributary Goldersbach (G). From source (cyan diamond at sampling site 1) to mouth (AM, cyan diamond downstream of sampling site 9), the Ammer River flows over 22 km; numbers in red circles indicate sampling sites (Table 1). Downstream of site 6 the Ammer bifurcates, only the Canal (purple line) was sampled. Before site 9, the canal and the stream merge again. The pie charts present the bioassay results at each sampling site and show the toxicological patterns (chart colors) and average cytotoxicity (chart size). The colors within the map illustrate urban areas (pale red), agricultural areas (yellow) and woodland (green)

considered for samples 4 and 5, and matrix effect of sample 8 was considered for samples 6, 7, 8 and 9.

In vitro bioassays

In this current study, seven in vitro reporter gene bioassays covering nine different endpoints were applied (Table 2). The ERα-GeneBLAzer [15], GR-GeneBLAzer [27, 32], AR-GeneBLAzer [15, 33] and PR-GeneBLAzer [15, 34] are reporter gene cell lines that generate a hormone receptor-mediated response when exposed to chemicals that trigger the estrogen receptor (ERα), the androgen receptor (AR), the glucocorticoid receptor (GR) and the progestagenic receptor (PR), respectively. The AR-GeneBLAzer and PR-GeneBLAzer were also measured in antagonistic mode to detect chemicals causing suppression of the effect of an agonist added at a constant concentration in the bioassay. The AhR-CALUX [31] mediates a measurable signal in the presence of chemicals having an affinity for the aryl hydrocarbon receptor (AhR), such as dioxin-like compounds. The PPARγ-GeneBLAzer [30] responds to chemicals binding to the peroxisome proliferator-activated receptor γ (PPARγ), a molecular target of several drugs that is involved in many cell metabolism pathways. The AREc32 [28, 29] indicates the activation of the oxidative stress response triggered by stressors like electrophilic chemicals or reactive oxygen species and is mediated via the antioxidant response element (ARE).

The experimental procedures of the bioassays are described in [15, 30]. All concentrations were expressed in units of relative enrichment factor (REF) which take the enrichment by SPE and the dilution in the assay into account [6]. The maximum concentration applied was REF 100.

Data treatment and presentation

The concentration-effect curve for cell viability was fitted with a log-sigmoidal model (Eq. 1), using slope of the curve and the inhibitory concentration causing 50% reduction in cell viability (IC_{50}) as the fit parameters.

$$\text{Cell viability} = \frac{1}{1 + 10^{\text{slope} \cdot (\log IC_{50} - \log \text{concentration})}} \quad (1)$$

Table 2 Overview of the in vitro bioassays, endpoints, reference compounds, EC values and literature source of the methods [EC_{10}: Concentration causing 10% effect relative to the maximum triggered by a positive control (Eq. 3); $EC_{IR1.5}$: Concentration causing an induction ratio of 1.5 (Eq. 4); $EC_{SR0.2}$: Concentration causing a suppression ratio of 0.2 in the presence of the agonist (Eq. 5)]

Assays	Mode of action	Reference compound	EC value	Reference method
ERα-GeneBLAzer	Estrogenicity	17β-Estradiol (E2)	EC_{10}	[15]
GR-GeneBLAzer	Glucocorticogenic activity	Dexamethasone	EC_{10}	[27, 32]
AR-GeneBLAzer	Androgenicity	Metribolone (R1881)	EC_{10}	[15, 33]
Anti AR-GeneBLAzer	Anti androgenicity	Cyproterone acetate (antagonist) Metribolone R1881 (agonist)	$EC_{SR0.2}$	[15, 33]
PR-GeneBLAzer	Progestagenic activity	Promegestone	EC_{10}	[15, 34]
Anti PR-GeneBLAzer	Anti progestagenic activity	Mifepristone RU-486 (antagonist) Promegestone (agonist)	$EC_{SR0.2}$	[15, 34]
AREc32	Oxidative stress response (adaptive stress response)	*t*-Butyl-hydroquinone (tBHQ)	$EC_{IR1.5}$	[28, 29]
PPARγ-GeneBLAzer	Peroxisome proliferation activation	Rosiglitazone	EC_{10}	[30]
AhR-CALUX	Aryl hydrocarbon receptor induction	2,3,7,8-Tetrachlorodibenzodioxin (TCDD)	EC_{10}	[31] with modifications of [16]

The concentration causing 10% cell death (IC_{10}) was calculated according to Eq. (2).

$$\log IC_{10} = \log IC_{50} - \left(\frac{1}{\text{slope}}\right)\log\left(\frac{10\%}{100\% - 10\%}\right) \quad (2)$$

For evaluation of the activation of the nuclear receptors and transcription factors, only concentrations below the IC_{10} for cytotoxicity were used. For the antagonistic mode of the AR and PR assays, concentrations above the IC_{01} were excluded to avoid false-positive antagonistic effects. Effect data above 40% or an induction ratio (IR) greater than 5 were also excluded to ensure linearity of the concentration-effect curves [9]. From the linear concentration-effect curves, the following effect concentrations (EC) were derived: the concentration causing 10% of the maximum effect (EC_{10}, Eq. 3), the concentration causing an induction ratio of 1.5 ($EC_{IR1.5}$, Eq. 4) or the concentration causing 20% suppression of the effects elicited by a constant concentration of the agonists R1881 ($8.81 \cdot 10^{-8}$ M) in Anti-AR and promegestone ($8.10 \cdot 10^{-9}$ M) in Anti-PR ($EC_{SR0.2}$, Eq. 5).

$$EC_{10} = \frac{10\%}{\text{slope}} \quad (3)$$

$$EC_{IR1.5} = \frac{0.5}{\text{slope}} \quad (4)$$

$$EC_{SR0.2} = \frac{0.2}{\text{slope}} \quad (5)$$

The standard errors (SE) of the EC_{10}, $EC_{IR1.5}$ and $EC_{SR0.2}$ were calculated according to Eqs. (6), (7) and (8).

$$SE(EC_{10}) = \frac{10\%}{\text{slope}^2} * SE_{\text{slope}} \quad (6)$$

$$SE(EC_{IR1.5}) = \frac{0.5}{\text{slope}^2} * SE_{\text{slope}} \quad (7)$$

$$SE(EC_{SR0.2}) = \frac{0.2}{\text{slope}^2} * SE_{\text{slope}} \quad (8)$$

The IC_{10} and EC values were transformed into toxic units (TU) because TU can better visualize toxicity as a high TU relates to a high effect. The cytotoxicity of a sample was expressed as $TU_{cytotoxicity}$ according to Eq. (9).

$$TU_{\text{cytotoxicity}} = \frac{1}{IC_{10_i}} \quad (9)$$

The specific effects of the bioassays (EC_{10}, $EC_{IR1.5}$ and $EC_{SR0.2}$) were expressed as $TU_{specific.effects}$ (Eq. 10).

$$TU_{\text{specific effects}} = \frac{1}{EC_{10}} \text{ or } \frac{1}{EC_{IR1.5}} \text{ or } \frac{1}{EC_{SR0.2}} \quad (10)$$

To achieve a measure comparable to other surface water case studies, the bioanalytical equivalent concentration (BEQ) was calculated with Eq. (11):

$$\mathrm{BEQ} = \frac{\mathrm{EC_{10}(reference)}}{\mathrm{EC_{10}(sample)}} \text{ or } \frac{\mathrm{EC_{IR1.5}(reference)}}{\mathrm{EC_{IR1.5}(sample)}} \text{ or } \frac{\mathrm{EC_{SR0.2}(reference)}}{\mathrm{EC_{SR0.2}(sample)}} \quad (11)$$

The error of the BEQ (SE(BEQ)) was calculated by error propagation with Eq. (12).

$$\mathrm{SE(BEQ)} = \sqrt{\left(\frac{1}{\mathrm{EC_{sample}}}\right)^2 \mathrm{SE(EC_{reference})}^2 + \left(\frac{\mathrm{EC_{reference}}}{\mathrm{EC_{sample}^2}}\right)^2 \mathrm{SE\left(EC_{sample}\right)}^2} \quad (12)$$

Results

In vitro bioassays

The concentrations causing cytotoxicity and effect IC_{10} and EC_{10} in the in vitro bioassays are presented in Table 3 and all concentration-effect curves, as well as the EC_{10} values of the reference compounds, are depicted in the Additional file 1: Table S4 and Figures S1–S7, respectively. All agonistic endpoints except for the PR-GeneBLAzer were triggered by at least one of the tested samples. The bioassays indicative of the hormone receptors AR-GeneBLAzer and PR-GeneBLAzer were also evaluated in antagonistic mode, i.e., in the presence of a constant concentration of agonist causing approximately 80% of the maximum effect, but showed no antagonistic effects ($EC_{SR0.2}$) (Additional file 1: Figures S3 and S4). The solvent blank caused no measurable response in any assay (Additional file 1: Figures S1–S7). The PPARγ-GeneBLAzer and AhR-CALUX were the most responsive assays, with activation observed in all samples and at very low EC_{10} values for the samples from sites 4 to 9 (appearing at a REF 1 to 6) compared to all other bioassays.

At site 1, no cytotoxicity was observed up to the highest tested REF of 100 with low effects in PPARγ-GeneBLAzer and AhR-CALUX. At site 2, with the exception of AhR-CALUX, all assays caused 10% cell death within the applied concentration range. With the exception of AR-GeneBLAzer and PPARγ-GeneBLAzer, cytotoxicity was detected in all assays along with low effects in ERα-GeneBLAzer, AREc32, PPARγ-GeneBLAzer and AhR-CALUX at site 3, upstream of the WWTP. The samples taken downstream of the WWTP at site 4 showed cytotoxicity and activation in all agonistic assays, except for PR-GeneBLAzer, and yielded the lowest IC_{10} and EC_{10} values of all samples from the Ammer River. This is not surprising as this WWTP effluent was already shown to have a distinct impact on the water quality of the Ammer River in an earlier study [35]. To gain a better understanding of the overall toxicological profile of the Ammer River, the results of the in vitro bioassays are visualized as pie charts integrated into the map of the catchment (Fig. 1). The size of the pie charts represents the average cytotoxicity (average $TU_{cytotoxicity}$) of the samples and shows the toxicological patterns by displaying the $TU_{specific\ effects}$ of all tested bioassays (Eq. 10). Sampling site 4, downstream of the WWTP, revealed the highest average cytotoxicity (average $TU_{cytotoxicity}$) and dominated the toxicity pattern of all downstream samples (sites 5–9). From site 5–9, only a slight decrease in the cytotoxicity (pie chart size), along with a rather marginally alteration of the effect pattern, was observed. In all agonistic assays, cytotoxicity and specific effects decreased at site 5. Within the stretch from site 6–9, the PPARγ and AhR assays did not show any distinct changes in their responses, while the response of AR slightly decreased. The assay for oxidative stress response AREc32 was not triggered continuously downstream of the WWTP but led to slight changes in the overall effect pattern at sampling sites 5, 7 and 9. After passing the WWTP, the toxicological pattern of the Ammer River shifted and included the newly activated assays ER, GR and AR for hormonal effects. This clearly reflects the input of estrogens and other hormones by the WWTP effluent. The bioanalytical response of ERα-GeneBLAzer and GR-GeneBLAzer attenuated from site 4 to 5 and only AR-GeneBLAzer was activated from site 6 on. Although these seven bioassay covering different toxicological pathways differ in sensitivity, it becomes apparent how important it is to combine different assays indicative of different endpoints to cover the largest possible number of organic micropollutants governing the water quality. Besides the main stem of the Ammer River, the samples from the tributaries Schönbrunnen (SB) and Mühlbach (MS) were measured as well, for detailed location see Table 1. Their effect patterns clearly differ from those of the main stem, which identified the WWTP as the dominant parameter determining the toxicological profile of the Ammer River, see Fig. 1. The small and remote Kleiner Goldersbach (G) creek located in the Schönbuch nature reserve was sampled as a potential control site. Although this creek is unaffected by domestic and industrial wastewaters, the impact of forest activities and ubiquitous dry and wet deposition needs to be considered. The bioassays revealed that cytotoxicity was similar to the Ammer River at sites 6–9, but with a different effect pattern. The most responsive bioassays were PPARγ-GeneBLAzer, AhR-CALUX and AREc32. Furthermore, the Kleiner Goldersbach creek caused the highest response in the AREc32 assay.

Table 3 Cytotoxicity (IC_{10}) and effect concentration (EC_{10}) values in REF units of the samples from site 1 to 9, the tributaries Schönbrunnen (SB W1 and SB W2) and Mühlbach (MS) in the Ammer catchment and site G in the Goldersbach catchment measured in the different in vitro bioassays

Sampling sites	ER		GR		AR		PR		AREc32		PPARy		AhR	
	IC_{10} ± SE	EC_{10} ± SE	IC_{10} ± SE	EC_{10} ± SE	IC_{10} ± SE	EC_{10} ± SE	IC_{10} ± SE	EC_{10} ± SE	IC_{10} ± SE	$EC_{IR1.5}$ ± SE	IC_{10} ± SE	EC_{10} ± SE	IC_{10} ± SE	EC_{10} ± SE
1	–	–	–	–	–	–	–	–	–	–	–	89.5 ± 24.2	–	35.0 ± 2.6
2	42.1 ± 8.7	–	61.2 ± 10.7	–	71.8 ± 9.1	–	82.4 ± 29.0	–	24.5 ± 4.2	–	59.0 ± 9.7	13.2 ± 0.6	–	26.2 ± 1.9
3	40.4 ± 7.2	37.9 ± 1.0	29.6 ± 5.8	–	–	–	30.7 ± 6.5	–	64.0 ± 6.6	33.7 ± 2.0	–	6.82 ± 0.29	74.0 ± 26.5	8.41 ± 0.48
4	4.84 ± 0.47	3.09 ± 0.13	7.18 ± 0.64	4.14 ± 0.21	19.3 ± 6.2	8.22 ± 0.18	9.67 ± 0.61	> 9	5.45 ± 1.22	> 5	5.41 ± 1.69	1.06 ± 0.07	31.7 ± 6.6	2.02 ± 0.81
5	17.4 ± 2.1	15.3 ± 1.1	11.5 ± 1.1	> 12	45.6 ± 14.7	34.1 ± 0.9	12.1 ± 2.3	–	32.4 ± 2.9	23.0 ± 1.6	48.9 ± 12.3	5.00 ± 0.29	54.2 ± 17.7	3.94 ± 0.21
6	13.7 ± 1.6	> 13	14.1 ± 1.3	> 14	54.5 ± 0.1	35.7 ± 1.2	40.7 ± 7.1	–	14.9 ± 3.0	> 14	30.0 ± 5.2	4.92 ± 0.29	–	5.75 ± 0.51
7	27.5 ± 7.7	> 27	16.3 ± 1.4	> 16	62.8 ± 12.9	43.5 ± 1.7	18.9 ± 3.0	–	23.8 ± 4.6	20.7 ± 1.5	53.3 ± 7.1	4.60 ± 0.24	61.9 ± 21.9	5.77 ± 0.49
8	15.3 ± 2.4	> 15	31.3 ± 4.2	> 31	54.2 ± 10.2	52.1 ± 2.8	31.5 ± 3.5	–	13.6 ± 1.9	> 13	22.0 ± 3.8	4.87 ± 0.31	65.5 ± 27.8	4.74 ± 0.32
9	16.6 ± 2.0	> 16	32.2 ± 4.0	> 32	58.8 ± 11.1	46.4 ± 3.2	40.2 ± 5.8	–	37.9 ± 4.3	24.8 ± 2.2	32.1 ± 7.0	4.47 ± 0.28	–	4.17 ± 0.29
G	16.9 ± 1.5	–	17.3 ± 2.8	–	81.1 ± 17.0	> 81	19.1 ± 3.9	–	22.5 ± 4.3	19.5 ± 1.1	34.5 ± 10.6	8.31 ± 0.67	53.1 ± 12.1	24.3 ± 1.5
SB W1	–	48.0 ± 4.4	18.7 ± 5.3	–	–	–	17.9 ± 5.1	–	–	57.6 ± 6.7	–	27.3 ± 2.3	–	23.4 ± 0.9
SB W2	–	–	28.1 ± 8.1	–	–	–	19.5 ± 6.9	–	–	37.9 ± 2.2	–	36.4 ± 2.7	–	21.3 ± 1.8
MS	–	68.3 ± 6.0	–	–	–	–	–	–	–	–	–	15.1 ± 0.8	–	24.5 ± 1.7

In some samples, no specific effects were observed, for instance in the PR assay (see Table 3), but the IC_{10} values could still be derived within the applied concentration range of REF 0.1 to 100. This turns cytotoxicity into an additional and valuable measure in evaluating changes in the water quality within a stream such as the Ammer River.

Chemical analysis

A total of 79 compounds were selected based on their environmental relevance, suitability as indicator chemicals and occurrence in previous studies [1, 36], including 50 substances present in European River systems with hazard quotients $> 10^{-4}$ as estimated by Busch et al. [37]. The hazard quotient is defined as the quotient of a measured environmental concentration and an effect concentration (EC).

In the samples taken at sites 1 to 9 of the Ammer River and the tributaries Schönbrunnen (SB) and Mühlbach (MS), 21 out of the 79 target analytes could be detected in at least one sample and these were assigned to the concentration classes shown in Fig. 2 (concentrations are given in Additional file 1: Table S5). Among them, 14 pharmaceuticals (including three commonly applied antibiotics: sulfamethoxazole, trimethoprim, metronidazole), the pharmaceutical metabolite metoprolol acid, the insecticide thiamethoxam, four herbicides (isoproturon, fluconazole, diuron, bentazone), and the herbicide metabolite atrazine-desethyl were detected. Except for atrazine-desethyl and bentazone, all target compounds occurred downstream of the WWTP at sites 4 to 9. Eight pharmaceuticals including metoprolol acid representing the most abundant class of substances with a concentration range between 0.26 and 1.9 µg L^{-1}. Only hydrochlorothiazide, a diuretic and antihypertensive drug, occurred at a concentration above 1 µg L^{-1}. With the exception of atrazine-desethyl and bentazone, the maximum concentration levels of the 19 remaining analytes were detected at site 4 and showed a more or less decreasing trend between sites 4 and 6. Lamotrigine, irbesartan, sulfamethoxazole, and carbamazepine showed rather constant concentration levels between sites 6 and 9 indicating a rather conservative behavior along this river stretch. Hydrochlorothiazide, tramadol, venlafaxine, thiamethoxam, sotalol, and acetaminophen showed a decreasing trend between sites 4 and 9, which indicates compound attenuation. Other compounds like oxcarbazepine, isoproturon, trimethoprim, fluconazole, gabapentin, atenolol, and metronidazole were only detected at site 4. A few pharmaceuticals (hydrochlorothiazide, lamotrigine, carbamazepine and acetaminophen), bentazone, and atrazine-desethyl also occurred upstream of the WWTP, indicating further input sources. Except for atrazine-desethyl, none of the target chemicals were detected in the tributaries SB and MS.

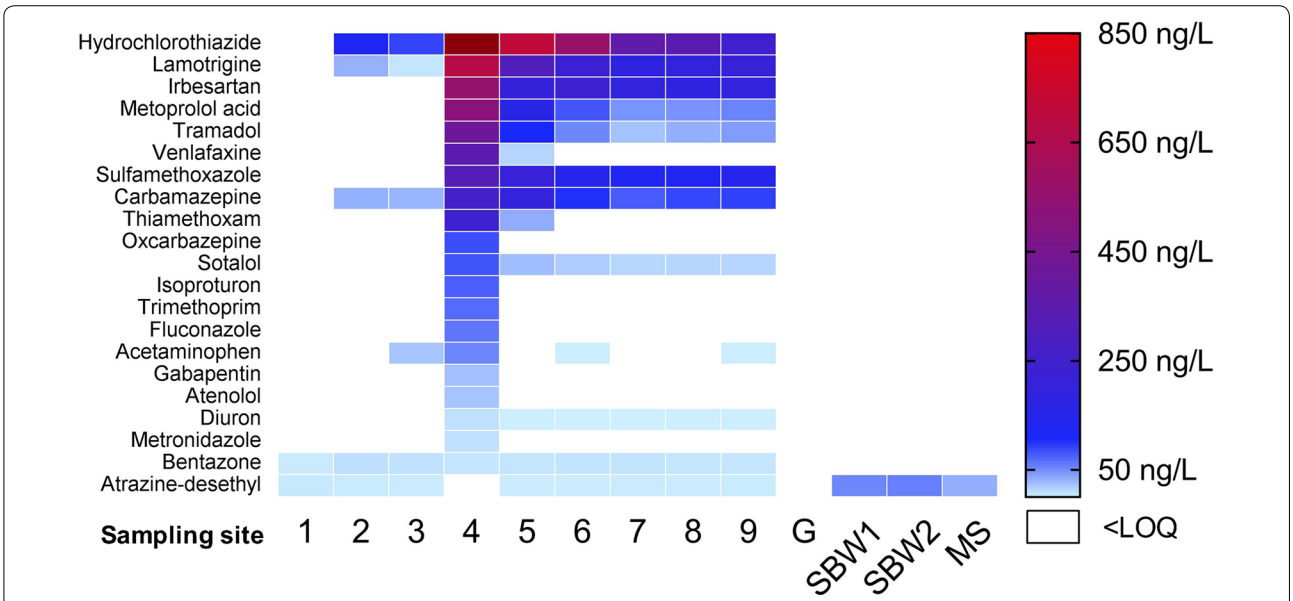

Fig. 2 Detected target pollutants from sampling sites 1 to 9 along the Ammer River, the tributaries Schönbrunnen (SB) and Mühlbach (MS) and from one sample of the Kleiner Goldersbach (G) creek. The concentration of hydrochlorothiazide at site 4 was 1.9 µg L^{-1} which exceeds the concentration scale and is colored in dark red

Discussion

Evaluation of bioassay results with effect-based trigger values and benchmarking against other water samples

To evaluate the mixture risk of the Ammer River, the BEQ values for each sample in each bioassay were calculated (Additional file 1: Table S6) and compared to other studies on wastewater and surface water, as well as to tentative effect-based trigger values (EBT) for surface water. The EBTs were derived from Environmental Quality Standards (EQS) of the European Union by read across and mixture toxicity considerations [38]. These EBTs represent levels of effect that differentiate acceptable from unacceptable water quality and can, therefore, serve to estimate the environmental risk of organic micropollutants in water. The EBTs listed in Additional file 1: Table S4 are preliminary as they were derived from an insufficient dataset in some cases, but at least for the estrogenic effect they provide a fairly robust estimate [38]. The estradiol equivalent concentrations EEQ directly downstream of the WWTP, 2.19 ng_{E2} L^{-1} at site 4 and 0.44 ng_{E2} L^{-1} at site 5, exceeded the proposed EBT-EEQ of 0.34 ng_{E2} L^{-1} for the ERα-GeneBLAzer assay by factors of 6.4 and 1.3, respectively. The EEQ-level was of no concern in all tributaries, and downstream of site 5 the estrogenic effect was masked by cytotoxicity. The EEQs in the river were similar to those for agricultural and WWTP impacted surface waters in Australia [39]. Another Australian river in South East Queensland was characterized by EEQ values that were up to a factor of 6 lower than measured downstream of the WWTP in the Ammer River [9].

No EBT could be derived for the GR assay because none of the regulated chemicals in the EU were active in this assay and, hence, there were no EQS available for the read across. Jia et al. [40] derived bioanalytical equivalent concentrations based on dexamethasone as the reference compound (Dexa-EQ) in the GR-GeneBLAzer of 39 to 155 $ng_{dexamethasone}$ L^{-1} for four WWTP effluents in the US, which is within the same range as the value measured downstream of the WWTP at site 4.

For AREc32, the preliminary EBT was based on dichlorvos with an EBT-dichlorvos-EQ of 156 $\mu g_{dichlorvos}$ L^{-1}. All samples tested here would have been compliant with this EBT for oxidative stress response. The dichlorvos-EQs detected in this study were also substantially lower than in previous studies on WWTPs and surface water [9, 16, 28].

For PPARγ-GeneBLAzer, the proposed EBT-rosglitazone-EQ was 36 $ng_{rosiglitazone}$ L^{-1}. While the Ammer River at site 3, upstream of the WWTP, complied with this EBT, all sites in the Ammer River downstream of the WWTP were just around the EBT, with only samples SB W1 and SB W2 and G being lower than the EBT-rosglitazone-EQ. Previous work identified similar ranges in the Danube River, where the rosglitazone-EQ was 67 $ng_{rosiglitazone}$ L^{-1} at a site where untreated wastewater was introduced, but a value far below the EBT was observed a couple of km up- and downstream of the discharge site [15].

The BEQs in the AhR-CALUX assay were presented in an earlier study as benzo(a)pyrene equivalents (B(a)P-EQ) and the EBT-B(a)P-EQ for surface water was proposed as 6.36 ng L^{-1}. This EBT is much smaller than any B(a)P-EQ encountered in this study (Additional file 1: Table S6). An earlier study on the treatment efficacy of conventional and intensified treatment wetlands reported a B(a)P-EQ of 130 $ng_{B(a)P}$ L^{-1} for an WWTP effluent at the same time of the year as the current study (July) [16], which is higher than what we detected in the sample of site 4, downstream of the WWTP.

In summary, site 4 with the highest BEQs in all bioassays, except for AREc32, would not comply with the proposed EBTs for estrogenicity, and activation of PPARγ and AhR. This is not astonishing given that 81% of the water volume at site 4 stemmed from the WWTP (Additional file 1: Section S1).

Chemical analysis

In the sample of the Ammer source, only the herbicide bentazone and the metabolite atrazine-desethyl were detected among all target compounds. The occurrence of the pharmaceuticals hydrochlorothiazide, lamotrigine, and carbamazepine at site 2, downstream of the pump station in Herrenberg, and furthermore acetaminophen at site 3 indicates the impact of wastewater, for example, from contaminated groundwater from the city of Herrenberg, storm water overflows or leaking sewers that are installed parallel to the Ammer. Interestingly, the herbicide diuron was detected only at and downstream of site 4 at concentrations up to 8 ng L^{-1}, indicating its use in urban areas presumably for protection of facades and other construction materials. Its use as a herbicide in agriculture is no longer authorized by the German government since 2008 [41]. However, atrazine-desethyl, the major degradation product of atrazine, was measured at concentrations ranging from 2 to 3 ng L^{-1} in the main stem and 33 to 56 ng L^{-1} in the tributaries Schönbrunnen (SB) and Mühlbach (MS). Atrazine, which was banned in the European Union in 2004 [42], was not detected in any sample. The relatively higher concentrations of atrazine-desethyl in the tributaries, which are located in agricultural areas, point to the previous use of atrazine at these sites. As atrazine-desethyl was the only target compound detected in the tributaries SB and MS, no major impact by agriculture on the water quality of the Ammer River is concluded. None of the detected chemicals listed in the

Water Framework Directive [4] (bentazone, diuron, isoproturon) exceeded the EQS.

To reflect changes of the water quality along the River Ammer, five pharmaceuticals, carbamazepine (CAR), sulfamethoxazole (SUL), tramadol (TRA), sotalol (SOT) and venlafaxine (VEN), were selected as indicator chemicals with WWTP effluents as predominant input source. Their concentrations along the river relative to their maximum concentration, expressed as C_i/C_{max}, are depicted in Fig. 3. CAR and SUL were selected as indicators for dilution processes, because both are expected to show a rather conservative behavior in surface water. CAR shows environmental persistence, high water solubility and negligible sorption to the sediment [43]. The antibiotic SUL is rather stable during wastewater treatment and against photodegradation under neutral pH conditions [44] and it also prevents bacterial growth [45]. Figure 3 shows a significant decrease of 63 and 55% of CAR and SUL, respectively, between sites 4 and 6 indicating dilution processes within this stretch under the assumption of a more or less constant input function over time if not the same parcel of water is sampled. Further downstream of site 6 towards the river mouth the concentrations of CAR and SUL are rather unchanged (−3 and +2%, respectively) suggesting no further dilution or additional sources. The drug TRA is rather persistent but moderately photolabile [46], whereas SOT is prone to slow biodegradation, hydrolysis and indirect photolysis [47, 48]. Between sites 4 and 6, the concentrations of TRA and SOT drop faster than CAR and SUL by 87 and 78%, respectively (Fig. 3). Both TRA and SOT are less stable than CAR and SUL but stable enough to pass the distance from sampling site 6 to 9 without any further dissipation. VEN is even better degradable and dissipates faster from the water phase than all other indicator chemicals (Fig. 3). Therefore, TRA and SOT can be considered as degradable tracer compounds in this study, indicating potential in-stream attenuation processes.

Comparison of chemical analysis and bioassays

Similar to the results from the bioassays, the target screening also identified the WWTP in the Ammer River as a dominant source of pollutants considerably affecting the river water quality. The information obtained from the list of detected target compounds and the effects found by bioassays are complementary. For example, no hormones or nonpolar compounds detectable by the bioassays ER, GR, AR, PR and AhR have been included in the target screening. Herbicides from the target list are, on the contrary, not detected specifically by the bioassays. Moreover, none of the target compounds were found in the Kleiner Goldersbach even though the bioassays revealed that cytotoxicity was similar to the Ammer River, which underlines the complementarity of both approaches.

The average cytotoxicity of all bioassays (average $TU_{cytotoxicity}$) at each sampling site was plotted together with the five indicator chemicals in Fig. 3. Interestingly, the cytotoxicity curve aligns between CAR and SOT; thus, the decrease in cytotoxicity between sites 4 and 6

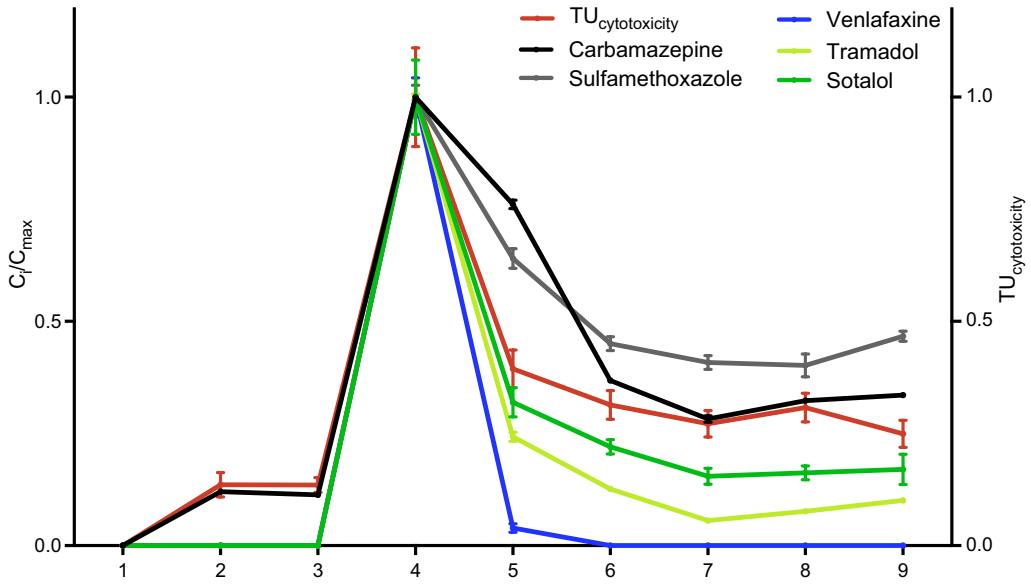

Fig. 3 Concentrations of carbamazepine (CAR), sulfamethoxazole (SUL), tramadol (TRA), sotalol (SOL) and venlafaxine (VEN) and the cytotoxicity expressed as $TU_{cytotoxicity}$ relative to the maximum concentration and maximum cytotoxicity, respectively, along the Ammer River

(69%) can be mainly attributed to dilution effects. Furthermore, similar to the indicator chemicals, the cytotoxicity remains rather stable from site 6 to 9. Further work is required to show whether the changes in the toxicological profile or the average cytotoxicity, both of which are surrogates for the chemical burden, can be explained by the use of indicator chemicals.

Conclusions

Both approaches, in vitro bioassays and targeted chemical analysis, identified the WWTP as a major input source of organic micropollutants dominantly influencing the water quality of the Ammer River. Hence, this method could also be used to characterize the impact and influence of WWTP effluents and possibly also agricultural and industrial activities on a catchment in surveillance monitoring. Further, the application of tentative EBTs forms an innovative way to account for mixture toxicity and toxicologically relevant pollutants that are not regulated yet.

Specifically, the combination of target analysis and in vitro bioassays uncovered (1) a reduction in cytotoxic potential between sampling site 4 and 6 mainly attributed to dilution by additional water inputs, (2) no substantial dilution and only little or no loss occurred between sampling sites 6 and 9, suggesting that (3) the consistent effect patterns and cytotoxic potential at the sampling sites 6, 7, 8 and 9 was primarily caused by the discharge of poorly degradable substances from the WWTP. This study showed the combination of these two complementary approaches to be a suitable way to identify input sources of organic micropollutants and to trace changes in the water quality along the Ammer River. Furthermore, the implementation of this combined approach into comprehensive, mass flux-based investigations of reactive transport may be promising to further elucidate and distinguish between different in-stream transformation and loss processes. The Ammer river is a 4th order stream with an extraordinarily high base flow. Hence, the water quality situation is very much dependent on local and possibly highly fluctuating inputs. It is likely that seasonal changes will impact on the input of pesticides and the WWTP effluent may have a higher contribution to the overall flow under dry summer conditions. Such seasonal effects will be investigated in future studies. Benchmarking against other surface water studies and comparison with tentative EBTs already provides an indication that we need to pay more attention to lower order streams because unlike in large higher order streams like the Danube river, where even the release of untreated sewage hardly results in the exceedance of EBTs due to the high dilution factor [15]; in the Ammer, the impact of the WWTP was still noticeable at a few sampling sites below the inflow. Despite being situated in an active agricultural area, this study has not registered a major chemical impact from agriculture. This might be partially due to sampling in late summer after the end of the major spraying activities but also because the bioassays targeted more effluent-derived micropollutants. Herbicide- and insecticide-specific bioassays should complement the test battery for a better differentiation between urban and agricultural impact.

Additional file

Additional file 1: Table S1. Usage, CAS-number, vendor and detection limit in ng L^{-1} of the detected target analytes of Table S3. **Table S2.** Target analytes that were included in the analytical method but not detected at sampling sites 1 to 9, the tributaries Schönbrunnen and Mühlbach, the Goldersbach and the SPE blank. **Section S1.** Estimation of the contribution of treated wastewater at site 4. **Table S3.** Electrical conductivity, temperature (T) and pH of sampling site 3, 4 and the WWTP effluent. **Table S4.** EC_{10} values of the used reference compounds in all agonistic bioassays. Proposed effect-based trigger values EBT-BEQ from Escher et al. [1]. **Figure S1.** Concentration-effect curves of all measured samples, SPE blank and the reference compound 17β-estradiol in the ER assay. **Figure S2.** Concentration-effect curves of all measured samples, SPE blank and the reference compound dexamethasone in the GR assay. **Figure S3.** Concentration-effect curves of all measured samples, SPE blank and the reference compounds R1881 and cyproterone acetate in agonistic and antagonistic mode in the AR assay. **Figure S4.** Concentration-effect curves of all measured samples, SPE blank and the reference compounds promegestone and RU486 in agonistic and antagonistic mode in the PR assay. **Figure S5.** Concentration-effect curves of all measured samples, solvent blank and the reference compound tBHQ in the AREc32 assay. **Figure S6.** Concentration-effect curves of all measured samples, SPE blank and the reference compound rosiglitazone in the PPARγ assay. **Figure S7.** Concentration-effect curves of all measured samples, SPE blank and the reference compound TCDD in the AhR assay. **Table S5.** Detected target analytes and measured concentrations in ng L^{-1} at sampling sites 1 to 9 of the Ammer main stem, the tributaries Schönbrunnen (SB W1 and SB W2) and Mühlbach (MS), the Goldersbach (G) and the SPE blank. **Table S6.** BEQ values of all sampling sites in the agonistic bioassays.

Abbreviations

AhR: aryl hydrocarbon receptor; AIF: All-Ion Fragmentation; AM: Ammer mouth; Anti-AR: anti androgenicity; Anti-PR: anti progestagenic activity; AR: androgen receptor; B(a)P-EQ: benzo(a)pyrene equivalent concentration; BEQ: bioanalytical equivalent concentration; CAR: carbamazepine; Dexa-EQ: dexamethasone equivalent; dichlorvos-EQ: dichlorvos equivalent; EBT: effect-based trigger value; EC: effect concentration; EEQ: estradiol equivalent concentration; EQS: environmental quality standard; ER: estrogen receptor; ESI: electrospray ionization; FBF: Find by Formula; GR: glucocorticoid receptor; IC: inhibitory concentration; IR: induction ratio; LC/MS: liquid chromatography/mass spectrometry; LC–HRMS: liquid chromatography–high resolution mass spectrometry; MS: Mühlbach source; PE: population equivalent; PES: polyethersulfone; PPARγ: peroxisome proliferator activated receptor; PR: progesterone receptor; Q-TOF-MS: quadrupole time-of-flight mass spectrometry; R1881: metribolone; REF: relative enrichment factor; rosglitazone-EQ: rosglitazone equivalent concentration; SB: Schönbrunnen; SE: standard error; SOT: sotalol; SPE: solid phase extraction; SR: suppression ratio; SUL: sulfamethoxazole; TCDD: 2,3,4,7-tetrachlorodibenzo-*p*-dioxin; TRA: tramadol; TU: toxic unit; VEN: venlafaxine; W: weir; WWTP: wastewater treatment plant.

Authors' contributions
MEM conducted the study including sampling, sample preparation, chemical analysis, evaluation of the bioassay results, interpretation of data and the initial design of all figures. He is the main author of the manuscript, gave his final approval of the version to be published and agreed to be accountable for all aspects of the work. BIE made substantial contributions to conception and design, bioassay measurements and analysis and interpretation of data, including the initial design of all figures. She was involved in drafting the manuscript, gave her final approval of the version to be published and agreed to be accountable for all aspects of the work. MS made substantial contributions to sampling, acquisition and interpretation of data. He was involved in revising the manuscript critically for important intellectual content, gave his final approval of the version to be published and agreed to be accountable for all aspects of the work. MW made all contributions to the chemical analysis and interpretation of data. She was involved in revising the manuscript critically for important intellectual content, gave her final approval of the version to be published and agreed to be accountable for all aspects of the work. CZa made a contribution to conception, design and interpretation of data. She was involved in revising the manuscript critically for important intellectual content, gave her final approval of the version to be published and agreed to be accountable for all aspects of the work. CZw made substantial contributions to conception and design, chemical analysis and interpretation of data. He was involved in drafting the manuscript, gave his final approval of the version to be published and agreed to be accountable for all aspects of the work. All authors read and approved the final manuscript.

Author details
[1] Center for Applied Geoscience, Eberhard Karls University of Tübingen, 72074 Tübingen, Germany. [2] UFZ-Helmholtz Centre for Environmental Research, 04318 Leipzig, Germany.

Acknowledgements
We would like to thank the excellent support of the bioassay laboratory team Maria König, Lisa Glauch and Rita Schlichting at UFZ, and Stephanie Nowak at University of Tübingen. We thank Peta A. Neale for proof-reading of the manuscript.

Competing interests
The authors declare that they have no competing interests.

Availability of data and materials
The datasets supporting the conclusions of this article are included either within the article or its Additional file 1.

Ethics approval and consent to participate
Not applicable.

Funding
This work was supported by the Collaborative Research Centre 1253 CAMPOS (Project P1: Rivers), funded by the German Research Foundation (DFG, Grant Agreement SFB 1253/1 20147).

Publisher's Note

Received: 5 March 2018 Accepted: 6 June 2018
Published online: 18 June 2018

References

1. Loos R, Gawlik BM, Locoro G, Rimaviciute E, Contini S, Bidoglio G (2009) EU-wide survey of polar organic persistent pollutants in European river waters. Environ Pollut 157:561–568. https://doi.org/10.1016/j.envpol.2008.09.020
2. Kuzmanović M, Ginebreda A, Petrović M, Barceló D (2015) Risk assessment based prioritization of 200 organic micropollutants in 4 Iberian rivers. Sci Tot Environ 503–504:289–299. https://doi.org/10.1016/j.scitotenv.2014.06.056
3. Heeb F, Singer H, Pernet-Coudrier B, Qi W, Liu H, Longrée P, Müller B, Berg M (2012) Organic micropollutants in rivers downstream of the megacity Beijing: sources and mass fluxes in a large-scale wastewater irrigation system. Environ Sci Technol 46:8680–8688. https://doi.org/10.1021/es301912q
4. European Commission (2013) Directive 2013/39/EU of the European Parliament and the Council amending Directives 2000/60/EC and 2008/105/EC as regards priority substances in the field of water policy. L 226/1-L226/17
5. Brack W, Dulio V, Ågerstrand M, Allan I, Altenburger R, Brinkmann M, Bunke D, Burgess RM, Cousins I, Escher BI, Hernández FJ, Hewitt LM, Hilscherová K, Hollender J, Hollert H, Kase R, Klauer B, Lindim C, Herráez DL, Miège C, Munthe J, O'Toole S, Posthuma L, Rüdel H, Schäfer RB, Sengl M, Smedes F, van de Meent D, van den Brink PJ, van Gils J, van Wezel AP, Vethaak AD, Vermeirssen E, von der Ohe PC, Vrana B (2017) Towards the review of the European Union Water Framework Directive: recommendations for more efficient assessment and management of chemical contamination in European surface water resources. Sci Tot Environ 576:720–737. https://doi.org/10.1016/j.scitotenv.2016.10.104
6. Escher BI, Leusch F (2012) Bioanalytical tools in water quality assessment. IWA publishing, London
7. Maruya KA, Dodder NG, Mehinto AC, Denslow ND, Schlenk D, Snyder SA, Weisberg SB (2016) A tiered, integrated biological and chemical monitoring framework for contaminants of emerging concern in aquatic ecosystems. Integr Environ Assess Manag 12:540–547. https://doi.org/10.1002/ieam.1702
8. Wernersson A-S, Carere M, Maggi C, Tusil P, Soldan P, James A, Sanchez W, Dulio V, Broeg K, Reifferscheid G, Buchinger S, Maas H, Van Der Grinten E, O'Toole S, Ausili A, Manfra L, Marziali L, Polesello S, Lacchetti I, Mancini L, Lilja K, Linderoth M, Lundeberg T, Fjällborg B, Porsbring T, Larsson DJ, Bengtsson-Palme J, Förlin L, Kienle C, Kunz P, Vermeirssen E, Werner I, Robinson CD, Lyons B, Katsiadaki I, Whalley C, den Haan K, Messiaen M, Clayton H, Lettieri T, Carvalho RN, Gawlik BM, Hollert H, Di Paolo C, Brack W, Kammann U, Kase R (2015) The European technical report on aquatic effect-based monitoring tools under the water framework directive. Environ Sci Eur 27:7. https://doi.org/10.1186/s12302-015-0039-4
9. Escher BI, Allinson M, Altenburger R, Bain PA, Balaguer P, Busch W, Crago J, Denslow ND, Dopp E, Hilscherova K, Humpage AR, Kumar A, Grimaldi M, Jayasinghe BS, Jarosova B, Jia A, Makarov S, Maruya KA, Medvedev A, Mehinto AC, Mendez JE, Poulsen A, Prochazka E, Richard J, Schifferli A, Schlenk D, Scholz S, Shiraishi F, Snyder S, Su G, Tang JYM, Bvd Burg, Linden SCvd, Werner I, Westerheide SD, Wong CKC, Yang M, Yeung BHY, Zhang X, Leusch FDL (2014) Benchmarking organic micropollutants in wastewater, recycled water and drinking water with in vitro bioassays. Environ Sci Technol 48:1940–1956. https://doi.org/10.1021/es403899t
10. Mehinto AC, Jia A, Snyder SA, Jayasinghe BS, Denslow ND, Crago J, Schlenk D, Menzie C, Westerheide SD, Leusch FDL, Maruya KA (2015) Interlaboratory comparison of in vitro bioassays for screening of endocrine active chemicals in recycled water. Water Res 83:303–309. https://doi.org/10.1016/j.watres.2015.06.050
11. Tousova Z, Oswald P, Slobodnik J, Blaha L, Muz M, Hu M, Brack W, Krauss M, Di Paolo C, Tarcai Z, Seiler T-B, Hollert H, Koprivica S, Ahel M, Schollée JE, Hollender J, Suter MJF, Hidasi AO, Schirmer K, Sonavane M, Ait-Aissa S, Creusot N, Brion F, Froment J, Almeida AC, Thomas K, Tollefsen KE, Tufi S, Ouyang X, Leonards P, Lamoree M, Torrens VO, Kolkman A, Schriks M, Spirhanzlova P, Tindall A, Schulze T (2017) European demonstration program on the effect-based and chemical identification and monitoring of organic pollutants in European surface waters. Sci Tot Environ 601–602:1849–1868. https://doi.org/10.1016/j.scitotenv.2017.06.032
12. Van der Linden SC, Heringa MB, Man HY, Sonneveld E, Puijker LM, Brouwer A, Van der Burg B (2008) Detection of multiple hormonal activities in wastewater effluents and surface water, using a panel of steroid receptor CALUX bioassays. Environ Sci Technol 42:5814–5820. https://doi.org/10.1021/es702897y
13. Žegura B, Heath E, Černoša A, Filipič M (2009) Combination of in vitro bioassays for the determination of cytotoxic and genotoxic potential of wastewater, surface water and drinking water samples. Chemosphere 75:1453–1460. https://doi.org/10.1016/j.chemosphere.2009.02.041
14. Miège C, Gabet V, Coquery M, Karolak S, Jugan ML, Oziol L, Levi Y, Chevreuil M (2009) Evaluation of estrogenic disrupting potency in aquatic environments and urban wastewaters by combining chemical

and biological analysis. Trends Anal Chem 28:186–195. https://doi.org/10.1016/j.trac.2008.11.007
15. König M, Escher BI, Neale PA, Krauss M, Hilscherová K, Novák J, Teodorović I, Schulze T, Seidensticker S, Kamal Hashmi MA, Ahlheim J, Brack W (2017) Impact of untreated wastewater on a major European river evaluated with a combination of in vitro bioassays and chemical analysis. Environ Pollut 220:1220–1230. https://doi.org/10.1016/j.envpol.2016.11.011
16. Nivala J, Neale PA, Haasis T, Kahl S, König M, Müller RA, Reemtsma T, Schlichting R, Escher BI (2018) Application of cell-based bioassays to evaluate treatment efficacy of conventional and intensified treatment wetlands. Environ Sci Water Res Technol 4:206–217. https://doi.org/10.1039/c7ew00341b
17. Roberts J, Bain PA, Kumar A, Hepplewhite C, Ellis DJ, Christy AG, Beavis SG (2015) Tracking multiple modes of endocrine activity in Australia's largest inland sewage treatment plant and effluent-receiving environment using a panel of in vitro bioassays. Environ Toxicol Chem 34:2271–2281. https://doi.org/10.1002/etc.3051
18. Margot J, Kienle C, Magnet A, Weil M, Rossi L, de Alencastro LF, Abegglen C, Thonney D, Chèvre N, Schärer M, Barry DA (2013) Treatment of micropollutants in municipal wastewater: ozone or powdered activated carbon? Sci Tot Environ 461–462:480–498. https://doi.org/10.1016/j.scitotenv.2013.05.034
19. Neale PA, Ait-Aissa S, Brack W, Creusot N, Denison MS, Br Deutschmann, Hilscherová K, Hollert H, Krauss M, Novak J, Schulze T, Seiler T-B, Serra H, Shao Y, Escher BI (2015) Linking in vitro effects and detected organic micropollutants in surface water using mixture-toxicity modeling. Environ Sci Technol 49:14614–14624. https://doi.org/10.1021/acs.est.5b04083
20. Jin X, Peldszus S (2012) Selection of representative emerging micropollutants for drinking water treatment studies: a systematic approach. Sci Tot Environ 414:653–663. https://doi.org/10.1016/j.scitotenv.2011.11.035
21. Wolf L, Zwiener C, Zemann M (2012) Tracking artificial sweeteners and pharmaceuticals introduced into urban groundwater by leaking sewer networks. Sci Tot Environ 430:8–19. https://doi.org/10.1016/j.scitotenv.2012.04.059
22. Jobelius C, Ruth B, Griebler C, Meckenstock RU, Hollender J, Reineke A, Frimmel FH, Zwiener C (2010) Metabolites indicate hot spots of biodegradation and biogeochemical gradients in a high-resolution monitoring well. Environ Sci Technol 45:474–481. https://doi.org/10.1021/es1030867
23. Helwig K, Hunter C, MacLachlan J, McNaughtan M, Roberts J, Cornelissen A, Dagot C, Evenblij H, Klepiszewski K, Lyko S (2013) Micropollutant point sources in the built environment: identification and monitoring of priority pharmaceutical substances in hospital effluents. J Environ Anal Toxicol 3:1–10. https://doi.org/10.4172/2161-0525.1000177
24. Drewes JE, Anderson P, Denslow N, Olivieri A, Schlenk D, Snyder SA, Maruya KA (2012) Designing monitoring programs for chemicals of emerging concern in potable reuse—what to include and what not to include? Water Sci Technol 67:433–439. https://doi.org/10.2166/wst.2012.520
25. Götz CW, Stamm C, Fenner K, Singer H, Schärer M, Hollender J (2010) Targeting aquatic microcontaminants for monitoring: exposure categorization and application to the Swiss situation. Environ Sci Pollut Res Int 17:341–354. https://doi.org/10.1007/s11356-009-0167-8
26. Jekel M, Dott W, Bergmann A, Dünnbier U, Gnirß R, Haist-Gulde B, Hamscher G, Letzel M, Licha T, Lyko S, Miehe U, Sacher F, Scheurer M, Schmidt CK, Reemtsma T, Ruhl AS (2015) Selection of organic process and source indicator substances for the anthropogenically influenced water cycle. Chemosphere 125:155–167. https://doi.org/10.1016/j.chemosphere.2014.12.025
27. Huang R, Xia M, Cho M-H, Sakamuru S, Shinn P, Houck KA, Dix DJ, Judson RS, Witt KL, Kavlock RJ (2011) Chemical genomics profiling of environmental chemical modulation of human nuclear receptors. Environ Health Perspect 119:1142. https://doi.org/10.1289/ehp.1002952
28. Escher BI, Dutt M, Maylin E, Tang JYM, Toze S, Wolf CR, Lang M (2012) Water quality assessment using the AREc32 reporter gene assay indicative of the oxidative stress response pathway. J Environ Monit 14:2877–2885. https://doi.org/10.1039/c2em30506b
29. Escher BI, van Daele C, Dutt M, Tang JYM, Altenburger R (2013) Most oxidative stress response in water samples comes from unknown chemicals: the need for effect-based water quality trigger values. Environ Sci Technol 47:7002–7011. https://doi.org/10.1021/es304793h
30. Neale PA, Altenburger R, Aït-Aïssa S, Brion F, Busch W, de Aragão Umbuzeiro G, Denison MS, Du Pasquier D, Hilscherová K, Hollert H, Morales DA, Novák J, Schlichting R, Seiler T-B, Serra H, Shao Y, Tindall AJ, Tollefsen KE, Williams TD, Escher BI (2017) Development of a bioanalytical test battery for water quality monitoring: fingerprinting identified micropollutants and their contribution to effects in surface water. Water Res 123:734–750. https://doi.org/10.1016/j.watres.2017.07.016
31. Brennan JC, He G, Tsutsumi T, Zhao J, Wirth E, Fulton MH, Denison MS (2015) Development of species-specific Ah receptor-responsive third generation CALUX cell lines with enhanced responsiveness and improved detection limits. Environ Sci Technol 49:11903–11912. https://doi.org/10.1021/acs.est.5b02906
32. Invitrogen (2007) Validation & Assay Performance Summary. GeneBLAzer® GR-UAS-bla HEK 293T Cells. https://assets.thermofisher.com/TFS-Assets/LSG/manuals/geneblazer_GRblaHEK293T_man.pdf. Accessed 13 June 2018
33. Invitrogen (2010) Validation & Assay Performance Summary. GeneBLAzer® AR-UAS-bla GripTite™ Cells. https://tools.thermofisher.com/content/sfs/manuals/geneblazer_ARGripTite_man.pdf. Accessed 26 May 2018
34. Invitrogen (2007) Validation & Assay Performance Summary. GeneBLAzer® PR-UAS-bla HEK293T Cells. https://assets.thermofisher.com/TFS-Assets/LSG/manuals/geneblazer_PRUASblaHEK293T_man.pdf. Accessed 13 June 2018
35. Selle B, Schwientek M, Lischeid G (2013) Understanding processes governing water quality in catchments using principal component scores. J Hydrol 486:31–38. https://doi.org/10.1016/j.jhydrol.2013.01.030
36. Moschet C, Wittmer I, Simovic J, Junghans M, Piazzoli A, Singer H, Stamm C, Leu C, Hollender J (2014) How a complete pesticide screening changes the assessment of surface water quality. Environ Sci Technol 48:5423–5432. https://doi.org/10.1021/es500371t
37. Busch W, Schmidt S, Kühne R, Schulze T, Krauss M, Altenburger R (2016) Micropollutants in European rivers: a mode of action survey to support the development of effect-based tools for water monitoring. Environ Toxicol Chem 35:1887–1899. https://doi.org/10.1002/etc.3460
38. Escher BI, Aït-Aïssa S, Behnisch PA, Brack W, Brion F, Brouwer A, Buchinger S, Crawford SE, Du Pasquier D, Hamers T, Hettwer K, Hilscherová K, Hollert H, Kase R, Kienle C, Tindall AJ, Tuerk J, van der Oost R, Vermeirssen E, Neale PA (2018) Effect-based trigger values for in vitro and in vivo bioassays performed on surface water extracts supporting the environmental quality standards (EQS) of the European Water Framework Directive. Sci Total Environ 628–629:748–765. https://doi.org/10.1016/j.scitotenv.2018.01.340
39. Scott PD, Coleman HM, Khan S, Lim R, McDonald JA, Mondon J, Neale PA, Prochazka E, Tremblay LA, Warne MSJ, Leusch FDL (2018) Histopathology, vitellogenin and chemical body burden in mosquitofish (*Gambusia holbrooki*) sampled from six river sites receiving a gradient of stressors. Sci Tot Environ 616–617:1638–1648. https://doi.org/10.1016/j.scitotenv.2017.10.148
40. Jia A, Wu S, Daniels KD, Snyder SA (2016) Balancing the budget: accounting for glucocorticoid bioactivity and fate during water treatment. Environ Sci Technol 50:2870–2880. https://doi.org/10.1021/acs.est.5b04893
41. European Commission (2008) 08/91/EC, Reg. (EU) No 540/2011
42. European Commission (2004) 2004/248/EC: Commission Decision of 10 March 2004 concerning the non-inclusion of atrazine in Annex I to Council Directive 91/414/EEC and the withdrawal of authorisations for plant protection products containing this active substance (Text with EEA relevance) (notified under document number C(2004) 731)
43. Clara M, Strenn B, Kreuzinger N (2004) Carbamazepine as a possible anthropogenic marker in the aquatic environment: investigations on the behaviour of Carbamazepine in wastewater treatment and during groundwater infiltration. Water Res 38:947–954. https://doi.org/10.1016/j.watres.2003.10.058
44. Zhou W, Moore DE (1994) Photochemical decomposition of sulfamethoxazole. Int J Pharm 110:55–63. https://doi.org/10.1016/0378-5173(94)90375-1
45. Martindale W (1993) The extra pharmacopoeia, 30th edn. Pharmaceutical Press, London

46. Bergheim M, Gieré R, Kümmerer K (2012) Biodegradability and ecotoxicitiy of tramadol, ranitidine, and their photoderivatives in the aquatic environment. Environ Sci Pollut Res Int 19:72–85. https://doi.org/10.1007/s11356-011-0536-y
47. Letzel M (2008) Verhalten prioritärer organischer Stoffe der Wasserrahmenrichtlinie in Kläranlagen und beim Eintrag in oberirdische Gewässer. Bayerisches Landesamt für Umwelt (LfU), München
48. Piram A, Salvador A, Verne C, Herbreteau B, Faure R (2008) Photolysis of β-blockers in environmental waters. Chemosphere 73:1265–1271. https://doi.org/10.1016/j.chemosphere.2008.07.018

Publication 2

Mitochondrial toxicity of selected micropollutants, their mixtures and surface water samples measured by the oxygen consumption rate in cells

Maximilian E. Müller [a], Sofia Vikstrom [b], Maria König [c], Rita Schlichting [c], Christiane Zarfl [a], Christian Zwiener [a], and Beate I. Escher [a,c]

[a]Eberhard Karls University of Tübingen, Center for Applied Geoscience, Tübingen, Germany

[b]Agilent Technologies, Golstrup, Denmark

[c]UFZ – Helmholtz Centre for Environmental Research, Leipzig, Germany

Published in *Environmental Toxicology and Chemistry*, DOI: 10.1002/etc.4396

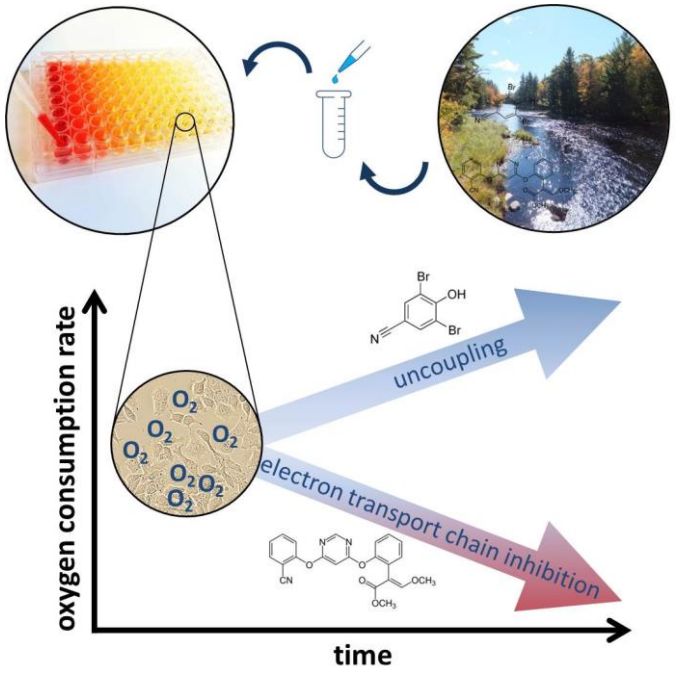

Environmental Toxicology and Chemistry—Volume 38, Number 5—pp. 1000–1011, 2019
Received: 20 December 2018 | Revised: 11 February 2019 | Accepted: 13 February 2019

Environmental Toxicology

Mitochondrial Toxicity of Selected Micropollutants, Their Mixtures, and Surface Water Samples Measured by the Oxygen Consumption Rate in Cells

Maximilian E. Müller,[a] Sofia Vikstrom,[b] Maria König,[c] Rita Schlichting,[c] Christiane Zarfl,[a] Christian Zwiener,[a] and Beate I. Escher[a,c,*]

[a]Eberhard Karls University of Tübingen, Center for Applied Geoscience, Tübingen, Germany
[b]Agilent Technologies, Glostrup, Denmark
[c]UFZ–Helmholtz Centre for Environmental Research, Leipzig, Germany

Abstract: Some environmental pollutants impair mitochondria, which are of vital importance as energy factories in eukaryotic cells. Mitochondrial toxicity was quantified by measuring the change of the oxygen consumption rate (OCR) of HepG2 cells with the Agilent Seahorse XF^{e}96 Analyzer. Various mechanisms of mitochondrial toxicity, including inhibition of the electron transport chain or adenosine triphosphate (ATP) synthase as well as uncoupling of oxidative phosphorylation, were differentiated by dosing the sample in parallel with reference compounds following the OCR over time. These time–OCR traces were used to derive effect concentrations for 10% inhibition of the electron transport chain or 10% of uncoupling. The low effect level of 10% was necessary because environmental mixtures contain thousands of chemicals; only few of them interfere with mitochondria, but the others cause cytotoxicity. The OCR bioassay was validated with environmental pollutants of known mechanism of mitochondrial toxicity. Binary mixtures of uncouplers or inhibitors acted according to the mixture model of concentration addition. Uncoupling and/or inhibitory effects were detected in extracts of river water samples without apparent cytotoxicity. Uncoupling effects could only be quantified in water samples if inhibitory effects occurred at lower concentrations because no uncoupling can be detected without an appreciable membrane potential built up. The OCR bioassay can thus complement chemical analysis and in vitro bioassays for monitoring micropollutants in water. *Environ Toxicol Chem* 2019;38:1000–1011. © 2019 SETAC

Keywords: Oxidative phosphorylation; Uncoupling; Inhibition of electron transport; Inhibition of ATP synthesis; Seahorse XF^{e}96 Analyzer; In vitro bioassay

INTRODUCTION

Mitochondria are ubiquitous in most eukaryotic organisms and play an important role in cellular physiology. Mitochondria are responsible for the majority of the cellular energy production by generating adenosine triphosphate (ATP) through oxidative phosphorylation (Dykens et al. 1999; McBride et al. 2006) and are also a crucial component in many important metabolic processes, such as regulation of apoptosis, synthesis of macromolecules, and generation of intracellular messengers such as Ca^{2+} and reactive oxygen species. Hence, there are plenty of processes in mitochondria that can be disrupted and lead to mitochondrial dysfunction. These disruptions of mitochondrial respiration are triggered by many pesticides such as the fungicide group of strobilurins, which inhibit the fungal electron transport chain (Bartlett et al. 2002), or substituted phenols such as bromoxynil, which act as uncouplers (Terada 1990). Furthermore, many pharmaceuticals introduced by treated wastewater into environmental water bodies interfere with mitochondrial functions (Sahdeo et al. 2014), for example, the analgesic diclofenac (Syed et al. 2016), the antiepileptics lamotrigine and carbamazepine (Berger et al. 2010), and the antidiabetic agent metformin (Thakur et al. 2018), all of which were detected in surface waters (Müller et al. 2018; Singer et al. 2010; Tisler and Zwiener 2018). Detection methodologies for mitochondrial toxicity in environmental samples are by no means straightforward (Divakaruni et al. 2014). Because micropollutants that disturb mitochondrial functions by different modes of action (MoA) share the common outcome of an altered oxygen consumption rate (OCR), we hypothesized that the modes of action can be identified and

This article includes online-only Supplemental Data.
* Address correspondence to beate.escher@ufz.de
Published online 19 February 2019 in Wiley Online Library (wileyonlinelibrary.com).
DOI: 10.1002/etc.4396

quantified by measuring cellular oxygen consumption in vitro using the Agilent Seahorse XF^{e}96 Extracellular Flux Analyzer.

Besides addressing cell metabolism and physiology in medical and health-care efforts (Beeson et al. 2010; Gupta et al. 2016; Nonnenmacher et al. 2017; Shah-Simpson et al. 2016), the Seahorse XF^{e}96 was used to assess effects of environmentally relevant drugs (Sahdeo et al. 2014; Zhang et al. 2017) and micropollutants (Attene-Ramos et al. 2013) on cells, as well as polycyclic aromatic hydrocarbons (Raftery et al. 2017) and biocides such as triclosan (Shim et al. 2016) in zebrafish embryos and larvae. The Seahorse XF^{e}96 was also applied on environmental samples such as soil extracts (Probert et al. 2018) but not in a quantitative way that accounts for the absolute effect of a sample relative to a reference chemical and distinguishes between different modes of action.

Oxidative phosphorylation in mitochondria has 3 main components that alter the OCR of cells to a measurable extent when interacting with a disruptor (Figure 1). The first component comprises several protein complexes that are involved in the electron transport chain and build up the electrochemical gradient. If the electron transport chain is partly or completely inhibited (e.g., by a mix of rotenone and antimycin A [Rot/AA]), the proton gradient cannot be built up completely, which is directly associated with a decrease in the OCR. The second component is the membrane itself, forming the barrier necessary for an electrochemical proton gradient. Chemicals that uncouple the inner and outer mitochondrial membrane (e.g., 2,4-dinitrophenol [2,4-DNP]) break down this gradient as they transport the protons across the membrane and thereby short-circuit ATP production. To rebuild the electrochemical proton gradient, the mitochondrial respiration is up-regulated in response to uncouplers, and thus the OCR is increasing to its maximum. The third component is the ATP synthase protein complex. Chemicals that inhibit this protein complex (e.g., oligomycin) inhibit ATP production, which leads to an increasing proton gradient in the intermembrane space and induces a decreasing OCR as the cell tries to maintain a constant electrochemical proton gradient (Nicholls and Ferguson 2002).

We present 3 different experimental designs with which one can quantify the potency of a sample to 1) inhibit ATP synthase, 2) uncouple the mitochondrial membrane potential, or 3) inhibit the electron transport chain based on measuring the extracellular oxygen flux of HepG2 cells with a Seahorse XF^{e}96 Analyzer.

These experimental designs were used to characterize environmental pollutants that are known to occur in river water, including the herbicide bromoxynil; the fungicides fluazinam, azoxystrobin, and pyraclostrobin; and the biocide tributyltin. Moreover, water extracts from a small river near Tübingen, Germany, were collected 0.5 and 3.5 km downstream of a wastewater-treatment plant and tested for uncoupling and inhibition of the electron transport chain. Finally, the measured effects of the water extracts were validated with binary mixture experiments. The hypothesis of the mixture experiments was that 2 chemicals that show activity in one of the OCR bioassay designs act together according to concentration addition, which is the mixture toxicity concept applicable to mixtures of chemicals with the same modes of action (Backhaus and Faust 2012). In a binary mixture with an environmental sample that shows the OCR trace typical for uncouplers, such a concentration addition mixture effect would be a confirmation that the complex mixture behaves as if it has one mode of action only, despite the fact that complex environmental mixtures contain hundreds of thousands of chemicals with presumably hundreds of modes of action.

THEORY

Experimental designs for differentiating modes of action

To differentiate the 3 mechanisms of mitochondrial toxicity (ATP synthase inhibition, uncoupling, electron transport chain inhibition; Figure 1) by OCR measurements, we registered time-resolved traces of OCR measurements and consecutively applied reference compounds for inhibition of ATP synthase (oligomycin), uncoupling (2,4-DNP), and inhibition of the electron transport chain (Rot/AA). The OCR traces were generated by consecutive measurement cycles involving the lowering of the sensor probes to obtain a small chamber, measuring the OCR for 3 min, followed by 3 min of aeration and mixing. These traces were finally compared to parallel measurements, where one of the reference compounds was replaced by the sample or by a negative control (buffer; Supplemental Data, Figure S1).

Figure 2 provides a conceptual scheme of the OCR profiles measured for the 3 detection methods for inhibition of ATP synthase, uncoupling, and electron transport chain inhibition. Importantly, this OCR change was normalized to the basal

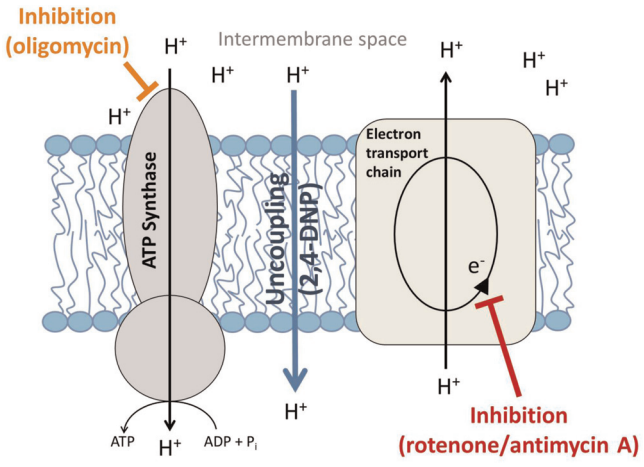

FIGURE 1: Illustration of the main components involved in oxidative phosphorylation, which are the inner mitochondrial membrane that contains the electron transport chain and adenosine triphosphate (ATP) synthase. The ATP synthase can be inhibited by the reference chemical oligomycin and the electron transport chain by a mix of rotenone and antimycin A. 2,4-Dinitrophenol is used as the reference chemical for uncoupling the proton gradient by allowing protons to pass the membrane barrier without ATP production. 2,4-DNP = 2,4-dinitrophenol.

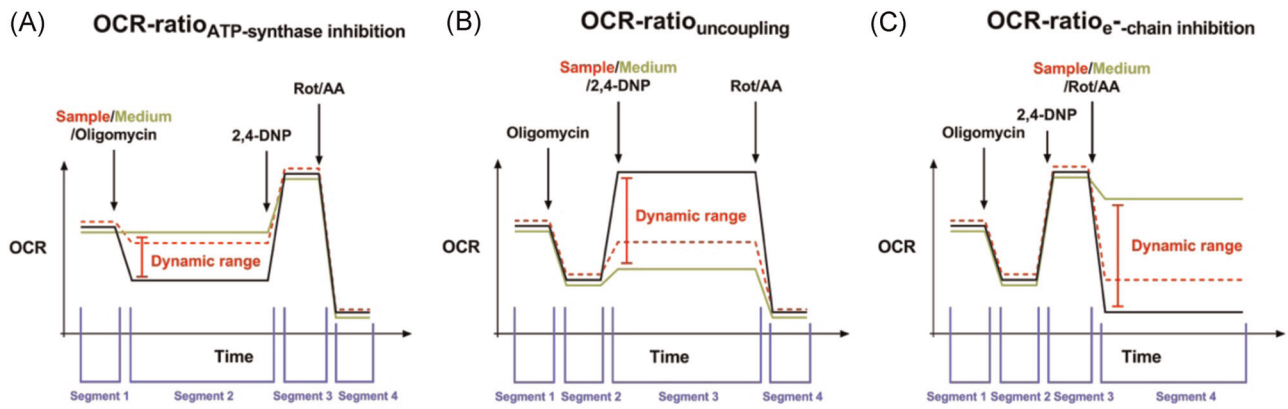

FIGURE 2: Oxygen consumption rate (OCR) profiles over time in the experimental test designs for (**A**) adenosine triphosphate (ATP) synthase inhibition, (**B**) uncoupling, and (**C**) electron transport chain inhibition. The OCR profiles of the positive control (injection of oligomycin, followed by 2,4-dinitrophenol and then rotenone and antimycin A (Rot/AA), black arrows) is illustrated as a black line. The OCR profile of the negative control is displayed as a green line. The OCR profile of a sample tested for the given mode of action is depicted as a dashed red line. The dynamic range of each experiment is indicated by the red vertical line. Each experimental design is separated into 4 time segments, illustrated by the blue brackets. 2,4-DNP = 2,4-dinitrophenol; Rot/AA = rotenone and antimycin A.

respiration of the respective well to reduce variability attributable to variations in cell numbers.

ATP synthase inhibition. To assess the potency of a sample to interfere with ATP synthase, the sample (dashed red line) was injected in parallel to assay medium only (green line, negative control) and to oligomycin at 1 μM (black line, positive control), after the basal respiration was measured for 3 measurement cycles, as illustrated in Figure 2A. After injection, the OCR was measured for 9 measurement cycles, corresponding to an incubation time of 54 min. This is a longer incubation time than for most routine Seahorse applications but was chosen to increase the robustness of the assay and to assure sufficient time for cellular uptake kinetics (Fischer et al. 2018). At the next stage, the uncoupler 2,4-DNP was added to the cells (previously exposed to either sample, medium, or oligomycin) at 80 μM (causing 95% of maximum OCR), and the OCR was measured for 3 measurement cycles. Subsequently, Rot/AA (0.5 μM), completely inhibiting the electron transport chain, was added and the OCR measured for another 3 measurement cycles.

The dynamic range indicated in Figure 2A ranges from 0% inhibition set at the OCR of cells that underwent an injection of medium and 100% inhibition by 1 μM oligomycin, which completely inhibits ATP synthase. Because inhibition of the electron transport chain would also lead to a decrease in OCR, the specificity of the inhibitory effect on ATP synthase was assessed by subsequently injecting 80 μM of 2,4-DNP. If the cells exposed to the sample did not reach an increased OCR with 80 μM 2,4-DNP as high as in the negative control, the sample inhibits the electron transport chain rather than the ATP synthase. If the electron transport chain is inhibited, the electrochemical gradient cannot be built up and consequently cannot be uncoupled. Hence, the cells would be unable to reach their maximum respiration rate.

Uncoupling. For the quantitative assessment of the potency of a chemical to uncouple the mitochondrial membrane, the OCR was brought down by 1 μM oligomycin after the basal respiration was measured in 3 measurement cycles, to increase the dynamic range (Figure 2B). After 3 measurement cycles, the cells were exposed to the sample (dashed red line). In parallel, 80 μM of 2,4-DNP marked the upper effect level (positive control, black line) and assay medium marked the no-effect level (negative control, green line). A negative control is indispensable because the OCR is gradually recovering back to basal respiration (green line in Figures 1B and 3) after the oligomycin injection. Subsequent to the sample–2,4-DNP–medium injection, the OCR was measured in 9 measurement cycles for a total period of 54 min. At last 0.5 μM Rot/AA was injected to the cells and measured in 3 measurement cycles.

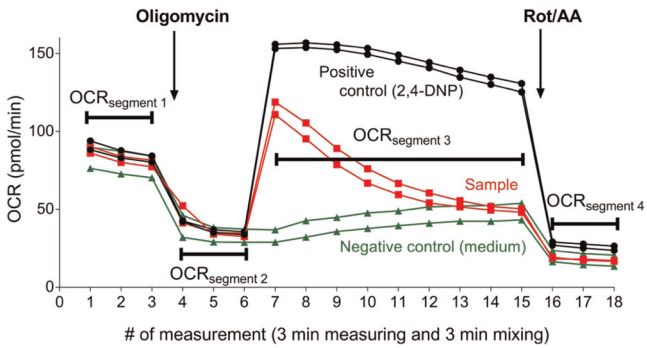

FIGURE 3: Oxygen consumption rate (OCR) profile over time (expressed as number of measurements) in the experimental design for measuring the uncoupling activity, OCR ratio$_{uncoupling}$, of a sample (100 μM bromoxynil, red lines) relative to the positive control (80 μM 2,4-dinitrophenol, black line) and the negative control (medium, green line). Each line represents the OCR of one single well. All wells had the same treatment with oligomycin (after measurement 3) and rotenone and antimycin A (after measurement 15) and differed only in the treatment after measurement 6. Bold black brackets indicate time segments 1, 2, 3, and 4 (OCR$_{segment\ 1}$, OCR$_{segment\ 2}$, OCR$_{segment\ 3}$, OCR$_{segment\ 4}$). 2,4-DNP = 2,4-dinitrophenol; Rot/AA = rotenone and antimycin A.

Electron transport chain inhibition. For testing chemicals that interfere with the electron transport chain, basal respiration was measured in 3 measurement cycles. Then, 1 µM oligomycin was added to the cells to ensure an OCR decrease after sample addition not being caused by ATP synthase inhibition. After 3 measurement cycles, the OCR was brought up by injecting 80 µM 2,4-DNP to increase the dynamic range, followed by another 3 measurement cycles. Finally, the cells were exposed either to the sample, to 0.5 µM Rot/AA, or to medium (Figure 2C). The decreased OCR caused by Rot/AA marks 100% electron transport chain inhibition (positive control, black line in Figure 2C), and the OCR after medium injection marks the no-effect level (negative control, green line in Figure 2C). Again, a medium control is indispensable because the OCR is gradually recovering back to basal resiration after exposure to 2,4-DNP (green line in Figure 2C).

Data evaluation

OCR measurements. As the first step in quantitatively assessing the activity of a sample, the OCR–time profile was separated into 4 time segments (Figure 2), compiling the 3 to 9 OCR measurements made while measuring the basal respiration or between 2 injections. The data evaluation procedure is illustrated in the example of the uncoupling activity, OCR $\text{ratio}_{\text{uncoupling}}$, of 100 µM bromoxynil as sample in Figure 3. For each well the OCR values measured within a time segment were averaged ($\text{OCR}_{\text{segment 1}}$, $\text{OCR}_{\text{segment 2}}$, $\text{OCR}_{\text{segment 3}}$, $\text{OCR}_{\text{segment 4}}$).

For each well the OCR change induced by the sample, negative or positive control (for uncoupling the difference between the $\text{OCR}_{\text{segment 2}}$ and $\text{OCR}_{\text{segment 3}}$, see Figure 3), was normalized to the basal respiration ($\text{OCR}_{\text{segment 1}}$) in that well and expressed as ΔOCR. For the experimental designs ATP synthase inhibition, uncoupling, and e^--chain inhibition the ΔOCR values were calculated according to Equations 1–3, respectively, with *i* referring to the wells for the sample or negative control or positive controls (oligomycin for ATP synthase inhibition, 2,4-DNP for uncoupling, and Rot/AA for electron transport chain inhibition). The ΔOCR values of the same treatment were then averaged. For ATP synthase inhibition:

$$\Delta\text{OCR}_i = \frac{\text{OCR}_{\text{segment 1}} - \text{OCR}_{\text{segment 2}}}{\text{OCR}_{\text{segment 1}}} \quad (1)$$

For uncoupling:

$$\Delta\text{OCR}_i = \frac{\text{OCR}_{\text{segment 3}} - \text{OCR}_{\text{segment 2}}}{\text{OCR}_{\text{segment 1}}} \quad (2)$$

For electron transport chain inhibition:

$$\Delta\text{OCR}_i = \frac{\text{OCR}_{\text{segment 3}} - \text{OCR}_{\text{segment 4}}}{\text{OCR}_{\text{segment 1}}} \quad (3)$$

OCR ratios for each modes of action were subsequently calculated by Equation 4 using the ΔOCR_i of the appropriate modes of action according to Equation 1, 2, or 3.

$$\text{OCR ratio}_{\text{MoA}} = \frac{\Delta\text{OCR}_{\text{sample}} - \Delta\text{OCR}_{\text{negative control}}}{\Delta\text{OCR}_{\text{positive control}} - \Delta\text{OCR}_{\text{negative control}}} \quad (4)$$

For all wells belonging to the same treatment the average and standard deviation of this OCR ratio were derived. The standard deviation of the OCR ratio was derived according to the Gauss law of error propagation, reflected in Equation 5:

$$\text{SD OCR ratio}_{\text{MoA}} = \sqrt{\left(\begin{array}{l}\left(\left(\frac{1}{\Delta\text{OCR}_{\text{positive control}} - \Delta\text{OCR}_{\text{negative control}}}\right)^2 \times \left(\text{SD}_{\Delta\text{OCR}_{\text{sample}}}\right)^2\right) + \\ \left(\left(\frac{\Delta\text{OCR}_{\text{negative control}} - \Delta\text{OCR}_{\text{sample}}}{\left(\Delta\text{OCR}_{\text{positive control}} - \Delta\text{OCR}_{\text{negative control}}\right)^2}\right)^2 \times \left(\text{SD}_{\Delta\text{OCR}_{\text{positive control}}}\right)^2\right) + \\ \left(\left(-\frac{\Delta\text{OCR}_{\text{positive control}} - \Delta\text{OCR}_{\text{sample}}}{\left(\Delta\text{OCR}_{\text{positive control}} - \Delta\text{OCR}_{\text{negative control}}\right)^2}\right)^2 \times \left(\text{SD}_{\Delta\text{OCR}_{\text{negative control}}}\right)^2\right)\end{array}\right)} \quad (5)$$

Concentration–response curves. The full concentration–response curves (CRCs) showed a typical sigmoidal shape and can be fitted using logarithmic concentrations and a 2-parameter logistic fit from 0 and 100% effect (Equation 6).

$$\text{OCR ratio} = \frac{100\%}{1 + 10^{\text{slope}(\log\text{EC50} - \log\text{concentration})}} \quad (6)$$

In Equation 6 EC50 is the median effect concentration. Because the activation in a bioassay by an environmental sample that contains many different compounds can be masked and attenuated by cytotoxicity and other nonspecific effects, concentrations above the maximum effect of the sample causing concentration and revealing <80% of the maximum effect within an experiment were excluded from the fit. For environmental samples the exclusion of cytotoxic concentrations leads in many cases to a CRC that does not even reach 50% of maximum effect. Hence, we focused on the lower portion of the CRC for the data evaluation, where CRCs on a linear concentration scale exhibit an approximately linear behavior up to 40% of the maximum effect level (Escher et al. 2018), described by Equation 7.

$$\text{OCR ratio} = \text{slope} \times \text{concentration} \quad (7)$$

The EC10 was calculated with Equation 8 from the slope of the linear regression of concentration versus the percent effect.

$$\text{EC10} = \frac{10\%}{\text{slope}} \quad (8)$$

The standard error of the EC10 was calculated according to Equation 9:

$$\text{SE(EC10)} = \frac{10\%}{\text{slope}^2} \times \text{SE}_{\text{slope}} \quad (9)$$

MATERIALS AND METHODS

Cell line

We used a modified HepG2 cell line, the CellSensor® ARE-bla HepG2 cell line, for the OCR experiments. To avoid the cells growing in multiple layers and as a compromise between cell viability and a suitable oxygen consumption, 15 000 cells per well, which attained an average OCR of 75 pmol min^{-1}, were seeded onto XF96 Cell Culture Microplates that were previously coated with poly-D-lysine. After seeding, the cells were incubated between 18 and 24 h at 37 °C and 5% CO_2. A detailed workflow is described in König et al. (2017). To avoid any misinterpretations attributable to cytotoxicity, all samples tested in the present study were checked for cytotoxicity after an incubation time of 24 h in the applied concentration ranges based on measuring the cell area coverage (Escher et al. 2018).

Assay

Hydration, media exchange, and cell imaging. The XF^{e}96 sensor cartridges were incubated in sterile water overnight in a humidified non-CO_2 incubator at 37 °C. At least 1 h before the experiment the sterile water was exchanged with XF calibrant solution, and the sensor cartridge was incubated until the measurement under the same conditions. The medium was exchanged with the Seahorse XF assay medium prior to the measurement. The culture medium was aspirated using a BioTek® 405 TS washer, leaving 20 µL in each well. Each well was refilled to a final volume of 180 µL with prewarmed Seahorse XF Assay Medium (Agilent Technologies) supplemented with 10 mM glucose, 1 mM pyruvate, 2 mM glutamine, and 5 mM HEPES and adjusted to pH 7.4. After this step was repeated 3 times, the microplate was incubated at 37 °C in a non-CO_2 incubator for at minimum of 1 h and a maximum of 2 h. Prior and subsequent to every experiment the cells were visually checked by microscopy with a Leica DMi1 for morphological alterations, such as cell rounding and loss of adherence, that go along with changes in cell viability (Rello et al. 2005).

Loading the XF^{e}96 sensor cartridge. In every experiment irrespective of the experimental design a reference test profile (positive control) was performed by injecting the reference chemicals oligomycin (10 µM), 2,4-DNP (0.8 mM), and Rot/AA (5 µM) as follows: port A → port B → port C. These positive controls were prepared and injected in 10 times concentrations. This combination causes complete ATP synthase inhibition, 95% uncoupling (Supplemental Data, Figure S2), and complete electron transport chain inhibition and serves as the reference, to which all samples were compared. To characterize the potency of a chemical to inhibit the mitochondrial ATP synthase, the chemical or sample of interest was loaded into port A in the desired concentration instead of oligomycin. To evaluate the potency of a chemical to uncouple the mitochondrial membrane, the sample was loaded into port B in the desired concentration instead of 2,4-DNP. To assess the potency of a compound to inhibit the mitochondrial electron transport chain, the sample was loaded into port C instead of Rot/AA. Because the OCR went back to basal respiration over time, a negative control was added on the same plate. For the negative control, the Seahorse assay medium was loaded into port A, port B, or port C instead of oligomycin, 2,4-DNP, or Rot/AA, respectively. Finally, the plate contained the following treatments: positive control (port A, oligomycin; port B, 2,4-DNP; port C, Rot/AA), negative control (medium filled into port A, B or C instead of oligomycin, 2,4-DNP, or Rot/AA, respectively), sample (loaded into either port A, B, or C instead of oligomycin, 2,4-DNP, or Rot/AA, respectively), background (wells containing no cells but treated equally to the positive control), and medium background (medium loaded into ports A, B, and C). After injection of the sample as well as in parallel the positive and negative controls, the OCR was measured in 9 measurement cycles for a total period of 54 min to provide enough time for the sample to enter the cells and cause an effect, which is important especially for environmental samples. One measurement cycle consisted of 3 min of measuring the cellular OCR and 3 min of mixing by lifting the sensors up and down. All other injections were only measured by 3 measurement cycles. As a trade-off between sufficient statistical effect size and a high number of samples on one microplate, 4 replicates for each sample were found to be a pragmatic choice. To assure the robustness of the test system, the replicates for the positive control, negative control, and backgrounds (cells exposed to medium only and no cells exposed to the positive control) were set at a number of 8. Wells that underwent an unsuccessful injection, apparent from incompletely emptied injection ports, or a premature injection attributable to the pipetting procedure were declared technical outliers and discarded. Wells attaining a basal respiration ≤ 40 pmol min^{-1} were also excluded from the data evaluation.

To assess the assays' performance, we derived the Z factor (Zhang et al. 1999) for every experimental design according to Equation 10, based on the OCR ratios and standard deviations of the positive and negative controls:

$$Z = 1 - \frac{3\mathrm{SD}\ \Delta\mathrm{OCR}_{\text{positive control}} + 3\mathrm{SD}\ \Delta\mathrm{OCR}_{\text{negative control}}}{\left|\text{mean}\ \Delta\mathrm{OCR}_{\text{positive control}} - \text{mean}\ \Delta\mathrm{OCR}_{\text{negative control}}\right|} \quad (10)$$

Every performed experiment was taken into consideration using all replicates of the positive control ($n = 8$) and the negative control ($n = 8$) unless they fell under the criteria of technical outliers.

Testing of water samples

In June 2018, river water samples from a German river (see Müller et al. 2018) were enriched with large-volume solid-phase extraction (LV-SPE; Maxx Meß- und Probenahmetechnik) according to Schulze et al. (2017) with minor modifications. Each water extract integrated 20 L of river water sampled over 6 h using an HR-X sorbent (Chromabond®; Macherey-Nagel) with a sorbent to sample ratio of

0.2 g L^{-1}. The exact geographical coordinates are 48°33′ 40.9"N 8°54′10.7"E for sampling site 1 (SS1), approximately 500 m downstream of a wastewater-treatment plant, and 48°32′28.8"N 8°55′15.4"E for sampling site 2 (SS2), which is located approximately 3 km downstream of SS1. The sampling was conducted in 2 intervals, A and B. At SS1 sampling interval A (SS1-A) was performed from 12:00 to 18:00 and sampling interval B (SS1-B) from 18:00 to 24:00. At SS2 the sampling was 2 h and 13 min (SS2-A and SS2-B) delayed because the water needed that time to pass the distance from SS1 to SS2. The concentrations of water are reported in units of relative enrichment factor (REF; Escher et al. 2009).

Binary mixtures

In environmental samples chemicals are present in and act as mixtures. The conventional wisdom for mixture toxicity is that chemicals that act according to the same modes of action act by concentration addition in mixtures (Backhaus and Faust 2012). For binary mixtures the concordance or deviation from the concept of concentration addition can easily be tested and visualized by an isobologram (Altenburger et al. 1990). For this purpose, the toxic units (TUs) of mixture components A (TU_A) and B (TU_B) are plotted against each other. Components A and B can be single compounds or environmental samples, and they can also have different concentration scales because the units for the concentrations C_A and C_B and the respective effect concentrations ($EC10_A$ and $EC10_B$) cancel out in the equation for toxic unit (Equation 11).

$$TU_A = \frac{C_A}{EC10_A} \text{ and } TU_B = \frac{C_B}{EC10_B} \quad (11)$$

The mixtures were designed in such a way that on one plate 2 concentrations of each component A and B was dosed (to confirm the earlier single-component CRC) and then 3 different mixture ratios constituting at the highest dose 75% of the EC30 of A with 25% of the EC30 of B, 50% of the EC30 of A with 50% of the EC30 of B, and 25% of the EC30 of A with 75% of the EC30 of B. For each mixture a CRC was constructed by plotting the sum of the concentrations of components A and B in the chosen concentration ratio (dilution of a mixture) against the measured effect. The $EC10_{mix}$ was derived from the linear CRC, using Equation 8. The mixture designs were planned with slightly different EC10 values but then evaluated with all final data together. The final toxic unit in the mixture was then calculated with Equation 12, where the fraction f_A of component A in a mixture is the concentration of the component relative to the sum of the concentrations of all components and likewise for B.

$$TU_A = \frac{f_A \times EC10_{mix}}{EC10_A} \text{ and } TU_B = \frac{f_B \times EC10_{mix}}{EC10_B} \quad (12)$$

The model of concentration addition holds if the sum of both toxic units of A and B in the mixture, which is expressed as sumTU and calculated according to Equation 13, is equal to 1.

$$\text{sumTU} = \frac{f_A \times EC10_{mix}}{EC10_A} + \frac{f_B \times EC10_{mix}}{EC10_B} \quad (13)$$

If sumTU $\gg$ 1, then the mixture acts antagonistically; if sumTU $\ll$ 1, then the mixture acts synergistically.

RESULTS AND DISCUSSION

Assay performance

For all 3 experimental designs excellent *Z* factors as a measure of statistical effect size and for the assay performance were derived (Table 1), justifying their applicability as bioassays for the detection of mitochondrial toxicity. The *Z* factor reflects the separation of negative and positive control and can vary between 0 and 1, with a value between 0.5 and 1 identifying an assay as performant (Zhang et al. 1999).

The limit of detection of effect (LOD, percentage) was defined as 3 times the standard deviation of the negative controls (0% effect) averaged over all experiments with reference chemicals (Table 1). To derive robust EC10 values from the linear CRCs, the maximum measured effects must be higher than the LOD, and the CRC must show a monotonous upward trend. The LODs approximately 10% were obtained for OCR $ratio_{e^-\text{-chain inhibition}}$ and OCR $ratio_{uncoupling}$ (Table 1), which is within the linear range of the CRC up to 40%, allowing a robust derivation of EC10 values. In contrast, the LOD for OCR $ratio_{ATP\text{-synthase}}$ was 16.6%, which renders the window for the linear CRC rather small. Although for OCR $ratio_{ATP\text{-synthase}}$ a robust derivation of an EC10 is in principle possible, we do not deem it appropriate for screening of environmental samples given the rather small window of the linear CRC.

Visually checking the cell morphology immediately before and after every experiment by microscopy did not uncover any changes in cell viability in all experiments performed in the present study. Given an incubation time of approximately 2 h, the morphological alterations of dying cells might not be detected as such. During an OCR assay experiment cytotoxicity caused by a sample would result in a decrease of the OCR. Consequently, the effect of cytotoxic samples was underestimated in the experimental design for uncoupling and overestimated or misinterpreted in the experimental

TABLE 1: Assay performance of the experimental designs for assessing ATP synthase inhibition, uncoupling and e^--chain inhibition described by the *Z* factor according to Zhang et al. (1999) and the limits of detection related to the reference chemicals

Experimental design	OCR ratio ATP synthase inhibition	OCR ratio uncoupling	OCR ratio e^--chain inhibition
Reference chemical	Oligomycin	2,4-DNP	Rot/AA
Z factor	0.64 ± 0.15	0.61 ± 0.12	0.69 ± 0.10
LOD (% effect)	16.6%	11.3%	9.6%

2,4-DNP = 2,4-dinitrophenol; LOD = limit of detection; Rot/AA = rotenone and antimycin A.

designs for ATP synthase inhibition and electron transport chain inhibition. In that regard, all single and reference chemicals were, in addition, applied to the same cell line separately and incubated for 24 h. Changes in cell viability after 24 h are depicted in Supplemental Data, Figure S3. The reference chemical rotenone had a 10% inhibition concentration (IC10) value below the concentration used in the assay, whereas antimycin A and oligomycin exhibited 10% cell death in concentrations slightly higher than those used in the assay. Because the IC10 is dependent on the incubation time, cytotoxicity is only of concern if it occurs within the duration of the experiment. For instance, in our proposed assay Rot/AA needed to be applied in a concentration of 0.5 µM to achieve complete inhibition of the electron transport chain. During the incubation time of 54 min in the OCR assay, the OCR level provoked by this mix stayed rather consistent with no further decrease that may be attributed to cell death (Supplemental Data, Figure S1), but declining cell viability was detected after an incubation time of 24 h (Supplemental Data, Figure S3).

Quantitative assessment of environmentally relevant single chemicals

Uncouplers. The chemicals 2,4-DNP, bromoxynil, and fluazinam—representative of environmentally relevant chemicals that uncouple the mitochondrial membrane—were chosen to validate the presented experimental design for testing uncouplers. Fluazinam is described in Supplemental Data, Figure S4.

New reference compound (2,4-DNP) for testing of uncoupling activity—The compound 2,4-DNP was chosen as the reference chemical for testing samples for uncoupling activity because it held the increased OCR over the entire testing period of segment 3 (Figure 3). Exposing the cells to concentrations exceeding the maximum uncoupling effect resulted in an attenuated increase of the OCR. Even though no immediate changes in cell viability were observed at 2,4-DNP concentrations above the one that causes maximum respiration, they led to lower OCR of the cells (Supplemental Data, Figure S2). To achieve a dynamic range as wide as possible in testing uncouplers and to avoid "oversaturation," the concentration of 2,4-DNP as the reference chemical was set to 80 µM, which triggers an uncoupling effect of 95% (Supplemental Data, Figure S2). The EC10 derived from the linear portion of the CRC (Figure 4A) was 6.46 ± 0.83 µM.

Bromoxynil is a widely used postemergence herbicide that interferes with photosynthetic electron transport and uncouples the oxidative phosphorylation in mitochondria (Droppa et al. 1981). In Germany it was used in quantities of 25 to 100 t reported for the year 2017 (Federal Office of Consumer Protection and Food Safety 2017) and therefore can potentially be present in the aquatic environment. A full CRC for bromoxynil ranging from 1 to 130 µM was determined, and there was an excellent overlap of 5 independent repetitions of the experiment at different concentrations (Supplemental Data, Figure S5). Before bromoxynil reached the maximum uncoupling effect (as set by the effect of 80 µM 2,4 DNP), the effects declined again, possibly by other, inhibitory effects or cytotoxicity

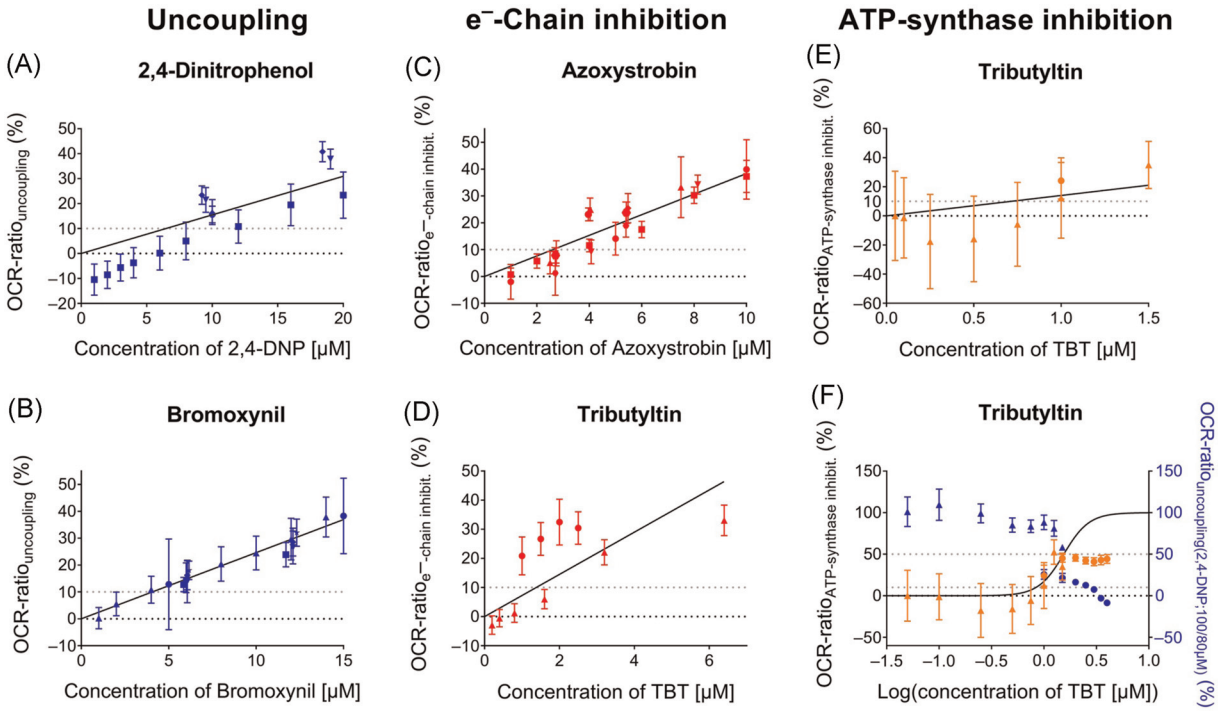

FIGURE 4: Oxygen consumption rate ratios of environmentally relevant single chemicals in the experimental designs for (**A, B**) uncoupling, (**C, D**) electron transport chain inhibition, and (**E, F**) adenosine triphosphate (ATP) synthase inhibition. Error bars indicate the standard deviation. 2, 4-DNP = 2,4-dinitrophenol; OCR = oxygen consumption rate; TBT = tributyltin.

(Supplemental Data, Figure S5). The EC10 derived from the linear portion of the CRC (Figure 4B) was 4.06 ± 0.09 μM.

Inhibitors of the electron transport chain in oxidative phosphorylation. For validation of the experimental design, the commonly used strobilurin fungicides azoxystrobin and pyraclostrobin were tested for inhibitory activity of the electron transport chain. In addition, the organotin compound tributyltin was tested for electron transport chain inhibition as well as inhibition of ATP synthase because it is known that tributyltin affects protein complexes and acts as an uncoupler (Hunziker et al. 2002).

A full CRC of azoxystrobin is depicted in Supplemental Data, Figure S6, with an e^--chain inhibition activity beyond 95% relative to Rot/AA at concentrations > 79 μM. The EC10 derived from the linear portion of the CRC (Figure 4C) was 2.61 ± 0.13 μM. Pyraclostrobin is described in Supplemental Data, Figure S7. The EC10 derived from the linear portion of the CRC was 1.18 ± 0.11 μM. Azoxystrobin and pyraclostrobin belong to the strobilurins a group of agrochemical fungicides. Strobilurins inhibit complex III of the oxidative phosphorylation because they impede the electron transport from ubiquinol to cytochrome *c* by binding to the ubiquinol oxydation center of cytochrome *b* (Mansfield and Wiggins 1990). The selectivity of strobilurins is based on differences in degradation and penetration in various organisms rather than on their general modes of action. Thus, they can potentially be toxic to a broad range of nontarget organisms (Maltby et al. 2009). Liess and Von Der Ohe (2005) and Berenzen et al. (2005) found maximum concentrations of 11.1 and 29.7 μg L^{-1} azoxystrobin in German river waters; hence, with an EC10 of 1105 μg L^{-1} it could in principle be detected in environmental samples at a REF of 100. Also, pyraclostrobin can potentially occur in environmental compartments such as surface waters and rivers (European Food Safety Authority 2010).

Organotin compounds such as tributyltin were widely used as biocides, especially as antifouling paintings for ships and fishing nets (Almeida et al. 2007). Among other inorganic compounds, tributyltin interferes with the oxidative phosphorylation in mitochondria in a number of ways simultaneously (Hunziker et al. 2002). They inhibit electron transport (Aldridge 1958; Saxena 1987), uncouple the mitochondrial membrane (Bragadin et al. 2003), and inhibit ATP synthase (Aldridge and Street 1964; Matsuno-Yagi and Hatefi 1993). Tributyltin was tested in the assay for electron transport chain inhibition, and the EC10 was 1.38 ± 0.26 μM (Figure 4D). The full logarithmic CRC of tributyltin is depicted in Supplemental Data, Figure S8.

Inhibitors of ATP synthase. Inhibition of the ATP synthase of tributyltin was assessed relative to 1 μM oligomycin (Figure 4E,F). At concentrations > 1.50 μM a maximum effect level of approximately 50% appears to be reached and not exceeded. The EC10 was 0.71 ± 0.33 μM. After tributyltin was added to the cells and an incubation time of 54 min, 80 or 100 μM 2, 4-DNP, respectively, was added to test if ATP synthase is inhibited and maximum respiration would still be possible to achieve. The OCR $ratio_{uncoupling}$ decreased in a dose-dependent manner (blue data points in Figure 4F). Even at tributyltin concentrations that already reached a plateau of OCR $ratio_{ATP\ synthase\ inhibition}$ at 50%, OCR $ratio_{uncoupling}$ continued to decrease with increasing tributyltin concentrations. This observation is consistent with our previous findings that tributyltin can, in addition, act as an inhibitor of the electron transport chain.

Summary of environmentally relevant single chemicals and cytotoxicity. A summary of the effect concentrations of the tested environmentally relevant single chemicals is given in Supplemental Data, Table S1. The EC10 values derived from the linear portion of the CRC are within the 95% confidence interval of the EC10 derived from the sigmoidal logarithmic CRC. This confirms that the linear CRC evaluation is appropriate despite the LOD being around or slightly above 10% effect. Linear CRCs for EC10 derivation are advantageous for environmental samples because they require only the 0 to 40% effect range, and the sample is less prone to interference by nonspecific effects (Escher et al. 2018). Bromoxynil, 2,4-DNP, azoxystrobin, and pyraclostrobin showed high precision and reproducibility and confirmed the experimental designs OCR $ratio_{e^-\text{-chain inhibition}}$ and OCR $ratio_{uncoupling}$ applicable for the assessment of single chemicals (Supplemental Data, Table S1). The results of tributyltin tested in the experimental designs on OCR $ratio_{ATP\ synthase\ inhibition}$ and OCR $ratio_{e^-\text{-chain inhibition}}$ showed that the OCR assay reached its limits when it comes to chemicals targeting multiple sites in mitochondrial respiration or samples that include multiple components exhibiting different modes of action. The experimental design OCR $ratio_{ATP\ synthase\ inhibition}$ cannot distinguish between chemicals that inhibit ATP synthase and those that inhibit the electron transport chain because in both cases the OCR decreases. On the other hand, ATP synthase inhibitors do not interfere with the experimental design on OCR $ratio_{e^-\text{-chain inhibition}}$ because ATP synthase is already inhibited by oligomycin and protons predominantly pass the membrane barrier by 2,4-DNP carriage. The experimental design OCR $ratio_{ATP\ synthase\ inhibition}$ showed a relatively high LOD of 16.6%, which makes it difficult to derive robust EC10 values. Moreover, even though it has been proven by other researchers that tributyltin uncouples the mitochondrial membrane, this effect is masked by inhibition of the electron transport chain and therefore cannot be detected by measuring the extracellular oxygen flux. The absolute level of the membrane potential is also affected by inhibitors; hence, to differentiate uncoupling from inhibition, one needs to perform kinetic measurements of the decay of the membrane potential, as in the work by Hunziker et al. (2002).

The binary mixture experiments listed in Supplemental Data, Table S2, showed the OCR $ratio_{e^-\text{-chain inhibition}}$ and OCR $ratio_{uncoupling}$ of 2 mixtures of the inhibitor azoxystrobin and the uncoupler bromoxynil in different concentration ratios. In both mixtures the uncoupling effect was completely masked by the electron transport chain inhibition that revealed effects in the same range as in the single-chemical experiments with azoxystrobin. Thus, if the electron and proton gradients are not built

up, they cannot be destroyed by uncoupling. Thus, inhibitors will always mask uncouplers in the OCR bioassay. In contrast, inhibitors have the same effect regardless of whether an uncoupler is present. An alternative measure to shed light on the interference of chemicals with different modes of action present in a sample could be the extracellular acidification rate (ECAR; see Supplemental Data). The OCR measurements in the present study were performed in the presence of buffer to stabilize the OCR, and consequently the ECAR did not change much in the presence of uncouplers (Supplemental Data, Figure S9). The energy maps plotting OCR versus ECAR (Supplemental Data, Figure S10) also serve only as a diagnostic tool but cannot be used to derive CRCs and effect concentrations for the different modes of action of mitochondrial toxicity.

Environmental samples

Water extracts. The water extracts SS1-A, SS2-A, SS1-B, and SS2-B were measured in the experimental designs for uncoupling and for electron transport chain inhibition. A background control of the LV-SPE devices was tested for uncoupling and for electron transport chain–inhibiting activity. The effects were below the effect threshold of 10% up to a REF of 200 (the results are described in Supplemental Data, Figure S11).

Water extract SS1-A exhibited an uncoupling activity in 4 independent experiments, displayed in Figure 5A. An EC10 value of 97.9 ± 12.4 REF was determined based on the linear portion of the CRC. The highest uncoupling activity of 29% relative to 80 µM 2,4-DNP was obtained at a REF of 200 in the first experiment. In 2 experiments (diamond and square symbols in Figure 5A) the sample was tested at REF 194 and 97 in 2 independent binary mixture experiments that will be described in more detail in the following. In these 2 experiments, a REF of 97 caused OCR ratio$_{uncoupling}$ of 7.74 ± 4.81 and 11.3 ± 2.9%, which is consistent with the full CRC of the 2 first experiments. However, exposing the cells to REF 194 did not exceed 10% OCR ratio$_{uncoupling}$ in these 2 experiments.

Water extract SS1-A was also tested in the experimental design for electron transport chain inhibition but did not have any activity (Figure 5B). Water extract SS2-A acted as an inhibitor of the electron transport chain (Figure 5D) but did not show any uncoupling activity in the applied concentration range (Figure 5C). The EC10 for inhibition of the electron transport chain derived from the linear portion of the CRC was 9.34 ± 1.77 REF. Importantly, causing a 10% effect when enriched < 10-fold implies and highlights the high environmental relevance of mitochondria-disrupting chemicals that can sentence a cell to death (Meyer et al. 2013).

Water extract SS1-B did not yield effects exceeding 10% OCR ratio$_{uncoupling}$ in the experimental design for uncouplers (Figure 5E). However, a linear regression revealed a calculated EC10 of 179 REF, which is just within the applied concentration range. In the experimental design for inhibitors of the electron transport chain, water extract SS1-B did not exceed the 10% level either (Figure 5F). The calculated EC10 based on the linear CRC was 303 ± 64 REF, which is an extrapolation beyond the applied concentration range and consequently not reliable. The second water extract collected during sampling interval B at SS2, SS2-B, yielded no uncoupling activity but electron transport chain inhibition with an EC10 of 23.6 ± 2.0 REF (Figure 5G,H).

Within the first sampling interval uncoupling activity was measured at SS1 that turned into electron transport chain inhibition at SS2. These data indicate degradation of uncouplers or additional inputs of inhibitors between SS1 and SS2. Both samples at SS2, SS2-A and SS2-B, showed only inhibitory effects.

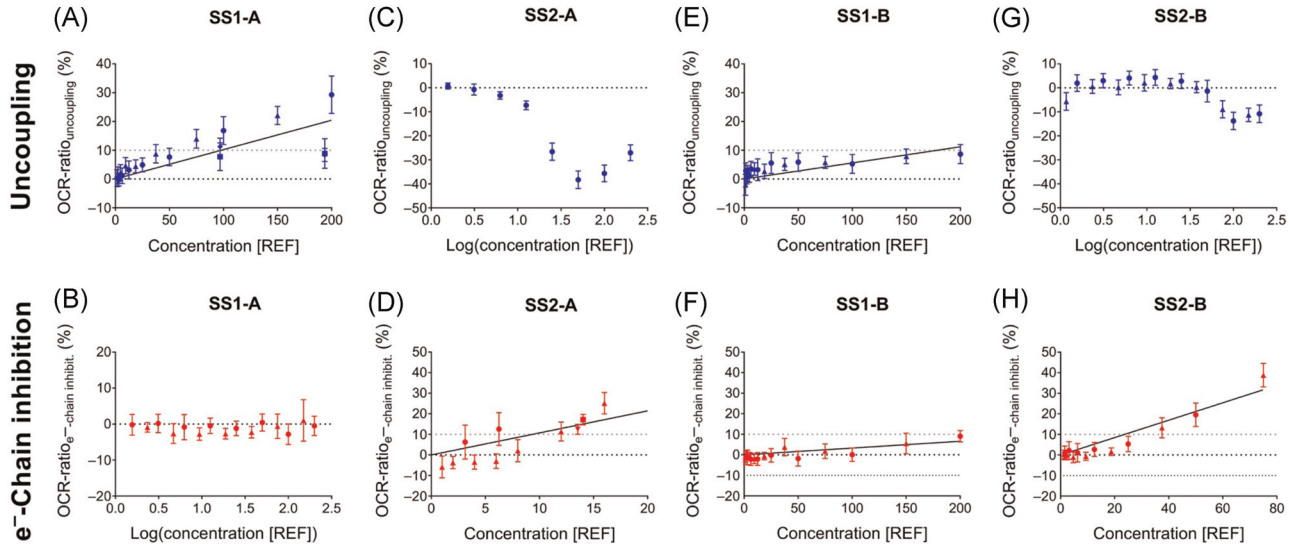

FIGURE 5: Water extracts SS1-A, SS2-A, SS1-B, and SS2-B tested in the experimental designs for uncoupling (**A, C, E**, and **G**) and for electron transport chain inhibition (**B, D, F**, and **H**). (**A, D, E, F**, and **H**) represent the linear portion of the concentration–response curve, others are depicted on a logarithmic concentration scale. Error bars indicate the standard deviation. OCR = oxygen consumption rate; REF = relative enrichment factor; SS = sampling site.

Cytotoxicity. The water extracts did not show any changes in cell viability during the OCR experiments, but some cytotoxicity was detected after 24 h of incubation (Supplemental Data, Figure S3). The 24-h IC10 values within concentration ranges of the linear portions of the OCR-CRC were determined only for water extracts SS1-A and SS1-B. In both extracts uncoupling activity was detected. The detected uncoupling might be partially a cytotoxicity artifact because nonspecifically acting compounds can also disturb membrane structure and hence may lead to proton leakages attributable to baseline toxicity (narcosis). In fact, as studies on isolated energy-transducing membranes have shown, the decay of the membrane potential is accelerated by uncouplers and baseline toxicants alike, the latter only at much higher concentrations (Escher et al. 2002).

Mixtures

The binary mixture experiments of bromoxynil with 2,4-DNP demonstrated that the 2 uncouplers acted in a concentration-additive way (Figure 6A). One of the 3 independent experiments was slightly off toward synergy, but given the small quantities to be pipetted, this could also be a pipetting error because the single compound 2,4-DNP showed in the mixture experimental plate a slightly enhanced effect level compared to the CRC (see diamonds in Figure 4A).

Because the uncoupling experiments with the water samples could not clearly differentiate between specific uncoupling and a baseline toxic effect, we also tested a combination of bromoxynil with SS1-A. Figure 6B shows some variability and a slight trend toward antagonism, but all mixture ratios were close to sumTU = 1. Thus, concentration addition is essentially confirmed, implying that the uncoupler bromoxynil and the water extract SS1-A have the same modes of action of uncoupling.

To confirm the applicability of the experimental design for electron transport chain inhibition and to assess whether 2 electron transport chain inhibitors act in a concentration-additive way, 2 binary mixture experiments of azoxystrobin with pyraclostrobin were conducted. Both chemicals belonging to the strobilurin family inhibit the electron transport chain at the level of complex III (Mansfield and Wiggins 1990). Both experiments confirmed concentration addition of the 2 components acting together (Figure 6C). For one experiment (diamonds) the concentration addition model perfectly held because a sumTU of 1.0 was within the error range of all mixtures, but also the second experiment (squares) came very close to a sumTU of 1.0 (Supplemental Data, Figure S12). Thus, also for inhibitors of the electron transport chain, concentration addition for binary mixtures can be measured by the proposed OCR bioassay.

A binary mixture of azoxystrobin with water sample SS2-A was also tested to assess whether the electron transport chain–inhibiting activity measured in water extract SS2-A was exerted by the same mode of action as azoxystrobin, which inhibits complex III. In 2 independent experiments concentration addition was confirmed (Figure 6D) because the sumTU of 1.0 was within the error range of all applied mixtures with one outlier (Supplemental Data, Figure S13). The electron transport chain involves several protein complexes that are not linearly interacting and can substitute for each other in their function as they form a complex redox system. Although both azoxystrobin and SS2-A caused 100% electron transport chain inhibition when measured independently, they might act on different sites of the electron transport chain, or the water sample might have multiple inhibitory sites.

CONCLUSION

OCR bioassay design

We have presented 2 experimental designs for cellular OCR measurements, which yielded excellent and statistically significant effect sizes and with which one can precisely and reproducibly assess uncoupling and electron transport chain inhibition.

A third experimental design for assessing ATP synthase inhibition was presented but revealed a relatively high detection limit of 16.6% given the small dynamic range. Because we recommend target effect levels up to 40% of maximum effects of

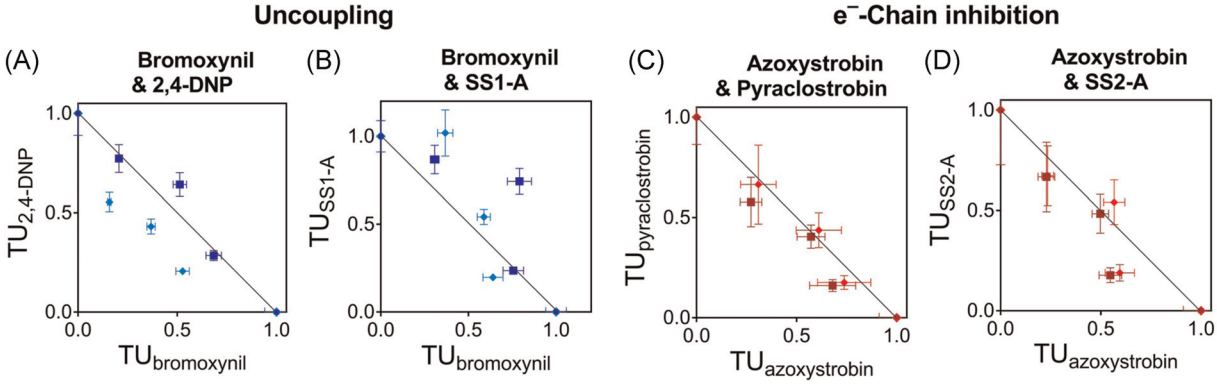

FIGURE 6: Binary mixtures of bromoxynil and 2,4-dinitrophenol (**A**), bromoxynil and SS1-A (**B**), azoxystrobin and pyraclostrobin (**C**), and azoxystrobin and SS2-A (**D**). The experiments represented by (**A** and **B**) were performed in the experimental design for uncoupling, and the experiments represented by (**C** and **D**) were performed in the experimental design for electron transport chain inhibition. Error bars indicate the standard errors derived by error propagation. 2,4-DNP = 2,4-dinitrophenol; SS = sampling site; TU = toxic unit.

the reference chemicals to avoid any matrix interference and cytotoxicity interference as well as to achieve high sensitivity, the LOD of the experimental design for ATP synthase inhibition is too high to derive a robust and precise EC10.

The short duration of an OCR experiment has both benefits and disadvantages. The experiment, which lasts approximately 2 h, is rather short compared with other in vitro bioassays and therefore allows a higher throughput. However, it simultaneously hinders an accurate determination of cell viability. Even though fully destroying energy production sentences a cell ultimately to death, 2 h may be too short for using cell morphology as a surrogate for cell viability. A decrease in OCR could therefore also be caused by nonspecific cytotoxicity. Because mitochondria are crucial for the energy production of almost all eukaryotic organisms, the impairment of their functions by organic micropollutants is inevitably associated with cell viability and thus highlights the environmental relevance of such chemicals.

Limitations of the OCR bioassay for application to environmental samples

For the testing of samples with unknown constituents, we recommend a tiered approach of the experimental designs in the order OCR ratio$_{e^-\text{-chain inhibition}}$ → OCR ratio$_{uncoupling}$ → OCR ratio$_{ATP\ synthase\ inhibition}$, to overcome the interference of inhibitors of the electron transport chain with ATP synthase inhibitors and uncouplers.

If a sample shows significant electron transport chain inhibition in the first step, no further steps will be necessary because this inhibitory effect would mask the effect of uncouplers and ATP synthase inhibitors that may also be present in the sample. If no electron transport chain inhibition is detected, it is recommended that the activity of uncouplers be tested subsequently. If the sample shows uncoupling activity, a further testing for ATP synthase is obsolete because an OCR decrease could not be induced when the protons can pass the membrane barrier facilitated by an uncoupler. If neither electron transport chain inhibition nor uncoupling activity was measured, testing for ATP synthase inhibition would be possible but, given the small dynamic range, might be rather limited. With the example of tributyltin we showed that multiple modes of action cannot be deconvoluted because the dominant effect will mask the other effects. There are other methods that directly measure the electron transport chain and the membrane potential that can quantitatively differentiate between the 3 modes of action of triorganotin compounds (Hunziker et al. 2002). Because organotin compounds have been phased out in agricultural applications and no other ATP synthase inhibitors are known to be present in environmental waters, this endpoint is not expected to be of high environmental relevance.

Applicability of the OCR bioassay to environmental samples

The proposed OCR bioassay was applicable for environmental samples such as water extracts and identified mitochondrial toxicity against a background of a large quantity of nonspecifically acting compounds. For 4 water extracts we uncovered uncoupling or electron transport chain inhibition with this test system and confirmed the samples' dominant modes of action by binary mixture experiments with chemicals of known modes of action.

We propose this test system as a suitable addition to chemical analysis and environmentally relevant in vitro bioassays (Müller et al. 2018) to identify input sources and trace changes of organic micropollutants in the environment. Given the high toxicological relevance of chemicals disrupting mitochondrial respiration, it is all the more surprising that the most active measured environmental sample caused 10% OCR ratio$_{e^-\text{-chain inhibition}}$ when enriched < 10-fold. In this context, we emphasize the consideration of mitochondrial respiration–disrupting chemicals in regulatory monitoring efforts.

Supplemental Data—The Supplemental Data are available on the Wiley Online Library at DOI: 10.1002/etc.4396.

Acknowledgment—The authors thank Agilent Technologies for material support and the loan of a Seahorse XF^{e}96 Analyzer. We thank J. John, A. Hajosch, and O. Nied for experimental assistance. The present study was supported by the Collaborative Research Centre 1253 CAMPOS (Project P1: Rivers), funded by the German Research Foundation (grant SFB 1253/1 20147).

Disclaimer—S. Vikström declares being employed by Agilent Technologies, the financial institution providing the Agilent Seahorse XF^{e}96 Analyzer. All other authors have no interest to declare. The views expressed in the present study are solely those of the authors.

Data Accessibility—Unprocessed data are available on request to maximilian-eckhard.mueller@uni-tuebingen.de.

REFERENCES

Aldridge W, Street B. 1964. Oxidative phosphorylation. Biochemical effects and properties of trialkyltins. Biochem J 91:287–297.

Aldridge WN. 1958. The biochemistry of organotin compounds. Trialkyltins and oxidative phosphorylation. Biochem J 69:367–376.

Almeida E, Diamantino TC, de Sousa O. 2007. Marine paints: The particular case of antifouling paints. *Prog Org Coat* 59:2–20.

Altenburger R, Bödeker W, Faust M, Grimme LH. 1990. Evaluation of the isobologram method for the assessment of mixtures of chemicals: Combination effect studies with pesticides in algal biotests. *Ecotoxicol Environ Saf* 20:98–114.

Attene-Ramos MS, Huang R, Sakamuru S, Witt KL, Beeson GC, Shou L, Schnellmann RG, Beeson CC, Tice RR, Austin CP, Xia M. 2013. Systematic study of mitochondrial toxicity of environmental chemicals using quantitative high throughput screening. *Chem Res Toxicol* 26:1323–1332.

Backhaus T, Faust M. 2012. Predictive environmental risk assessment of chemical mixtures: A conceptual framework. *Environ Sci Technol* 46:2564–2573.

Bartlett DW, Clough JM, Godwin JR, Hall AA, Hamer M, Parr-Dobrzanski B. 2002. The strobilurin fungicides. *Pest Manag Sci* 58:649–662.

Beeson CC, Beeson GC, Schnellmann RG. 2010. A high-throughput respirometric assay for mitochondrial biogenesis and toxicity. *Anal Biochem* 404:75–81.

Berenzen N, Lentzen-Godding A, Probst M, Schulz H, Schulz R, Liess M. 2005. A comparison of predicted and measured levels of runoff-related

pesticide concentrations in small lowland streams on a landscape level. *Chemosphere* 58:683–691.

Berger I, Segal I, Shmueli D, Saada A. 2010. The effect of antiepileptic drugs on mitochondrial activity: A pilot study. *J Child Neurol* 25:541–545.

Bragadin M, Marton D, Manente S, Scutari G, Toninello A. 2003. Tributyltin and mitochondria: New evidence in support of an uncoupling mechanism and a further characterisation of the transport mechanism. *Inorganica Chim Acta* 348:225–228.

Divakaruni AS, Paradyse A, Ferrick DA, Murphy AN, Jastroch M. 2014. Analysis and interpretation of microplate-based oxygen consumption and pH data. *Methods Enzymol* 547:309–354.

Droppa M, Horváth G, Vass I, Demeter S. 1981. Mode of action of photosystem II herbicides studied by thermoluminescence. *Biochim Biophys Acta Bioenerg* 638:210–216.

Dykens JA, Davis RE, Moos WH. 1999. Introduction to mitochondrial function and genomics. *Drug Dev Res* 46:2–13.

Escher BI, Bramaz N, Ort C. 2009. JEM spotlight: Monitoring the treatment efficiency of a full scale ozonation on a sewage treatment plant with a mode-of-action based test battery. *J Environ Monit* 11:1836–1846.

Escher BI, Eggen RI, Schreiber U, Schreiber Z, Vye E, Wisner B, Schwarzenbach RP. 2002. Baseline toxicity (narcosis) of organic chemicals determined by in vitro membrane potential measurements in energy-transducing membranes. *Environ Sci Technol* 36:1971–1979.

Escher BI, Neale PA, Villeneuve DL. 2018. The advantages of linear concentration–response curves for in vitro bioassays with environmental samples. *Environ Toxicol Chem* 37:2273–2280.

European Food Safety Authority. 2010. 2008 annual report on pesticide residues according to article 32 of regulation (EC) no 396/2005. Parma, Italy. [cited 2018 November 8]. Available from: https://www.efsa.europa.eu/de/efsajournal/pub/1646.

Federal Office of Consumer Protection and Food Safety. 2017. Domestic sales and export of plant protection products in 2017. Berlin, Germany. [cited 2018 November 8]. Available from: https://www.bvl.bund.de/EN/04_PlantProtectionProducts/01_ppp_tasks/02_ppp_AuthorisationReviewActSub/03_ppp_DomesticSalesExport/PPP_domesticSales_and_Export_node.html

Fischer FC, Abele C, Droge ST, Henneberger L, König M, Schlichting R, Scholz S, Escher BI. 2018. Cellular uptake kinetics of neutral and charged chemicals in in vitro assays measured by fluorescence microscopy. *Chem Res Toxicol* 31:646–657.

Gupta P, Jordan CT, Mitov MI, Butterfield DA, Hilt JZ, Dziubla TD. 2016. Controlled curcumin release via conjugation into PBAE nanogels enhances mitochondrial protection against oxidative stress. *Int J Pharm* 511:1012–1021.

Hunziker RW, Escher BI, Schwarzenbach RP. 2002. Acute toxicity of triorganotin compounds: Different specific effects on the energy metabolism and role of pH. *Environ Toxicol Chem* 21:1191–1197.

König M, Escher BI, Neale PA, Krauss M, Hilscherová K, Novák J, Teodorovic I, Schulze T, Seidensticker S, Kamal Hashmi MA, Ahlheim J, Brack W. 2017. Impact of untreated wastewater on a major European river evaluated with a combination of in vitro bioassays and chemical analysis. *Environ Pollut* 220:1220–1230.

Liess M, Von Der Ohe PC. 2005. Analyzing effects of pesticides on invertebrate communities in streams. *Environ Toxicol Chem* 24:954–965.

Maltby L, Brock TC, van den Brink PJ. 2009. Fungicide risk assessment for aquatic ecosystems: Importance of interspecific variation, toxic mode of action, and exposure regime. *Environ Sci Technol* 43:7556–7563.

Mansfield RW, Wiggins TE. 1990. Photoaffinity labelling of the β-methoxyacrylate binding site in bovine heart mitochondrial cytochrome BC1 complex. *Biochim Biophys Acta Bioenerg* 1015:109–115.

Matsuno-Yagi A, Hatefi Y. 1993. Studies on the mechanism of oxidative phosphorylation. ATP synthesis by submitochondrial particles inhibited at F0 by venturicidin and organotin compounds. *J Biol Chem* 268:6168–6173.

McBride HM, Neuspiel M, Wasiak S. 2006. Mitochondria: More than just a powerhouse. *Curr Biol* 16:R551–R560.

Meyer JN, Leung MC, Rooney JP, Sendoel A, Hengartner MO, Kisby GE, Bess AS. 2013. Mitochondria as a target of environmental toxicants. *Toxicol Sci* 134:1–17.

Müller ME, Escher BI, Schwientek M, Werneburg M, Zarfl C, Zwiener C. 2018. Combining in vitro reporter gene bioassays with chemical analysis to assess changes in the water quality along the Ammer River, southwestern Germany. *Environ Sci Eur* 30:20.

Nicholls DG, Ferguson SJ. 2002. Bioenergetics, *CA, USA* (3rd ed). Elsevier, San Diego

Nonnenmacher Y, Palorini R, d'Herouël AF, Krämer L, Neumann-Schaal M, Chiaradonna F, Skupin A, Wegner A, Hiller K. 2017. Analysis of mitochondrial metabolism in situ: Combining stable isotope labeling with selective permeabilization. *Metab Eng* 43:147–155.

Probert PM, Leitch AC, Dunn MP, Meyer SK, Palmer JM, Abdelghany TM, Lakey AF, Cooke MP, Talbot H, Wills C, McFarlane W, Blake LI, Rosenmai AK, Oskarsson A, Figueiredo R, Wilson C, Kass GE, Jones DE, Blain PG, Wright MC. 2018. Identification of a xenobiotic as a potential environmental trigger in primary biliary cholangitis. *J Hepatol* 69:1123–1135.

Raftery TD, Jayasundara N, Di Giulio RT. 2017. A bioenergetics assay for studying the effects of environmental stressors on mitochondrial function in vivo in zebrafish larvae. *Comp Biochem Physiol C Pharmacol Toxicol* 192:23–32.

Rello S, Stockert J, Moreno V, Gamez A, Pacheco M, Juarranz A, Cañete M, Villanueva A. 2005. Morphological criteria to distinguish cell death induced by apoptotic and necrotic treatments. *Apoptosis* 10:201–208.

Sahdeo S, Tomilov A, Komachi K, Iwahashi C, Datta S, Hughes O, Hagerman P, Cortopassi G. 2014. High-throughput screening of FDA-approved drugs using oxygen biosensor plates reveals secondary mitofunctional effects. *Mitochondrion* 17:116–125.

Saxena AK. 1987. Organotin compounds: Toxicology and biomedicinal applications. *Appl Organomet Chem* 1:39–56.

Schulze T, Ahel M, Ahlheim J, Aït-Aïssa S, Brion F, Di Paolo C, Froment J, Hidasi AO, Hollender J, Hollert H, Hu M, Kloß A, Koprivica S, Krauss M, Muz M, Oswald P, Petre M, Schollée JE, Seiler TB, Shao Y, Slobodnik J, Sonavane M, Suter MJF, Tollefsen KE, Tousova Z, Walz KH, Brack W. 2017. Assessment of a novel device for onsite integrative large-volume solid phase extraction of water samples to enable a comprehensive chemical and effect-based analysis. *Sci Total Environ* 581:350–358.

Shah-Simpson S, Pereira CF, Dumoulin PC, Caradonna KL, Burleigh BA. 2016. Bioenergetic profiling of *Trypanosoma cruzi* life stages using Seahorse extracellular flux technology. *Mol Biochem Parasitol* 208:91–95.

Shim J, Weatherly LM, Luc RH, Dorman MT, Neilson A, Ng R, Kim CH, Millard PJ, Gosse JA. 2016. Triclosan is a mitochondrial uncoupler in live zebrafish. *J Appl Toxicol* 36:1662–1667.

Singer H, Jaus S, Hanke I, Lück A, Hollender J, Alder AC. 2010. Determination of biocides and pesticides by on-line solid phase extraction coupled with mass spectrometry and their behaviour in wastewater and surface water. *Environ Pollut* 158:3054–3064.

Syed M, Skonberg C, Hansen SH. 2016. Mitochondrial toxicity of diclofenac and its metabolites via inhibition of oxidative phosphorylation (ATP synthesis) in rat liver mitochondria: Possible role in drug induced liver injury (DILI). *Toxicol In Vitro* 31:93–102.

Terada H. 1990. Uncouplers of oxidative phosphorylation. *Environ Health Perspect* 87:213–218.

Thakur S, Daley B, Gaskins K, Thakur S, Daley B, Gaskins K, Vasko VV, Boufraqech M, Patel D, Sourbier C, Reece J, Cheng SY, Kebebew E, Agarwal S, Klubo-Gwiezdzinska J. 2018. Metformin targets mitochondrial glycerophosphate dehydrogenase to control rate of oxidative phosphorylation and growth of thyroid cancer in vitro and in vivo. *Clin Cancer Res* 24:4030–4043.

Tisler S, Zwiener C. 2018. Formation and occurrence of transformation products of metformin in wastewater and surface water. *Sci Total Environ* 628:1121–1129.

Zhang J-H, Chung TD, Oldenburg KR. 1999. A simple statistical parameter for use in evaluation and validation of high throughput screening assays. *J Biomol Screen* 4:67–73.

Zhang J-L, Souders CL, II, Denslow ND, Martyniuk CJ. 2017. Quercetin, a natural product supplement, impairs mitochondrial bioenergetics and locomotor behavior in larval zebrafish (*Danio rerio*). *Toxicol Appl Pharmacol* 327:30–38.

Supplemental Data

Mitochondrial toxicity of selected micropollutants, their mixtures and surface water samples measured by the oxygen consumption rate in cells

Maximilian E. Müller[a], Sofia Vikstrom[b], Maria König[c], Rita Schlichting[c], Christiane Zarfl[a], Christian Zwiener[a], Beate I. Escher[a,c]*

[a]Eberhard Karls University of Tübingen, Center for Applied Geoscience, 72074 Tübingen, Germany

[b]Agilent Technologies, 2600 Glostrup, Denmark

[c]UFZ – Helmholtz Centre for Environmental Research, 04318 Leipzig, Germany

*corresponding author

Table of contents

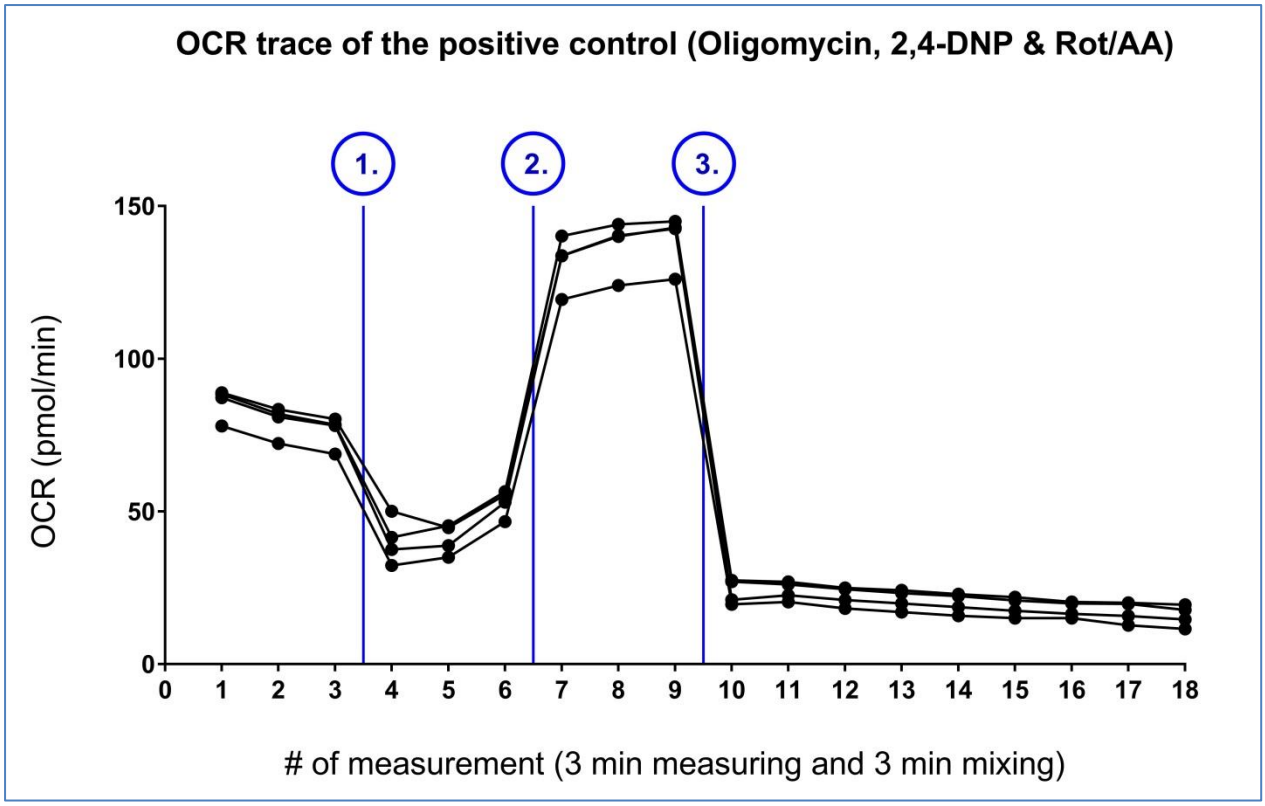

Figure S 1: OCR trace of the positive control in the experimental design for inhibitors of the electron transport chain using the reference kit provided by Agilent. The positive control was measured by injecting (1.) 1.0 µM oligomycin between the measurements 3 and 4, (2.) 80 µM 2,4-DNP between the measurements 6 and 7 and (3.) 0.5 µM of a mixture of rotenone and antimycin A (Rot/AA) between the measurements 9 and 10. The reference chemicals were prepared in tenfold concentrations to achieve the final concentrations mentioned above. In the experimental design for inhibitors of the electron transport chain, in parallel to the positive control, the sample was injected instead of Rot/AA between the measurements 9 and 10. In the experimental designs for ATP-synthase inhibition and uncoupling the sample would be injected instead of oligomycin between the measurements 3 and 4 and 2,4-DNP between the measurements 6 and 7, respectively.

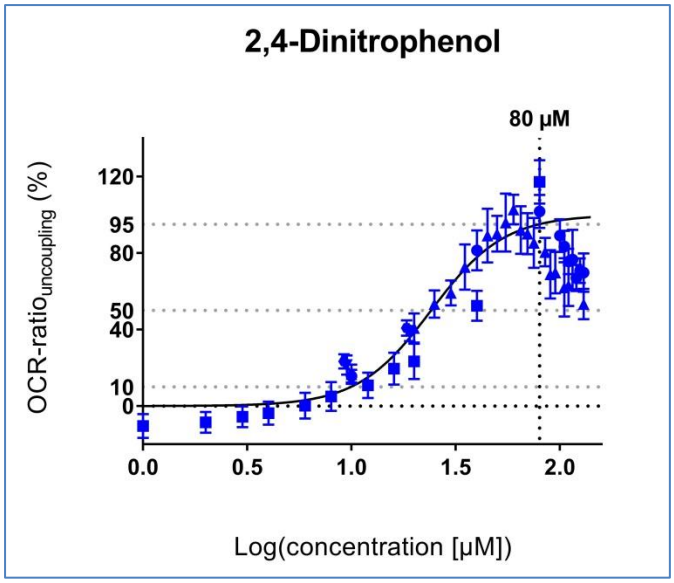

Figure S 2: Full CRC of 2,4-DNP with drawn line fitted using Eq. (5), measured in the experimental design for testing uncouplers. The concentration 80 µM triggering an uncoupling effect of 95% and used as reference in the experimental design for testing uncouplers is indicated by a dashed black line.

Cell viability after 24 h exposure

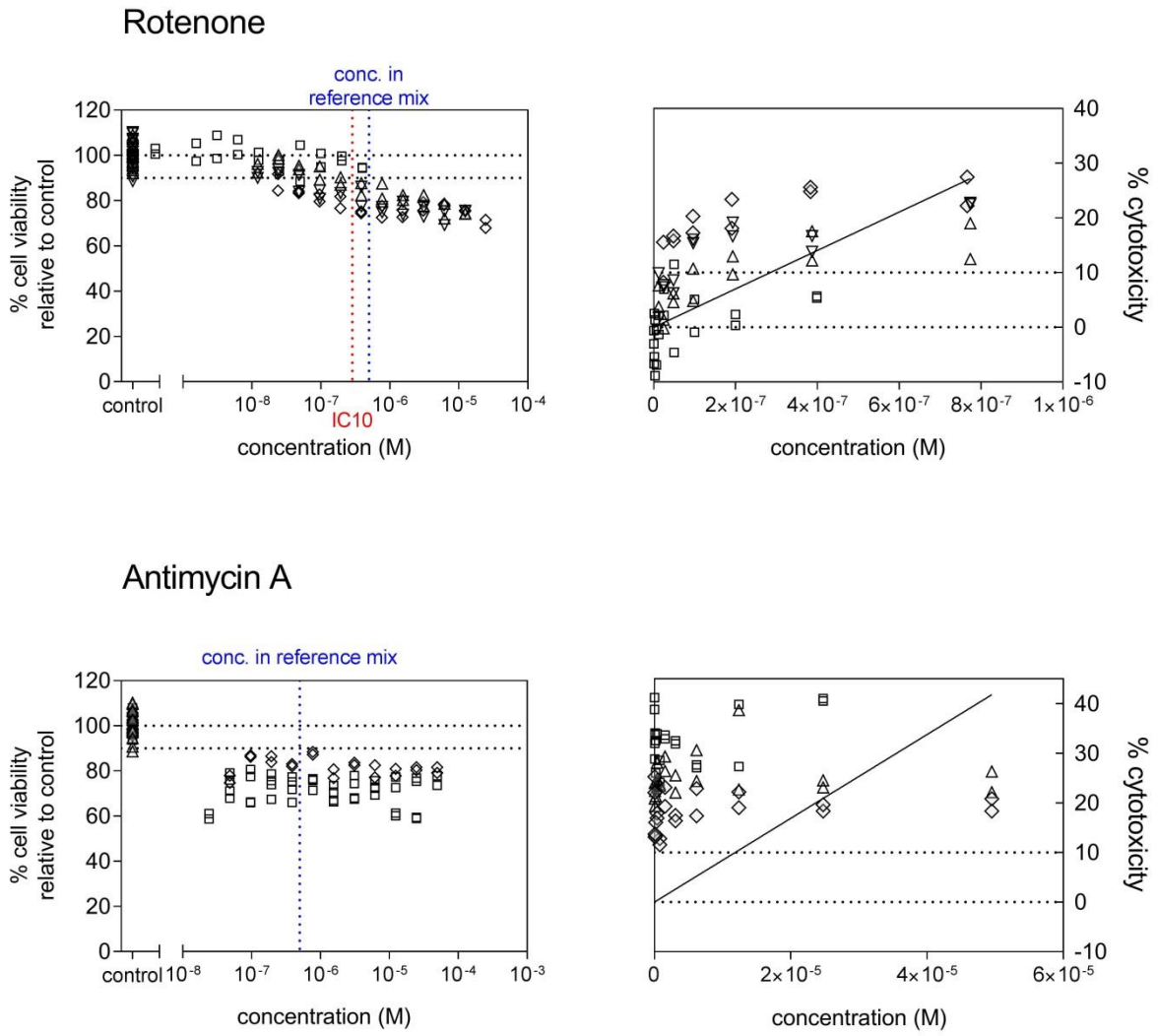

Figure S 3: Cell viability of HepG2 cells after the incubation of rotenone, antimycin A, oligomycin, 2,4-DNP, bromoxynil, fluazinam, azoxystrobin, pyraclostrobin, TBT and the water extracts SS1-A, SS2-A and SS1-B for 24 hours. The inhibitory concentrations for 10% reduction of cell numbers IC10 derived from the linear portion of the CRC is depicted as a red line. The concentrations of the chemicals of the positive control used for the OCR measurements are highlighted by a blue dotted line and the tested concentration ranges for the investigated chemicals are highlighted by yellow boxes.

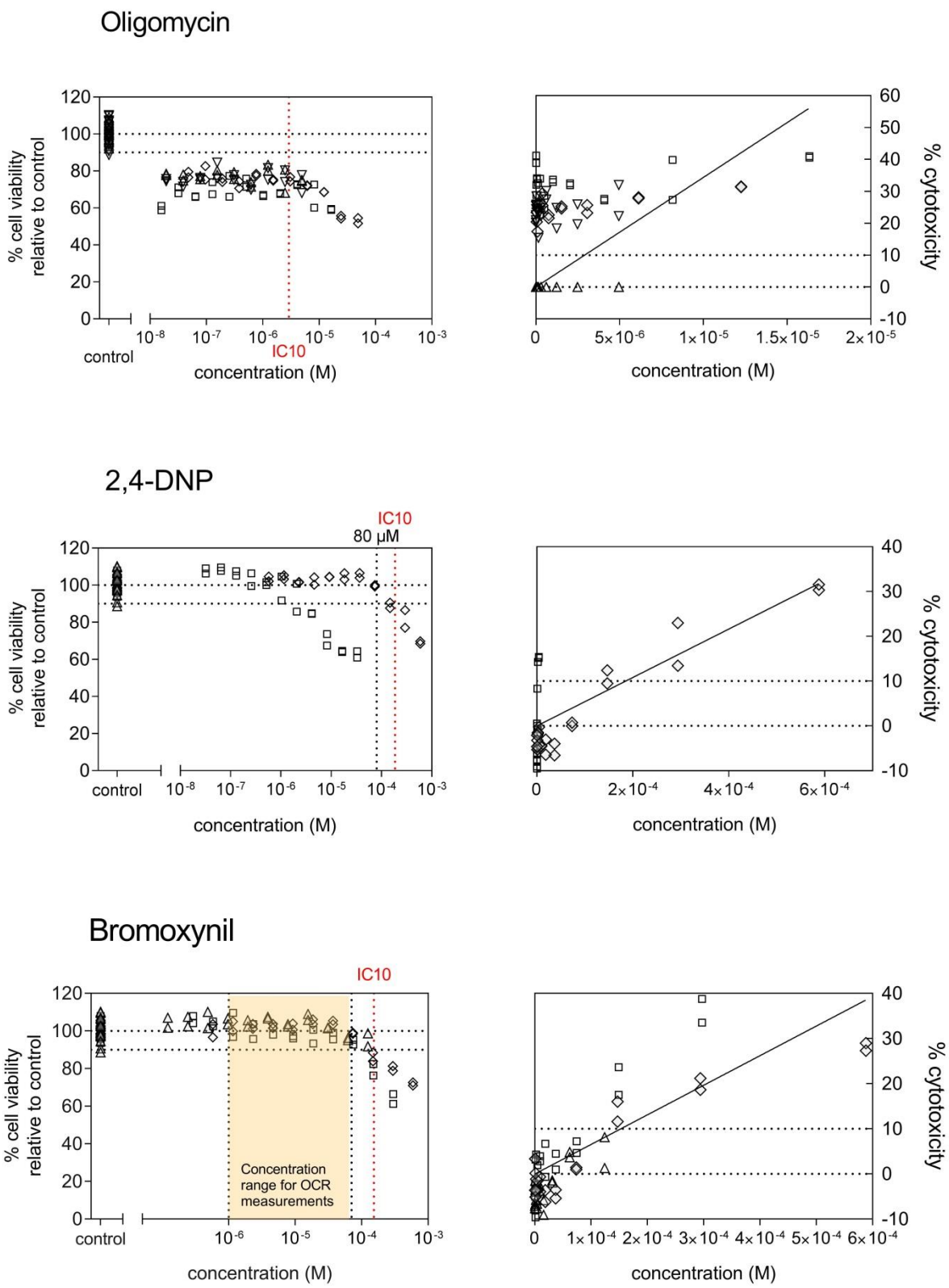

Figure S 3 continued.

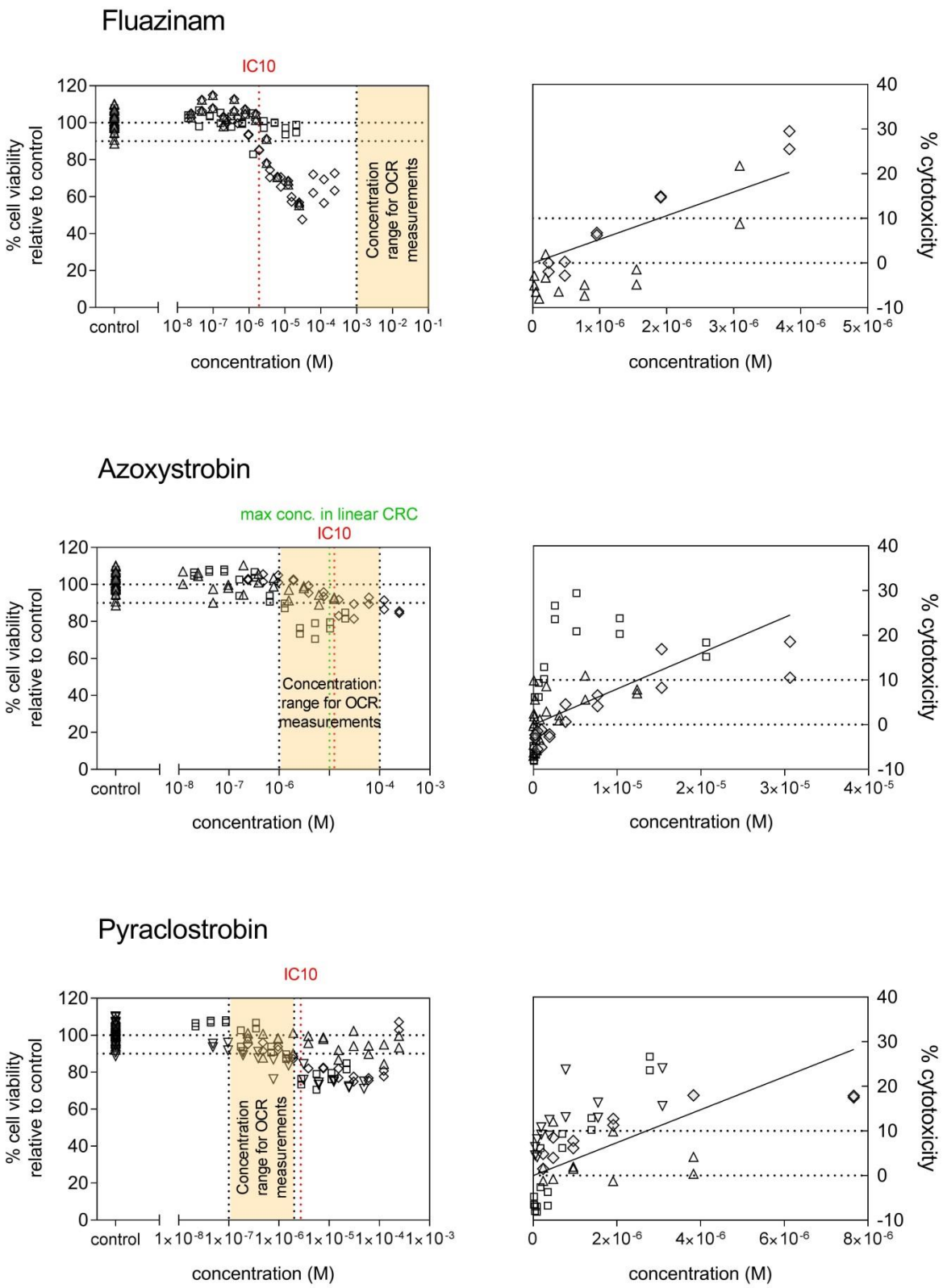

Figure S 3 continued.

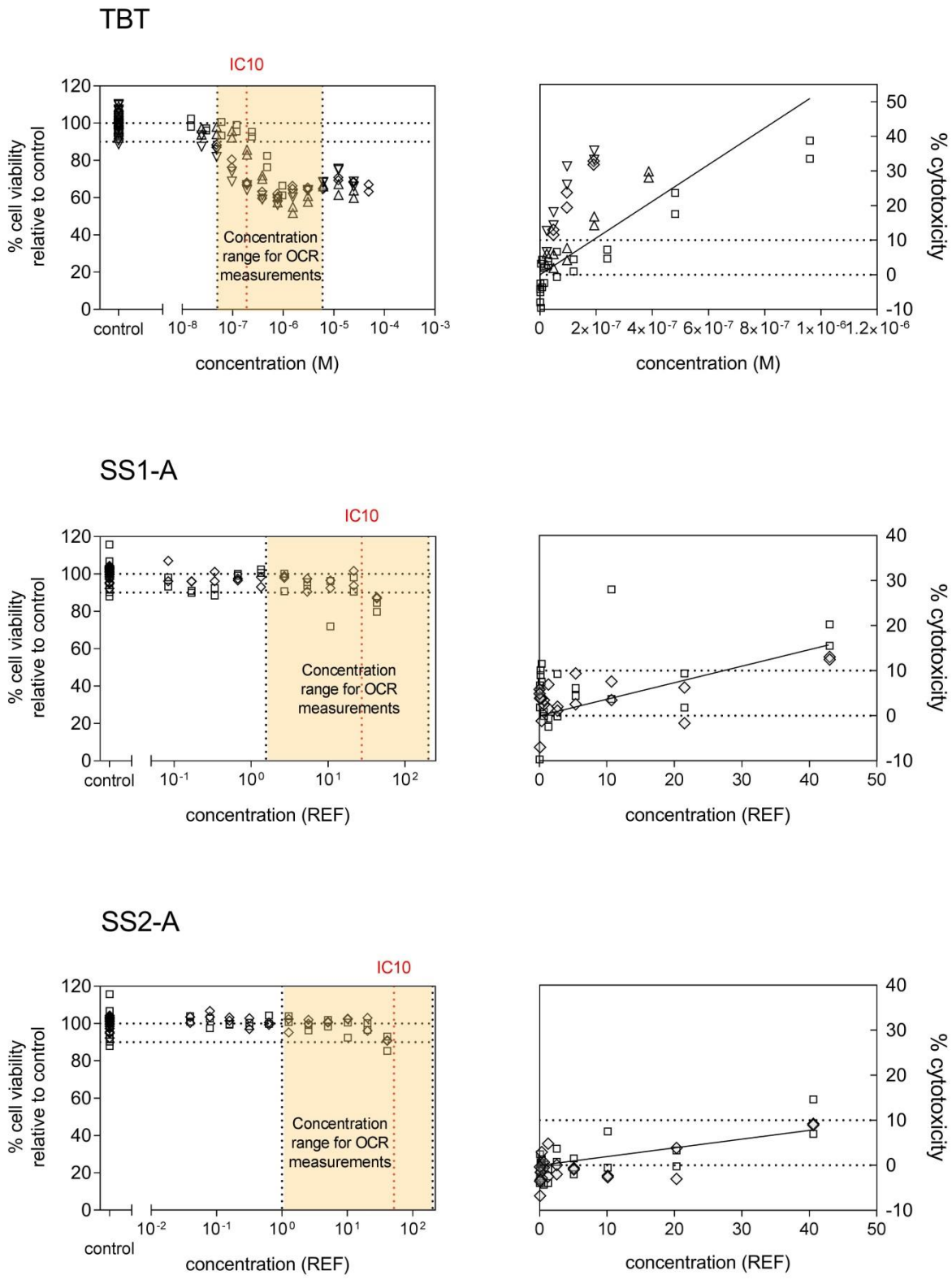

Figure S 3 continued.

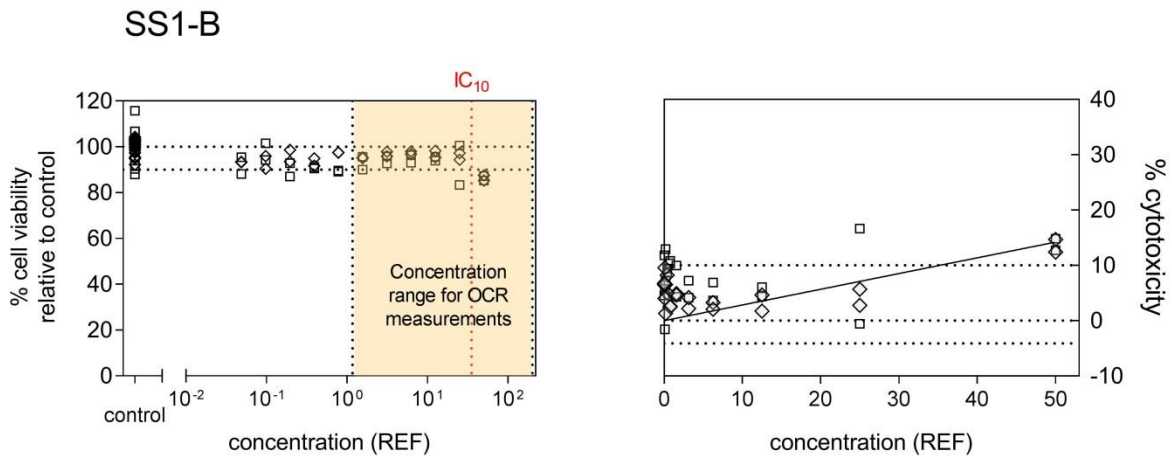

Figure S 3 continued.

Fluazinam

Fluazinam was reported to be an extremely potent uncoupler of the oxidative phosphorylation in mitochondria (Guo et al. 1991) and in isolated energy-transducing membrane (Spycher et al. 2008), which is used as a broad spectrum fungicide in agriculture and also known to affect non-target organisms (Wang et al. 2018). Fluazinam did not show any uncoupling effects in the tested concentration ranges (**Figure S 4**). Exposing the cells to 5 to 30 µM fluazinam revealed a negative %OCR-ratio$_{uncoupling}$, which can be an indication for electron transport chain inhibition activity, see **Figure S 4 B**, or cytotoxicity. The cytotoxicity IC10 for fluazinam after an incubation time of 24 hours was 1.9 µM, which is in the lower part of the applied concentration range. Although visually checking cell viability prior and subsequent to every OCR-experiment did not show any changes interference of cytotoxicity and an induced OCR increase cannot be excluded. Experiments for electron transport chain inhibition were not performed. Guo et. al. (1991) observed that fluazinam is metabolized in rat-liver cells, probably by GSH conjugation, which could be an explanation for fluazinam not reaching 10% OCR-ratio$_{uncoupling}$ if the used ARE-bla HepG2 cells were metabolically active, which is not certain.

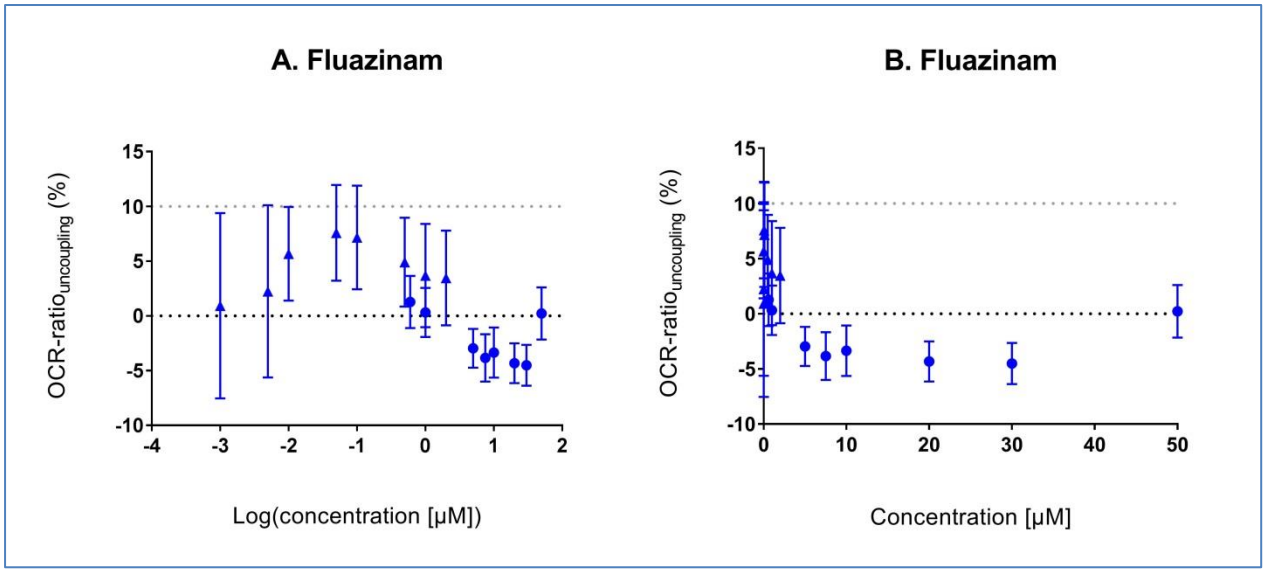

Figure S 4: CRC for OCR-ratio$_{uncoupling}$ of fluazinam on a logarithmic (A) and a linear (B) concentration scale measured in the experimental design for testing uncouplers.

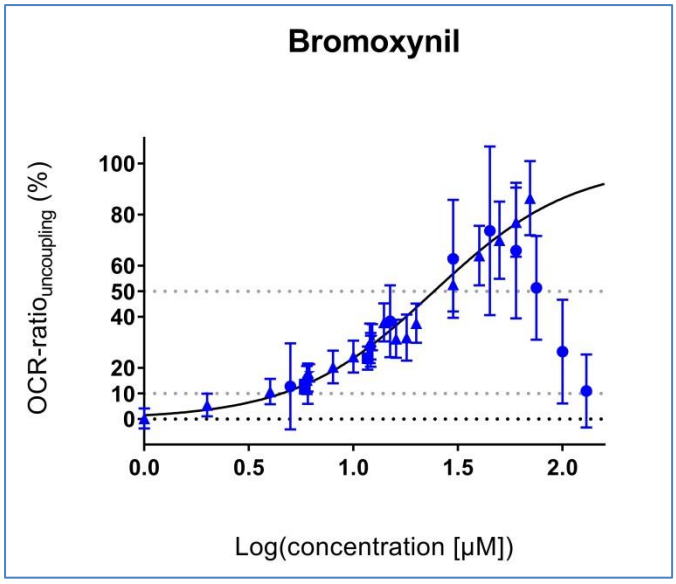

Figure S 5: The full CRC of bromoxynil with drawn line fitted using Eq. (5), measured in the experimental design for testing uncouplers.

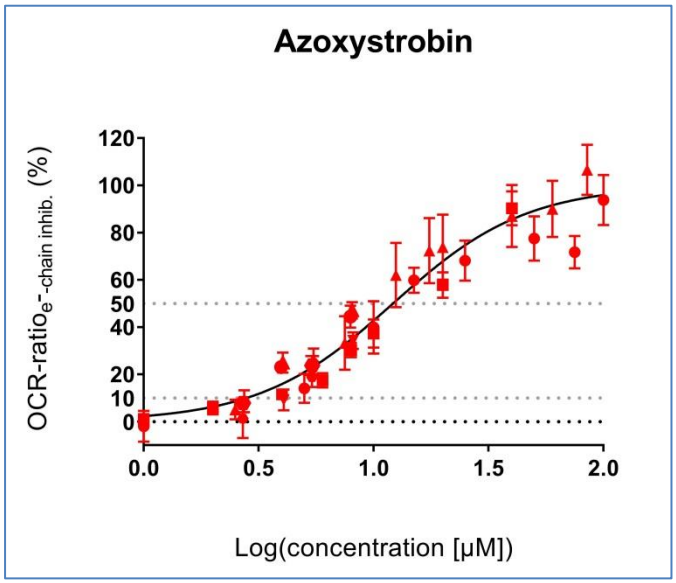

Figure S 6: The full CRC of azoxystrobin with drawn line fitted using Eq. (5), measured in the experimental design for testing inhibitors of the electron transport chain.

Pyraclostrobin

Pyraclostrobin is also a member of the strobilurin group and widely used as fungicide in agriculture (EFSA 2010). A full CRC was determined within the range of 0.1 and 100 µM and displayed an unusually steep slope of 11.3 (**Figure S 7A**). The CRC on a linear concentration scale up to 30% electron transport chain inhibition (**Figure S 7B**) was used to derive the EC10 at 1.18 ± 0.11 µM.

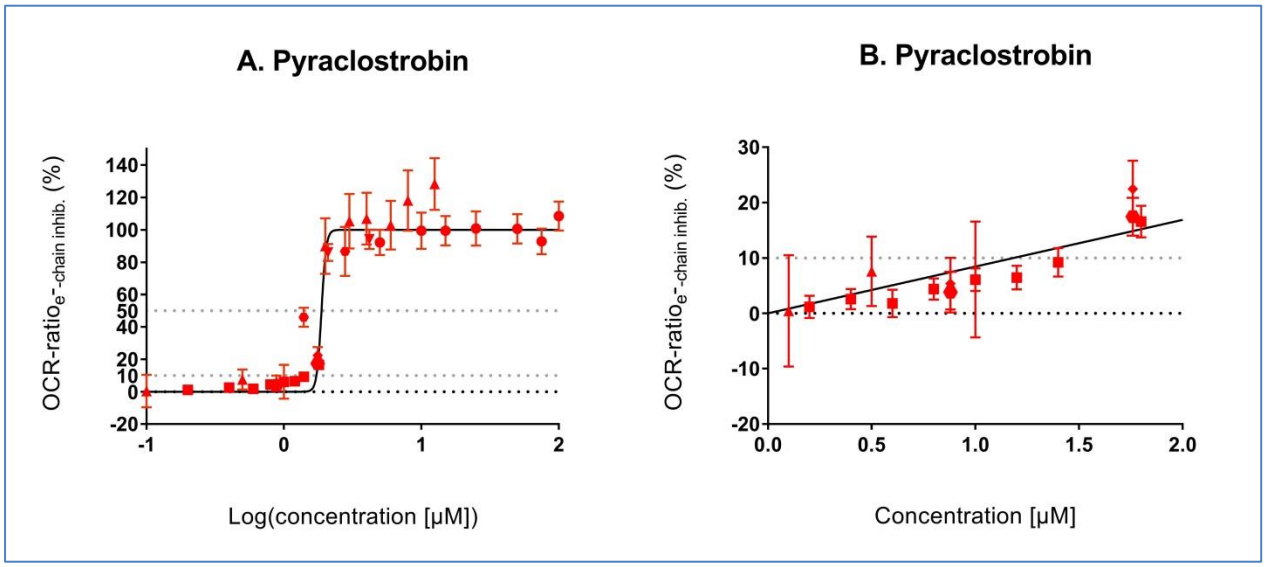

Figure S 7: (A) Full CRC of Pyraclostrobin with drawn line fitted using Eq. (5). (B) Linear portion of the CRC with drawn line fitted using Eq. (6). Pyraclostrobin was measured in the experimental design for testing inhibitors of the electron transport chain.

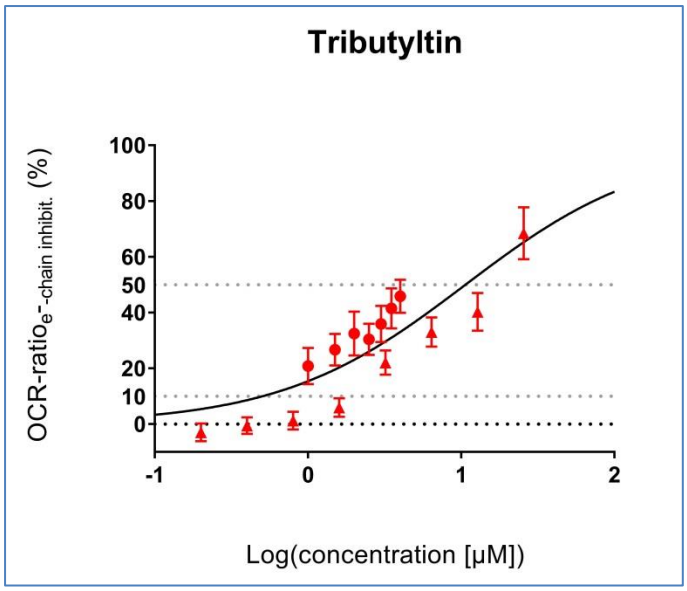

Figure S 8: The full CRC of TBT with drawn line fitted using Eq. (5), measured in the experimental design for testing inhibitors of the electron transport chain.

Table S 1: Summary of the EC50 and EC10 values derived from the sigmoidal-log CRC and the EC10 values derived from the linear portion of the CRC for the single chemicals.

Sample	Active endpoint	EC50 [µM]/ (sigmoidal-log CRC)	EC10 [µM] (sigmoidal-log CRC)	EC10 [µM] (linear CRC)
2,4-DNP	%OCR-ratio $_{uncoupling}$	24.1 (95%CI: 21.7 – 26.8)	9.93 (95%CI: 7.73 – 12.4)	6.46 ± 0.83
Bromoxnil	%OCR-ratio $_{uncoupling}$	24.3 (95%CI: 22.8 – 25.9)	4.53 (95%CI: 3.91 – 5.18)	4.06 ± 0.09
Fluazinam	%OCR-ratio $_{uncoupling}$	-	-	-
Azoxystrobin	%OCR-ratio $_{e^-\text{-chain inhibition}}$	12.2 (95%CI: 10.9 – 13.6)	2.79 (95%CI: 2.22 – 3.44)	2.61 ± 0.13
Pyraclostrobin	%OCR-ratio $_{e^-\text{-chain inhibition}}$	1.88 (95%CI: 1.85 – 1.94)	1.73 (95%CI: 1.59 – 1.82)	1.18 ± 0.11
TBT	%OCR-ratio $_{e^-\text{-chain inhibition}}$	10.7 (95%CI: 6.54 – 24.2)	0.50 (95%CI: 0.14 – 1.08)	1.38 ± 0.26
TBT	%OCR-ratio $_{ATP\text{-synthase inhibition}}$	1.55 (95%CI: 1.29 – 2.60)	0.84 (95%CI: 0.47 – 1.15)	0.71 ± 0.33

Table S 2: OCR-ratio$_{uncoupling}$ and OCR-ratio$_{e^-\text{-chain inhibition}}$ of the two mixes and the single compounds in the same concentrations as in the mixes. Note that this experiments was performed with a preliminary setup not considering an extended incubation time of the sample.

	OCR-ratio$_{uncoupling}$ (%)	OCR-ratio$_{e^-\text{-chain inhibition}}$ (%)
Bromoxynil [30 µM]	55	-
Azoxystrobin [75 µM]	-	~ 28
Mix 1	-42.9	31.3
Bromoxynil [75 µM]	88	-
Azoxystrobin [15 µM]	-	25
Mix 2	-13.1	28.0

Extracellular acidification rate (ECAR)

Impairment of mitochondrial functions can result in an increased or decreased glycolysis that can be detected by the extracellular acidification rate (ECAR). As these changes do not occur as a direct result of chemicals that interfere with mitochondrial respiration our primary aim was set on OCR measurements. Furthermore, the performance of ECAR measurements require the use of non-buffered assay media which is not guaranteeing the measured activity of a sample to be exerted at neutral pH and therewith under environmental relevant conditions. An example of an ECAR trace is given in **Figure S 9**. The simultaneous assessment of both, OCR and ECAR, could be a way to check whether two or more chemicals with different MoAs are present in a sample and that would mask their effect in the OCR assay alone. The energetic states of the cells during assessing the uncoupling activity of 100 µM bromoxynil in the experimental design for testing uncouplers are depicted in Figure S 10 by displaying both OCR and ECAR. Nonetheless, further research on the combined assessment of OCR and ECAR is necessary.

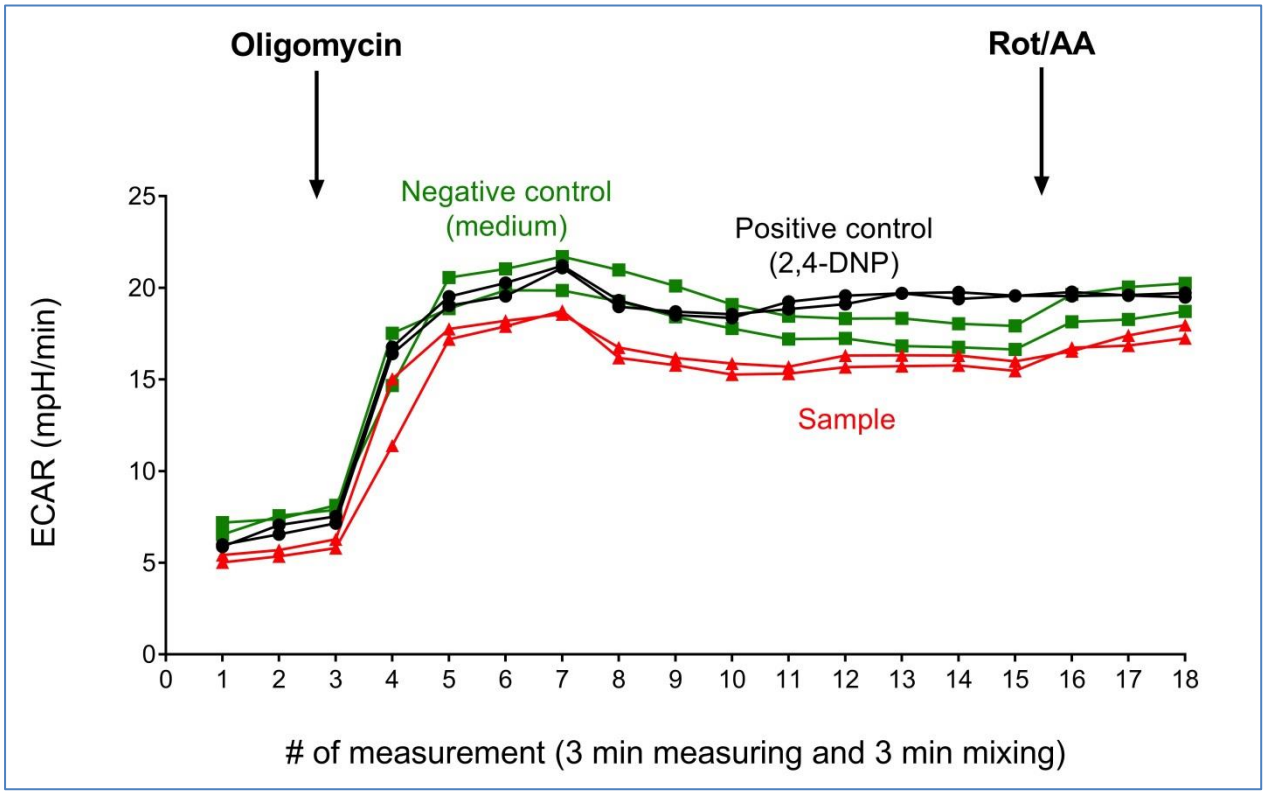

Figure S 9: Extracellular acidification rate (ECAR) over time in the experimental design for measuring the uncoupling activity OCR-ratio$_{uncoupling}$ of 100 µM bromoxynil (red line) relative to 80 µM 2,4-DNP (black line). Each line represents the ECAR, respectively, of one single well. The ECARs of the negative control (medium is injected instead of sample/reference chemical) is represented by a green line. The depicted data refers to the OCR data presented in Figure 3 of the main manuscript.

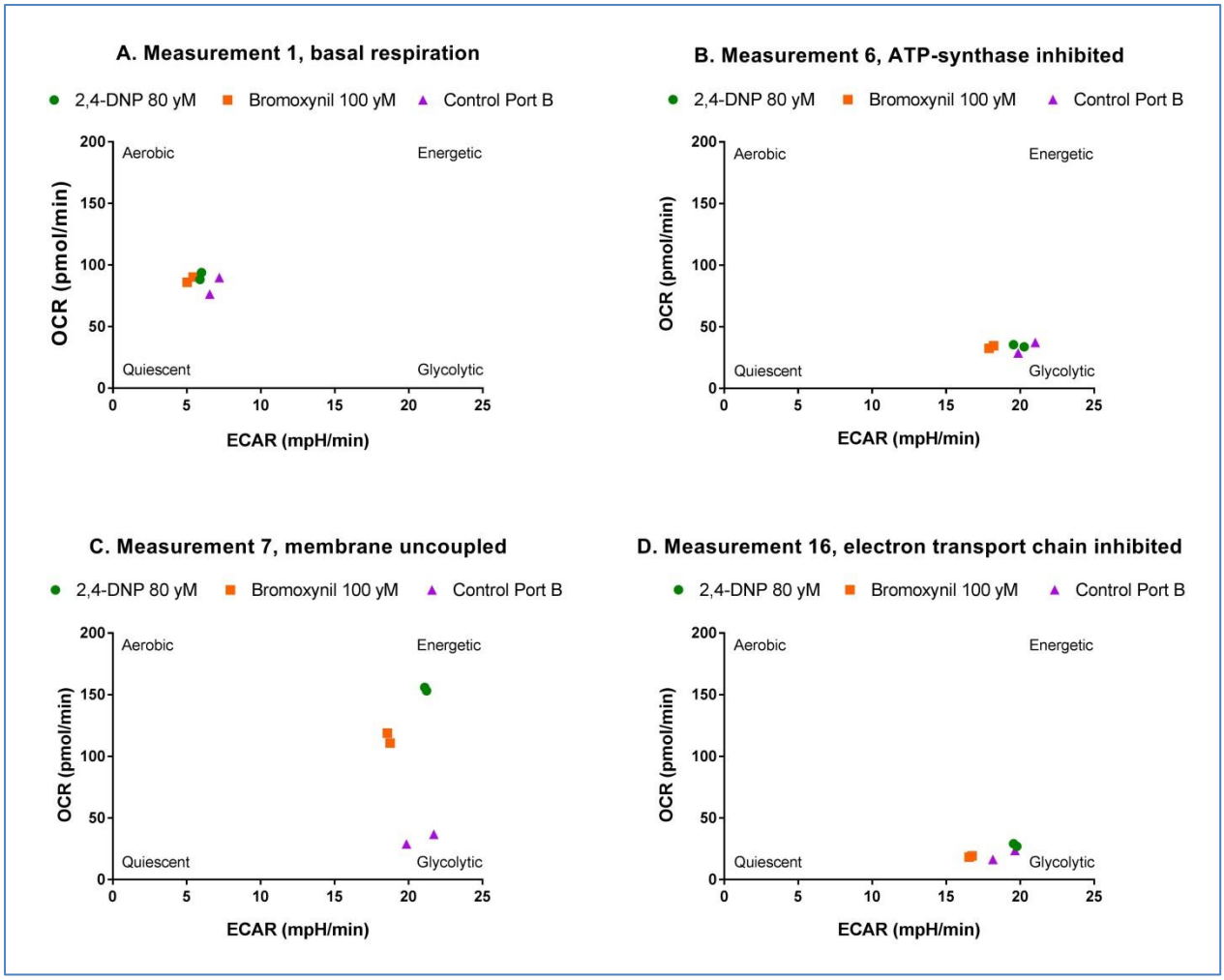

Figure S 10: Energy maps reflecting the cellular energetic states during assessing the uncoupling activity of 100 µM bromoxynil in the experimental design for testing uncouplers. (A) displays the energetic state of the basal respiration, (B) after the ATP-synthase was inhibited by oligomycin at measurement 6, (C) after the membrane was uncoupled by applying 2,4-DNP and (D) after complete electron transport chain inhibition. Each symbol represent one well with the respective treatment.

LV-SPE Blank

A background control of the LV-SPE devices was tested for uncoupling and for electron transport chain inhibiting activity, in each case in three independent experiments (**Figure S 11**). The LV-SPE Blank had no uncoupling activity (with OCR-ratio$_{uncoupling}$ in all three experiments being negative, down to -17.5 ± 2.5 % OCR-ratio$_{uncoupling}$). The LV-SPE Blank attained an electron transport chain inhibiting activity in a dose-dependent manner, see **Figure S 11A&B**. The EC10 was 150 ± 16.0 REF. Although the LV-SPE Blank exhibits an electron transport chain inhibiting potency this is rather small effect compared to the results of all other LV-SPE samples that were measured. Thus, the background signal can be neglected.

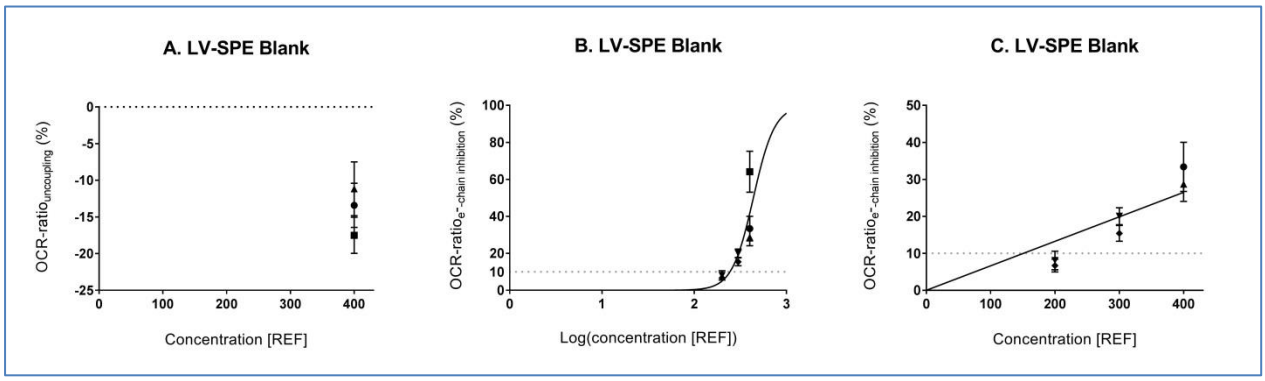

Figure S 11: (A) OCR-ratio$_{uncoupling}$ of the LV-SPE Blank at REF 400. CRC of OCR-ratio$_{e^-\text{-chain inhibition}}$ (B) and its linear portion (C) of the LV-SPE Blank.

Mixtures

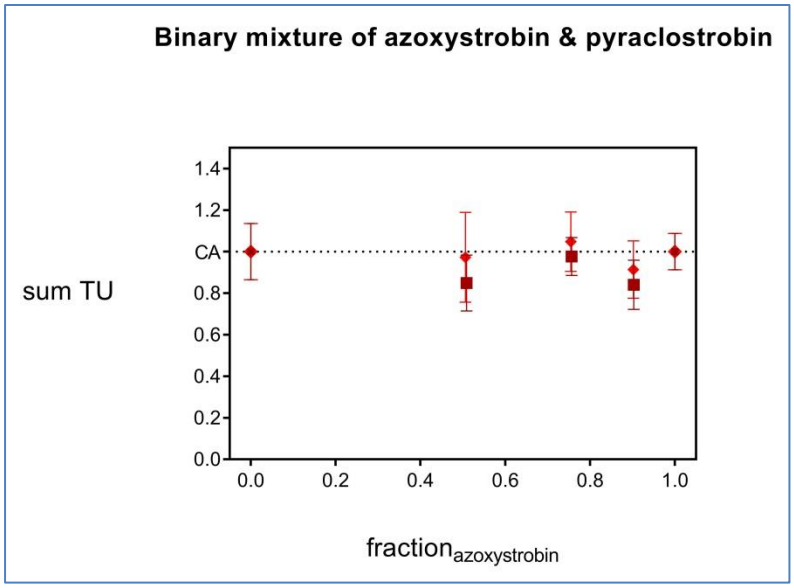

Figure S 12: Toxic units of the binary mixtures of azoxystrobin and pyraclostrobin. The figure shows the concordance and deviation from CA of the sumTU of each mixture. The experiment was performed in the experimental design for electron transport chain inhibitors.

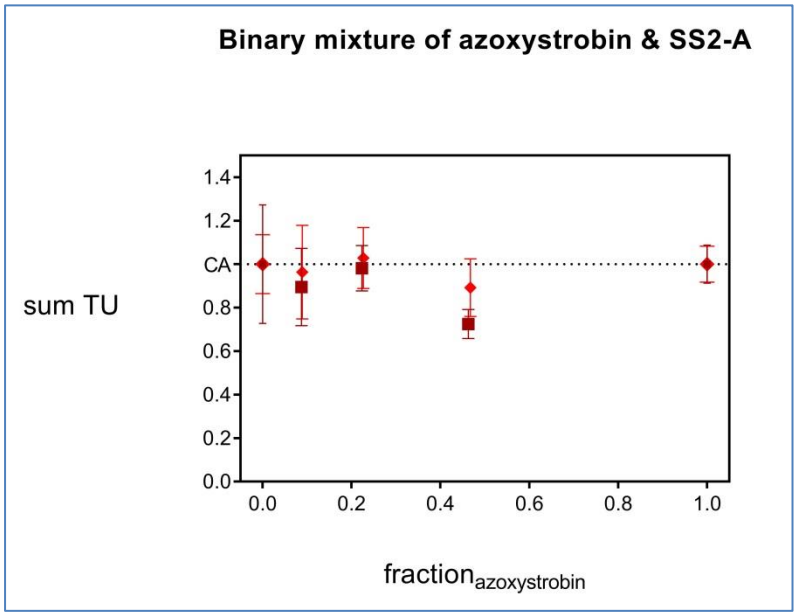

Figure S 13: Toxic units of the binary mixtures of azoxystrobin and water extract SS2-A. The figure shows the concordance and deviation from CA of the sumTU of each mixture. The experiment was performed in the experimental design for electron transport chain inhibitors.

References

EFSA. European Food Safety Authority. 2010. 2008 annual report on pesticide residues according to article 32 of regulation (EC) no 396/2005.

Guo Z-j, Miyoshi H, Komyoji T, Haga T, Fujita T. 1991. Uncoupling activity of a newly developed fungicide, fluazinam [3-chloro-n-(3-chloro-2, 6-dinitro-4-trifluoromethylphenyl)-5-trifluoromethyl-2-pyridinamine]. *Biochim Biophys Acta Bioenerg* 1056:89-92.

Spycher S, Smejtek P, Netzeva TI, Escher BI. 2008. Toward a class-independent quantitative structure− activity relationship model for uncouplers of oxidative phosphorylation. *Chem Res Toxicol* 21:911-927.

Wang XH, Zheng SS, Huang T, Su LM, Zhao YH, Souders II CL, Martyniuk CJ. 2018. Fluazinam impairs oxidative phosphorylation and induces hyper/hypo-activity in a dose specific manner in zebrafish larvae. *Chemosphere* 210:633-644.

Publication 3

Influence of emission sources and tributaries on the spatial and temporal patterns of micropollutant mixtures and associated effects in a small river

Maximilian E. Müller[a], Martina Werneburg[a], Clarissa Glaser[a], Marc Schwientek[a], Christiane Zarfl[a], Beate I. Escher[a, b] and Christian Zwiener[a]

[a]Eberhard Karls University of Tübingen, Center for Applied Geoscience, Tübingen, Germany

[b]UFZ – Helmholtz Centre for Environmental Research, Leipzig, Germany

Published in *Environmental Toxicology and Chemistry*, DOI: 10.1002/etc.4726

The Supplemental Information is published “Open Access” and available on

https://doi.org/10.1002/etc.4726

Environmental Toxicology and Chemistry—Volume 39, Number 7—pp. 1382–1391, 2020
Received: 7 February 2020 | Revised: 28 February 2020 | Accepted: 13 April 2020

Environmental Toxicology

Influence of Emission Sources and Tributaries on the Spatial and Temporal Patterns of Micropollutant Mixtures and Associated Effects in a Small River

Maximilian E. Müller,[a] Martina Werneburg,[a] Clarissa Glaser,[a] Marc Schwientek,[a] Christiane Zarfl,[a] Beate I. Escher,[a,b] and Christian Zwiener[a,*]

[a]Center for Applied Geoscience, Eberhard Karls University of Tübingen, Tübingen, Germany
[b]UFZ–Helmholtz Centre for Environmental Research, Leipzig, Germany

Abstract: Organic micropollutants of anthropogenic origin in river waters may impair aquatic ecosystem health and drinking water quality. To evaluate micropollutant fate and turnover on a catchment scale, information on input source characteristics as well as spatial and temporal variability is required. The influence of tributaries from agricultural and urban areas and the input of wastewater were investigated by grab and Lagrangian sampling under base flow conditions within a 7.7-km-long stretch of the Ammer River (southwest Germany) using target screening for 83 organic micropollutants and 4 in vitro bioassays with environmentally relevant modes of action. In total, 9 pesticides and transformation products, 13 pharmaceuticals, and 6 industrial and household chemicals were detected. Further, aryl hydrocarbon receptor induction, peroxisome proliferator–activated receptor activity, estrogenicity, and oxidative stress response were measured in the river. The vast majority of the compounds and mixture effects were introduced by the effluent of a wastewater-treatment plant, which contributed 50% of the total flow rate of the river on the sampling day. The tributaries contributed little to the overall load of organic micropollutants and mixture effects because of their relatively low discharge but showed a different chemical and toxicological pattern from the Ammer River, though a comparison to effect-based trigger values pointed toward unacceptable surface water quality in the main stem and in some of the tributaries. Chemical analysis and in vitro bioassays covered different windows of analyte properties but reflected the same picture. *Environ Toxicol Chem* 2020;39:1382–1391.

Keywords: Chemical analysis; Bioassays; Catchment scale; Micropollutant mixtures; Lagrangian sampling

INTRODUCTION

Intentionally and unintentionally released anthropogenic organic micropollutants may enter the aquatic environment via different pathways. Most household applications of compounds, such as pharmaceuticals, protection agents, personal care products, and flame retardants, are discharged to municipal sewerage systems. A substantial part of these pollutants is designed to be rather stable (e.g., pharmaceuticals, flame retardants) and in many cases highly mobile in water, thus facilitating the passage of pollutants through wastewater-treatment plants (WWTPs) into surface waters without complete removal (Schwarzenbach et al. 2016; Munz et al. 2017). In densely populated countries of Europe like Germany the impact of treated wastewater to rivers and small streams is quite common and dominates pollution input, especially during dry summer periods (Loos et al. 2009; Bueno et al. 2012; Englert et al. 2013). Other compounds such as pesticides are introduced directly into the environment. Thus, runoff and leachate from agricultural but also urban areas can lead to high micropollutant concentrations in surface and ground waters (Loos et al. 2009; Masoner et al. 2014; Kuzmanović et al. 2015; Szöcs et al. 2017; Lee et al. 2019). These mixtures of organic micropollutants may pose a risk to environmental organisms, reduce biodiversity, and affect drinking water quality and environmental services (Alpizar et al. 2019; European Environment Agency 2019).

The overarching aim of the present study was to identify the emission sources and the influence of tributaries on the contaminant concentrations and loads in a small river, the Ammer

This article contains online-only Supplemental Data.

* Address correspondence to christian.zwiener@uni-tuebingen.de
Published online 22 June 2020 in Wiley Online Library (wileyonlinelibrary.com).
DOI: 10.1002/etc.4726

River in southwest Germany. Chemical analysis and in vitro bioassays are complementary screening approaches which capture a broad range of organic micropollutants and have previously been used to assess the quality of treated and untreated wastewater and their impact on river water quality (Farré and Barceló 2003; König et al. 2017; Neale et al. 2017b) or to track pesticides in surface water from agricultural areas (Lundqvist et al. 2019). Whereas chemical analysis provides information on the identity and quantity of individual micropollutants (Gago-Ferrero et al. 2019), in vitro bioassays give information on the combined effect of all bioactive compounds present in a sample and on their mode of action (Neale et al. 2017b; Müller et al. 2019). In the present study a battery of 4 in vitro bioassays was applied that covered the environmentally relevant modes of action, aryl hydrocarbon receptor induction (Brennan et al. 2015), peroxisome proliferator–activated receptor activity (Neale et al. 2017a), estrogenicity (König et al. 2017), and oxidative stress response (Escher et al. 2012, 2013b). Because each compound present in a sample can potentially affect the viability of a cell, the cytotoxicity measured in the bioassays can reflect the total chemical load of a sample.

Our hypotheses are that 1) inputs from agricultural and urban areas show different compound and effect patterns, and 2) organic micropollutant and effect patterns and their temporal variability change with increasing distance from their input sources. To address hypothesis 1), each tributary and the main stem were investigated by grab sampling. For hypothesis 2), we followed individual water parcels using a Lagrangian sampling technique (Writer et al. 2011; Schwientek et al. 2016).

MATERIALS AND METHODS

Study site and sampling

The present study was conducted on 19 June 2018 on a 7.7-km-long section of the Ammer River, near Tübingen, southwest Germany. In this section the Ammer River receives input from 10 tributaries out of 15 (data on discharge are given in Table 1) and 2 WWTPs. This allowed comparison of the micropollutant burden of river water unaffected and affected by treated wastewater and river water affected by tributaries from agricultural and/or urban areas (Figure 1). Until the most downstream sampling site (autosampler 3 [AS3]) the Ammer catchment integrates an area of 134 km² with agricultural (71%), urban (17%), and forestry (12%) land use (Grathwohl et al. 2013). The large WWTP1 with 80 000 person equivalents is located upstream of Altingen approximately 250 m upstream of AS1 and contributed 50% of the discharge of the Ammer downstream of the WWTP1 on 19 June 2018 (Table 1). The much smaller WWTP2 with 9000 person equivalents is located in Hailfingen, discharging into Kochhart Creek (T8). One-liter grab samples were collected from each tributary and the Ammer River closely upstream of each confluence. All samples were taken from the middle of the water body 5 cm beneath the water surface, assuming well-mixed conditions. Moreover, 1-h composite samples (250 mL every 15 min) were collected over 24 h at 3 sampling sites, AS1, AS2, and AS3, which define reaches 1 and 2 (Figure 1). To sample the same water parcel at downstream sites AS2 and AS3, the travel time of water was considered for sampling similar water parcels and estimated as described (C. Glaser et al., Center for Applied Geoscience, University of Tübingen, Germany, unpublished manuscript, 2019a). Travel times were 135 min for reach 1 between AS1 and AS2 and 165 min for reach 2 between AS2 and AS3. All samples were taken in glass bottles, stored at 4 °C, and processed within 48 h after sampling.

TABLE 1: Discharges, in liters per second (Ls^{-1}), of the Ammer River and its tributaries[a]

Tributary/sampling site		Q (Ls^{-1})
Ammer (main stem)	Am-T0	270 ± 20
	AS1	540 ± 34
	AS2	577 ± 30
	AS3	743 ± 23
WWTP1 effluent		274 ± 38
Tributaries	T1	2
	T2	16
	T3	6
	T4	35
	T8	8
	T9	2
	T10	120[b]
	T11	1
	T12	1
	T15	12

[a]Discharges were determined as described in C. Glaser et al. (Center for Applied Geoscience, University of Tübingen, Tübingen, Germany, unpublished manuscript, 2019a). Discharges at autosamplers AS1, AS2, and AS3 were averaged over the 24 h of sampling at each site, thus leading to standard deviations (±) because of the daily discharge fluctuation of the wastewater-treatment plant (WWTP). The 24-h measurement of the WWTP effluent was performed with an offset of 22 min to account for the water travel time to AS1.
[b]C. Glaser et al. (Center for Applied Geoscience, University of Tübingen, Tübingen, Germany, unpublished manuscript, 2019b).
Q = discharge; T = tributary; WWTP = wastewater-treatment plant.

Chemicals and reagents

Methanol, acetonitrile, water, acetic acid, and ammonium acetate were all liquid chromatography/mass spectrometry (LC/MS) grade and purchased from Thermo Fisher Scientific. Ethyl acetate was purchased from Acros Organics, Thermo Fisher Scientific. The 83 monitored target analytes as well as their usages and vendors are listed in Supplemental Data, Table S1.

Sample preparation

Water samples were passed through a pleated cellulose filter (Whatman 595 1/2, pore size 4–7 μm) to remove suspended particulate matter. Filtrates were enriched by solid-phase extraction (SPE) using Waters Oasis HLB, 6CC, 200-mg cartridges preconditioned with 5 mL methanol, 5 mL ethyl acetate, and 5 mL ultrapure water. One liter of filtered water sample was passed through the extraction cartridges using a vacuum manifold. After this, extraction cartridges were flushed with 5 mL ultrapure water and aspirated to dryness by vacuum. Subsequently, they were eluted with 5 mL methanol, followed

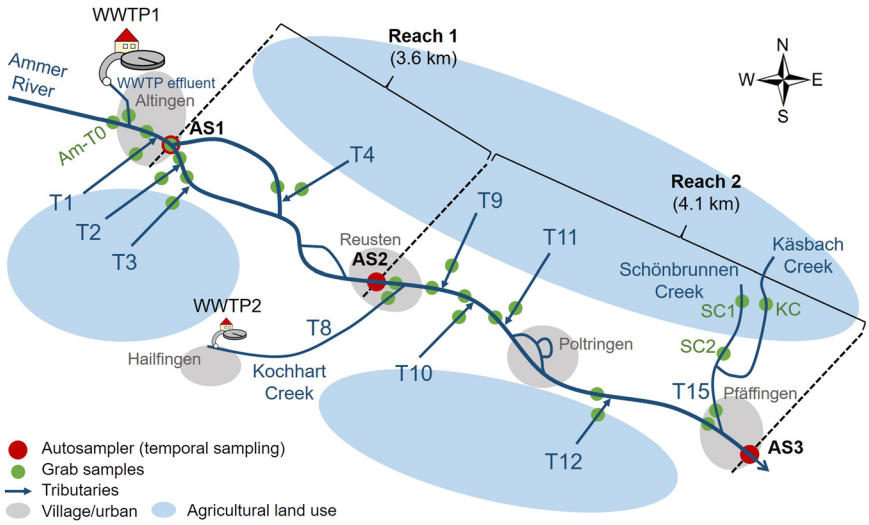

FIGURE 1: Conceptual map of the study site. Autosamplers AS1, AS2, and AS3 were located at the beginning, the center, and the end of the study site for 24-h sampling (red dots). Grab samples from the tributaries are marked green and named as the tributary (T2–T4, T8–T12, T15, SC1, SC2, and KC). Sample names of the grab samples taken from the Ammer River are named according to the adjacent downstream tributary (Am-T1, Am-T4, Am-T8–Am-12, Am-T15), except for Am-T0 upstream of the wastewater-treatment plant effluent and AS1. WWTP = wastewater-treatment plant.

by 5 mL ethyl acetate. Eluates were combined, evaporated under a gentle stream of nitrogen at 40 °C, and dissolved in methanol to achieve an enrichment factor of 1000. Final extracts were filtered (Agilent Captiva Premium Syringe filter, polyethersulfone, 0.2 µm) and stored at –20 °C until measurement. Blanks were prepared by SPE of 1 L MilliQ (GenPure Pro UV-TOC; Thermo Fisher Scientific). Prior to measurements, extracts were diluted 1:100, to minimize matrix effects (Villagrasa et al. 2007; Kruve et al. 2009), in water/acetonitrile (98/2 v/v) at room temperature. All volumes for reuptake and dilution were determined gravimetrically.

Chemical analysis

Eighty-three organic micropollutants were quantified by liquid chromatography (1260 Infinity HP-LC; Agilent Technologies) coupled to tandem mass spectrometry (6490 iFunnel Triple Quadrupole; Agilent Technologies). Separation was achieved on an Agilent Poroshell 120 EC-C18 column (2.7 µm particle size, 4.6 × 150 mm) at 40 °C with a gradient elution program using water with 0.1 mM ammonium acetate and acetonitrile, both with 0.1% formic acid. Positive ionization and negative ionization of target compounds were achieved by electrospray ionization. An external calibration with standard solutions was used for quantification of the target compounds, for which generally 2 mass transitions (qualifier, quantifier) were acquired. The lowest external calibration level within ±20% deviation from the method calibration curve was defined as the limit of quantification (LOQ; signal-to-noise ratio ≥10, quantifier/qualifier ion ratio within ±20% of the average of calibration standards from the same sequence and target compound). If analytes were detected in the SPE blank, the LOQ was defined as the mean blank concentration plus 10 times its standard deviation. Measurement uncertainty was assessed based on repeated standard solution measurements (coefficient of variance, $n = 10$, 5.0 µg L^{-1} of each analyte). Matrix effects caused by the WWTP1 effluent were investigated by standard addition of all target compounds to samples from all 3 sampling sites of the Ammer (AS1, AS2, AS3) at 3 sampling times (AS1_1, AS1_12, AS1_24, AS2_1, AS2_12, AS2_24, AS3_1, AS3_12, and AS_24) each at 2 different spiking levels (0.24 and 1 µg L^{-1}). Results of target compounds exceeding 20% signal suppression or enhancement were corrected according to the following scheme: the mean matrix effect of samples AS1_1, AS1_12, and AS1_24 was considered for samples WWTP effluent, Am-T1, and all samples of AS1, Am-T2, Am-T3, Am-T4; the mean matrix effect of samples AS2_1, AS2_12, and AS2_24 was considered for all samples of AS2, Am-T8, Am-T9, Am-T10, Am-T11, Am-T12, and T15; the mean matrix effect of samples AS3_1, AS3_12, and AS3_24 was considered for all samples of AS3. Recoveries during the SPE procedure of the target compounds were assessed by extracting 1 L MilliQ water spiked with standard solution mix, including all target compounds, to a final concentration of 100 ng L^{-1} ($n = 2$). Results of target compounds with <70% recovery were corrected. Information on mass transitions, collision energies, LOQs, relative standard deviation, recoveries during the SPE, and matrix effects of the target compounds is given in Supplemental Data, Tables S2 and S3.

In vitro bioassays

The in vitro bioassays AhR-CALUX (Brennan et al. 2015), AREc32 (Escher et al. 2012, 2013b), PPARγ-GeneBLAzer (Neale et al. 2017a), and ER-GeneBLAzer (König et al. 2017) covered 4 different environmentally relevant endpoints. For each

bioassay cytotoxicity was measured. More information on their mode of action, environmental relevance, and experimental procedures can be found in König et al. (2017) and Neale et al. (2017a). All effect concentrations (ECs) and cytotoxic inhibition concentrations (ICs) were expressed in units of relative enrichment factors, taking the enrichment during the extraction procedure and the dilution in the assay into consideration. A detailed description on the EC and IC derivation is provided in the Supplemental Data. The derived concentrations causing a 10% effect (EC10) in AhR-CALUX, PPARγ-GeneBLAzer, and ER-GeneBLAzer and concentrations causing an induction ratio of 1.5 (ECIR1.5) in AREc32 of each sample were then converted to bioanalytical equivalent concentration (BEQ; Equation 1) and effect units (Equation 2). The concentrations causing 10% cell growth inhibition (IC10) were converted to toxic units (TUs; Equation 3). This serves for a better visualization because high BEQ and toxic unit relate to high effects and cytotoxicity and allow comparison to other surface water case studies.

$$\text{BEQ} = \frac{\text{EC10 (reference)}}{\text{EC10 (sample)}} \text{ or } \frac{\text{ECIR1.5 (reference)}}{\text{ECIR1.5 (sample)}} \quad (1)$$

$$\text{Effect unit} = \frac{1}{\text{EC10}} \text{ or } \frac{1}{\text{IR1.5}} \quad (2)$$

$$\text{Toxic unit} = \frac{1}{\text{IC10}} \quad (3)$$

A list of the reference chemicals in each assay and their EC10 values can be found in Supplemental Data, Table S4. The errors of the BEQ, effect unit, and toxic unit were calculated by error propagation as described (Escher et al. 2018b).

Calculation of the influence of tributaries on the spatial effect and micropollutant dynamics in the main stem

The concentrations ($C_{downstream}$) and effects ($BEQ_{downstream}$) in the Ammer downstream of the respective tributary were obtained using a mass balance approach including concentrations and effects in the Ammer upstream of the tributary and in the tributary (Equations 4 and 5). Discharges (Q in liters per second, Ls^{-1}) are listed in Table 1, and effects (BEQ in nanograms of reference compound per liter) or concentrations (C, in nanograms per liter) from the Ammer and the tributaries are in Supplemental Data, Tables S5 and S6.

$$C_{downstream} = \frac{C_{upstream} \times Q_{upstream} + C_{tributary} \times Q_{tributary}}{Q_{upstream} + Q_{tributary}} \quad (4)$$

$$BEQ_{downstream} = \frac{BEQ_{upstream} \times Q_{upstream} + BEQ_{tributary} \times Q_{tributary}}{Q_{upstream} + Q_{tributary}} \quad (5)$$

Because the Ammer River splits into 2 smaller branches downstream of AS1 which reunite after approximately 900 m, discharges, effects, and concentrations of tributaries T2, T3, and T4 of both branches were combined and considered as one unit in reach 1. Consequently, the effects and concentrations of target compounds measured in the grab sample at AS1 were considered as the input of that unit. For each tributary confluence, the river discharge $Q_{upstream}$ was determined as the sum of all upstream tributary inputs and the discharge of the Ammer River Am-T0 (according to Table 1). To derive $Q_{downstream}$, the respective $Q_{tributary}$ was added. The mass fluxes J_i of target compounds (i) and the effect fluxes E_a measured in the bioassays (a) upstream and downstream of the tributary inlets were calculated with Equations 6 and 7.

$$J_i = Q \times C_i \quad (6)$$

$$E_a = Q \times BEQ_a \quad (7)$$

The mass flux increases of target compounds (ΔJ) and effects (ΔE) in the Ammer main stem downstream of the tributaries were calculated with Equations 8 and 9.

$$\Delta J_{i,Tx} = \frac{J_{i,downstream}}{J_{i,upstream}} - 1 \quad (8)$$

$$\Delta E_{a,Tx} = \frac{E_{a,downstream}}{E_{a,upstream}} - 1 \quad (9)$$

Similarity of either compound or effect profiles among the grab samples from the Ammer and the tributaries was assessed by a hierarchical cluster analysis with the unweighted pair-group method using arithmetic averages.

To give an equal weight to each individual target compound, their mass fluxes in all hourly water parcels at AS1, AS2, and AS3 were normalized each to the corresponding mass flux of water parcel 10 sampled at AS1 (if a target compound was not detected in AS1_10 the calculation referred to AS1_8 or AS1_9) according to Equation 10. Sample AS1_10 was used as a reference because it contained a high number of detected target compounds.

$$\text{Overall chemical burden} = \sum \frac{J_i}{J_{i,(AS1\_10)}} \quad (10)$$

RESULTS AND DISCUSSION

Impact of tributaries on the micropollutant and effect patterns in the river

The WWTP effluent had a mean discharge of $274 \pm 38\ Ls^{-1}$, which was on average 51% of the Ammer discharge during the 24 h of sampling at AS1 ($540 \pm 34\ Ls^{-1}$). Sample extracts were screened for 83 target compounds relevant for surface water, which included 38 pesticides, 28 pharmaceuticals and antibiotics, 6 transformation products, and 11 industrial, household and personal care products (Supplemental Data, Table S1). This includes pesticides currently used in the Ammer catchment (personal communication with local farmers), for example, strobilurine (pyraclostrobin) and triazole fungicides (epoxiconazole) or the sulfonyl urea herbicide nicosulfuron. In total, 28 compounds were detected in water samples, mostly in the nanograms per liter range (Supplemental Data, Table S5).

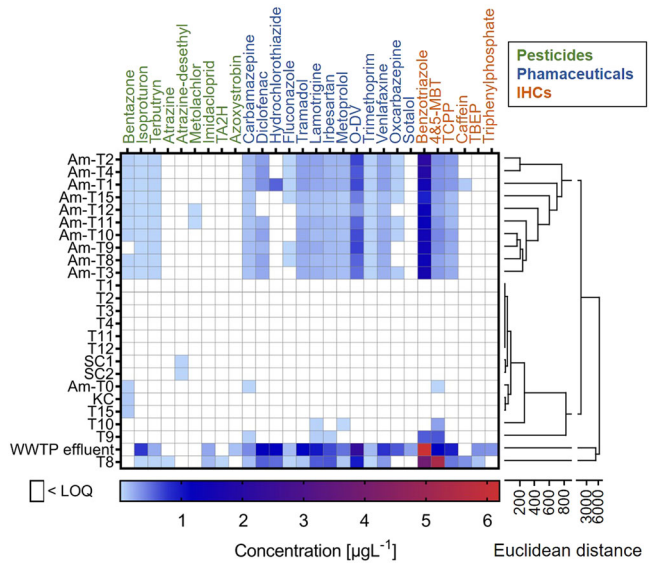

FIGURE 2: Target compounds in the Ammer main stem, the tributaries, the wastewater-treatment plant effluent, and Schönbrunnen Creek and Käsbach Creek, the tributaries of T15. Pesticides are highlighted in green, pharmaceuticals and antibiotics in blue, and industrial and household chemicals in orange. Similarity of compound profiles among samples is represented in a hierarchical cluster analysis with the unweighted pair-group method using arithmetic averages. Differences between samples and groups are expressed by the Euclidean distance. Am-T = Ammer tributary; IHCs = industrial and household chemicals; KC = Käsbach Creek; LOQ = limit of quantification; 4&5-MBT = 4&5-methylbenzotriazole; O-DV = O-desmethylvenlafaxine; SC = Schönbrunnen Creek; TA2H = terbuthylazine-2-hydroxy; TBEP = tris(2-butoxyethyl)phosphate; TCPP = tris(1-chloro-2-propyl)phosphate; WWTP = wastewater-treatment plant.

Among them were 9 pesticides and transformation products thereof, 13 pharmaceuticals, and 6 industrial, household and personal care products. The samples from the main stem downstream of the WWTP and from the tributaries clustered differently in a hierarchical cluster analysis, indicating clearly different compound profiles (see Figure 2). The compound profiles of the WWTP1 effluent and T8 impacted by WWTP2 appeared to be rather unique. Organic micropollutant concentrations in the Ammer main stem were considerably impacted by the input of WWTP1. Upstream of WWTP1 only the wastewater indicators carbamazepine and 4&5-methylbenzotriazole and the herbicide bentazone, which was previously detected in the Ammer source (Müller et al. 2018), occurred at approximately 20 to 60 ng L^{-1}. In the WWTP effluent 4 pesticides (azoxystrobin, imidacloprid, isoproturon, and terbutryn), 5 industrial, household and personal care products (benzotriazole, 4&5-methylbenzotriazole, tris[2-butoxyethyl]phosphate [TBEP], tris[1-chloro-2-propyl]phosphate [TCPP], and triphenylphosphate [TPP]), and 13 pharmaceuticals (e.g., carbamazepine, diclofenac, fluconazole, hydrochlorothiazide, metoprolol, tramadol) were detected. Concentrations were high for benzotriazole at 6 µg L^{-1}, O-demethylvenlafaxine at 2.3 µg L^{-1}, for 4&5-methylbenzotriazole at 1 µg L^{-1}, hydrochlorothiazide at 1 µg L^{-1}, diclofenac at 1 µg L^{-1}, and tramadol at 1 µg L^{-1}; pesticides ranged between 100 and 750 ng L^{-1} and other pharmaceuticals between 100 and 900 ng L^{-1}. Only caffeine and the 5 pesticides atrazine, atrazine-desethyl, bentazone, metolachlor, and terbuthylazine-hydroxy were absent in the WWTP effluent.

Farther downstream 5 pollutants decreased by >70% to concentrations below LOQ and did not occur any more at site Am-T1: azoxystrobin, imidacloprid, sotalol, TBEP, and TPP. Biodegradation, however, is not a reasonable process because of the short travel time of approximately 5 min between the WWTP1 input and Am-T1. Therefore, we speculate that sorption to suspended particulate matter (SPM) in the WWTP effluent and sedimentation may be considerable removal processes. This is supported by the relatively high octanol–water partition constant (log K_{OW}) of 2.5 for azoxystrobin (European Food Safety Authority 2010), 3.65 for TBEP (Van der Veen and de Boer 2012), and 4.59 for TPP (Hansch et al. 1995). Sotalol and imidacloprid have log K_{OW} values of the neutral species below 1 (ChemSpider 2020), and they are positively charged at neutral pH and therefore cannot be assessed by the K_{OW}. Also, charge interaction with negatively charged SPM and organic matter has to be considered in this case. Dilution and incomplete mixing can be ruled out based on the results of other pollutants (e.g., carbamazepine). The antihypertensive drug hydrochlorothiazide was detected in the river only once above the LOQ and was therefore not further considered. Other pollutants were transported throughout the river stretch and still appeared at Am-T15, the farthest downstream site: 3 pesticides (terbutryn at 27 ng L^{-1}, bentazone at 13 ng L^{-1}, isoproturon at 13 ng L^{-1}), 3 industrial, household and personal care products (benzotriazole at 850 ng L^{-1}, 4&5-methylbenzotriazole at 270 ng L^{-1}, TCPP at 140 ng L^{-1}), and 10 pharmaceuticals (e.g., O-desmethylvenlafaxine at 430 ng L^{-1}, tramadol at 150 ng L^{-1}, venlafaxine at 140 ng L^{-1}, lamotrigine at 120 ng L^{-1}, carbamazepine at 90 ng L^{-1}; see Supplemental Data, Table S5).

In tributaries T1, T2, T3, T4, T11, and T12 none of the pollutants could be detected. In T15, which is dominated by agricultural activity, only the herbicide bentazone was detected. A tributary of T15 (Schönbrunnen Creek) also contained atrazine-desethyl, the metabolite of the legacy herbicide atrazine. In T8, 5 pesticides (atrazine, imidacloprid, isoproturon, terbutryn, and terbuthalazine-2-hydroxy), 11 pharmaceuticals (e.g., carbamazepine, diclofenac, fluconazole, hydrochlorothiazide, tramadol), and 5 industrial, household and personal care products (e.g., caffeine, benzotriazole, 4&5-methylbenzotriazole, TCPP) were found; T8 receives WWTP effluents and inputs from agricultural land. The highest concentrations were measured for 4&5-methylbenzotriazole at 5.2 µg L^{-1} and benzotriazole at 3.8 µg L^{-1}. Caffeine, an indicator for untreated wastewater (Buerge et al. 2003), reached 336 ng L^{-1}. It appears that tributaries T9 and T10 were also impacted by WWTP2 effluent because the typical wastewater pollutants occurred: in T9, carbamazepine, irbesartan, lamotrigine, and benzotriazole; in T10, only lamotrigine, metoprolol, and 4&5-methylbenzotriazole. A likely explanation is wastewater from T8 percolating into the karstic groundwater, which enters farther downstream T9, T10, and the Ammer River, as shown in an earlier study (Harreß 1973). This is supported by the input of additional 22 Ls^{-1} water at AS3 that

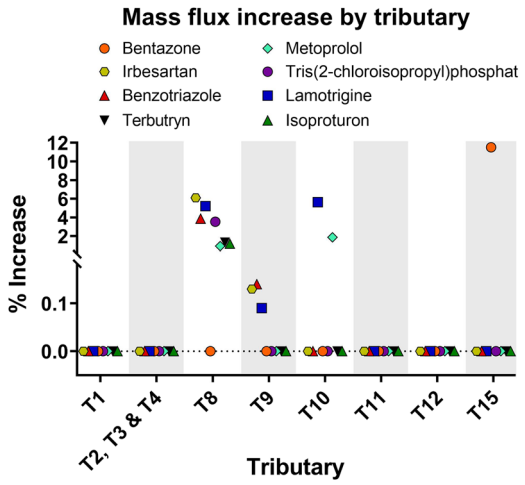

FIGURE 3: Mass flux increases in the Ammer main stem downstream of the tributaries (ΔJi, increase in percentage) of bentazone, metoprolol, irbesartan, tris(2-chloroisopropyl)phosphate, benzotriazole, lamotrigine, terbutryn, and isoproturon.

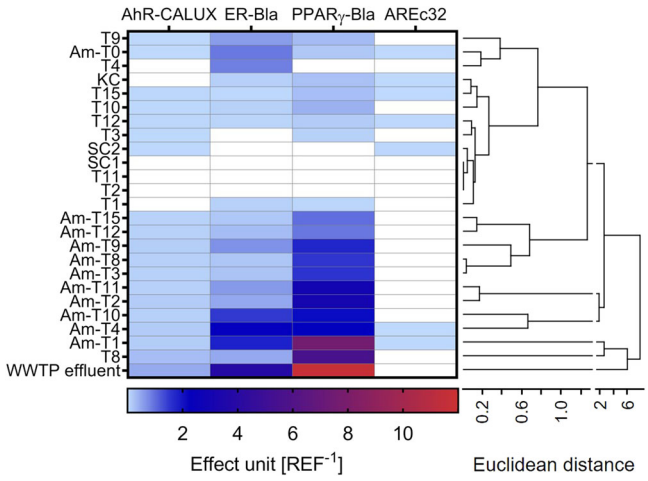

FIGURE 4: Effect units of the extracts from the Ammer main stem, the tributaries, the wastewater-treatment plant effluent, and the tributaries of T15, Schönbrunnen Creek and Käsbach Creek, measured in the in vitro bioassays AhR-CALUX, PPARγ-GeneBLAzer, ER-GeneBLAzer, and AREc32. Similarities of compound profiles among samples are represented in a hierarchical cluster analysis with the unweighted pair-group method using arithmetic averages. Differences between samples and groups are expressed by the Euclidean distance. Am-T = Ammer tributary; ER-Bla = ER-GeneBLAzer; KC = Käsbach Creek; PPARγ-Bla = PPARγ-GeneBLAzer; SC = Schönbrunnen Creek; WWTP = wastewater-treatment plant.

could not be attributed to any tributaries between AS2 and AS3 (see discharges in Table 1). Pollutants are subjected to dilution and attenuation processes during seepage passages, leading to reduced concentrations and the disappearance of compounds in T9 and T10 compared to T8 (e.g., diclofenac, irbesartan, lamotrigine, metoprolol, venlafaxine, 4&5-methylbenzotriazole, and TCPP).

To assess the influence of the tributaries on the compound pattern and abundance in the main stem, mass flux increases in the main stem caused by tributaries were calculated based on Equation 8 exemplarily for 8 compounds: the herbicides bentazone, isoproturon, and terbutryn; the pharmaceuticals metoprolol, lamotrigine, and irbesartan; the flame retardant tris (2-chloroisopropyl)phosphate; and the corrosion inhibitor benzotriazole (Figure 3). These chemicals represent different applications and thus diffusive (e.g., pesticides) and point source (via treated wastewater) inputs to the river. The influence of the tributaries on the compound profile and abundance in the main stem was generally insignificant apart from T8, T9, T10, and T15, with the highest mass flux increase for bentazone (10.4%) in T15. Most of the target compounds in Figure 3 were introduced by T8 (see Figure 2), though overall T8 had a rather low influence on the main stem because of its relatively low discharge (see Table 1). In contrast, T10 had a relatively high discharge but low compound concentrations except for lamotrigine and thus had little influence on the main stem as well.

The samples of the tributaries and the Ammer itself were further analyzed by in vitro bioassays AhR-CALUX, PPARγ-Bla, ER-Bla, and AREc32 (see Figure 4; Supplemental Data, Table S6. Similar to the compound profiles, the effect profiles of the tributaries clustered in a hierarchical cluster analysis as well as the samples of the Ammer main stem downstream of WWTP1. The samples that were most similar to the WWTP1 effluent were Am-T1 and T8. This finding is different from the chemical analysis but can be rationalized because Am-T1 and T8 are strongly influenced by WWTP effluents. The effect profiles of the Ammer clustered in a similar way as for the chemical analysis. The influence of the tributaries on the effect fluxes in the Ammer were generally significant (Figure 5). The highest effect flux increase in the Ammer was observed in ER-Bla, with 6.4% in reach 1 by T2, T3, and T4 together. Effect fluxes in the Ammer, measured in AhR-CALUX, PPARγ-Bla, and ER-Bla, increased approximately 1 to 5% by input from T8 and T10.

Although the chemical analysis and the in vitro bioassays covered different analytes and compound classes, they revealed similar pollution patterns and uncovered the tributaries as minor input sources of organic micropollutants and

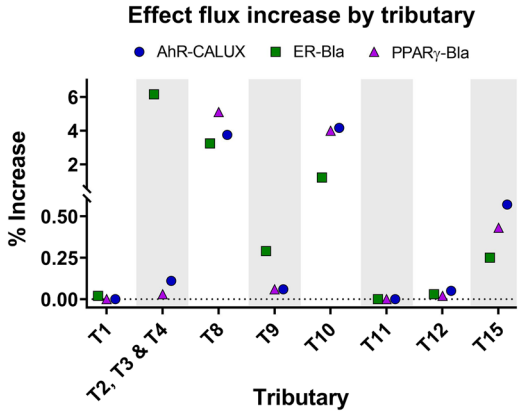

FIGURE 5: Effect flux increases in the Ammer main stem downstream of the tributaries measured in the bioassays AhR-CALUX, PPARγ-GeneBLAzer, and ER-GeneBLAzer. ER-Bla = ER-GeneBLAzer; PPARγ-Bla = PPARγ-GeneBLAzer.

associated effects. The tributaries had little impact on the Ammer because of their low discharge.

Temporal and spatial effects, cytotoxicity, and micropollutant dynamics in the main stem

In hourly composite water samples taken at the autosamplers, 23 of the target compounds were detected at AS1, AS2, and AS3 (Supplemental Data, Table S7). A different pollution profile at AS1 was found compared to AS2 and AS3, each of which clustered in a principal component analysis (PCA; see Supplemental Data, Figure S1A). The separation of the 3 groups occurred along principal component 1 (PC1), which explained 63.6% of the total variance. The compounds benzotriazole, 4-&5-methylbenzotriazole, and TCPP showed dominant negative loadings (Supplemental Data, Figure S1B). All are highly mobile in water, are rather stable toward degradation processes, and do not sorb considerably (Hem et al. 2003; Hart et al. 2004; Meyer and Bester 2004). Therefore, their concentrations did not decrease. O-Desmethylvenlafaxine and diclofenac showed dominant positive loadings (see Supplemental Data, Figure S1B) and consequently dissipated from the water phase more readily (Supplemental Data, Table S7). Both compounds are photodegradable under solar irradiation (Rúa-Gómez and Püttmann 2013; Baena-Nogueras et al. 2017). Principal component 2 explained 13.8% of the total variance and was mostly affected by the compounds diclofenac and mesotrione (Supplemental Data, Figure S1C). All of these compounds usually find their way into the environment by treated wastewater. Hydrochlorothiazide was not considered in the PCA because it was barely detected above the relatively high LOQ.

To consider the overall chemical burden of the Ammer River, normalized mass fluxes of the samples obtained over the course of 24 h at sampling sites AS1, AS2, and AS3 were summed up using Equation 10 (Figure 6A; named as "overall chemical burden"). The WWTP effluent had a high contribution to the Ammer main stem (51% of the Ammer discharge at AS1), and the WWTP discharge showed a temporal variability that cross-correlated moderately with the overall chemical burden at AS1 ($r_s = 0.52$). Hence, temporal dynamics of compounds from WWTPs can partially be explained by the effluent discharge, but the diurnal pattern of each individual target compound is still unknown. The coefficient of variation of the overall chemical burden over time was 18.7, 15.9 and 7.8% at AS1, AS2, and AS3, respectively, indicating a damping of temporal variability with increasing distance from the WWTP. The average cytotoxicity, $TU_{average}$, acquired from the in vitro bioassays AhR-CALUX, PPARγ-Bla, ER-Bla, and AREc32 (Supplemental Data, Table S8), was derived by Equation 3 and can reflect the total chemical load of a sample (Figure 6B). The average cytotoxicity was declining along the river flow with a slightly decreasing standard deviation and therewith a slightly declining variability over time (on average 0.040 ± 0.006 at AS1, 0.035 ± 0.006 at AS2, and 0.029 ± 0.004 toxic unit at AS3). The average attenuation of the mean $TU_{average}$ was 12.3 and 17.8%, which is mainly a result of dilution (10.3% in reach 1 and 22.7% in reach 2, based on data in Table 1). Similar to the overall chemical burden at AS1, the discharge of the WWTP effluent over time cross-correlated moderately ($r_s = 0.50$) with the $TU_{average}$ at AS1. However, no cross-correlation was observed with the $TU_{average}$ at AS2 and AS3.

Similar to the target compounds, the effects measured in the in vitro bioassays AhR-CALUX, PPARγ-Bla, ER-Bla, and AREc32 (Supplemental Data, Table S9) showed a different effect profile at AS1 compared to AS3 in a PCA (Supplemental Data, Figure S2A). The effect profiles of all individual samples appeared to cluster according to sampling sites, and separation between AS1 and AS3 occurred along the PC2 axis; PC2 explained 24.9% of the total variance, with strong loadings by AhR-CALUX (negative loading) and ER-Bla (positive loading) and weak loadings by PPARγ-Bla (positive loading) and AREc32 (negative loading; see Supplemental Data, Figure S2C). The differences between the effect profiles at AS1, AS2, and AS3 were mainly driven by the effects measured in AhR-CALUX and ER-Bla, which is in accordance with the data depicted in

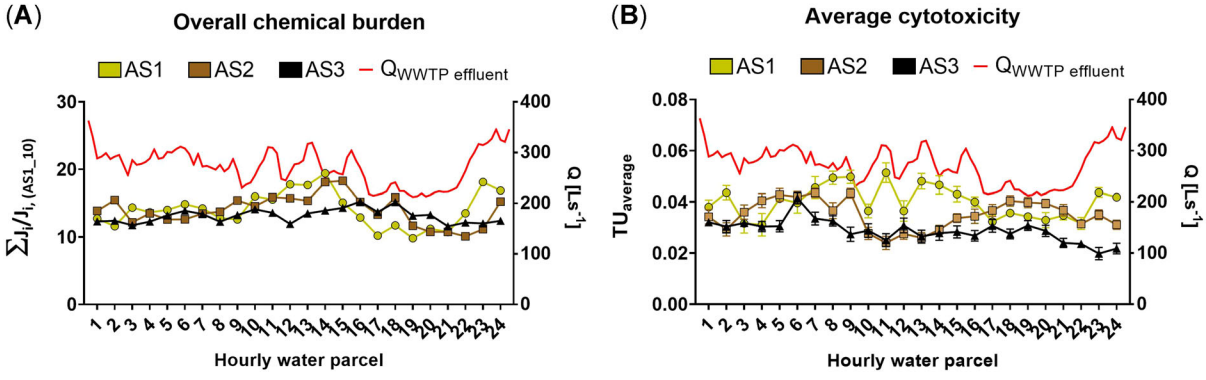

FIGURE 6: Overall chemical burden and average cytotoxicity in the Ammer main stem at autosamplers AS1, AS2, and AS3 over 24 h. (**A**) Sum of normalized mass fluxes of pollutants (chemical burden) measured by liquid chromatography tandem mass spectrometry. (**B**) Average cytotoxicity measured in the assays AhR-CALUX, PPARγ-GeneBLAzer, ER-GeneBLAzer, and AREc32. The discharge of the WWTP1 effluent is displayed on the second *y*-axis. Average cytotoxicity is expressed as toxic unit (see Equation 3), and the overall mass flux is expressed as the sum of the mass fluxes of each detected compound, normalized to the corresponding mass flux of water parcel 10 at AS1 ($\sum J_i/J_{i,(AS1\_10)}$). Error bars in (**B**) indicate standard errors calculated by error propagation. Q = discharge; TU = toxic unit; WWTP = wastewater-treatment plant.

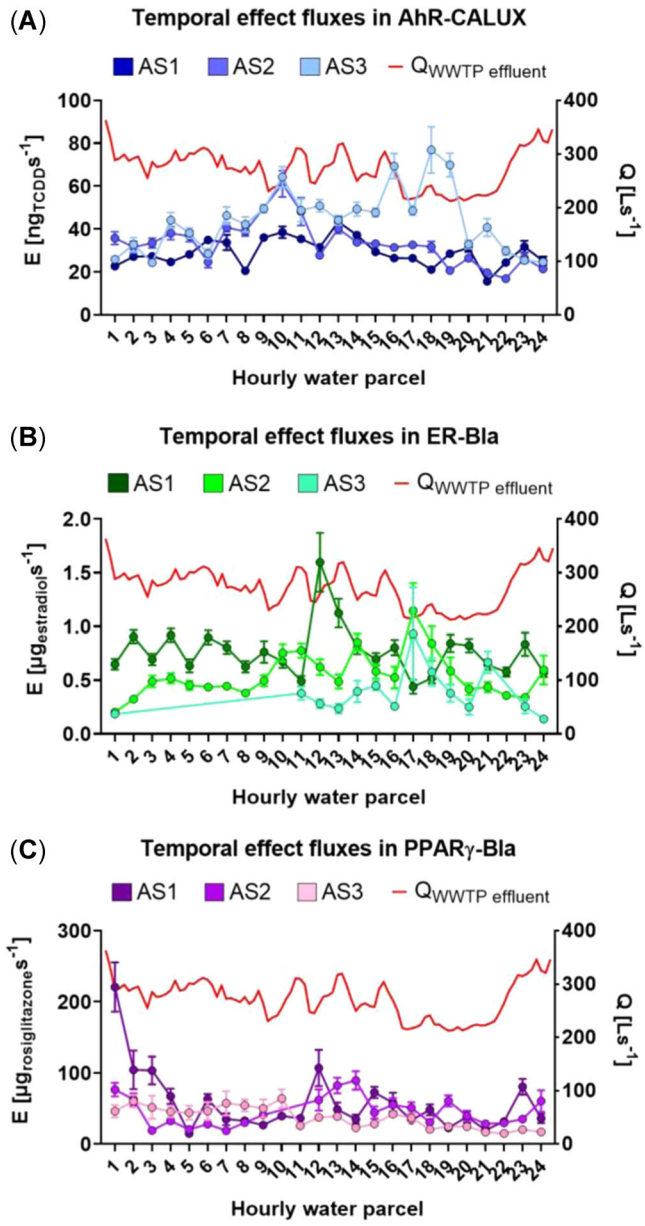

FIGURE 7: Effect fluxes expressed as amount of reference compound per second, in the Ammer main stem at autosamplers AS1, AS2, and AS3 over 24 h measured by the assays AhR-CALUX (**A**), ER-GeneBLAzer (**B**), and PPARγ-GeneBLAzer (**C**). Discharge Q of the WWTP1 effluent, expressed as Ls^{-1}, is displayed as a red line on the right vertical axis. Error bars in indicate standard errors. E = effect flux; ER-Bla = ER-GeneBLAzer; PPARγ-Bla = PPARγ-GeneBLAzer; Q = discharge; WWTP = wastewater-treatment plant.

Figure 7A and B. The effect fluxes averaged over 24 h increased in AhR-CALUX and decreased in ER-Bla along the river flow. The effect fluxes measured in AhR-CALUX, PPARγ-Bla, and ER-Bla (Figure 7A–C) showed temporal dynamics not following the discharge of the WWTP. Overall dynamics over 24 h were not large under these base flow conditions for the day of sampling.

The effect-based data were compared to tentative effect-based trigger values (EBT-BEQ) proposed by (Escher et al. 2018a), representing effect threshold levels for unacceptable surface water quality. These EBT-BEQs were derived from environmental quality standards of the European Union and help in estimating environmental risks of organic micropollutants. The EBT-EQ for benzo[*a*]pyrene is 6.4 $ng_{benzo[a]pyrene}L^{-1}$ for AhR CALUX, the EBT-EQ for 17ß-estradiol is 0.34 $ng_{17ß\text{-}estradiol}L^{-1}$ for ER-Bla, the EBT-rosiglitazone-EQ is 36 $ng_{rosiglitazone}L^{-1}$ for PPARγ-Bla, and the EBT-dichlorvos-EQ is 156 $\mu g_{dichlorvos}L^{-1}$ for AREc32 (Escher et al. 2018a). At AS1, AS2, and AS3 these proposed EBT-BEQs were exceeded in all bioassays except AREc32, where also in many samples the effects were masked by cytotoxicity (Supplemental Data, Tables S10 and S11). Compliant with the EBTs were many of the tributaries and the Ammer at Am-T0 (except for the EBT-EQ for 17ß-estradiol) prior to the WWTP effluent coming in. Aside from the wastewater-contaminated T8, the proposed EBT-BEQs were also exceeded by tributaries T1, T2, T9, T10, and KC in ER-Bla; T9 and T10 in PPARγ-Bla; and T12, T15, KC, and SC2 in AREc32 (see Supplemental Data, Table S6). Although only a few or no target compounds were detected in most tributaries, the measured effects point toward potential problems with the water quality stemming from other sources. One year earlier, in July 2017, the chemical and effect profiles of the Ammer catchment were investigated (Müller et al. 2018). The proportion of treated wastewater deriving from WWTP1 was higher in 2017 with 81% compared to 50% in 2018, and therefore, the effects measured in AhR-CALUX, ER-Bla, and AREc32 were slightly higher in 2017 than in 2018. Although the EBT-BEQs exceeded the measured effects, they were still in the same range as those derived for similar surface water samples by other research groups (Escher et al. 2012, 2013a; Scott et al. 2018).

CONCLUSION

The characterization of input sources and pathways of organic micropollutants in the aquatic environment is important to assess water quality but also a challenging task. The study site is representative of other small river systems in densely populated countries. The present study revealed treated wastewater as the primary input source of organic micropollutants and associated effects in rivers during dry weather periods. Tributaries from agricultural and urban areas carried only a few of the monitored target compounds but exceeded effect-based trigger values, pointing toward unacceptable water quality. However, the contribution of tributaries to the mass and effect fluxes in the main river were negligible under base flow conditions. Increased discharge during rain events may change this situation. Increased runoff from agricultural and urban areas may change the pollution profile, mass and effect fluxes, and therefore the contribution of tributaries to the main river. We therefore recommend further catchment-scale studies to reveal the role of rain events for the water quality of small rivers.

Supplemental Data—The Supplemental Data are available at the Wiley Online Library at https://doi.org/10.1002/etc.4726.

Acknowledgment—The authors thank C. Adolphi for her assistance in chemical analysis, M. Ebner for his advice on

statistical data treatment, S. Novak for her laboratory assistance in Tübingen, and M. König, J. John, and R. Schlichting for performing the in vitro bioassays at UFZ. The present study was supported by the Collaborative Research Centre 1253 CAMPOS (Project P1: Rivers), funded by the German Research Foundation (grant SFB 1253/1 2017).

Disclaimer—All authors have no interest to declare. The views expressed in the present study are solely those of the authors.

Author Contribution Statement—M.E. Müller: conceiving and conducting the sampling, sample preparation, conducting the evaluation and interpretation of chemical analysis and bioassay data, in vitro bioassay data acquisition, writing the manuscript, initial design of all figures except for Figure 1; M. Werneburg: conceiving the sampling, sample preparation, chemical analysis, data acquisition and evaluation, drafting the manuscript; C. Glaser: sampling, revising the manuscript, making substantial contributions to designing Figure 1, conceiving the sampling; M. Schwientek: conceiving and conducting the sampling, revising the manuscript; C. Zarfl: conceiving the sampling, revising the manuscript; B.I. Escher: conceiving the sampling, making substantial contributions to bioassay measurements, analysis and interpretation of data, and drafting the manuscript; C. Zwiener: conceiving the sampling and making substantial contributions to chemical analysis, interpretation of data, drafting and revising the manuscript.

Data Availability Statement—Data, associated metadata, and calculation tools are available from the corresponding author (christian.zwiener@uni-tuebingen.de).

REFERENCES

Alpizar F, Backhaus T, Decker N, Eilks I, Escobar-Pemberthy N, Fantke P, Geiser K, Ivanova M, Jolliet O, Kim H-S. 2019. Global Chemicals Outlook II: From legacies to innovative solutions. Implementing the 2030 agenda for sustainable development. United Nations Environment Programme, Nairobi, Kenya.

Baena-Nogueras RM, González-Mazo E, Lara-Martín PA. 2017. Degradation kinetics of pharmaceuticals and personal care products in surface waters: Photolysis vs biodegradation. *Sci Total Environ* 590:643–654.

Brennan JC, He G, Tsutsumi T, Zhao J, Wirth E, Fulton MH, Denison MS. 2015. Development of species-specific Ah receptor-responsive third generation CALUX cell lines with enhanced responsiveness and improved detection limits. *Environ Sci Technol* 49:11903–11912.

Bueno MM, Gomez M, Herrera S, Hernando M, Agüera A, Fernández-Alba A. 2012. Occurrence and persistence of organic emerging contaminants and priority pollutants in five sewage treatment plants of Spain: Two years pilot survey monitoring. *Environ Pollut* 164:267–273.

Buerge IJ, Poiger T, Müller MD, Buser H-R. 2003. Caffeine, an anthropogenic marker for wastewater contamination of surface waters. *Environ Sci Technol* 37:691–700.

ChemSpider. 2020. Sotalol, imidacloprid. [cited 2020 April 2]. Available from: http://www.chemspider.com/Chemical-Structure.5063.html

Englert D, Zubrod JP, Schulz R, Bundschuh M. 2013. Effects of municipal wastewater on aquatic ecosystem structure and function in the receiving stream. *Sci Total Environ* 454:401–410.

Escher BI, Aït-Aïssa S, Behnisch PA, Brack W, Brion F, Brouwer A, Buchinger S, Crawford SE, Du Pasquier D, Hamers T. 2018a. Effect-based trigger values for in vitro and in vivo bioassays performed on surface water extracts supporting the environmental quality standards (EQS) of the European Water Framework Directive. *Sci Total Environ* 628:748–765.

Escher BI, Allinson M, Altenburger R, Bain PA, Balaguer P, Busch W, Crago J, Denslow ND, Dopp E, Hilscherova K. 2013a. Benchmarking organic micropollutants in wastewater, recycled water and drinking water with in vitro bioassays. *Environ Sci Technol* 48:1940–1956.

Escher BI, Dutt M, Maylin E, Tang JYM, Toze S, Wolf CR, Lang M. 2012. Water quality assessment using the AREc32 reporter gene assay indicative of the oxidative stress response pathway. *J Environ Monit* 14:2877–2885.

Escher BI, Neale PA, Villeneuve DL. 2018b. The advantages of linear concentration–response curves for in vitro bioassays with environmental samples. *Environ Toxicol Chem* 37:2273–2280.

Escher BI, van Daele C, Dutt M, Tang JY, Altenburger R. 2013b. Most oxidative stress response in water samples comes from unknown chemicals: The need for effect-based water quality trigger values. *Environ Sci Technol* 47:7002–7011.

European Environment Agency. 2019. The European environment—State and outlook 2020: Knowledge for transition to a sustainable Europe. Publications Office of the European Union, Luxembourg.

European Food Safety Authority. 2010. Conclusion on the peer review of the pesticide risk assessment of the active substance azoxystrobin. *EFSA J* 8:1542.

Farré M, Barceló D. 2003. Toxicity testing of wastewater and sewage sludge by biosensors, bioassays and chemical analysis. *Trends Anal Chem* 22:299–310.

Gago-Ferrero P, Bletsou AA, Damalas DE, Aalizadeh R, Alygizakis NA, Singer HP, Hollender J, Thomaidis NS. 2019. Wide-scope target screening of >2000 emerging contaminants in wastewater samples with UPLC-Q-TOF-HRMS/MS and smart evaluation of its performance through the validation of 195 selected representative analytes. *J Hazard Mater* 387:121712.

Grathwohl P, Rügner H, Wöhling T, Osenbrück K, Schwientek M, Gayler S, Wollschläger U, Selle B, Pause M, Delfs J-O. 2013. Catchments as reactors: A comprehensive approach for water fluxes and solute turnover. *Environ Earth Sci* 69:317–333.

Hansch C, Leo A, Hoekman D. 1995. *Exploring QSAR: Fundamentals and Applications in Chemistry and Biology*. American Chemical Society, Washington, DC.

Harreß HM. 1973. Hydrogeologische Untersuchungen im Oberen Gäu. PhD thesis, University of Tübingen, Tübingen, Germany.

Hart D, Davis L, Erickson L, Callender T. 2004. Sorption and partitioning parameters of benzotriazole compounds. *Microchem J* 77:9–17.

Hem LJ, Hartnik T, Roseth R, Breedveld GD. 2003. Photochemical degradation of benzotriazole. *J Environ Sci Health A* 38:471–481.

König M, Escher BI, Neale PA, Krauss M, Hilscherová K, Novák J, Teodorović I, Schulze T, Seidensticker S, Hashmi MAK, Ahlheim J, Brack W. 2017. Impact of untreated wastewater on a major European river evaluated with a combination of in vitro bioassays and chemical analysis. *Environ Pollut* 220:1220–1230.

Kruve A, Leito I, Herodes K. 2009. Combating matrix effects in LC/ESI/MS: The extrapolative dilution approach. *Anal Chim Acta* 651:75–80.

Kuzmanović M, Ginebreda A, Petrović M, Barceló D. 2015. Risk assessment based prioritization of 200 organic micropollutants in 4 Iberian rivers. *Sci Total Environ* 503:289–299.

Lee H-J, Kim KY, Hamm S-Y, Kim M, Kim HK, Oh J-E. 2019. Occurrence and distribution of pharmaceutical and personal care products, artificial sweeteners, and pesticides in groundwater from an agricultural area in Korea. *Sci Total Environ* 659:168–176.

Loos R, Gawlik BM, Locoro G, Rimaviciute E, Contini S, Bidoglio G. 2009. EU-wide survey of polar organic persistent pollutants in European river waters. *Environ Pollut* 157:561–568.

Lundqvist J, von Brömssen C, Rosenmai AK, Ohlsson Å, Le Godec T, Jonsson O, Kreuger J, Oskarsson A. 2019. Assessment of pesticides in surface water samples from Swedish agricultural areas by integrated bioanalysis and chemical analysis. *Environ Sci Eur* 31:53.

Masoner JR, Kolpin DW, Furlong ET, Cozzarelli IM, Gray JL, Schwab EA. 2014. Contaminants of emerging concern in fresh leachate from landfills in the conterminous United States. *Environ Sci Process Impacts* 16:2335–2354.

Meyer J, Bester K. 2004. Organophosphate flame retardants and plasticisers in wastewater treatment plants. *J Environ Monit* 6:599–605.

Müller ME, Escher BI, Schwientek M, Werneburg M, Zarfl C, Zwiener C. 2018. Combining in vitro reporter gene bioassays with chemical analysis to assess changes in the water quality along the Ammer River, southwestern Germany. *Environ Sci Eur* 30:20.

Müller ME, Vikstrom S, König M, Schlichting R, Zarfl C, Zwiener C, Escher BI. 2019. Mitochondrial toxicity of selected micropollutants, their mixtures, and surface water samples measured by the oxygen consumption rate in cells. *Environ Toxicol Chem* 38:1000–1011.

Munz NA, Burdon FJ, De Zwart D, Junghans M, Melo L, Reyes M, Schönenberger U, Singer HP, Spycher B, Hollender J. 2017. Pesticides drive risk of micropollutants in wastewater-impacted streams during low flow conditions. *Water Res* 110:366–377.

Neale PA, Altenburger R, Aït-Aïssa S, Brion F, Busch W, de Aragão Umbuzeiro G, Denison MS, Du Pasquier D, Hilscherová K, Hollert H. 2017a. Development of a bioanalytical test battery for water quality monitoring: Fingerprinting identified micropollutants and their contribution to effects in surface water. *Water Res* 123:734–750.

Neale PA, Munz NA, Aït-Aïssa S, Altenburger R, Brion F, Busch W, Escher BI, Hilscherová K, Kienle C, Novák J. 2017b. Integrating chemical analysis and bioanalysis to evaluate the contribution of wastewater effluent on the micropollutant burden in small streams. *Sci Total Environ* 576:785–795.

Rúa-Gómez PC, Püttmann W. 2013. Degradation of lidocaine, tramadol, venlafaxine and the metabolites O-desmethyltramadol and O-desmethylvenlafaxine in surface waters. *Chemosphere* 90:1952–1959.

Schwarzenbach RP, Gschwend PM, Imboden DM. 2016. *Environmental Organic Chemistry*, 3rd ed. John Wiley & Sons, Hoboken, NJ, USA.

Schwientek M, Guillet G, Rügner H, Kuch B, Grathwohl P. 2016. A high-precision sampling scheme to assess persistence and transport characteristics of micropollutants in rivers. *Sci Total Environ* 540:444–454.

Scott PD, Coleman HM, Khan S, Lim R, McDonald JA, Mondon J, Neale PA, Prochazka E, Tremblay LA, Warne MSJ. 2018. Histopathology, vitellogenin and chemical body burden in mosquitofish (*Gambusia holbrooki*) sampled from six river sites receiving a gradient of stressors. *Sci Total Environ* 616:1638–1648.

Szöcs E, Brinke M, Karaoglan B, Schäfer RB. 2017. Large scale risks from agricultural pesticides in small streams. *Environ Sci Technol* 51: 7378–7385.

Van der Veen I, de Boer J. 2012. Phosphorus flame retardants: Properties, production, environmental occurrence, toxicity and analysis. *Chemosphere* 88:1119–1153.

Villagrasa M, Guillamón M, Eljarrat E, Barceló D. 2007. Matrix effect in liquid chromatography–electrospray ionization mass spectrometry analysis of benzoxazinoid derivatives in plant material. *J Chromatogr A* 1157: 108–114.

Writer JH, Keefe SK, Ryan JN, Ferrer I, Thurman ME, Barber LB. 2011. Methods for evaluating in-stream attenuation of trace organic compounds. *Appl Geochem* 26(Suppl):S344–S345.

Publication 4

Storm event-driven occurrence and transport of dissolved and sorbed organic micropollutants and associated effects in the Ammer River, Southwestern Germany

Maximilian E. Müller[a], Christian Zwiener[a] and Beate I. Escher[a, b]

[a]Eberhard Karls University of Tübingen, Center for Applied Geoscience, Tübingen, Germany

[b]UFZ – Helmholtz Centre for Environmental Research, Leipzig, Germany

Published in *Environmental Toxicology and Chemistry*, DOI: 10.1002/etc.4910

The Supplemental Information is published “Open Access” and available on

https://doi.org/10.1002/etc.4910

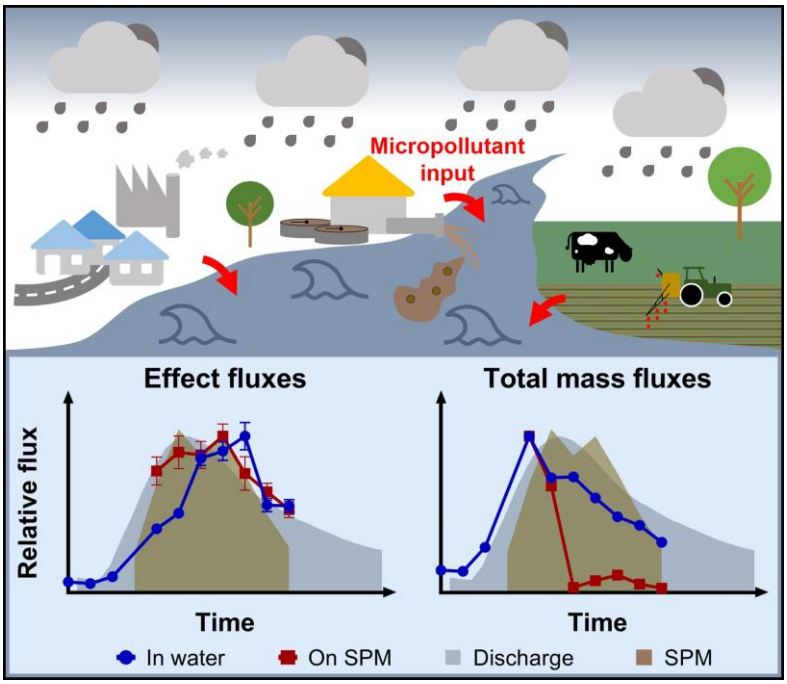

Environmental Toxicology and Chemistry—Volume 00, Number 00—pp. 1–12, 2020
Received: 17 July 2020 | Revised: 11 August 2020 | Accepted: 16 October 2020

Environmental Chemistry

Storm Event–Driven Occurrence and Transport of Dissolved and Sorbed Organic Micropollutants and Associated Effects in the Ammer River, Southwestern Germany

Maximilian E. Müller,[a] Christian Zwiener,[a] and Beate I. Escher[a,b,*]

[a]Center for Applied Geoscience, Eberhard Karls University of Tübingen, Tübingen, Germany
[b]Department of Cell Toxicology, UFZ–Helmholtz Centre for Environmental Research, Leipzig, Germany

Abstract: Storm events lead to agricultural and urban runoff, to mobilization of contaminated particulate matter, and to input from combined sewer overflows into rivers. We conducted time-resolved sampling during a storm event at the Ammer River, southwest Germany, which is representative of small river systems in densely populated areas with a temperate climate. Suspended particulate matter (SPM) and water from 2 sampling sites were separately analyzed by a multi-analyte liquid chromatography–tandem mass spectrometry (LC–MS/MS) method for 97 environmentally relevant organic micropollutants and with 2 in vitro bioassays. Oxidative stress response (AREc32) may become activated by various stressors covering a broad range of physicochemical properties and induction of aryl hydrocarbon receptor–chemical-activated luciferase gene expression (AhR-CALUX) by hydrophobic compounds such as dioxins and dioxin-like molecules. Compound numbers, concentrations, their mass fluxes, and associated effect fluxes increased substantially during the storm event. Micropollutants detected in water and on SPM pointed toward inputs from combined sewer overflow (e.g., caffeine, paracetamol), urban runoff (e.g., mecoprop, terbutryn), and agricultural areas (e.g., azoxystrobin, bentazone). Particle-facilitated transport of triphenylphosphate and tris(1-chloro-2-propyl) phosphate accounted for up to 34 and 33% of the total mass flux even though SPM concentrations were <1 g L^{-1}. Effect fluxes attributed to SPM were similar or higher than in the water phase. The important role of SPM-bound transport emphasizes the need to consider not only concentrations but also mass and effect fluxes for surface water quality assessment and wastewater/stormwater treatment options. *Environ Toxicol Chem* 2020;00:1–12. © 2020 The Authors. *Environmental Toxicology and Chemistry* published by Wiley Periodicals LLC on behalf of SETAC.

Keywords: Storm event; Organic micropollutants; Chemical analysis; In vitro bioassays; Water quality

INTRODUCTION

More and more anthropogenic organic compounds are being used in a broad range of applications and have become indispensable to our modern society. Because of high usage and consumption, they are regularly found in the aquatic environment (Casado et al. 2019; Bradley et al. 2020). Due to their use-specific properties, such as high persistence of flame retardants or effects of pesticides and pharmaceuticals on biological organisms (Daughton and Ternes 1999), they may pose a hazard to ecosystems and drinking water quality (Alpizar et al. 2019; European Environment Agency 2019). Ideally, pharmaceuticals and personal care products are collected after application and managed by municipal sewers and wastewater treatment systems. Other compounds such as pesticides are directly dispersed in agriculture and urban environments. Biocides, used to preserve outdoor materials, facades, and roofs, may leach and be flushed into surface waters by rainfall (Berenzen et al. 2005; Tran et al. 2019; Spahr et al. 2020).

The chemical status of surface waters is generally only assessed by snapshots of individual compound concentrations in regulatory monitoring (Brack et al. 2018). The water quality of small river systems can be highly dynamic (Jordan and Cassidy 2011), and as a recent study on 128 cumulative water samples

This article includes online-only Supplemental Data.

* Address correspondence to beate.escher@ufz.de
Published online 20 October 2020 in Wiley Online Library (wileyonlinelibrary.com).
DOI: 10.1002/etc.4910

taken during rain events at 44 different small streams in Germany demonstrated, each rain event showed a different chemical and effect profile (Neale et al. 2020). Depending on their physicochemical properties, organic micropollutants can sorb to organic carbon or mineral surfaces of soils and sediments (Schwarzenbach et al. 2016). Micropollutant-loaded soil or sediment particles may be released and suspended in rivers during storm events. With increased river discharge during storms, suspended particulate matter (SPM) represents a potential transport vector of organic micropollutants in rivers (Gasperi et al. 2009; Lepom et al. 2009; da Silva et al. 2011; Zgheib et al. 2011; Boulard et al. 2019). Storm and flood events can cause combined sewer overflows and thereby the release of untreated wastewater, including sewage sludge particles, into surface waters (Phillips et al. 2012; Madoux-Humery et al. 2013). Furthermore, remobilization of contaminants from sediments has to be considered (Eggleton and Thomas 2004; de Weert et al. 2010; Müller et al. 2019).

We investigated the impact of a storm event on the concentrations and mass fluxes of dissolved and particle-associated micropollutants and their associated effects, in high temporal resolution at 2 sampling sites at the Ammer River in southwest Germany. Water and SPM were analyzed separately by liquid chromatography–mass spectrometry (LC–MS) and 2 in vitro bioassays. The chemical analysis targeted 97 environmentally relevant organic micropollutants including 45 pesticides, 31 pharmaceuticals, 12 industrial and household chemicals, and 9 other compounds, that have been found regularly in surface waters (Ruff et al. 2015; Casado et al. 2019; van Gils et al. 2020). Mixture effects of all chemicals in water and SPM were quantified with 2 in vitro bioassays that cover the environmentally relevant modes of action of aryl hydrocarbon receptor (AhR) induction and oxidative stress response. Induction of AhR may be activated by hydrophobic compounds such as dioxins and dioxin-like molecules (i.e., planar polychlorinated biphenyls, polychlorinated dibenzodioxins, and dibenzofurans), but also by polycyclic aromatic hydrocarbons; the assay is commonly used to assess sediment quality and the bioavailability and toxicity of sediment-associated contaminants (Li et al. 2013; Eichbaum et al. 2014; Bräunig et al. 2016). Oxidative stress response is induced by a broad range of stressors and has been used for sediment and water quality assessment (Escher et al. 2012; Li et al. 2013; Bräunig et al. 2016).

In the present study we addressed the following questions: 1) What are the dynamics of the total organic micropollutant and effect fluxes in a river during a storm event? 2) How much does SPM-facilitated transport contribute to the total flux of micropollutants and bioactive mixtures? and 3) What is the concentration ratio between water and SPM for micropollutants and effects and does it change during the event?

MATERIALS AND METHODS

Sampling

In the night of 27 July 2019, from 18:30 to 22:45 (all times given as Central European Summer Time, Coordinated Universal Time [UTC] + 2 h) a thunder cell came from the southwest and passed the upper Ammer catchment with precipitation up to 80 mm h^{-1} (Supplemental Data, Figure S1). The precipitation sum for 27 July 2019 was 29 mm at the meteorological station in Herrenberg/Gäufelden, Germany (Baden-Württemberg State Institute for the Environment, Survey and Nature Conservation 2020b). With a discharge maximum of 8772 L s^{-1} at autosampler (AS) AS2 (gauge station in Pfäffingen, Germany) the investigated storm event almost reached the German classification of a biennial flood HQ2 (HQ2: ≥ 11 650 L s^{-1} at the gauge station in Pfäffingen; Baden-Württemberg State Institute for the Environment, Survey and Nature Conservation 2020a). At 2 sampling sites (AS1 and AS2) at the Ammer River, which were located upstream and downstream of a wastewater treatment plant (WWTP1, 80 000 person equivalents, annual mean flow: 100–120 L s^{-1}) and 7.7 km apart, 1 L of river water was sampled every 30 min for a total period of 6 h using ISCO 3700 autosamplers (Teledyne ISCO; Figure 1). The first samples taken at AS1 (AS1_1 at 20:09) and at AS2 (AS2_1 at 21:03) were set as origins (0 h) of the respective time scales (time [h]). A second smaller WWTP (WWTP2, annual mean flow: 12–15 L s^{-1}) with 9000 person equivalents discharges into the Kochart Creek, a tributary of the Ammer River upstream of AS2.

After 14 h, when discharge decreased toward base flow conditions, 1 L of river water was collected at each sampling site. The AS2 samples were taken 53 min after the AS1 samples to capture full hydrographs of both sampling sites. All samples were kept cool at 4 °C and processed within the next 48 h. At AS1 and AS2, discharges were derived from measured water levels (using online probes from UIT) and pre-established rating curves. Discharges (Q) of 15-min intervals (Supplemental Data, Table S1) and amounts of SPM (Supplemental Data, Table S2) have been reported by Glaser et al. (2020). The SPM amounts were derived by filtering (250 mL of replicate samples, 1.5-µm cellulose membrane) according to the German industrial standard Deutsche Industrienorm 38409-2 (1987). At both sampling sites sampling and discharge measurements were not performed at the exact same time. Therefore, the discharge corresponding to a given sample of AS1 was estimated by linear interpolation between the 2 adjacent samples. The discharge for a given sample of AS2 referred to the closest discharge measurement (Supplemental Data, Table S3). The SPM fluxes ($kg_{dry\ weight}\ s^{-1}$) were determined as the SPM amount (Supplemental Data, Table S2) times the discharge (Supplemental Data, Table S3).

Chemicals and reagents

All solvents used were LC–MS grade. Acetonitrile was purchased from Honeywell Riedel-de Haen™. Methanol (Optima®) and water (Optima®) were obtained from Thermo Fisher Scientific. Ethyl acetate was purchased from Acros Organics, Thermo Fisher Scientific. Acetone (SupraSolv®) was obtained from Merck. A list of all analytical standards is given in the Supplemental Data, Table S4.

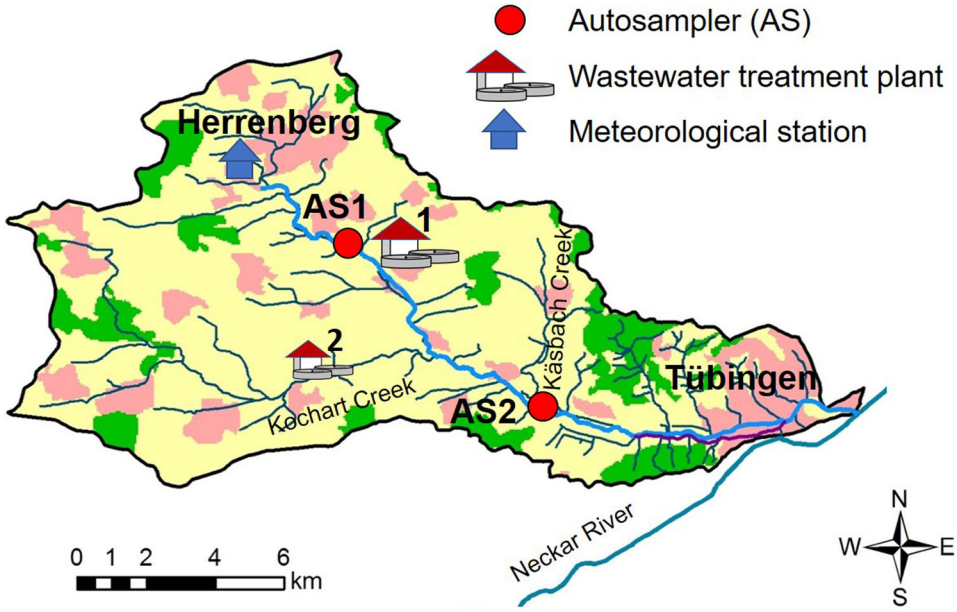

FIGURE 1: Study site in the Ammer catchment near Tübingen, Germany. At 2 sampling sites, autosamplers (AS) AS1 and AS2 (red dots) were installed, and run during the storm event. AS2 was located at the river water gauge station in Pfäffingen. Wastewater treatment plants are located at the Ammer main stem downstream of AS1 (WWTP1, 80 000 PE) and at the Kochart Creek (WWTP2, 9000 PE). The meteorological station (blue house symbol) is located upstream of AS1. The Ammer main stem is highlighted in light blue. Land uses are illustrated in yellow for agriculture, pink for urban areas, and green for forestry. Figure adapted from Müller et al. (2018).

Sample preparation

Accelerated solvent extraction. The SPM from 1 L of river water was separated from the water phase using a cellulose filter (Whatman 595 1/2, pore size: 4–7 µm), frozen at –20 °C overnight, and then freeze-dried for 24 h (Alpha 1-4 LSCplus freeze drier; Martin Christ). Freeze-dried cellulose filters with attached SPM were extracted by accelerated solvent extraction (ASE; Dionex ASE 300 system, Thermo Fisher Scientific). Extraction was performed with acetone:ethyl acetate (50:50, v/v) in 2 cycles, each with 5-min preheat, 10-min static time at 80 °C and 100 bar, a flush volume of 60%, and a purge time of 60 s. More information is provided in the Supplemental Data, S1. The ASE blanks were derived by extracting freeze-dried cellulose filters. The ASE extracts were evaporated to dryness using a rotary evaporator (Rotapovator® R-215; Büchi) and reconstituted with 1 mL methanol. The exact final volumes were determined gravimetrically.

Solid phase extraction. First, 1 L of filtered river water samples was preconcentrated by a factor of 2000 by solid phase extraction (SPE) using cartridges with 200 mg hydrophilic–lipophilic balanced material (Oasis HLB 6 cc; Waters). Further information is provided in the Supplemental Data, S1. For SPE blanks, pure water was used. Finally, all water and SPM extracts, blanks, and samples for assessing extraction recoveries were filtered with a polyethersulfone 0.2-µm filter (Agilent Captiva Premium Syringe filter), to avoid clogging of the high-performance liquid chromatography (HPLC) system, and stored at –20 °C until measurement. Exact volumes of all extracts were determined gravimetrically.

ASE and SPE recoveries

Uncertainty systematically arising from the sample preparation was considered in the result reported (Barwick and Ellison 2000; Cordeiro et al. 2018; Mateos et al. 2020). Therefore, with respect to the absence of sufficient sample volume and the avoidance of internal standards that would lead to signal interference in the bioassays, ASE recovery was assessed by extracting cellulose filters spiked with standard solutions (50 µL of 100 µg L^{-1}, $n = 3$). The SPE recoveries were determined with pure water (Milli-Q) spiked with a standard mix including all target compounds (5 ng L^{-1}, $n = 3$). It was assumed that the systematic analyte loss during SPE and ASE was constant throughout the samples and not affected by the sample matrix.

Chemical analysis

Analyte separation was achieved by a 1260 Infinity HPLC device (Agilent Technologies) using a Poroshell 120 EC-C18 column (2.7-µm particle size, 4.6 × 150 mm; Agilent) at 40 °C. Carrier liquids were water with 0.1 mM ammonium acetate and 17.5 mM acetic acid (A) and acetonitrile with 17.5 mM acetic acid (B). Chromatographic separation was performed with the following gradient program: 0 to 17 min, 95 to 20% A, 17 to 23 min 0% A, 23 to 33 min 95% A. Target screening for 97 target compounds was performed by tandem mass spectrometry (MS/MS; 6490 iFunnel triple quadrupole mass spectrometer; Agilent) using electrospray ionization and 2 mass transitions/analyte (Supplemental Data, Table S5). For 11 target compounds, quantification was performed by internal standard

calibration (internal standard spiked to the samples to a concentration of 5 µg L^{-1}, using an Agilent 1260 Infinity Standard Autosampler prior to LC–MS/MS measurement). For all other target compounds, external standard calibration (9-point calibration) was applied.

Matrix effects were assessed in representative samples by standard addition and 2 concentration levels (0.83 and 3.33 µg L^{-1}, $n = 1$; Supplemental Data, S1 and Table S6). Because the average relative standard deviation of all target compounds (Supplemental Data, Table S8) was 7%, correction for matrix effects of the quantitative results (Supplemental Data, Table S7) was deemed appropriate if the signal suppression or enhancement was outside a range of ±20%. The limit of quantification (LOQ) was defined as the lowest calibration level for which the signal-to-noise ratio was ≥10 and for which the quantifier-to-qualifier ratio was within ±20% of the average ratio of analytical standards. If an analyte was detected in the blank, the 5-fold blank concentration was used as the LOQ. Prior to LC–MS/MS measurements, water extracts were diluted 1:50 in methanol:water (30:70 v/v) to reduce matrix effects (Villagrasa et al. 2007; Kruve et al. 2009). The relative standard deviations of ASE and SPE recoveries of all target compounds were on average 11 and 29%, respectively. Only concentrations of analytes with recoveries <70% were corrected (Supplemental Data, Table S8). Analytes with recoveries <20% were not further considered. Recoveries of acesulfame, citalopram, fluoxetin, and gabapentin were <20%, and these compounds were therefore omitted from further analysis. The relative standard deviations of replicate LC–MS measurements, of a standard solution at 5.0 µg L^{-1}, of each analyte ($n = 10$) are provided in the Supplemental Data, Table S8. In addition, analyte concentrations on SPM were corrected for residual water co-extracted with the SPM filters (Supplemental Data, S1).

Given the available amount of 250-mL sample for determining the SPM concentration (Glaser et al. 2020) and the high uncertainty resulting from subtracting 2 relatively large gravimetric values, we omitted data for compound concentrations in SPM extracts of water sample with SPM concentration <50 $mg_{dry\ weight}\ L^{-1}$ (AS1_12, AS2_1, AS2_2, AS2_3, and AS2_12; Supplemental Data, Table S2) because no reliable and robust results were obtained.

In vitro bioassays

All extracts were tested with 2 in vitro reporter gene bioassays that were indicative for activation of metabolism (activation of aryl hydrocarbon receptor–chemical-activated luciferase gene expression [AhR-CALUX]; Brennan et al. 2015) and activation of oxidative stress response (AREc32; Escher et al. 2012, 2013). Detailed methods are given in König et al. (2017) and Neale et al. (2017). The effect concentration ECIR1.5 (concentration in the assay causing an induction ratio (IR) of 1.5 relative to unexposed cells) for AREc32 and the EC10 (concentration in the assay causing 10% effect relative to 2,3,7,8-tetrachlorodibenzodioxin) for AhR-CALUX were derived based on the linear regression of the lower portion (up to an IR of 4 in AREc32 and up to 30% effect in AhR-CALUX) of the concentration–response curve, according to Escher et al. (2018b). For each bioassay, cell growth inhibition was assessed by measuring the cell area coverage by live cell imaging as described in Escher et al. (2019) and expressed as concentration causing 10% cell growth inhibition (IC10). The ECIR1.5, EC10, and IC10 values of water extracts were expressed as relative enrichment factors (REFs), taking into account the enrichment during the sample preparation procedure and the dilution in the assay. The REFs are in units of $L_w\ L_{bioassay}^{-1}$ for water extracts and $mg_{dry\ weight}\ L_{bioassay}^{-1}$ for SPM extracts. Effect concentrations were then translated into bioanalytical equivalent concentrations (BEQs) by relating the effect of the extract to a reference chemical (Escher et al. 2018a), using Equation 1.

$$\text{BEQ} = \frac{\text{EC10 (reference)}}{\text{EC10 (sample)}} \text{ or } \frac{\text{ECIR1.5 (reference)}}{\text{ECIR1.5 (sample)}} \quad (1)$$

A list of the quality control reference chemicals (tert-butylhydroquinone and 2,3,7,8-tetrachlorodibenzodioxin) and the reference chemicals dichlorvos and benzo[*a*]pyrene (BaP) for derivation of the BEQ (dichlorvos-EQ and BaP-EQ) and their ECs is given in the Supplemental Data, Table S9. Because low effects were detected in the SPE and ASE blanks, the effects of the samples were corrected by blank subtraction ($\text{BEQ} = \text{BEQ}_{sample} - \text{BEQ}_{blank}$). During this process, the effects (BEQ) measured in the SPE and ASE blanks were converted to the matching enrichment factor of the sample. This was necessary because enrichment factors of SPM extracts differed widely, resulting in higher relative background of samples with small SPM amounts. Blanks showed no cytotoxicity in the bioassays. Analogously to the chemicals analysis (Supplemental Data, Equation S1), results of the SPM extracts were corrected for the cytotoxicity using toxic units (Müller et al. 2018) and effects (BEQ) ascribed to the co-extracted water in the SPM filters. Similar to the chemical analysis, we omitted effect data of SPM extracts from samples with SPM concentrations <50 $mg_{dry\ weight}\ L^{-1}$.

Calculation of mass and effect fluxes

Mass fluxes were calculated from analyte concentrations in water (µg L^{-1}) and on SPM (µg $g_{dry\ weight}^{-1}$) by multiplication with the flow rate Q (L s^{-1}) and the SPM flux (g s^{-1}), respectively (Equations 2 and 3).

$$J_{i,\text{water}} = Q \times C_{i,\text{water}} \quad (2)$$

$$J_{i,\text{SPM}} = \text{SPM flux} \times C_{i,\text{SPM}} \quad (3)$$

where $J_{i,\text{water}}$ is the mass flux in water and $J_{i,\text{SPM}}$ is the mass flux attributed to SPM, of compound i. The fraction f_{SPM} describes the portion of the total mass flux that was attributed to SPM and was calculated using Equation 4.

$$f_{\text{SPM}} = \frac{J_{i,\text{SPM}}}{(J_{i,\text{SPM}} + J_{i,\text{water}})} \quad (4)$$

Bioanalytical effect fluxes (BEFs; mass of reference compound equivalent effect in the respective bioassay/second) were calculated using Equation 5 for water (dichlorvos-BEF_{water} and BaP-BEF_{water}) and Equation 6 for SPM (dichlorvos-BEF_{SPM} and BaP-BEF_{SPM}) from the BEQ measured in water (dichlorvos-EQ_{water} [$\mu g_{dichlorvos}\ L^{-1}$] in AREc32, and BaP-$EQ_{water}$ [$ng_{BaP}\ L^{-1}$] in AhR-CALUX) or SPM extracts (dichlorvos-EQ_{SPM} [$\mu g_{dichlorvos}\ g_{dry\ weight}^{-1}$] in AREc32 and BaP-$EQ_{SPM}$ [$ng_{BaP}\ g_{dry\ weight}^{-1}$] in AhR-CALUX).

$$BEF_{water} = Q \times BEQ_{water} \quad (5)$$

$$BEF_{SPM} = \text{SPM flux} \times BEQ_{SPM} \quad (6)$$

Distribution between micropollutants in water and on SPM

The concentration ratio (R_i in $L\,kg^{-1}$) of a compound *i* between water and SPM was calculated using Equation 7, based on the compound concentration measured in the water ($C_{i,water}$ in $\mu g\ L^{-1}$) and on SPM ($C_{i,SPM}$ in $\mu g\ kg_{dry\ weight}^{-1}$) extract.

$$R_i = \frac{C_{i,SPM}}{C_{i,water}} \quad (7)$$

The BEQ ratio R_{BEQ} between water and SPM was calculated analogously to Equation 7. Partitioning of a compound *i* between water and organic carbon of SPM at equilibrium (K_d) was estimated from the octanol/water partition coefficient (K_{OW}), the organic carbon content of SPM, and an empirical correlation from Karickhoff (1981), using Equation 8. This empirical correlation only accounts for hydrophobic compounds that are not ionized and was only applied to compounds that were shown to predominantly partition to the organic carbon of SPM. The organic carbon content (f_{OC}) was derived from the amount of sampled SPM, the dissolved organic carbon (DOC), which refers to organic carbon after 0.45-µm filtration, and the total organic carbon concentration; these data were obtained from replicate samples as reported in Glaser et al. (2020; Supplemental Data, Table S2). The K_{OW} values of target compounds detected in water and SPM extracts are provided in the Supplemental Data, Table S10.

$$K_d = f_{OC} \times K_{OC} = f_{OC} \times 0.41 \times K_{OW} \quad (8)$$

We need to note that the DOC of the water samples was defined as the organic carbon dissolved in water and on particles <0.45 µm. The SPM measured by chemical analysis and bioassays was defined as the particle fraction size in the water samples >4 to 7 µm. The concentration of SPM measured in the water samples was defined as the particle fraction size in the water samples >1.5 µm.

RESULTS AND DISCUSSION

Chemical analysis

Micropollutants in water. At AS1, 27 of 97 target compounds were detected (11 pesticides, 9 pharmaceuticals, and 7 industrial and household chemicals). At AS2, 33 of 97 target compounds were detected (10 pesticides, 17 pharmaceuticals, and 6 industrial and household chemicals), with 25 compounds detected at both sites. Between AS1 and AS2 the compounds perfluorohexanoic acid and propiconazole disappeared, and 8 additional compounds were detected at AS2, along with fluconazole, sotalol, oxcarbazepine, sulfamethoxazole, and trimethoprim. The latter were demonstrably introduced by WWTP1 under dry weather conditions (Müller et al. 2020). Measured concentrations of all target compounds in the water extracts and quantification limits are provided in the Supplemental Data, Tables S11 and S12.

For a better understanding and visualization of the mass flux dynamics and potential input sources, the detected compounds were subdivided into 3 major groups. This division was made on the basis of their mass flux dynamics at AS1 and AS2 (groups 1, 2, and 3; Supplemental Data, Table S13), and thus compounds from different groups showed different courses of mass fluxes over time. Group 1 compounds showed higher or equally high average mass fluxes at AS1 compared with AS2. Group 2 compounds showed 10× higher average mass fluxes at AS2. Group 3 comprised compounds that were detected at AS1 and showed moderately increased average mass fluxes (below a factor of 10) at AS2. One-half of the LOQ was used as a substitute for all samples with concentrations below the LOQ, as recommended by the US Environmental Protection Agency (2000). It is important to note that interpretation of data with nondetects is generally biased (Helsel 1990; Kayhanian et al. 2002). The mass flux dynamics of the 3 groups are shown in Figure 2.

Group 1 compounds were more abundant at AS1 compared with AS2 (Figure 2A and B) and thus were introduced from different input sources of the upper Ammer catchment, such as stormwater from agricultural and urban areas and combined sewer overflows. Storm water input from urban areas is suggested by the biocides carbendazim, diuron, and propiconazole, which are used to preserve outdoor materials and façades. The presence of the plasticizer and flame retardant triphenyl phosphate (TPP) also indicates input from urban areas and wastewater. At AS1, caffeine and paracetamol were detected; both are anthropogenic markers for untreated wastewater (Buerge et al. 2003; Kasprzyk-Hordern et al. 2009). Interestingly, the concentrations of caffeine and paracetamol at AS1 kept increasing throughout the storm event (Supplemental Data, Figure S2A), indicating an increasing portion of untreated wastewater in the Ammer, perhaps through combined sewer overflows.

Many compounds ascribed to group 2 were pharmaceuticals and industrial and household chemicals, which typically find their way into rivers by the route of treated wastewater, indicating a major influence of WWTP1 on the dynamics of group 2 compounds. Indeed, flow measurements showed that WWTP1 released much more water during the storm event. At 20:00 (27 July 2019), the WWTP1 influent substantially increased and exceeded the maximum influent capacity (Supplemental Data, Figure S3), leading to a maximum flow rate of $690\ L\,s^{-1}$ through the WWTP and redirection of the spillover into storm water

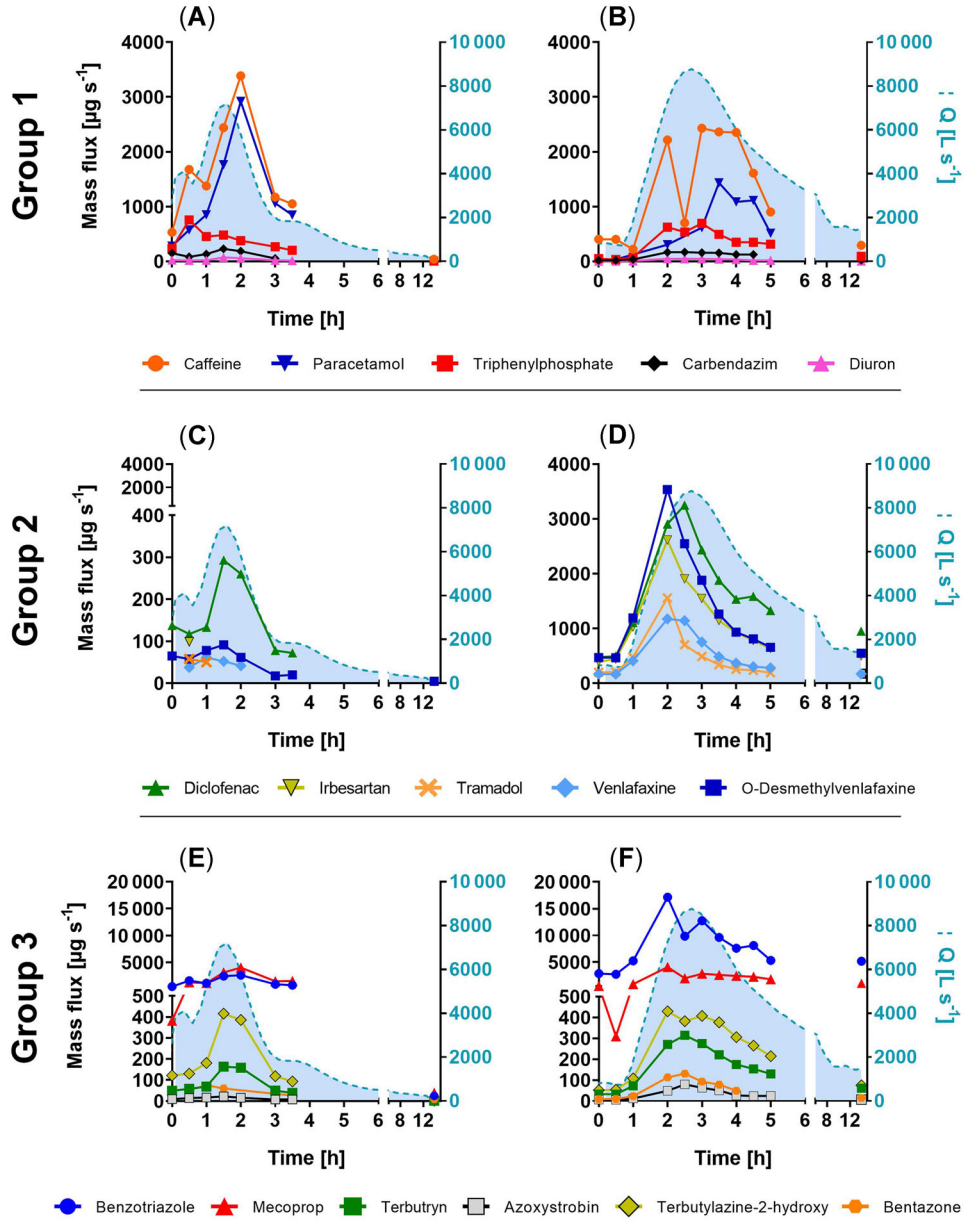

FIGURE 2: Mass fluxes (µg s^{-1}) of selected compounds in water during the storm event that fell into 3 groups. Chemicals in group 1 showed a higher or equally high average mass flux at autosampler (AS) AS1 (**A**) compared with AS2 (**B**). Group 2 showed a 10× higher average mass flux at AS2 (**D**) than at AS1 (**C**). Group 3 chemicals were detected at AS1 (**E**) with moderately increased (below a factor of 10) average mass fluxes compared with AS2 (**F**). Mass fluxes are depicted on the left vertical axis, and discharge is depicted as light blue area and on the right vertical axis. MCPA = (4-chloro-2-methylphenoxy)acetic acid.

retention basins. At AS1, a few pharmaceuticals had already appeared due to input from combined sewer overflows. The mass fluxes of selected compounds at AS1 and AS2 (Figure 2C and D) increased with increasing discharge and roughly followed the hydrograph. Interestingly and considering the concentrations, group 2 compounds at AS2 increased even before the discharge increased (Supplemental Data, Figure S2D). An explanation could be a "first flush" upstream of AS2, that is, contaminated storm water leading to high concentrations in the receiving river, early in the storm hydrograph (Bertrand-Krajewski et al. 1998; Lee et al. 2002; Peter et al. 2020). Similar dynamics were observed by Madoux-Humery et al. (2013) and Phillips et al. (2012), who found generally higher pollutant concentrations in the beginning of storm events when inputs were high and dilution low, which decreased when dilution kicked in.

Compounds of group 3 (Supplemental Data, Table S13) were detected at AS1 and showed moderately increased mass fluxes at AS2, hinting at inputs upstream of AS1 and between AS1 and AS2. The corrosion inhibitor benzotriazole showed the highest mass fluxes of all detected compounds and was likely introduced by a combined sewer overflow and in large amounts by WWTP1. Pesticides commonly applied in agriculture (bentazone, azoxystrobin, mecoprop) and a pesticide

transformation product (terbutylazine-2-hydroxy), pointed toward inputs from agricultural areas. Szöcs et al. (2017) identified agricultural land use as a substantial input source of pesticides in streams and detected a higher number of pesticides following rainfall. Moreover, mecoprop is applied as a biocide against root penetration in bituminous sealings and felts on flat roofs, and terbutryn is used in façade paintings. Rainfall may wash both of them off into surface waters (Bucheli et al. 1998; Burkhardt et al. 2011). Propiconazole (a group 1 compound) was detected at the maximum discharge at AS1. It is used as fungicide in wood preservation and has been found during storm event conditions by other researchers in an urban catchment (Gasperi et al. 2008). Because mecoprop and propiconazole were not detected in the Ammer River under dry weather conditions (Müller et al. 2020), they could potentially be used as storm water indicators in future studies.

Remarkably, the numbers, concentrations, and mass fluxes of the target compounds investigated in the present study were generally higher during the storm event compared with dry weather conditions, according to data from previous studies at the Ammer River in 2017 (Müller et al. 2018) and 2018 (Müller et al. 2020). At base flow, compounds introduced by wastewater and/or from agricultural areas occurred at AS2 in the lower ng L^{-1} range. These compounds showed higher concentrations under storm event conditions by factors of 4 for benzotriazole, 7 for tris(1-chloro-2-propyl) phosphate (TCPP), 3 for 4- and 5-methylbenzotriazole, 3 for carbamazepine, 2 for isoproturon, and 3 for bentazone. The mass fluxes of the same compounds, however, increased by factors of 26 for benzotriazole, 77 for TCPP, 26 for 4- and 5-methylbenzotriazole, 17 for carbamazepine, 15 for isoproturon, and 18 for bentazone during the storm event. The absolute total mass of all compounds (detected then and now) passing AS2 over 12 h was 122 g during the same time period in 2018 and during base flow, but it was 1028 g in the present study, although only 18 compounds were detected then, and now we can estimate a pollutant load difference of 1 order of magnitude between dry and wet weather conditions. Moreover, in 2017 and 2018, 9 and 15 of the now detected compounds were in concentrations below the limit of detection. Thus, during the investigated storm event, micropollutant numbers and concentrations increased considerably along with a generally even more pronounced mass flux increase.

Micropollutants sorbed to SPM. The compounds isoproturon, tebuconazole, and terbutryn were found in the majority of the SPM samples. Highest concentrations were found for the organophosphates TPP, TCPP, and tris(2-butoxyethyl) phosphate (TBEP; Supplemental Data, Tables S14 and S15). In total 16 compounds, comprising 10 pesticides, 2 pharmaceuticals, and 4 industrial and household chemicals, were detected in the SPM extracts. Fenofibrate, azoxystrobin, and carbendazim were exclusively detected in SPM extracts of AS1 and perfluorooctanesulfonic acid (PFOS), atrazine, and prochloraz exclusively in SPM extracts of AS2. The SPM fluxes in the Ammer River followed the hydrographs at AS1 and AS2 and were at maximum 7.10 and 2.93 $kg_{dry\ weight}$ s^{-1} (after 1.5 and 3.4 h, respectively; Supplemental Data, Table S3). Glaser et al. (2020) found a broader discharge function at AS2 and a particle loss of approximately 13% between both sampling sites. Again, the target compounds detected in the SPM extracts from AS1 and AS2 can be subdivided into 3 groups in terms of the mass flux dynamics associated with SPM, similar to the compounds detected in the water extracts. In this case, only compounds detected 3 times in a row were considered.

Among the group 1 compounds, which showed higher or equally high average particle-associated mass fluxes at AS1 compared with AS2, was TPP (Figure 3), a typical wastewater pollutant widely used as a plasticizer and flame retardant (Meyer and Bester 2004; Kim et al. 2017). The presence of TPP points toward micropollutant input from a combined sewer overflow upstream of AS1, as already suggested by organic indicator chemicals (caffeine and paracetamol) in the water samples from AS1. Diflufenican is a pesticide commonly used in agriculture, and isoproturon is a biocide used in domestic

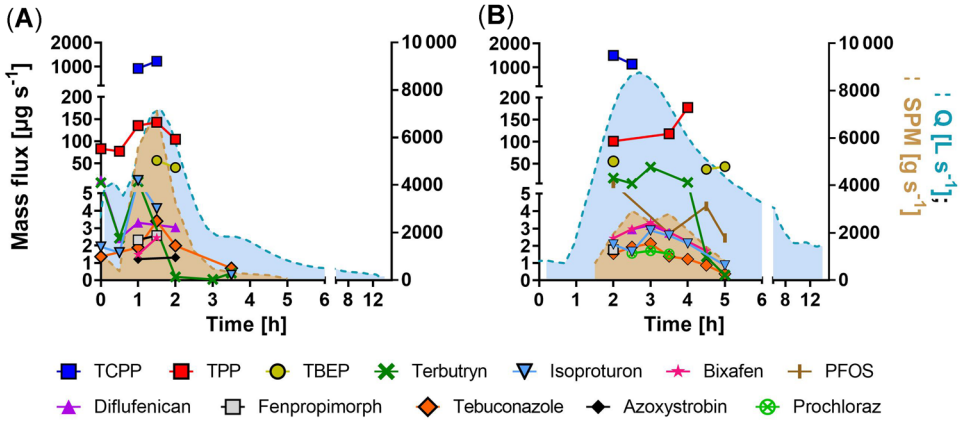

FIGURE 3: Mass fluxes associated with suspended particulate matter (µg s^{-1}) of detected compounds at the autosamplers (AS) AS1 (**A**) and AS2 (**B**) over time. Mass fluxes are depicted on the left vertical axis, and discharge and suspended particulate matter (SPM) flux are depicted on the right vertical axis as light blue and light brown areas. TCPP = tris(1-chloro-2-propyl) phosphate; TPP = triphenylphosphate; TBEP = tris(2-butoxyethyl) phosphate; PFOS = perfluorooctanesulfonic acid.

applications. This suggests inputs from agricultural and from urban areas.

Prochloraz, assigned to group 2, is used as fungicide in agriculture and could thus come from inputs of agricultural areas between AS1 and AS2, for instance, through the agriculturally impacted Käsbach Creek (Figure 1; Müller et al. 2020).

In group 3 the fungicides bixafen and tebuconazole and the biocide terbutryn were detected, which points to agricultural (bixafen) and urban input (tebuconzole, terbutryn).

Among all detected compounds, azoxystrobin, isoproturon, terbutryn, TPP, TCPP, and TBEP were found in, both water and SPM. A comparison of the mass fluxes in water and SPM of these compounds revealed dominant transport in water. The portion of the total mass fluxes attributed to SPM was at maximum 34% for TPP and TCPP at AS2 (Figure 4). For the organophosphate TBEP and the herbicide isoproturon, up to 15% of the total mass flux was attributed to SPM.

The log K_{OW} is 2.8 for isoproturon and TCPP, and >4 for azoxystrobin, TPP, and TBEP (Supplemental Data, Table S10). These compounds are neutral at pH 7.4 and predominantly partition to the organic carbon of SPM (Worrall et al. 1996; Kodešová et al. 2011; Kim et al. 2017). The comparison between the measured concentration ratios R_i between SPM and water (Equation 7) and the predicted partition coefficient K_d (Equation 8) depicted in Figure 5, gives an estimate of whether equilibrium was reached. For TPP, TBEP, and isoproturon at AS1 and AS2, the R_i agreed well with the K_d estimated on the basis of K_{OW}. Because environmental parameters and conditions in rivers (such as DOC and particle and ion concentrations) may change very quickly during storm events, it is all the more surprising that the results indicate that SPM and water could be equilibrated. An R_i 11 to 29 times higher than K_d was observed for TCPP, indicating particle-associated input of TCPP from particles with higher concentrations than found in the Ammer River. Azoxystrobin occurred at R_i 47 and 18 times lower than K_d. Therefore, input of azoxystrobin via the dissolved phase could be linked to direct agricultural application, especially because it was only found in AS1. However, this comparison should be considered with caution because chemicals sorbed to small particles below the applied filter cutoff of 4 to 7 μm would be attributed to the water phase. The fitting factor of 0.41 used in this approximation, empirically determined by Karickhoff (1981), might not apply to all compounds.

All compounds detected in the SPM extracts have log K_{OW} values >1.5. These compounds, except for fenpropimorph and PFOS, are not charged at pH 7.4 (Supplemental Data,

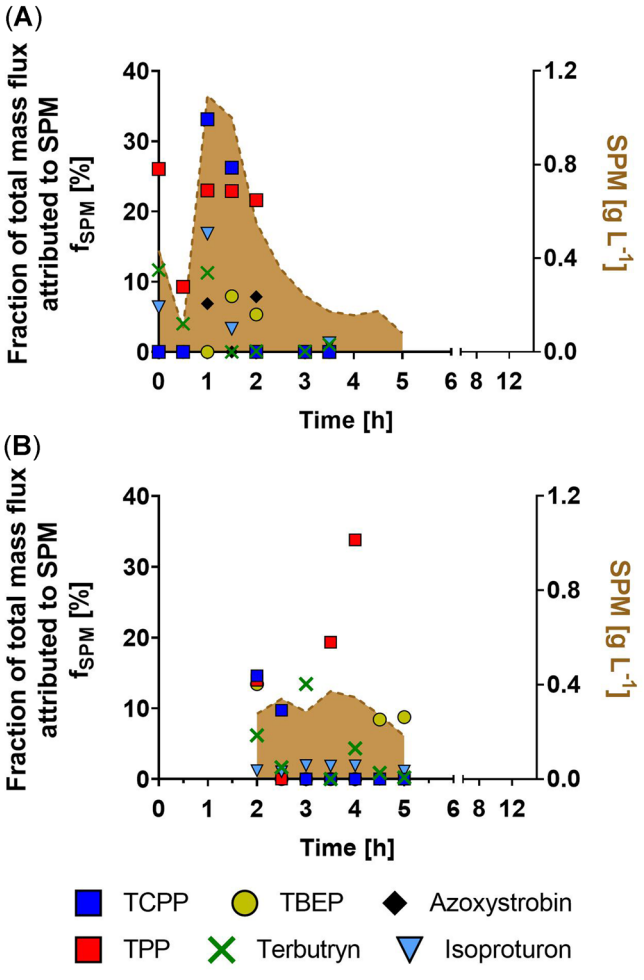

FIGURE 4: Fraction of the total mass flux attributed to suspended particulate matter (f_{SPM}; Equation 4) at the autosamplers (AS) AS1 (**A**) and AS2 (**B**) of compounds detected in water and SPM extracts. TCPP = tris(1-chloro-2-propyl) phosphate; TPP = triphenylphosphate; TBEP = tris(2-butoxyethyl) phosphate.

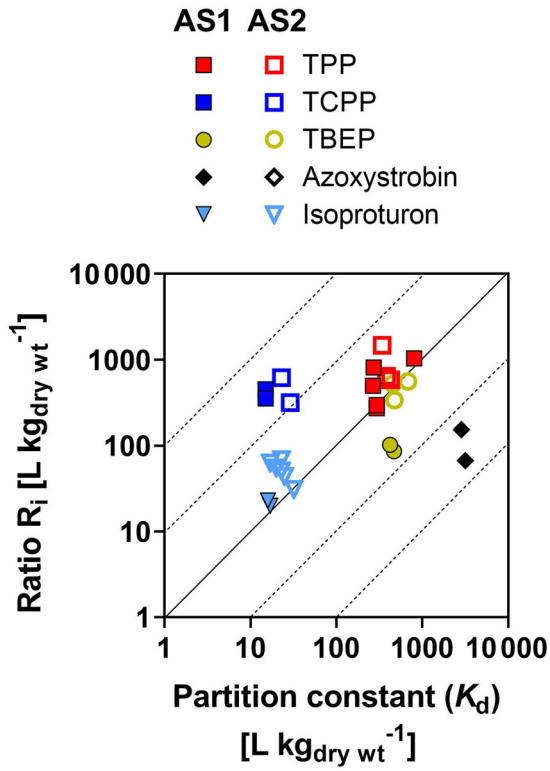

FIGURE 5: Observed concentration ratio (R_i in L kg^{-1}; Equation 7) versus the partition constant (K_d; Equation 8) between water and organic carbon of suspended particulate matter (SPM) during the storm event, for the compounds azoxystrobin, isoproturon, TPP (triphenylphosphate), TBEP (tris(2-butoxyethyl) phosphate), and TCPP (tris(1-chloro-2-propyl) phosphate), at the autosamplers (AS) AS1 (filled symbols) and AS2 (empty symbols).

Table S10) and partition predominantly to the organic carbon of SPM. Fenpropimorph is positively and PFOS negatively charged at pH 7.4, and sorption would not be expected to partition to organic carbon but rather bind via electrostatic attraction to oppositely charged surface sites.

In vitro bioassays

During the storm event the BEQs measured in the SPM extracts (Supplemental Data, Table S17) from AS1 in the AREc32 assay showed variability that increased toward the end of the event (Figure 6A). The BEQs in SPM extracts from AS2 stayed level before they also increased in the last 2 samples (Figure 6B). The BEQs measured in the water extracts were fairly constant, with coefficients of variation of only 32% at AS1 and 34% at AS2 (Figure 6A and B).

The effect distribution ratio R_{BEQ} of effects measured in the water and SPM extracts, from AS1 and AS2, varied between 1000 and 10 000 (Supplemental Data, Figure S4), indicating that most of the chemicals responsible for the measured effects were associated with SPM. The BEF associated with SPM, BEF_{SPM}, was as large or even larger than the BEF associated with water, BEF_{water}, at AS1 and AS2, despite the 1000 times lower mass of SPM than water (Figure 6C and D). The BEF_{water} followed the discharge with a delay of 0.5 h at AS1 (Figure 6C) and 1.5 h at AS2 (Figure 6D). Both BEF_{SPM} and BEF_{water} increased during the storm event at both sampling sites. At AS1, BEF_{SPM} was higher than BEF_{water} after 1 to 2 h, and then both went down parallel with *Q*. Both BEF_{SPM} and BEF_{water} increased by 3- and 2-fold at AS1 and by 26- and 8-fold at AS2 during the storm event (first sample compared with the sample taken at highest discharge). At both sampling sites the BEF_{SPM} followed the SPM flux.

In the AhR-CALUX assay, the BEQs in water and SPM (Supplemental Data, Table S18) at AS1 followed the water and SPM discharge during the storm event (Figure 7A). At AS2, effects in water increased following the discharge, with a 2-h delay, similar to that shown by AREc32 (Figure 7B). Most of the chemicals responsible for the effects in AhR-CALUX partitioned onto SPM, as revealed by the distribution ratio R_{BEQ} of effects measured in the water and SPM extracts from AS1 and AS2, which varied between 1000 and 100 000 (Supplemental Data, Figure S4). As a consequence, the BEF_{SPM} was generally higher than the associated BEF_{water}, although the SPM mass was approximately 1000 times smaller than the water. Similar to the AREc32 assay, the BEF_{SPM} and water BEF_{water} increased during the storm event at AS1 and AS2 in the AhR-CALUX assay (Figure 7C and D). Both BEF_{SPM} and BEF_{water} at AS1 were much higher than at AS2, in line with the SPM flux.

In 29 and 59% of the samples taken during the actual storm event, the major portion of effects in AREc32 and AhR-CALUX were transported via SPM. The distribution ratios R_{BEQ} of effects measured in the water and SPM extracts in AhR-CALUX and AREc32 were similar, being distribution constants between surface water and sediments, as determined by Bräunig et al. (2016), who investigated the same endpoints. Bräunig et al. (2016) measured higher distribution ratios in bed sediments of larger rivers and estuaries. In the present study, the BEQ_{water} values measured in water in AhR-CALUX were approximately 10 times higher than in 2018 (Müller et al. 2020), under dry weather conditions and in the same river section. In 2018 no or low effects were detected by AREc32.

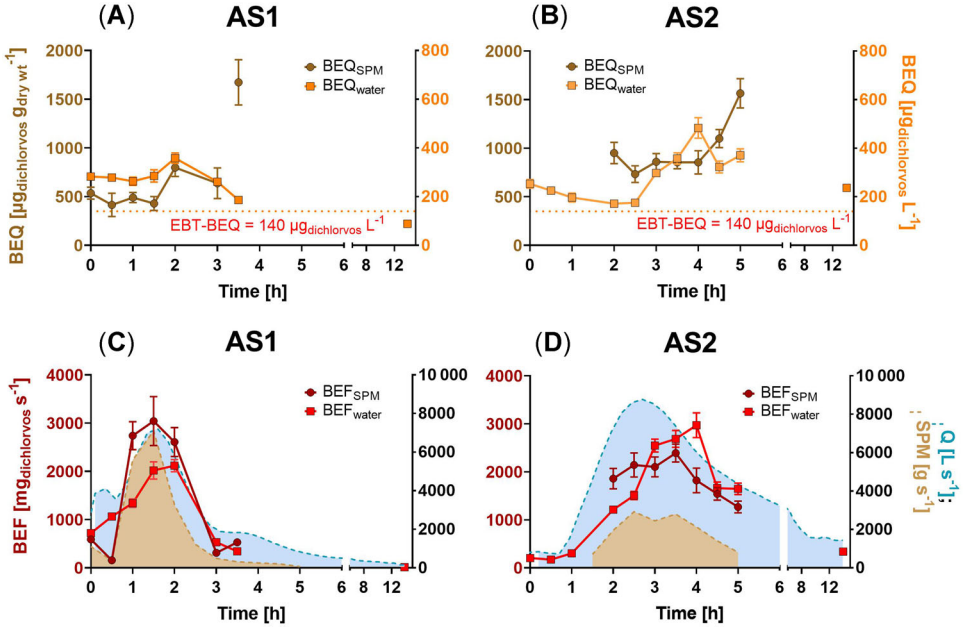

FIGURE 6: The time course of the bioanalytical equivalent concentrations (BEQs), specifically dichlorvos-EQ, in the AREc32 assay of extracted suspended particulate matter (BEQ_{SPM}) and water (BEQ_{water}) at the autosamplers (AS) AS1 (**A**) and AS2 (**B**) and bioanalytical effect fluxes (BEFs) in AREc32 associated with BEF_{SPM} and water (BEF_{water}) compared with discharge *Q* and SPM flux on the second vertical axis, at AS1 (**C**) and AS2 (**D**). The effect-based trigger value (EBT-EQ) for the oxidative stress response in AREc32, updated by Neale et al. (2020), is visualized by a dotted line. Error bars indicate standard errors.

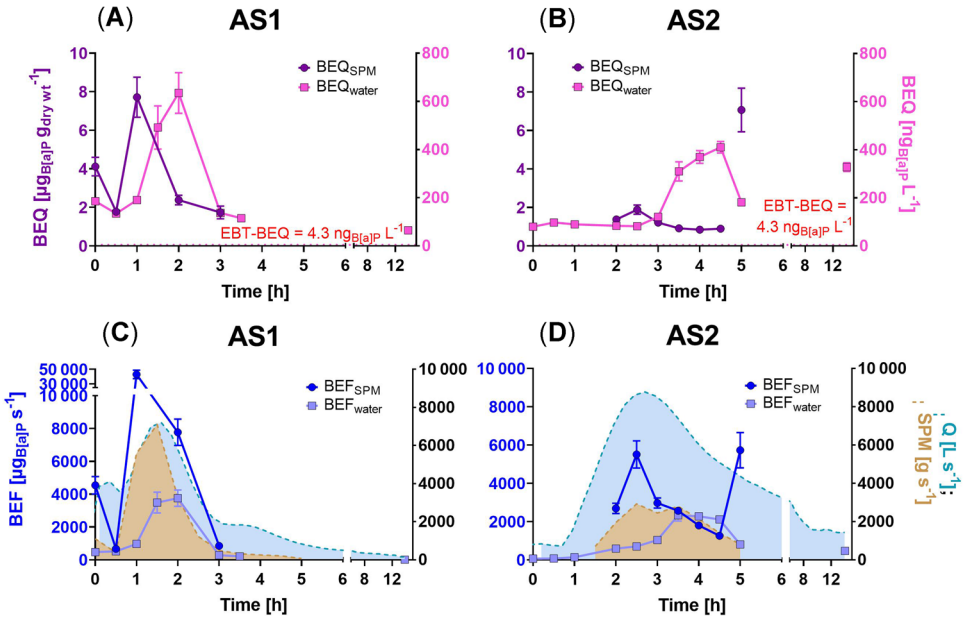

FIGURE 7: Time course of the bioanalytical equivalent concentration (BEQ), specifically benzo[*a*]pyrene-EQ, in the aryl hydrocarbon receptor (AhR–chemical-activated luciferase gene expression [AhR-CALUX]) of extracted suspended particulate matter (BEQ_{SPM}) and water (BEQ_{water}) at the autosamplers (AS) AS1 (**A**) and AS2 (**B**) and bioanalytical effect fluxes (BEFs) associated with BEF_{SPM} and water (BEF_{water}) compared with discharge *Q* and SPM flux on the second vertical axis, at AS1 (**C**) and AS2 (**D**). The effect-based trigger value (EBT-EQ) for AhR-CALUX, updated by Neale et al. (2020), is visualized by a dotted line. Error bars indicate standard errors.

Neale et al. (2020) performed an automated sampling of water at 44 sites in small German rivers, mostly influenced by agriculture and/or wastewater, triggered by rain events. They found a high spatial and temporal variability of the chemical and effect profile in water. Although the majority of samples showed lower effects in AhR-CALUX compared with the present study, the effects measured in AREc32 were in the same range in both studies. The bioassay data of the water extracts from AS1 and AS2 were further compared with tentative effect-based trigger values (EBT-BEQ; Escher et al. 2018a), which were derived from environmental quality standards of the European Union and can serve as effect thresholds indicating poor water quality if exceeded. The EBT-dichlorvos-EQ is 140 $\mu g_{dichlorvos}\ L^{-1}$ for AhR-CALUX, and the EBT-EQ for BaP is 4.3 $ng_{benzo[a]pyrene}\ L^{-1}$ for AREc32, as updated by Neale et al. (2020) using newly available single chemical effect data. The EBT-EQs were exceeded in AREc32 in all samples, except for AS1_12 (13.9 h at AS1) when discharge had returned to base flow after the storm event. Exceedance of EBT-EQ was much more pronounced for AhR-CALUX, pointing toward overall poor water quality with respect to these mixture effect endpoints.

In summary, the bioactive pollutants captured by the bioassays increased much more during the storm event than the individual chemicals analyzed. During the storm event, the BEFs attributed to SPM were as high or even higher than the BEFs attributed to water.

CONCLUSIONS

Storm events pose hazards to the aquatic environment. Numbers of micropollutants, concentrations, mass fluxes, and associated effects and effect fluxes substantially increased during the investigated storm event. Water and SPM originated from combined sewer overflow, urban and agricultural areas, and treated wastewater, with complex contributions that could not completely be traced back to the sources without detailed information on their origin. Water and SPM are inextricably intertwined and exchange organic micropollutants; some neutral compounds appear to occur in concentration ratios close to thermodynamic equilibrium. The SPM turned out to play a particularly important role in the transport of bioactive organic micropollutants, as demonstrated by the dominance of effect flux on SPM over water. The mixture effects of chemicals associated with SPM do not mean that these chemicals are bioavailable. We used the bioassays only to capture complex mixtures, not to form any conclusions with respect to organisms that ingest particles.

Further research would be necessary on whether these pollutants were transported into the Ammer River by particles flushed in during the storm event or whether they originated from mobilized riverbed sediment. For polycyclic aromatic hydrocarbons, it was shown that they rather stemmed from remobilized river sediment during the same event (Glaser et al. 2020), but the sources could be entirely different for the pesticides, consumer products, and pharmaceuticals we investigated.

Despite the much smaller mass contribution of SPM than water, effects and effect flux equivalents attributed to SPM were as high as or even higher than in the water phase. Our study emphasizes that micropollutant inputs triggered by storm events represent an important portion of the overall chemical load in a river. Further research should thus focus on elucidating the impact of different hydrological conditions on the

overall chemical load in a river and assessing their long-term influence on the aquatic environment. Furthermore, particle-facilitated transport of micropollutants, particularly those that may cause toxicity, cannot be neglected in terms of surface water quality monitoring and management.

Supplemental Data—The Supplemental Data are available on the Wiley Online Library at https://doi.org/10.1002/etc.4910.

Acknowledgment—The authors thank C. Zarfl, C. Glaser and M. Schwientek for their help in planning and conducting the sampling, S. Novak for her assistance with sample preparation in Tübingen, and M. König and R. Schlichting for performing the bioassays. We gratefully acknowledge access to the platform CITEPro (Chemicals in the Terrestrial Environment Profiler) funded by the Helmholtz Association. The present study was supported by the Collaborative Research Centre 1253 CAMPOS (Project P1: Rivers), funded by the German Research Foundation (grant SFB 1253/1 2017). Open access funding enabled and organized by Projekt DEAL.

Disclaimer—All authors have no interest to declare. The views expressed in the present study are solely those of the authors.

Author Contributions Statement—M.E. Müller planned and conducted the sampling, sample preparation, chemical analysis, and evaluation and interpretation of the data, wrote the manuscript, and created the initial design of all figures. C. Zwiener planned the sampling, made substantial contributions to the chemical analysis and interpretation of data, and revised the manuscript. B.I. Escher designed the sampling, developed all the bioassay methods and effect-based trigger values, supervised the bioassay measurements, analysis, and interpretation of data, and revised the manuscript.

Data Availability Statement—Data, associated metadata, and calculation tools are available from the corresponding author (beate.escher@ufz.de).

REFERENCES

Alpizar F, Backhaus T, Decker N, Eilks I, Escobar-Pemberthy N, Fantke P, Geiser K, Ivanova M, Jolliet O, Kim H-S. 2019. UN Environment Global Chemicals Outlook II—From legacies to innovative solutions: Implementing the 2030 agenda for sustainable development. United Nations, Geneva, Switzerland.

Baden-Württemberg State Institute for the Environment, Survey and Nature Conservation. 2020a. Daten- und Kartendienst der LUBW. Karlsruhe, Germany. [cited 2020 May 15]. Available from: https://udo.lubw.baden-wuerttemberg.de/projekte/api/processingChain?ssid=62abf969-105e-4ab2-8b20-b07c853b14d6&selector=abflussBW.Hochwasser.bwabfl%3Abwabfl_sel_hq_pegel.sel

Baden-Württemberg State Institute for the Environment, Survey and Nature Conservation. 2020b. Hochwasservorhersagezentrale Baden-Württemberg der LUBW. Karlsruhe, Germany. [cited 2020 May 15]. Available from: https://hvz.lubw.baden-wuerttemberg.de/pegel.html?id=00359

Barwick V, Ellison S. 2000. VAM project 3.2.1. Development and harmonization of measurement uncertainty principles. Part (d): Protocol for uncertainty evaluation from validation data. Report no. LGC/VAM/1998/088. LGC, Teddington, UK.

Berenzen N, Lentzen-Godding A, Probst M, Schulz H, Schulz R, Liess M. 2005. A comparison of predicted and measured levels of runoff-related pesticide concentrations in small lowland streams on a landscape level. *Chemosphere* 58:683–691.

Bertrand-Krajewski J-L, Chebbo G, Saget A. 1998. Distribution of pollutant mass vs volume in stormwater discharges and the first flush phenomenon. *Water Res* 32:2341–2356.

Boulard L, Dierkes G, Schlüsener MP, Wick A, Koschorreck J, Ternes TA. 2019. Spatial distribution and temporal trends of pharmaceuticals sorbed to suspended particulate matter of German rivers. *Water Res* 171:115366.

Brack W, Escher BI, Müller E, Schmitt-Jansen M, Schulze T, Slobodnik J, Hollert H. 2018. Towards a holistic and solution-oriented monitoring of chemical status of European water bodies: How to support the EU strategy for a non-toxic environment? *Environ Sci Eur* 30:1–11.

Bradley PM, Journey CA, Button DT, Carlisle DM, Huffman BJ, Qi SL, Romanok KM, Van Metre PC. 2020. Multi-region assessment of pharmaceutical exposures and predicted effects in USA wadeable urban-gradient streams. *PLoS One* 15:e0228214.

Bräunig J, Tang JY, Warne MSJ, Escher BI. 2016. Bioanalytical effect-balance model to determine the bioavailability of organic contaminants in sediments affected by black and natural carbon. *Chemosphere* 156:181–190.

Brennan JC, He G, Tsutsumi T, Zhao J, Wirth E, Fulton MH, Denison MS. 2015. Development of species-specific Ah receptor-responsive third generation CALUX cell lines with enhanced responsiveness and improved detection limits. *Environ Sci Technol* 49:11903–11912.

Bucheli TD, Müller SR, Voegelin A, Schwarzenbach RP. 1998. Bituminous roof sealing membranes as major sources of the herbicide (R, S)-mecoprop in roof runoff waters: Potential contamination of groundwater and surface waters. *Environ Sci Technol* 32:3465–3471.

Buerge IJ, Poiger T, Müller MD, Buser H-R. 2003. Caffeine, an anthropogenic marker for wastewater contamination of surface waters. *Environ Sci Technol* 37:691–700.

Burkhardt M, Zuleeg S, Vonbank R, Schmid P, Hean S, Lamani X, Bester K, Boller M. 2011. Leaching of additives from construction materials to urban storm water runoff. *Water Sci Technol* 63:1974–1982.

Casado J, Brigden K, Santillo D, Johnston P. 2019. Screening of pesticides and veterinary drugs in small streams in the European Union by liquid chromatography high resolution mass spectrometry. *Sci Total Environ* 670:1204–1225.

Cordeiro RM, Rosa CM, da Silva RJB. 2018. Measurements recovery evaluation from the analysis of independent reference materials: Analysis of different samples with native quantity spiked at different levels. *Accredit Qual Assur* 23:57–71.

da Silva BF, Jelic A, López-Serna R, Mozeto AA, Petrovic M, Barceló D. 2011. Occurrence and distribution of pharmaceuticals in surface water, suspended solids and sediments of the Ebro River basin, Spain. *Chemosphere* 85:1331–1339.

Daughton CG, Ternes TA. 1999. Pharmaceuticals and personal care products in the environment: Agents of subtle change? *Environ Health Perspect* 107(Suppl 6):907–938.

de Weert J, Streminska M, Hua D, Grotenhuis T, Langenhoff A, Rijnaarts H. 2010. Nonylphenol mass transfer from field-aged sediments and subsequent biodegradation in reactors mimicking different river conditions. *J Soils Sediments* 10:77–88.

Deutsche Industrienorm. 1987. 38409-2. German standard methods for the examination of water, waste water and sludge; parameters characterizing effects and substances (group H); determination of filterable matter and the residue on ignition (H 2). Berlin, Germany.

Eggleton J, Thomas KV. 2004. A review of factors affecting the release and bioavailability of contaminants during sediment disturbance events. *Environ Int* 30:973–980.

Eichbaum K, Brinkmann M, Buchinger S, Reifferscheid G, Hecker M, Giesy JP, Engwall M, van Bavel B, Hollert H. 2014. In vitro bioassays for detecting dioxin-like activity—Application potentials and limits of detection, a review. *Sci Total Environ* 487:37–48.

Escher BI, Dutt M, Maylin E, Tang JYM, Toze S, Wolf CR, Lang M. 2012. Water quality assessment using the AREc32 reporter gene assay indicative of the oxidative stress response pathway. *J Environ Monit* 14:2877–2885.

Escher BI, van Daele C, Dutt M, Tang JY, Altenburger R. 2013. Most oxidative stress response in water samples comes from unknown chemicals: The need for effect-based water quality trigger values. *Environ Sci Technol* 47:7002–7011.

Escher BI, Aït-Aïssa S, Behnisch PA, Brack W, Brion F, Brouwer A, Buchinger S, Crawford SE, Du Pasquier D, Hamers T, Hettwer K, Hilscherová K, Hollert H, Kase R, Kienle C, Tindall AJ, Tuerk J, van der Oost R, Vermeirssen E, Neale PA. 2018a. Effect-based trigger values for in vitro and in vivo bioassays performed on surface water extracts supporting the environmental quality standards (EQS) of the European water framework directive. *Sci Total Environ* 628–629:748–765.

Escher BI, Glauch L, König M, Mayer P, Schlichting R. 2019. Baseline toxicity and volatility cutoff in reporter gene assays used for high-throughput screening. *Chem Res Toxicol* 32:1646–1655.

Escher BI, Neale PA, Villeneuve DL. 2018b. The advantages of linear concentration-response curves for in vitro bioassays with environmental samples. *Environ Toxicol Chem* 37:2273–2280.

European Environment Agency. 2019. The European environment—State and outlook 2020: Knowledge for transition to a sustainable Europe. European Union, Luxembourg.

Gasperi J, Garnaud S, Rocher V, Moilleron R. 2008. Priority pollutants in wastewater and combined sewer overflow. *Sci Total Environ* 407: 263–272.

Gasperi J, Garnaud S, Rocher V, Moilleron R. 2009. Priority pollutants in surface waters and settleable particles within a densely urbanised area: Case study of Paris (France). *Sci Total Environ* 407:2900–2908.

Glaser C, Zarfl C, Rügner H, Lewis A, Schwientek M. 2020. Analyzing particle-associated pollutant transport to identify in-stream sediment processes during a high flow event. *Water* 12:1794.

Helsel DR. 1990. Less than obvious-statistical treatment of data below the detection limit. *Environ Sci Technol* 24:1766–1774.

Jordan P, Cassidy R. 2011. Assessing a 24/7 solution for monitoring water quality loads in small river catchments. *Hydrol Earth Syst Sci* 15: 3093–3100.

Karickhoff SW. 1981. Semi-empirical estimation of sorption of hydrophobic pollutants on natural sediments and soils. *Chemosphere* 10:833–846.

Kasprzyk-Hordern B, Dinsdale RM, Guwy AJ. 2009. Illicit drugs and pharmaceuticals in the environment—Forensic applications of environmental data, Part 2: Pharmaceuticals as chemical markers of faecal water contamination. *Environ Pollut* 157:1778–1786.

Kayhanian M, Singh A, Meyer S. 2002. Impact of non-detects in water quality data on estimation of constituent mass loading. *Water Sci Technol* 45:219–225.

Kim U-J, Oh JK, Kannan K. 2017. Occurrence, removal, and environmental emission of organophosphate flame retardants/plasticizers in a wastewater treatment plant in New York State. *Environ Sci Technol* 51: 7872–7880.

Kodešová R, Kočárek M, Kodeš V, Drábek O, Kozák J, Hejtmánková K. 2011. Pesticide adsorption in relation to soil properties and soil type distribution in regional scale. *J Hazard Mater* 186:540–550.

König M, Escher BI, Neale PA, Krauss M, Hilscherová K, Novák J, Teodorović I, Schulze T, Seidensticker S, Hashmi MAK. 2017. Impact of untreated wastewater on a major European river evaluated with a combination of in vitro bioassays and chemical analysis. *Environ Pollut* 220:1220–1230.

Kruve A, Leito I, Herodes K. 2009. Combating matrix effects in LC/ESI/MS: The extrapolative dilution approach. *Anal Chim Acta* 651:75–80.

Lee J, Bang K, Ketchum L Jr, Choe J, Yu M. 2002. First flush analysis of urban storm runoff. *Sci Total Environ* 293:163–175.

Lepom P, Brown B, Hanke G, Loos R, Quevauviller P, Wollgast J. 2009. Needs for reliable analytical methods for monitoring chemical pollutants in surface water under the European water framework directive. *J Chromatogr A* 1216:302–315.

Li JY, Tang JYM, Jin L, Escher BI. 2013. Understanding bioavailability and toxicity of sediment-associated contaminants by combining passive sampling with in vitro bioassays in an urban river catchment. *Environ Toxicol Chem* 32:2888–2896.

Madoux-Humery A-S, Dorner S, Sauvé S, Aboulfadl K, Galarneau M, Servais P, Prévost M. 2013. Temporal variability of combined sewer overflow contaminants: Evaluation of wastewater micropollutants as tracers of fecal contamination. *Water Res* 47:4370–4382.

Mateos R, Oliveira CM, Díez-Pascual AM, Vera-López S, San Andrés MP, da Silva RJB. 2020. Impact of recovery correction or subjecting calibrators to sample preparation on measurement uncertainty: PAH determinations in waters. *Talanta* 207:120274.

Meyer J, Bester K. 2004. Organophosphate flame retardants and plasticisers in wastewater treatment plants. *J Environ Monit* 6:599–605.

Müller A-K, Leser K, Kämpfer D, Riegraf C, Crawford SE, Smith K, Vermeirssen E, Buchinger S, Hollert H. 2019. Bioavailability of estrogenic compounds from sediment in the context of flood events evaluated by passive sampling. *Water Res* 161:540–548.

Müller ME, Escher BI, Schwientek M, Werneburg M, Zarfl C, Zwiener C. 2018. Combining in vitro reporter gene bioassays with chemical analysis to assess changes in the water quality along the Ammer River, Southwestern Germany. *Environ Sci Eur* 30:20.

Müller ME, Werneburg M, Glaser C, Schwientek M, Zarfl C, Escher BI, Zwiener C. 2020. Influence of emission sources and tributaries on the spatial and temporal patterns of micropollutant mixtures and associated effects in a small river. *Environ Toxicol Chem* 39:1382–1391.

Neale PA, Altenburger R, Aït-Aïssa S, Brion F, Busch W, de Aragão Umbuzeiro G, Denison MS, Du Pasquier D, Hilscherová K, Hollert H. 2017. Development of a bioanalytical test battery for water quality monitoring: Fingerprinting identified micropollutants and their contribution to effects in surface water. *Water Res* 123:734–750.

Neale PA, Braun G, Brack W, Carmona E, Gunold R, König M, Krauss M, Liebmann L, Liess M, Link M, Schäfer RB, Schlichting R, Schreiner VC, Schulze T, Vormeier P, Weisner O, Escher BI. 2020. Assessing the mixture effects in in-vitro bioassays of chemicals occurring in small agricultural streams during rain events. *Environ Sci Technol* 54:8280–8290.

Peter KT, Hou F, Tian Z, Wu C, Goehring M, Liu F, Kolodziej EP. 2020. More than a first flush: Urban creek storm hydrographs demonstrate broad contaminant pollutographs. *Environ Sci Technol* 54:6152–6165.

Phillips P, Chalmers A, Gray J, Kolpin D, Foreman W, Wall G. 2012. Combined sewer overflows: An environmental source of hormones and wastewater micropollutants. *Environ Sci Technol* 46:5336–5343.

Ruff M, Mueller MS, Loos M, Singer HP. 2015. Quantitative target and systematic non-target analysis of polar organic micro-pollutants along the river Rhine using high-resolution mass-spectrometry–identification of unknown sources and compounds. *Water Res* 87:145–154.

Schwarzenbach RP, Gschwend PM, Imboden DM. 2016. *Environmental Organic Chemistry*. John Wiley & Sons, Hoboken, NJ, USA.

Spahr S, Teixidó M, Sedlak DL, Luthy RG. 2020. Hydrophilic trace organic contaminants in urban stormwater: Occurrence, toxicological relevance, and the need to enhance green stormwater infrastructure. *Environ Sci Water Res* 6:15–44.

Szöcs E, Brinke M, Karaoglan B, Schäfer RB. 2017. Large scale risks from agricultural pesticides in small streams. *Environ Sci Technol* 51: 7378–7385.

Tran NH, Reinhard M, Khan E, Chen H, Nguyen VT, Li Y, Goh SG, Nguyen QB, Saeidi N, Gin KY-H. 2019. Emerging contaminants in wastewater, stormwater runoff, and surface water: Application as chemical markers for diffuse sources. *Sci Total Environ* 676:252–267.

US Environmental Protection Agency. 2000. Guidance for data quality assessment: Practical methods for data analysis. EPA QA/G-9 (QA00 update). Washington, DC.

van Gils J, Posthuma L, Cousins IT, Brack W, Altenburger R, Baveco H, Focks A, Greskowiak J, Kühne R, Kutsarova S. 2020. Computational material flow analysis for thousands of chemicals of emerging concern in European waters. *J Hazard Mater* 397:122655.

Villagrasa M, Guillamón M, Eljarrat E, Barceló D. 2007. Matrix effect in liquid chromatography–electrospray ionization mass spectrometry analysis of benzoxazinoid derivatives in plant material. *J Chromatogr A* 1157: 108–114.

Worrall F, Parker A, Rae J, Johnson A. 1996. Equilibrium adsorption of isoproturon on soil and pure clays. *Eur J Soil Sci* 47:265–272.

Zgheib S, Moilleron R, Saad M, Chebbo G. 2011. Partition of pollution between dissolved and particulate phases: What about emerging substances in urban stormwater catchments? *Water Res* 45:913–925.

